THE EFFECTS OF MACROPHAGE-STIMULATING PROTEIN AND GAMMA SYNUCLEIN ON THE DEVELOPMENT OF BRAINSTEM MOTOR SYSTEMS

by

Dr. Oliver Schmidt, M.B., Ch.B.

Submitted for the degree of Doctor of Philosophy

The University of Edinburgh

2002

This thesis is dedicated to my wife,

Siân

and to my parents

Astrid and Gerald

Alles will jetzt den Menschen von innen, von außen ergründen;
Wahrheit, wohin rettest du dich hin vor der wütenden Jagd?
Dich zu fangen, ziehen sie aus mit Netzen und mit Stangen,
Aber mit Geistestritt schreitest du mitten hindurch.

"Die Forscher", Friedrich Schiller, 1796

—

One and all now seeks to fathom man from inside out;
Truth, where dost thou flee the furious hunt?
To grasp thee, they fan out with nets and poles,
But with spirit's stride thou stepst straight through their midst.

"The researchers" by Friedrich Schiller, 1796

Declaration

I declare that I am the author of this thesis. All experiments described were carried out by myself under the supervision of Prof Alun M. Davies and Dr. Vladimir L. Buchman. Any contributions by third persons are clearly acknowledged. This thesis has not been submitted for any other degree or qualification.

Oliver Schmidt
November, 2002

Acknowledgements

I might be forgiven if I start long before work on this project began. My first thanks have to go to Klaus Unsicker, now Head of the Department of Neuroanatomy at the University of Heidelberg, Germany. His lectures on neuroanatomy and neurobiology arose my curiosity in the subject. Later he gave me the opportunity to work in his laboratory as an undergraduate. The experience of those months stayed with me during my clinical years and finally brought me back to neuroscience 10 years later.

Actual work on this thesis began with a thoroughly enjoyable trip to the south of France and a two week visit to the laboratory of Christopher E. Henderson at INSERM in Marseille. Special thanks go to Alain Garces who taught me the technique of purifying motoneurons during those two weeks. I am also indebted to Jean Livet, Vilma Arce and Odile deLapeyrièr who have supplied me with valuable information throughout the course of my thesis. And last but certainly not least, I am very grateful to Chris Henderson for allowing me to visit his lab on that and several other occasions and for kindly supplying me with the SC1-hybridoma cell line. I also wish to thank him and his group for the warm welcome I received every time I visited.

During the years in St. Andrews and Edinburgh, a range of people in Alun Davies' and Vladimir Buchman's labs have lent me their kind support in various ways. I especially wish to thank Epaminondas Doxakis who contributed the expression data for the MSP chapter and Natalia Ninkina for giving me access to her transgenic γ-synuclein mouse colony. Darren

Robertson has to be thanked for taking the tedious task of genotyping off my shoulders. He also conducted the affinity purification of the γ-synuclein antibody.

Many thanks go to Gayle Middleton who introduced me to the art of histology. I also thank her for reading my manuscript and pointing out when my English sounded too Victorian.

I wish to express my gratitude to Vladimir Buchman for giving me the chance to collaborate with his group (which I now have become a member of). I am especially thankful for his readiness to putting aside any work and giving my questions his full attention whenever I barged into his office. He has more than confirmed my belief that two minds often get further than one.

The final decision to go back to a subject that once had a special impact on me in medical school, couldn't possibly have found more support than in Alun Davies who invited me to join his lab in 1997. He gave me the freedom to venture into a project that was slightly out of the focus of his group and provided the "French Connection" needed for my undertaking.

I also want to thank Matthew Kaufman for kindly giving me access to his vast and superb histological collection of mouse embryos and for his expert advice on all matters of murine developmental anatomy. It was a great pleasure to work with a true and enthusiastic anatomist.

There can be no doubt that I owe the most debt to my wife Siân. What she often jokingly described as being a "Ph.D.-widow" is in fact a hard test

on any partner. And I can't thank her enough for her understanding, support and – most of all - immense patience throughout the lengthy process of writing this thesis.

This work was funded by the BBSRC and the Wellcome Trust

Abbreviations

AD	Alzheimer's disease
ALS	Amyotrophic lateral sclerosis
ANR	Anterior neural ridge
ATP	Adenosine triphosphate
BDNF	Brain-derived neurotrophic factor
BMP	Bone morphogenic protein
BSA	Bovine serum albumin
BSCG	Breast cancer specific gene
CAM	Cell adhesive molecule
cAMP	Cyclic adenosine monophosphate
cDNA	Complementary deoxyribonucleic acid
CLC	Cardiotrophin-1-like cytokine
CMF-PBS	Calcium-magnesium-free phosphate buffered saline
CNS	Central nervous system
CNTF	Ciliary neurotrophic factor
CO_2	Carbon dioxide
CSF	Cerebrospinal fluid
CT	Column of Terni
CT-1	Cardiotrophin-1
Cu/Zn-SOD	Copper/Zinc superoxide dismutase
DAB	3,3'-diaminobenzidine
DFF	DNA fragmentation factor
DHB	Dihydrobiopterin
DMSO	Dimethyl sulfoxide
DNA	Deoxyribonucleic acid

dNTP	Deoxy nucleotide triphosphate
dpc	Days post coitum
DPX	Dibutyl phthalate xylene
DRG	Dorsal root ganglion
En	Engrailed
ERK	Extracellular signal-regulated protein kinase
FAA	Formalin Alcohol Acetic Acid
FADD	Fas-associating protein
FALS	Familial amyotrophic lateral sclerosis
FBS	Fetal bovine serum
FCS	Fetal calf serum
FGF	Fibroblast growth factor
GA	Gestational age
GABA	γ-aminobutyric acid
GDNF	Glial-derived neurotrophic factor
GGF	Glial growth factor
GPe	Globus pallidus, external segment
GPi	Globus pallidus, internal segment
GPI	Glycosyl-phospatidylinositol
GTP	Guanosine triphosphate
H_2O_2	Hydrogen superoxide
HCl	Hydrochloric acid
HE	Haematoxylin/Eosin
HEPES	N-(2-hydroxyethyl)piperazine-N'-(2-ethanesulfonic acid)
HGF	Hepatocyte growth factor
HH	Hamburger Hamilton stage
IGF	Insulin-like growth factor

IPN	Interpeduncular nucleus
JNK	Jun N-terminal kinase
LBD	Lewy body disease
L-DOPA	L-Dihydroxyphenylalanin
LIF	Leukemia inhibitory factor
LMC_l	Lateral motor column, lateral part
LMC_m	Lateral motor column, medial part
MAO	Monoamino oxidase
MGNF	Motor neuron growth factor
MHJ	Midbrain-hindbrain junction
mM	Millimols
MMC_l	Medial motor column, lateral part
MMC_m	Medial motor column, medial part
mRNA	Messenger ribonucleic acid
MSC	Median stream of cells
MSP	Macrophage-stimulating protein
MPTP	N-methyl-4 phenyl-1,2,3,6, tetrahydropyridine
NAC	Non-Aβ component of Alzheimer's disease amyloid
NF	Neurofilament
NGF	Nerve growth factor
nM	Nanomols
NMDA	N-methyl-D-aspartic acid
NT	Neurotrophin
NTN	Neurturin
OM	Oncostatin M
PBS	Phosphate buffered saline
PCR	Polymerase chain reaction

PI	Phosphatidylinositol
PNAC	Precursor of NAC
PNS	Peripheral nervous system
PSP	Persephin
RA	Retinoic acid
RARE	Retinoic acid response element
RER	Rough endoplasmic reticulum
RTK	Receptor tyrosine kinase
RT-PCR	Reverse transcript polymerase chain reaction
SHH	Sonic hedgehog
SN	Substantia nigra
SNpc	Substantia nigra, pars compacta
SNpr	Substantia nigra, pars reticulata
STN	Subthalamic nucleus
TGF	Transforming growth factor
TH	Tyrosine hydroxylase
THB	Tetrahydrobiopterin
TNF	Tumour necrosis factor
TUNEL	TdT-mediated dUTP-biotin nick end labeling
UCH	Ubiquitin carboxy terminal hydroxylase
VLS	Ventrolateral stream of cells
VMAT	Vesicular monoamine transporter
VTA	Ventral tegmental area

Figures

Tables

Table of Contents

Abstract

Disorders of motility are among the most common and debilitating neurological ailments. In most cases, treatment of these conditions is at best palliative. This is mainly due to the apparent inability of central neurons to regenerate after a given noxious event. In the past, embryos have proven to be valuable objects to study the mechanisms of growth and death in nerve cells since both are physiological events in the developing nervous system. The discovery and study of an ever-growing list of molecules that are involved in these events has significantly furthered our understanding of the conditions that have to be met for individual nerve cell populations to develop into functional structures. It also has the potential to contribute significantly to the establishment of more targeted and efficient therapeutic strategies.

Here, the effects of macrophage-stimulating protein (MSP) and γ-synuclein on two systems in the developing brainstem involved in controlling movement have been studied: a) the cranial motoneurons and b) the dopaminergic neurons of the substantia nigra and the ventral tegmental area. MSP exerts a variety of biological actions on many cell types, but has no known functions in the brain. To investigate whether MSP is also capable of acting as a neurotrophic factor, hypoglossal motoneurons were purified from the embryonic chicken hindbrain because these neurons are known to express the MSP receptor tyrosine kinase RON. The study shows that MSP promotes the in vitro survival of these neurons during the period of naturally occurring neuronal cell death and enhances the growth of neurites from these neurons. Furthermore, MSP mRNA was detected in the developing tongue which is the

target tissue for hypoglossal neurons. These studies demonstrate that MSP is a neurotrophic factor for a distinct population of developing motoneurons.

γ-synuclein is a recently discovered member of the synuclein family. Another member of this family, α-synuclein has been implicated in the pathogenesis of Parkinson's disease. However, little is known about the function of γ-synuclein and it has not yet been directly implicated in the genesis of neurodegenerative conditions. Here, brainstems of transgenic mice lacking γ-synuclein have been analysed by means of immunohistochemical and histological techniques. The data obtained shows that γ-synuclein is expressed in the murine substantia nigra and in most cranial motor nuclei and that the localization of the protein undergoes a shift during development from a cytosomal to an axonal and synaptic localization. Mice lacking γ-synuclein have a deficit of neurons in these structures. In the context of recent studies which have revealed in vivo and in vitro interactions between the synucleins, this data suggests that a fine balance between α- and γ-synuclein seems critical to prevent the demise of certain neurons during the period of naturally occurring neuronal cell death. It also indicates that γ-synuclein may play a role in the pathogenesis of Parkinson's disease.

PREFACE

At the beginning of the 21st century modern neurology is still facing an old dilemma: the apparent disability of central neurons to regenerate and re-establish axonal or dendritic connections with other neurons or target organs. The functional deficits resulting from damage to central neurons are in many cases only partially or not at all reversible, and the prognosis of many diseases affecting the central nervous system is accordingly poor. In order to improve the status quo, one is ultimately faced with the question of how to facilitate neuronal regeneration.

Any regeneration strategy for a damaged neuron faces a set of objectives: The neuron has to survive the insult, and its branches have to be re-myelinated and need to re-establish contact with their original target and afferents to rebuild functional synapses. These requirements are essentially the same a neuron has to meet during ontogenesis in order to become a functional part of the nervous system. Thus the study of the developing nervous system has become a valuable tool in understanding the mechanisms of neuronal cell death and survival, neuritic outgrowth and guidance, and synaptic contact. The results of this research provide an important basis on which future therapeutic strategies can be built.

The studies reported in this thesis focus on specific aspects in the development of two systems involved in the generation of movement, the brainstem motor nuclei and the dopaminergic neurons of the substantia nigra. The former are part of a neuronal population that in a clinical context is often referred to as lower motoneurons. These motoneurons are directly responsible for the execution of movement. The latter group is involved in regulatory functions that finetune the brains motor output. Although damage to these structures can result from a whole range of noxious insults, they are particular targets of Amyotrophic Lateral Sclerosis and Parkinson's disease, respectively. The findings of the work reported here are discussed in their developmental context as well as in relation to the possible molecular mechanisms underlying these two diseases.

CHAPTER I

Introduction

1.1. Development of the Brainstem, Brainstem Motoneurons, and the Substantia Nigra

1.1.1. Early development of the central nervous system

The development of the nervous system commences shortly after gastrulation has taken place (week 3 in human embryos). At this stage, the embryo consists of three layers: the endoderm which will give rise to lungs, liver and gut, the mesoderm, from where the connective tissues, muscles and the vascular system will arise, and the outermost layer, the ectoderm which will differentiate into the epidermis of the skin and the nervous system.

The central nervous system (CNS) makes its first appearance as a slipper-shaped thickening of ectoderm. This thickened sheet of ectoderm, called the neural plate, consists of a uniform population of neural progenitor cells. The lateral edges of the neural plate soon start to elevate, becoming the neural folds. With further proliferation of neural progenitor cells, the folds approach each other in the midline. They finally fuse and form a tubular structure, called the neural tube (Fig. 1.1.1).

These early stages of neural development are characterised by extensive cell proliferation. However, the extent of proliferation is not uniform throughout the antero-posterior axis of the neural tube. Increased proliferation takes place at certain sites, leading to the expansion of three specialised regions, the primary brain vesicles. In rostro-caudal order they

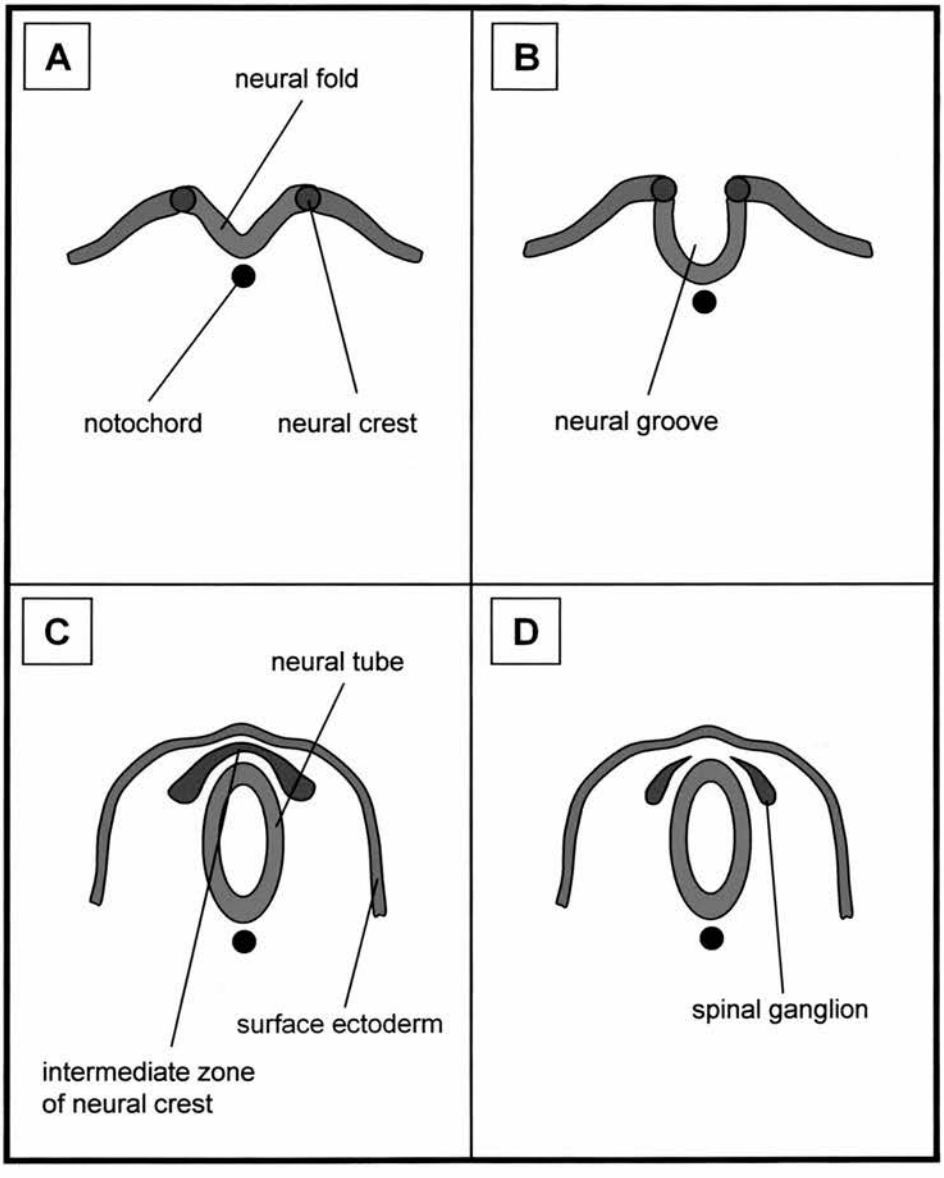

Fig. 1.1.1: Transverse sections through successive stages of the early development of the nervous system. **A,B:** Closing of neural groove; **C,D:** Separation of the neural crest and formation of (spinal and cranial) sensory ganglia (adapted from Langman's Medical Embryology)

give rise to the prosencephalon, the mesencephalon, and the rhombencephalon. Further divisions of the prosencephalon and the rhombencephalon give rise to telencephalon and diencephalon, and met- and myelencephalon respectively (Tab. 1.1.1).

At the same time, two flexures are formed in the anterior part of the neural tube. The uppermost of the two, the so-called cephalic flexure marks the border between midbrain and hindbrain. Further down, the cervical flexure marks the boundary between hindbrain and spinal cord. The cervical flexure as well as a later formed curvature, the pontine flexure are of a transient nature and straighten out during further development.

Three-Vesicle Stage	Five-Vesicle Stage	Main Derivatives
Prosencephalon (forebrain)	Telencephalon (endbrain)	Cerebral cortex, basal ganglia, hippocampus, amygdala
	Diencephalon	Thalamus, hypothalamus, sub- and epithalamus, optic tract and nerve, retina
Mesencephalon (midbrain)	Mesencephalon	Midbrain (upper brainstem)
Rhombencephalon	Metencephalon (afterbrain)	Pons, cerebellum (upper brainstem)
	Myelencephalon (medullary brain)	Medulla (lower brainstem)
Caudal part of neural tube	Caudal part of neural tube	Spinal cord

Tab. 1.1.1: Divisions of the developing and mature central nervous system

The newly formed neural tube consists of a pseudostratified epithelium, referred to as the neuroepithelial layer or neuroepithelium. From this layer of neural progenitor cells neuroblasts emerge which form a new layer around the neuroepithelium, the mantle layer. Due to further proliferation, the mantle layer shows a ventral and a dorsal thickening, the basal and the alar plate respectively. The ventral and dorsal midline portions of the neural tube give rise to populations of specialised glial cells and are referred to as floor plate (ventral) and floor plate (dorsal). In the caudal part of the neural tube - which is to become the spinal cord - neuroblasts of the basal plate differentiate into motoneurons and ventral interneurons, whereas neuroblasts in the alar plate give rise to dorsal sensory interneurons.

The fate of ectodermal cells differentiating into neural progenitor cells and the specialisation of neuroblasts arising from these progenitors into distinct subsets of neurons is regulated by a complex mechanism that involves inducing factors and intracellular signalling cascades that transduce the signal of the inducers to the cell nucleus. The interface between inducing factors and intracellular signalling is represented by different receptors located on the membrane of individual cells. Once an inducer molecule binds to its specific receptor, intracellular signalling cascades become activated by the receptor. This in turn directs the expression of specific genes within individual cells via transcription factors that lie at the downstream end of the intracellular signalling pathways.

Recent research has shown that ectodermal cells, when dissociated in culture and deprived from influences that are exerted on them by their *in situ* neighbourhood differentiate into neural tissue (Grunz and Tacke, 1989; Sato and Sargent, 1989). These findings seem to contrast with the historical paper of Spemann and Mangold who identified an area of mesoderm adjacent to the future neural plate that seemed to be responsible for the induction of neural tissue. They called this area the organiser region (Spemann and Mangold, 1924). The conflicting findings can be explained by the actions of bone morphogenetic proteins (BMPs), a subclass of transforming growth factor β (TGF-β)-related proteins (reviewed in Tanabe and Jessell, 1996). BMPs suppress neural differentiation and promote the formation of epidermis from ectoderm (Sasai et al., 1995; Schmidt et al., 1995). BMP signalling can in turn be suppressed by three different proteins: follistatin, noggin, and chordin, each of which are secreted by cells of the organiser region (Lamb et al., 1993; Lamb and Harland, 1995; Piccolo, 1996). The differentiation of neural plate tissue triggered by BMP signal suppression seems to involve the expression of transcription factors belonging to the Sox family (reviewed in Sasai, 1998).

Once the neural plate has developed into the neural tube, and the progenitor cells of the neuroepithelium give rise to neuroblasts, these neuroblasts rapidly acquire specialised properties. The fate of neuroblasts depends on their position inside the neural tube and is controlled by two different signalling systems. One of these systems controls the patterning along the rostrocaudal axis and will be discussed in connection with the

development of the brainstem in the following subchapter. The other signalling system directs patterning of the dorsoventral axis at any given segment of the neural tube.

The ventral half of the neural tube is controlled by a signalling system distinct from the signals directing the differentiation of neural crest cells and sensory interneurons in the dorsal half. The fate of ventral neural tube neurons is determined by the Sonic hedgehog protein which is expressed by floor plate cells as well as the notochord (Ecchelard et al., 1993; Riddle et al., 1993; Roelink et al., 1994, 1995). The notochord is made up from a solid strand of cells that underlies the neural tube and serves as a basis for the future axial skeleton. Sonic hedgehog induces the differentiation of floor plate cells, motoneurons and ventral interneurons by binding to a heterodimeric receptor complex on the membrane of these cells. The two transmembrane proteins forming the receptor are 'patched' and 'smoothened' (Marigo et al., 1996; Stone et al., 1996; Murone et al., 1999). Smoothened activates an intracellular signalling cascade involving several protein kinases leading to the activation of a group of cytosolic transcription factors, the 'gli' proteins (Lee et al., 1997; Ruiz I Altaba, 1998; Villavicencio et al., 2000). Once activated, the gli proteins enter the nucleus and induce the expression of several target genes. Smoothened activity is inhibited by the patched subunit of the receptor complex. Binding to patched sonic hedgehog relieves smoothened from the repression and induces its intracellular signalling.

Most notable is the ability of sonic hedgehog to direct different cell fates at different locations. Ericson and colleagues have shown that this process is dependent on the concentration of sonic hedgehog: neural tube cells exposed to low levels differentiate into ventral interneurons. Intermediate levels of sonic hedgehog induce motoneurons and high concentrations lead to the formation of floor plate cells (Ericson et al., 1997).

The concentration gradient of sonic hedgehog inside the neural tube needed for these differential specifications is achieved by means of affinity. Once secreted the protein undergoes autocatalytic cleavage. The active N-terminal protein fragment is then modified by the addition of a cholesterol molecule which attracts most of the molecules to the cell membranes of the notochord and the floor plate. Therefore, only a small amount of sonic hedgehog is able to diffuse further into the neural tube and initiate the formation of motoneurons and further again ventral interneurons (Roelink et al., 1995, Porter et al., 1996).

The patterning of the dorsal neural tube is directed by bone morphogenetic proteins that are initially secreted by the ectodermal cells flanking the elevating neural folds (Liem et al, 1995). After tube closure BMPs are produced by the floor plate. BMPs induce the differentiation of neural crest cells and dorsal interneurons by binding to a transmembrane serine-threonine kinase receptor complex. While BMP is binding to one subunit of the receptor complex the other subunit is transducing the signal to

the cell nucleus via phosphorylation of cytosolic SMAD proteins. Upon phosphorylation the SMADs enter the nucleus and control the expression of transcription factors that direct the specialisation of those cells (reviewed by Baker et al., 1997).

However, the whole picture of the early development of the central nervous system remains patchy, and little is known about the intermediate steps between the early induction of progenitor cells and final differentiation patterns. Many more factors than described above are likely to be involved in the patterning process. It has, for instance, been known for years that the homeobox gene *Islet-1* plays an important role in motoneuron differentiation (see below). There also seems to be involvement of members of the neurotrophin family in motoneuron specification(Jungbluth et al., 1997). Both will be discussed in the following subchapters.

1.1.2. Hindbrain development

1.1.2.1. General hindbrain pattern

The hindbrain or rhombencephalon lies between the rhombencephalic isthmus and the cervical portion of the spinal cord. It consists of the metencephalon rostrally and the myelencephalon caudally (see above; Tab.1.1.1).

The overall pattern of the hindbrain is similar to that of the spinal cord in the dorsoventral arrangement of motoneurons and sensory relay neurons, but it exhibits a somewhat higher degree of structural complexity.

The lateral walls of the hindbrain are everted, expanding the lumen of the neural tube to what will become the fourth ventricle. As is true for the spinal cord, efferent neurons are contained within the ventral basal plate and sensory relay nuclei are located in the alar plate. The plates contain three different neuronal groups each: somatic, special visceral and general visceral; the basal plate also contains a small group of efferent vestibuloacoustic neurons (Fig. 1.1.2; see below).

Of the three main motor groups in the basal plate, the most medial, the somato-efferent group forms the cephalic continuation of the anterior horn cells of the spinal cord. It reaches as far up as the mesencephalon and contains motoneurons that innervate the muscles of the tongue and external ocular muscles. Lateral to this discontinuous column of motoneurons lies the intermediate group of special visceral motoneurons (or branchiomotoneurons) that innervate striated muscles deriving from the mesoderm of the pharyngeal arches. The most lateral group contains pre-synaptic parasympathetic neurons whose axons terminate on peripheral (postsynaptic) neurons that innervate the lacrimal and salivary glands as well as the smooth muscles of the respiratory tract, the intestinal tract, and the cardio-vascular system. Similarly, but in a mirrored fashion, the alar plate contains a somatic afferent group of relay neurons at its most lateral extension. These neurons receive input from the ear and the surface of the head. The intermediate group of special visceral afferent neurons - like its efferent counterpart - receives input from derivates of the pharyngeal arches, namely the palate, the oropharynx, the epiglottis, and the taste buds of the

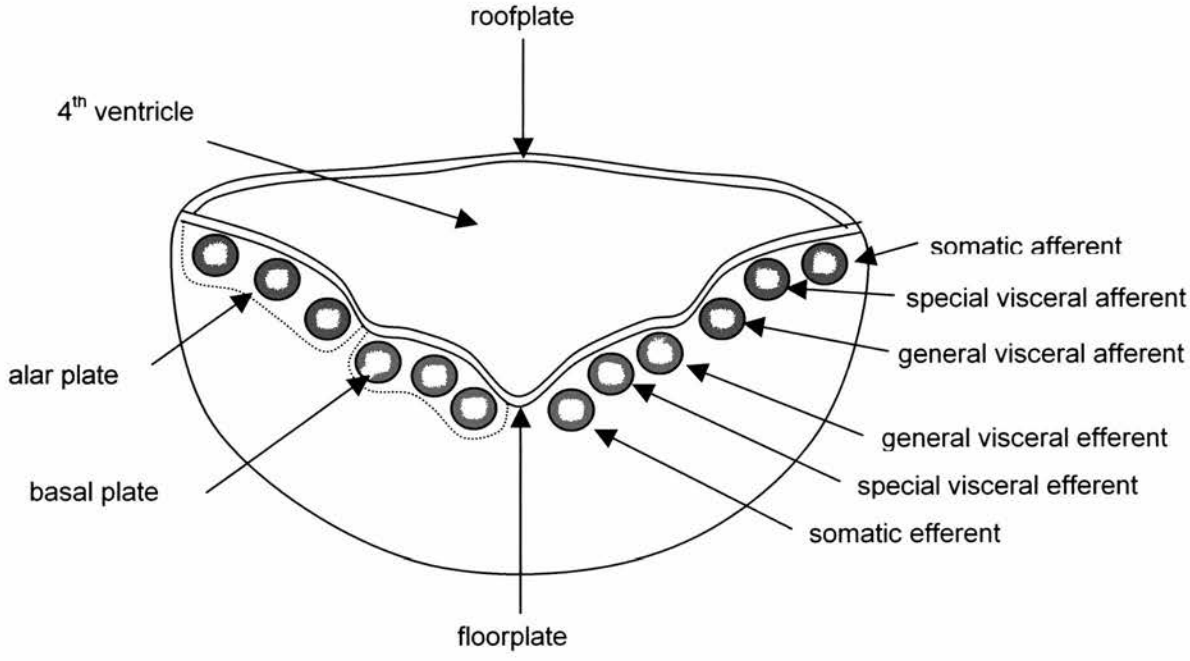

Fig. 1.1.2: Transverse section through the developing hindbrain showing the position of the nuclear groups in the basal and alar plates

tongue. More medially, adjacent to the sulcus limitans (see above) lies the general afferent group which receives interoceptive information from the gastrointestinal tract, the respiratory tract, and the heart.

Analogous to the spinal cord which gives rise to 31 nerve pairs, the brainstem displays 12 pairs of cranial nerves. Of these only numbers 3 to 12 are true peripheral nerves, conveying information from and to structures of face, head, and neck. The first two, the ophthalmic and the optic nerve are strictly speaking part of the central nervous pathways but are traditionally referred to as cranial nerves (Mayr, 1985).

1.1.2.2. Hindbrain segmentation

The most conspicuous and intriguing aspect of early hindbrain development is the transient formation of periodic neuroepithelial swellings along the rostro-caudal axis called rhombomeres. The boundaries between these rhombomeres appear as grooves on the pial surface and ridges on the ventricular side. Although rhombomeres have been recognised and described in a variety of vertebrates for a long time, their significance has only recently become apparent.

In the chick, hindbrain segmentation begins at Hamburger Hamilton stage (HH) 9⁻(Lumsden & Keynes, 1989). A constriction appears at a level between the future rhombomeres 5 and 6. Further subdivisions of the neuroepithelium rostral and caudal to the initial demarcation lead to the full set of eight rhombomeres by HH 12. The most rostral rhombomere (r1) is

separated from the midbrain by the rhombencephalic isthmus. Caudally the eighth rhombomere (r8) appears continuous with the spinal cord. The boundary between r7 and r8 is also less well defined than those rostral to it. The rhombomeric pattern becomes invisible once again by HH 24.

Since Lumsden and Keynes in their landmark paper in 1989 have for the first time presented strong evidence that the chick hindbrain develops in a segmental pattern, a plethora of subsequent research has advanced our understanding of the cellular and molecular mechanisms underlying this phenomenon. Rhombomeres can be viewed as an *"iteration of a comparatively uniform set of early cell types ... , a theme on which local variations are subsequently built"* (Clarke and Lumsden, 1993). The rhombomeric units are separated by boundaries that are morphologically and biochemically distinct from the central segment regions. Both at the light and the electron microscopic level, intercellular spaces in the boundaries are enlarged compared to those in the centres of the rhombomeres (Lumsden & Keynes, 1989; Heyman et al., 1993). Given a concentration of medially-directed axons (Lumsden and Keynes, 1989) and axons originating from developing branchiomotoneurons (Guthrie and Lumsden, 1992) in the boundary zones, the widened spaces might provide preferential routes for axons. How are these intercellular gaps achieved?

Forty years ago, Källén showed that mitoses in colchicine-treated embryos accumulate around the centres of rhombomeres and are much sparser in the boundaries (Källén, 1962). A more recent study has confirmed

the rhombomeres as mitotic centres and has also shown that the interkinetic nuclear migration pattern in the boundaries differs from the one usually found in the neuroepithelium (Guthrie et al., 1991). The nuclei of epithelial cells typically undergo migration from the apical to the basal pole of the cell and back during one cell cycle (Sauer, 1936). Mitosis takes place close to the ventricular surface. Guthrie and colleagues have shown that S-phase nuclei which are characteristically found in proximity to the basal (pial) border lie closer to the apical (ventricular) cell pole in the boundaries suggesting a reduced nuclear migration. Cells therefore become wedge-shaped with a broad apical surface. The investigators presume that this leads to a narrowing of basal endfeet and subsequently to widened intercellular spaces which might act as conduits for outgrowing axons (Guthrie et al., 1991).

Further support for a role of the boundary zones in axonal guidance comes from the finding that the extracellular matrix protein laminin as well as Ng-CAM/L1 are expressed locally in these zones (Lumsden and Keynes, 1989). Laminin has been proposed to play a role in axon guidance (Gordon-Weeks et al., 1989).

The appearance of rhombomeres coincides with the beginning of neurogenesis in the hindbrain. Reticular neurons and motoneurons first appear in even-numbered rhombomeres at HH 11/12 followed shortly by the onset of neuronal differentiation in the odd numbered rhombomeres (Lumsden and Keynes, 1989). Up to HH 20 the neuronal composition of each rhombomere is remarkably similar. By tracing the different axonal projection

pathways of newly generated neurons, Clarke and Lumsden found that each of rhombomeres 1 to 6 contains a nearly identical set of 8 different types of reticular neurons and at least one of the three types of cranial motoneurons (Clarke and Lumsden, 1993). Local specialisations inside each rhombomeric unit lead to diversification at later stages, giving rise to the final anatomical complexity of the brainstem. However, the cellular patterns of rhombomeres 7 and 8 deviate slightly from those seen in the other rhombomeres. Although some features like dorsal branchiomotor exit points, are in line with the other rhombomeres, the more continuous, non-segmented neuronal and axonal organisation already points towards the pattern seen in the developing spinal cord (Clarke and Lumsden, 1993).

The question that arises is how this segmented neuronal pattern is achieved. Fraser and colleagues studied the migration behaviour of neuronal cell clones in the chick hindbrain by marking single neuroepithelial cells between HH 6 and 12^{-} with a vital fluorescent dye (Fraser et al., 1990). All cell clones expanded inside the rhombomere of their precursor but did not cross boundaries into adjacent rhombomeres when marking was performed after the first appearance of segmentation. However, when labelled before boundaries become visible, the progeny of some cells but not all would extend into neighbouring rhombomeres. In contrast, cell clones inside the floor plate, which doesn't exhibit morphological signs of segmentation at any time in development, expanded freely along the unilateral rostro-caudal axis but did not cross into the adjacent basal plate. The authors suggested that the

formation of boundaries and the onset of migratory restrictions coincide with each other.

However tempting, one cannot deduce from these observations that the boundaries themselves act as a barrier for migration. Indeed, subsequent research has shone a different light on these events. Intrinsic differences in rhombomeres are already established at early stages. Rhombomeres keep their individual characteristics in terms of specific gene expression (see below) and motoneuron morphology even when transplanted to an ectopic location at a stage prior to visible boundary formation (Guthrie et al 1992, Simon et al., 1995; Grapin-Botton et al., 1995, 1997; Itasaki et al., 1996).

Heterospecific transplantation of quail rhombomeres into chick embryos between stages 10 and 12 revealed that cells from donor and host rhombomeres readily mixed with each other when the donor rhombomere was either placed adjacent to a host rhombomere of the same order (e.g. r3 next to r3) or to a rhombomere 2 segments away (e.g. r3 next to r5; Guthrie et al., 1993). Neither were any boundaries formed between the two rhombomeres. In contrast, the placement of an odd numbered rhombomere next to an even numbered one (e.g. r3 next to r4) led to boundary formation and prevented mixing of the neighbouring neuron populations. Moreover, the transplantation of smaller-sized rhombomere fragments (chick to chick) into a host hindbrain revealed a hierarchy of miscibility. Cell dispersal of the grafted fragments was most pronounced when the fragments were transplanted into rhombomeres of the same order number as their origin.

Slightly less pronounced dispersal was seen in odd/odd or even/even transplants where the order number of donor and host rhombomere was different. Grafts from r4 to r3 however led to a segregation of host and donor cell populations in most cases. The authors proposed *"that the generation of discrete but continuous blocks of tissue that manifest qualitatively and/or quantitatively different adhesive properties is one of the primary events in the creation of the rhombomeric pattern in the hindbrain"* (Guthrie et al., 1993). Furthermore, they deduced from their observations that there was an adhesive hierarchy brought about by different repertoires of cell surface molecules in individual rhombomeres.

1.1.2.3. Migration pattern of cranial neural crest cells

The segmental pattern of hindbrain development also becomes apparent in the migration behaviour of neural crest cells. Neural crest cells first appear during folding of the neural plate along each edge of the neural groove (Fig.1.1.1). After closure of the neural tube, the neural crest temporarily forms a continuous band of cells between the tube and the surface ectoderm, spreading along the entire length of the neural tube. Neural crest cells soon migrate ventrally and laterally from this position to give rise to a number of different structures (spinal ganglia, ganglia of the trigeminus, facial, vestibuloacoustic, glossopharyngeus, and vagus nerve, chromaffin cells of the sympathetic system, Schwann cells, melanocytes of the skin, and mesenchyme of the head).

In the trunk region, neural crest cells migrate in a segmented pattern which seems to be controlled solely by the adjacent mesoderm. The cells are directed towards the rostral half of each sclerotome (Rickmann et al., 1985). The caudal half of the sclerotomes appears to produce a variety of molecules that inhibit migration of neural crest cells (Stern et al., 1986; Davies et al., 1990; Wang et al., 1997; Eickholt et al., 1999). In the head region the segmentation of the mesoderm into distinct somites is absent. Lumsden and colleagues have studied the cranial migration pattern of neural crest cells in the chick embryo and found that the cells are segregated into 4 migratory groups along the rhombencephalic axis (Lumsden et al., 1991). The most rostral group originates from the posterior midbrain and rhombomeres 1 and 2, and contributes to the trigeminal ganglion as well as derivatives of the first branchial arch (Fig.1.1.3 on page 38), the mandibular process and to a small extent the maxillary process). The second group populates the otocyst, the geniculate and vestibular ganglia and the hyoid arch. It originates in rhombomere 4. The third group from rhombomere 6 migrates towards the third branchial arch and contributes towards the superior and petrosal ganglia. The fourth branchial arch seems to be populated by cells stemming from rhombomere 7. These results show a clear segmental migration pattern by which each group of neural crest cells is assigned to an individual branchial arch.

The fate of neural crest cells from the levels of r3 and r5 remained less clear in that study. The authors suggested two possibilities: firstly, increased death of crest cells in these rhombomeres, and secondly, a

recruitment of cells from r3 and r5 by adjacent rhombomeres. Indeed, neural crest cells from r3 and r5 are selectively eliminated as a result of signalling interactions between even- and odd-numbered rhombomeres involving the induction of Bmp-2 and msx-2 expression (Graham et al., 1993, 1994). When r3 and r5 are grafted to an ectopic site or isolated in an explant culture, both Bmp-4 and msx-2 are down-regulated and the cell death program is halted (Graham et al., 1994). These results not only support the hypothesis that neural crest is eliminated in these rhombomeres but also that neighbouring rhombomeres are by no means isolated blocks of cells but interact with each other (Graham and Lumsden, 1996). On the other hand, it has been shown that spreading of the neural crest progenitor region occurs along the rostro-caudal axis allowing cells from r3 and r5 to migrate to r2, r4 and r6 (Birgbauer et al., 1995). This suggests that a significant number of crest cells are removed from r3 and r5 by apoptosis and that those cells that survive elimination are recruited by adjacent rhombomeres. Neural crest fate mapping has revealed that cells from r3 and r5 contribute, in an albeit small manner, to the formation of the head skeleton. Most of them are restricted to skeletal and muscle connective tissue of the hyoid arch which derives from the 4^{th} rhombomere (Köntges and Lumsden, 1996).

The exact mechanisms that lead to segmentation of the neural crest in the hindbrain region are still unknown. A mesoderm-controlled mechanism as seen in the trunk region is unlikely since there is no obvious segmental pattern of mesoderm in the head region. A combination of guidance cues

from the ectoderm and inside the hindbrain neuroepithelium might be a plausible scenario (Lumsden et al., 1991, Löfberg et al., 1985).

1.1.2.4. Development of cranial motoneurons

Motoneurons are initially generated from a strip of neuroepithelium latero-adjacent to the floor plate (Van Straaten et al., 1985; Yamada et al., 1991). Postmitotic motoneurons form a continuous medial column in the mantle layer, extending the whole length of lower midbrain, hindbrain and spinal cord. Here they begin to grow axons and dendritic processes, and at the same time start migrating towards their final destinations (Simon et al., 1994). Different types of motoneurons take different migratory paths. In the spinal cord, the lateral somatic motoneurons move into the lateral part of the ventral horns, segregated from the medial somatic motoneurons (Heaton, 1977). The viscero-motoneurons of the spinal cord assume a dorsomedial position to form the Column of Terni (Levi-Montalcini, 1950). In the brainstem, 3 different classes of motoneurons are defined (see above): Somatic motoneurons maintain their medial position whereas branchio- and viscero-motoneurons migrate dorso-laterally. The axons of somatomotoneurons leave the neuroepithelium via ventral exit points, and the branchio- and visceromotoneurons exit laterally. In addition, a small, specialized group of vestibulo-acoustic efferent neurons has been described (Meredith, 1988; Simon and Lumsden, 1993). A minute number of motoneurons in every motor nucleus originates from the contralateral side and migrates across the midline floor plate (Tan and Le Douarin, 1991).

Most cranial motor nuclei originate in two consecutive rhombomeres. The branchiomotoneurons of nerves V, VII, and IX emerge from the rhombomere pairs r2/3, r4/5, and r6/7 respectively, with neurons in the even-numbered rhombomeres developing slightly ahead of those in odd-numbered rhombomeres (Lumsden and Keynes, 1989). The nucleus of the abducens nerve however, is one segment out of register; its neurons lie in r5and r6 in the chick and in r5 exclusively in rodents (Gilland and Baker, 1993). The segmental pattern of hindbrain development becomes very apparent in the three branchiomotor nerves: Emerging from paired rhombomeres, their exit points lie in the centres of the most rostral of the two segments (Lumsden and Keynes, 1989). The three nerves supply derivates of the first three branchial arches, whereby each rhombomere pair corresponds to a single arch. A similar pattern can be found in the migratory behaviour of neural crest cells (see above).

The first branchiomotor axons emerge from neurons in the even-numbered rhombomeres which they cross transversely, converging towards their lateral exit points. Axon pathfinding in odd-numbered rhombomeres is less straight forward: Retrograde labelling of early motoneurons through their exit points shows a somewhat stereotyped pathway of motor axons emerging from odd-numbered rhombomeres. After an initial transverse trajectory, they turn to cross the cranial adjacent boundary and head for the exit point. However, SC1 staining (see below) of outgrowing axons at earlier stages, before they have reached their exit points, reveals a less "confident " pattern of axonal pathfinding. Axons emerging from cells located in the most

rostral part of the rhombomere seem to follow a more or less straight course along the boundary before finally crossing the border and turning towards their exit point. Axons emerging further caudally can be seen meandering throughout the segment, a good portion of them even turning caudally before finally arcing back towards the rostro-adjacent rhombomere (Guthrie and Lumsden, 1992). A small minority of axons can be found crossing the caudal boundary and leaving the marginal layer through an inappropriate exit point.

The mechanism by which cranial motor axons are guided to their specific exit points is still not entirely understood. Essentially, two hypotheses can be proposed: a) axonal trajectories may be determined by polarity cues in the neuroepithelium, and b) axon guidance may depend on specific target-derived attractants. Rhombomere reversal experiments by which a single rhombomere was transplanted to the opposite side of the neuraxis, so that its rostro-caudal orientation was reversed, have shown that the majority of axons still found their appropriate exit point (Guthrie and Lumsden, 1992). Nevertheless, a substantial number of facial motor axons grew towards the wrong (caudal) exit point in r5 reversals. Interestingly, the proportion of trigeminal motor axons heading for the inappropriate exit point in r3 reversals was significantly smaller (only 10%) than in r5 reversals, suggesting a more specific affinity of trigeminus axons for their exit point than is the case with facial axons. Therefore, a combination of local and distributed cues might be involved in determining axon trajectories inside the rhombomeres.

There is strong evidence that the cells of the trigeminal sensory ganglion are involved in the early pathfinding of trigeminal motor axons. Ablation of the trigeminal ganglion anlage prevents the trigeminal motor root from exiting the brainstem. Furthermore, the motoneurons do not migrate laterally to form the trigeminal motor nucleus but maintain their medial postmitotic position (Moody and Heaton, 1983a). The trigeminal ganglion derives from two different anlagen: the epibranchial ectodermal placodes and the cranial neural crest. Sensory trigeminus neurons send their axons into the metencephalon shortly before motor axons begin to sprout (Windle, 1933; Windle and Fitzgerald, 1942, Heaton and Moody, 1980). Removal of the neural crest anlage of the trigeminus ganglion leads to a 2 day delay of ingrowth of sensory axons and subsequently to delayed migration of motoneurons. This suggests that the penetration of sensory axons rather than the mere presence of ganglion cell bodies is a prerequisite for the formation of the lateral trigeminal motor nucleus (Moody and Heaton, 1983b).

Guidance of cranial motor axons in the periphery is in accordance with the overall segmental pattern of the developing head. The highly segmental, segregated migratory streams of neural crest cells into the branchial arches(see above) might provide positional cues guiding motor axons outside the mesencephalon (Lumsden and Krumlauf, 1996). Although detailed studies on the complete set of cranial motor nerves are not available, research done on the trigeminal and facial nerves provides valuable insights into peripheral pathfinding of cranial motoneurons.

Trigeminal motor axons enter the trigeminal sensory ganglion and grow along the sensory fibres of the mandibular branch towards the muscle plate of the first branchial arch. In r3 reversal experiments a small amount of trigeminal axons exits via the inappropriate exit point of the facial nerve (see above). In the periphery, these aberrant fibres grow along the pathway taken by the branchiomotor portion of the facial nerve but never join the facial visceromotor axons (Warrilow and Guthrie, 1999). This indicates that different sets of guidance cues might exist for branchiomotor and visceromotoneurons, but not necessarily for different branchiomotor subpopulations. Although the trigeminal axons seem to be able to recognize guidance cues for the branchiomotor fibres of the facial nerve and subsequently innervate muscles of the second arch, studies of r3 reversed embryos at later stages show a reduction of aberrant trigeminal fibres in the second arch. Thus, misprojecting trigeminal axons might subsequently be eliminated. Furthermore, the study by Warrilow and Guthrie also showed that r3-derived axons only project to specific muscles both in the appropriate first and inappropriate second branchial arch. The authors point out that their findings are consistent with the fact that r2 and r3 motoneurons are located in the rostral and caudal half of the trigeminus motor nucleus (Marín and Puelles, 1995). Those muscles in the first branchial arch that were innervated by r3 motoneurons in the reversal studies normally receive input only from the most caudal portion of the trigeminus motor nucleus (Wild and Zeigler, 1980). It is tempting to propose a mechanism of programmed cell death by which the lack of specific neurotrophic factors for trigeminus motoneurons

(or motoneuron subpopulations) in inappropriate muscle targets is responsible for the elimination of those neurons. However, although a large array of factors is known to prevent physiological cell death in motoneurons, detailed studies of differential neurotrophic substances acting on different cranial motoneuron populations have still to be undertaken. The mechanism of cell death in motoneurons and its prevention by neurotrophic factors is subject of a later chapter.

In contrast to the trigeminal nerve, the facial nerve contains two different population of motoneuron axons. The branchiomotor axons, originating from the facial nucleus supply muscles derived from the second branchial arch. The second component is made up from visceromotor fibres emerging from the superior salivatory nucleus. In adult humans these axons together with afferent taste fibres form the intermediate nerve. Both components of the facial nerve leave the embryonic hindbrain via the exit point in r4 and project along a common pathway towards the geniculate ganglion. Here the two axon populations segregate to follow different trajectories: the branchiomotor axons turn caudally to grow towards the muscle plate of the second branchial arch via the hyoid nerve, whereas the visceromotor processes arc rostrally towards the sphenopalatine (pterygopalatine) ganglion. Cell bodies of the latter component are restricted to the 5th rhombomere whereas branchiomotoneurons are present in r4 as well as r5. However, only a minority of r5 branchiomotoneurons are intrinsic to that rhombomere, most of them having migrated from r4 to this more caudal position after the disappearance of rhombomere boundaries (Jacob

and Guthrie, 2000). It is worth mentioning that the extent of migration of r4-derived facial neurons varies between species: in rodents as well as in humans, these neurons migrate as far as r6 thereby forming a loop around the abducens nucleus, the so-called internal genu of the facial nerve. This loop is missing in chicks where the cell bodies assume their final position at the level of r5 lateral to the abducens nucleus.

The branchiomotoneurons of the facial nerve differ from those of the trigeminus nerve in respect to their pathfinding abilities after transplantation. Whereas caudally-transplanted r3 trigeminus neurons grow axons into the inappropriate second branchial arch, facial axons show a remarkable homing behaviour. Transposition of r5 into r3 position gives rise to two different pathways: ectopic facial axons either leave the hindbrain via the trigeminus exit point in r2 or course caudally in the neuroepithelium to exit in r4. In both cases, the axons home in on their appropriate intermediate target, the geniculate ganglion, once having exited the hindbrain (Jacob and Guthrie, 2000).

In summary, a variety of factors seem to be involved in peripheral axonal guidance of cranial motoneurons. Firstly, motor axons project into territories partially derived from neural crest cells of the same axial level. Secondly, target-derived factors can act as chemoattractive guidance cues. Caton and colleagues have shown that Hepatocyte Growth Factor which is produced in branchial arches to exert chemoattractive and growth-promoting influences on cranial motoneurons (Caton et al., 2000). Thirdly, for visceral

motoneurons, target ganglia seem to play an important role in pathfinding. The lack of the sphenopalatine ganglion in Phox2a mutant mice leads to disruption of the pathway of facial visceromotoneurons and the formation of an ectopic branch linking the geniculate ganglion with the otic ganglion, a target for visceromotoneurons of the glossopharyngeal nerve (Jacob et al., 2000).

1.1.2.5. The SC1 Antigen

Part of this work involved the study of chick hypoglossal motoneurons *in vitro*. To purify hypoglossal neurons advantage was taken of the fact that chick motoneurons transiently express the SC1 antigen during early development. This sub-chapter gives a brief overview of the antigen's properties, expression pattern during development and presumed function.

SC1 is a member of the immunoglobulin superfamily of cell adhesion molecules. It was first described by Tanaka and Obata in 1984. However, two more groups have subsequently identified and named the protein independently. The antigen is therefore also referred to as BEN or DM-GRASP in the literature. Here, the antigen will be referred to by the name it was first given by Tanaka and Obata: SC1.

SC1 is a glycoprotein that is expressed on the cell surfaces and processes of various neuronal and non-neuronal tissues. During the early development of the nervous system the protein is transiently expressed by motoneurons, floor plate cells, neurons of the dorsal root ganglia, and

sympathetic ganglion cells. However, the time course of its expression is dependent on the cell type. SC1 first appears on cells of the notochord between HH 11 and HH 15. By the time expression is strongest in the notochord (HH16/17), the first newborn motoneurons start expressing the protein. (Tanaka et al., 1984). Spinal motoneurons show the strongest expression of the SC1 antigen during stages 19 to 24. After that expression decreases, and by HH 32 hardly any SC1 can be detected on those neurons. At the time the protein starts to disappear from the cell bodies of spinal motoneurons, SC1 mRNA can be detected in ventral and dorsal muscle masses of the forelimb (Fournier-Thibault et al., 1999). Later in development SC1 expression can be detected in various other structures of the central nervous system, such as the inferior olivary nucleus and parts of the cerebellum (Pourquié et al., 1992). Interneurons never express SC1 (Pourquié et al., 1990).

Since SC1 is expressed on neuronal somata as well as their processes, and due to its homophilic (Tanaka et al., 1991) as well as heterophilic properties, notably with Ng-CAM (DeBernardo et al., 1996), the protein has been implied in several functions, namely: maintenance of structural integrity of neuronal clusters, path finding and fasciculation as well as axon-target interaction. Tanaka and colleagues have pointed out that SC1 is most strongly expressed on motoneurons very early in their development, shortly after their differentiation and until their axons have reached the target muscles. During that time motoneurons in the lateral motor column are very tightly packed, whereas with the disappearance of the SC1 signal around E7

(HH 31), cells become more loosely distributed. In accordance with that the group also observed SC1 expression in the peripheral nervous system at the time of ganglion formation. Pourquié and colleagues have stressed the co-expression of SC1 on axons of the peripheral as well as the central nervous system at a time when fasciculation takes place. Furthermore, the antigen's disappearance from these cells corresponds with the onset of glial cell proliferation in the dorsal root ganglia and the spinal cord. It also coincides with the beginning of ensheathment of axons by Schwann cells which disrupts the once established close axon-axon contacts (Pourquié et al., 1990).

At E7, SC1 has mainly disappeared from the somata and axons of spinal motoneurons and its expression is restricted to their intramuscular nerve terminals. Fournier-Thibault and colleagues have been able to show co-localisation of this restricted expression pattern with acetyl cholinesterase clusters. They also showed that in nerve-contacted myotubes the SC1 protein has disappeared from the muscle fibre and is restricted to the synaptic site. At the same time it is still expressed in non-innervated muscle cells (Fournier-Thibault et al., 1999). SC1 might therefore be involved in target recognition as well.

In accordance with events observed in the spinal cord, SC1 is also expressed by motoneurons of the brainstem. SC1 whole mount staining reveals immunostaining of the motoneuron column adjacent to the floor plate at HH 20 (Simon et al., 1994). SC1 expression can be found on all somato-,

branchio-, and viscero-motoneurons shortly after differentiation has taken place (Guthrie and Lumsden, 1992, Chang et al.,1992). Nevertheless, the antigen is down-regulated on cells of the branchiomotor and visceromotor subpopulation as soon as they start migrating laterally from the motor column (see above). As is the case with spinal motoneurons, the disappearance of the antigen is not an all-or-none event but a gradual process taking place while axons grow towards their muscle targets. Nevertheless, somatomotoneurons which do not migrate from their original position of differentiation continue to express the antigen. Whether they lose the antigen at a later stage in development has not yet been established. The transient expression of SC1 in the intact hindbrain motor column and its subsequent down-regulation by neurons migrating away from that column adds evidence to the hypothesis that the protein is important in the maintenance of temporarily created formation of like cells. However, it has yet to be shown whether SC1 down-regulation is an absolute requirement for migration or a consequence of this process (Simon et al., 1994).

1.1.3. Genetic control of brainstem development

1.1.3.1. Hox genes and hindbrain patterning

As has been shown in the preceding paragraphs, a significant amount of anatomical, cellular, and molecular evidence has been mounted during the last decade suggesting that the vertebrate brainstem develops in a truly segmental pattern. This makes it somewhat different to the spinal cord where the segmental arrangement of nerve roots is extrinsically regulated by

mesenchyme originating from paraxial mesoderm. Since ectodermal segmentation is a characteristic feature in many non-vertebrates like arthropods, one might assume that the spinal cord was originally segmented in a common ancestor but segmentation was lost during phylogeny in vertebrates (Krumlauf et al., 1993). Furthermore, in the head a majority of mesenchymal components does not originate from mesoderm. Instead, these structures derive from the cranial neural crest which is ectodermal in origin (see above). Rhombomeric segmentation may be crucial in patterning the cranial neural crest (see above, Krumlauf et al., 1993).

How is this segmentation genetically controlled? Segmentation has been extensively studied in Drosphila, and a plethora of genes has been identified that are involved in the early patterning of the fly embryo. One group of genes that plays a major role in establishing the body plan is the so-called homeotic gene complex (Hom-C; Lewis, 1978, Gehring 1986, Akam, 1987). Most of these genes are clustered on chromosome 3 in *Drosophila* in two complexes: the Antennapedia complex, which is responsible for specification of the head and the first two thoracic segments and the Bithorax complex which controls specification of the third thoracic and all abdominal segments. The striking feature of these genes is that their linear arrangement on the chromosome corresponds to their domains of expression and function in the embryo. That is, genes that are located more downstream (towards the 5' end of the DNA are expressed in more posterior parts of the embryo and vice versa (Lewis, 1978). The most 3' gene, *labial,* is required to generate the most anterior structures in the head whereas the most 5' gene, *Abd-B*,

specifies the development of the posterior abdomen. Their HOM-C gene products belong to a group of proteins called homeodomain proteins which are characterised by a 60 amino acid domain that binds DNA. The corresponding 180 base-pairs in the respective genes containing the code for these domains are commonly referred to as the homeobox. Homeotic genes act at a late stage in a genetic cascade that is initiated by maternal effector genes originating from the fly's ovaries and that controls segmentation of the embryo so that at the end of the cellular blastoderm stage each segment primordium has been given its individual identity (Tab.1.1.2; Levine and Harding, 1989, Wilkinson and Krumlauf, 1990).

The vertebrate homologues of the HOM-C homeotic genes are the Hox genes (Duboule and Dolle, 1989) which are predominantly expressed in the developing nervous system (Gaunt, 1988 and 1991, Graham et al., 1988 and 1991, Holland and Hogan, 1988). However, vertebrate genomes contain four copies of the homeotic set of genes found in *Drosophila* (Boncinelli et al., 1988; McGinnis and Krumlauf, 1992, Scott, 1992). The way these genes are ordered on the respective chromosomes is remarkably similar to *Drosophila*. So is their pattern of expression: those vertebrate genes homologous to *lab* in *Drosophila* are located at the most 3' end of the cluster and expressed most anteriorly in the embryo. According to the new nomenclature the Hox genes in each cluster are numbered from 1 to 13 whereby genes that are referred to by the same number show highest sequence homology and are called paralogous (e.g. Hoxa-1, Hoxb-1, Hoxc-1, Hoxd-1; see Tab. 1.1.3). Nevertheless, no cluster contains a full set of all 13 genes. It has been

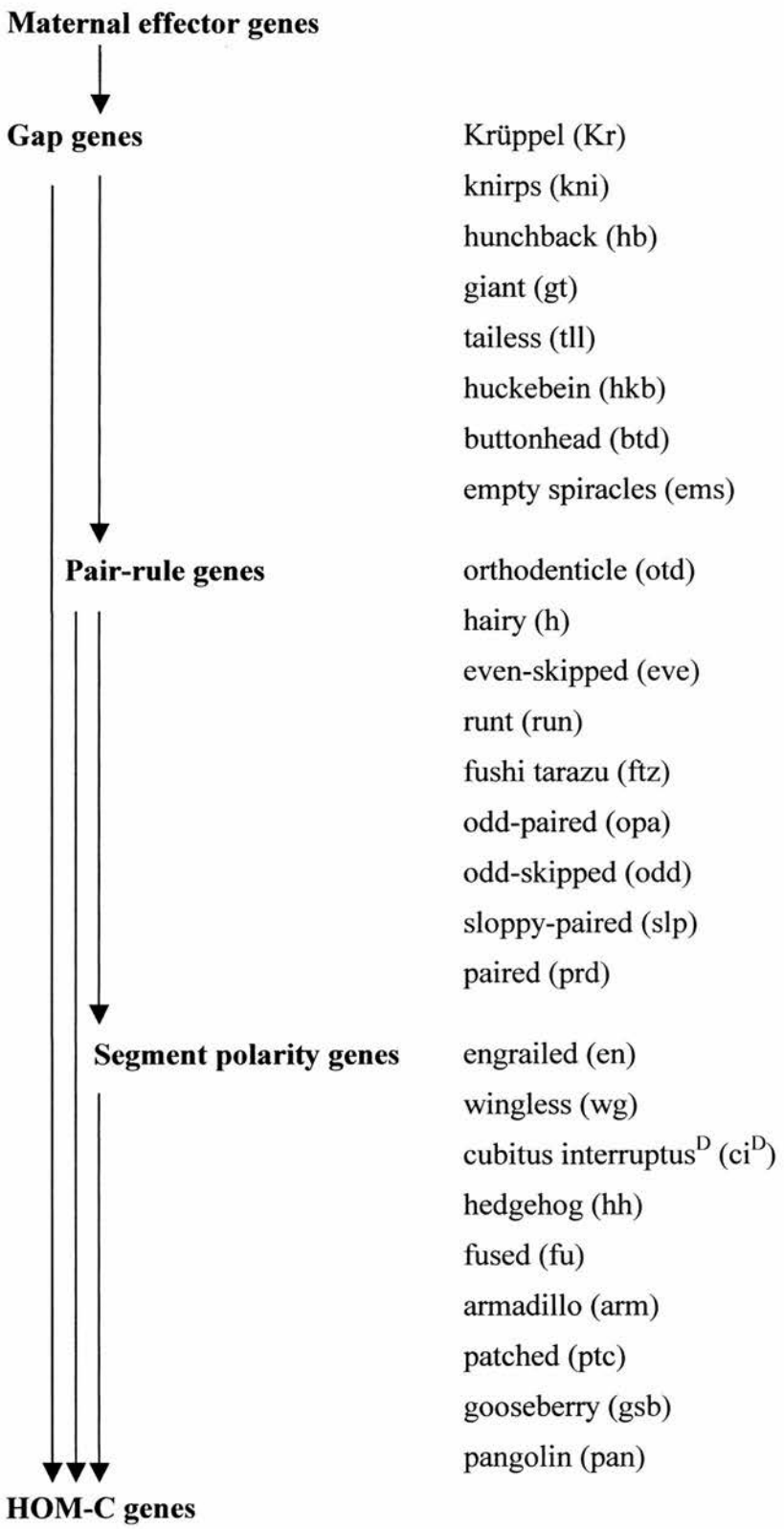

Tab. 1.1.2: Genes controlling the antero-posterior patterning in Drosophila; interaction of proteins of the gap, pair-rule, and segment polarity genes regulate expression of the homeotic genes (HOM-C complex; modified after Gilbert, 1997)

Drosophila (HOM-C)	ANT-C lab	pb		Dfd	Scr	Antp	BX-C Ubx	Abd-A	Abd-B				
Hox-a Hox-1 (6)	**a1** 1.6	**a2** 1.11	**a3** 1.5	**a4** 1.4	**a5** 1.3	**a6** 1.3	**a7** 1.1		**a9** 1.7	**a10** 1.8	**a11** 1.9		**a13** 1.10
Hox-b Hox 2 (11)	**b1** 2.9	**b2** 2.8	**b3** 2.7	**b4** 2.6	**b5** 2.1	**b6** 2.2	**b7** 2.3	**b8** 2.4	**b9** 2.5				
Hox-c Hox-3 (15)				**c4** 3.5	**c5** 3.4	**c6** 3.3		**c8** 3.1	**c9** 3.2	**c10** 3.6	**c11** 3.7	**c12**	**c13**
Hox-d Hox-4 (2)	**d1** 4.9		**d3** 4.1	**d4** 4.2				**d8** 4.3	**d9** 4.4	**d10** 4.5	**d11** 4.6	**d12** 4.7	**d13** 4.8
Paralogous groups	**1**	**2**	**3**	**4**	**5**	**6**	**7**	**8**	**9**	**10**	**11**	**12**	**13**
	3' hindbrain												trunk 5'

Tab 1.1.3: Alignment of *Drosophila* HOM-C and vertebrate Hox complexes. Genes grouped in columns are paralogous, that is, they show high sequence analogy and have evolved by duplication and divergence. The new Hox nomenclature is highlighted in bold print and the old nomenclature given underneath. The numbers in brackets in the old nomenclature indicate the murine chromosome the respective Hox complex is located on. The bottom row indicates the expression of the vertebrate paralogous groups in the hindbrain and in the trunk and their arrangement between the 3' and 5' ends. ANT-C, Antennapedia complex; BX-C, Bithorax complex. (Modified after Krumlauf et al, 1993)

proposed that the four vertebrate Hox clusters have evolved by duplication and divergence from a common ancestor (Boncinelli et al., 1989; Duboule and Dolle, 1989; Graham et al., 1989). Some Hox genes are so similar to their counterparts in *Drosophila* that they can substitute for one another. For instance, when the murine Hoxb-6 gene is transfected into *Drosophila* it can perform the regulatory functions of the fly's Antennapedia gene (Malicki et al., 1990).

In the central nervous system Hox genes are expressed from the most posterior portion to sharp anterior borders which map precisely to rhombomere boundaries (Murphy et al., 1989; Wilkinson et al., 1989; Hunt et al., 1991a, 1991b, Prince and Lumsden, 1994). Paralogous groups 1-4 are expressed in the hindbrain and expression of groups 5-13 is confined to the spinal cord (Tab. 1.1.3). Generally, members of the same paralogous group share the same anterior boundaries (Fig. 1.1.3). However, Hoxc-4 expression is one rhombomere short compared to the other genes in its group, and Hoxa-2 and Hoxb-2 are also shifted by one rhombomere (Krumlauf et al., 1993). With the exception of Hoxa-1 and Hoxb-1, the anterior expression limits of individual genes correspond with their relative chromosomal position, e.g., Hox b2 which lies closer to the 3' end than Hoxb-3 is expressed up to the r2/r3 boundary whereas Hoxb-3 expression terminates at the r4/r5 boundary. Moreover, the expression limits display a two-segment periodicity between paralogous groups (Fig. 1.1.3; Wilkinson et al., 1989). A similar pattern seems to exist within the trunk where Hox gene expression patterns correspond to somite boundaries (Kessel and Gruss, 1991).

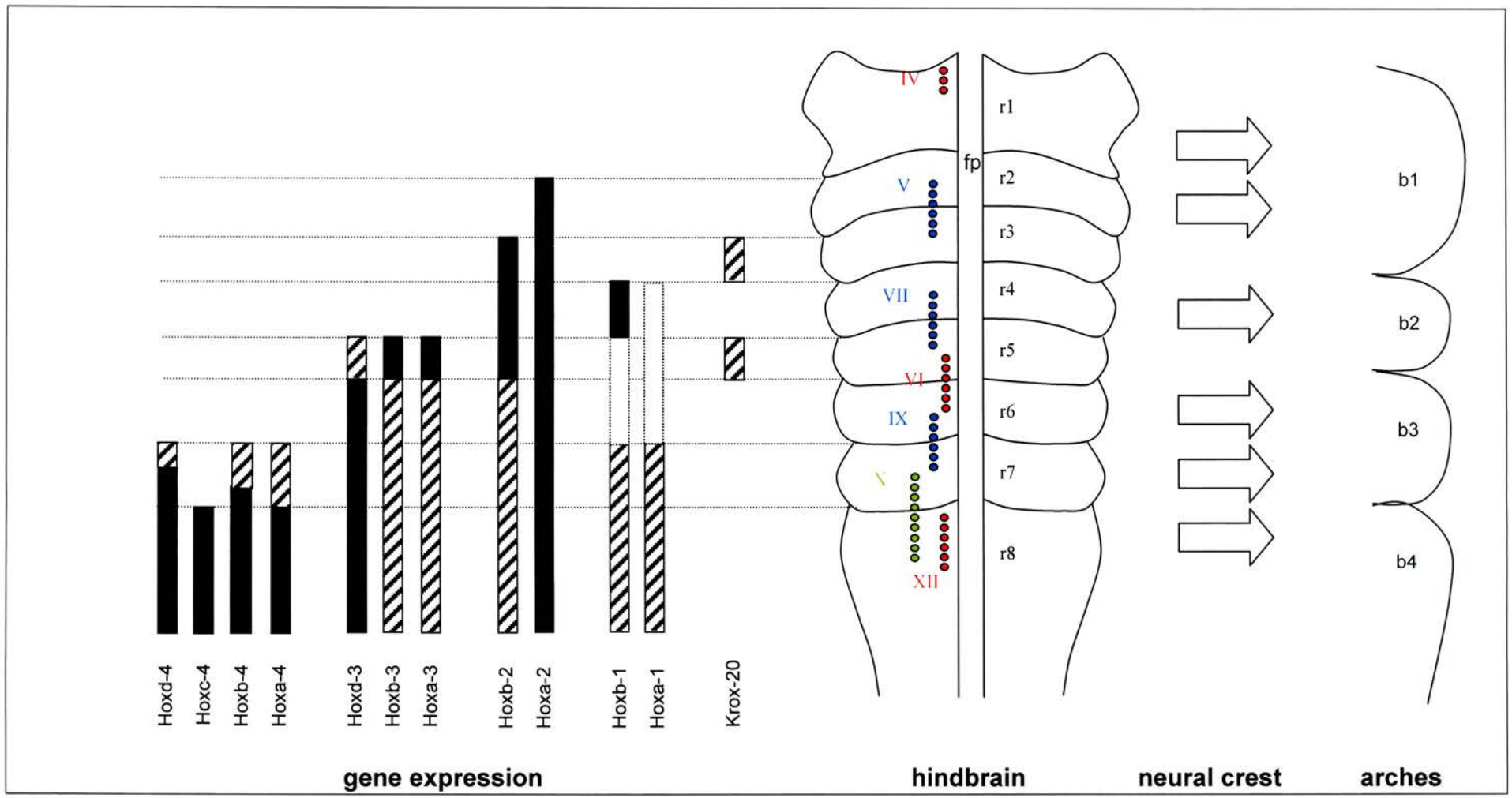

Fig. 1.1.3: Hox and Krox gene expression, position of motor nuclei, and origin of migrating neural crest cells in the developing hindbrain. Filled columns: strong gene expression; striped columns: medium expression; empty columns: weak expression. r1-r8: rhombomeres 1-8. b1-b4: branchial arches 1-4. fp: floorplate (adapted from Lumsden and Keynes, 1989; and Krumlauf et al., 1993)

Hox expression domains are established shortly before morphological segmentation of the hindbrain becomes visible and are maintained up to later stages of hindbrain development. However, Hoxa-1 is downregulated before the formation of boundaries (Krumlauf et al., 1993; Wingate and Lumsden, 1996). When hindbrain neuroepithelium is transplanted to more posterior regions at early neural plate stages, the graft expresses Hox genes and displays morphological features that are consistent with the new location (Grapin-Botton et al., 1995, 1997; Itasaki et al., 1996). However, if transplantation is performed at a later stage, i.e. shortly before or around the time of rhombomere formation, segmental identities and Hox expression of the graft are maintained (Guthrie et al., 1992; Kuratani and Eichele, 1993; Simon et al., 1995)

A number of knockout experiments have been conducted in recent years that have revealed a likely role of Hox genes in segmentation and specification of the hindbrain. For example, a null mutation of Hoxa-2 which is the only Hox gene expressed in r2 (Krumlauf et al., 1993, Prince and Lumsden, 1994) and co-expressed with Hoxb-2 in r3 (Krumlauf et al., 1993) results in a number of defects. The r1/r2 boundary is missing and the r2/r3 boundary only partially formed (Gavalas et al., 1997). Molecular identities of the region are significantly changed: the expression of Sek-1, an Eph receptor tyrosine kinase (RTK) involved in cell-cell recognition is abolished in r2. On the other hand, the expression of Engrailed-2 (En-2), a gene that plays a role in cerebellar development (Millen et al., 1994) and that is normally expressed in the mid-hindbrain region including r1 (Davis and

Joyner, 1988), is extended caudally. The same is true for the homeobox gene Sax-1, whose r1 expression in wild types (Schubert et al., 1995) is extended to at least r2 and possibly r3 (Gavalas et al. 1997). This suggests a switch in molecular identity from r2 to r1. Motor axon pathfinding is also affected in the Hoxa-2 mutants. Although an r2 root exit point is established, all axons from the r3 region and some from the r2 region are guided towards the second branchial arch via the caudal exit point of the facial nerve in r4. The second branchial arch itself shows homeotic transformation of its neural crest-derived skeletal elements (Gendron-Maguire et al., 1993; Rijli et al., 1993). Whereas Hoxa-1 mutants show segmentation and specification defects, this is not true for all Hox null mutations. Hoxb-1 mutants for example fail to form a facial motor nucleus but seem to establish a normal segmentation pattern (Goddard et al., 1996). The same is true for Hoxb2 mutants (Barrow and Capecchi, 1996).

Summarising these findings, one might postulate the following hypothesis: during the early neural plate stages a complex pattern of Hox gene expression is established along the antero-posterior axis which after a short period of plasticity, is maintained throughout further cell divisions of neuronal precursor cells. The role of the Hox genes in the hindbrain could then be twofold: firstly, they divide the neural tube into compartments (rhombomeres) by restricting proliferating neuronal precursors and their progeny to discrete cell blocks. This might be achieved by the means of segment-specific cell adhesion molecules. Secondly, they control cell

differentiation by laying out segment-specific developmental pathways (Rijli, et al., 1998).

1.1.3.2. The role of retinoic acid in Hox gene regulation

In *Drosophila*, the expression of HOM-C genes is regulated by other genes that lie upstream in a segmentation controlling cascade of genes initiated by maternal effector genes (see above). Yet, only little is known about the regulation of Hox gene expression in vertebrates. Nevertheless, there is strong evidence that retinoic acid plays a key-role in the regulation of at least some Hox genes: Retinoic acid (RA) exists in two isomeric forms, the all-trans and the 9-cis form, and exerts its effects by activating transcription factors of the steroid receptor superfamily (Leid et al., 1992). These receptors, once activated bind to specific DNA regions called retinoic acid response elements (RAREs). Some of these response elements have been found in 3 Hox genes, Hoxa-1, Hoxb-1, and Hoxd-4 (Langston et al., 1992; Pöpperl and Featherstone, 1993, Marshall et al, 1994; Ogura and Evans, 1995a,b). According to a model proposed by Nieuwkoop and colleagues in 1952, tissue interactions occurring during gastrulation establish an anterior or forebrain fate in the early embryo. In a second step, the posterior cells are activated by certain agents to generate posterior structures like the hindbrain and spinal cord (posterior transformation; Nieuwkoop et al., 1952). Indeed, in the mouse the Otx2 gene (a homolog of the head-specific orthodenticle homeobox gene in *Drosophila*) is expressed throughout the whole embryo during gastrulation but is maintained only in the anterior regions that give rise to fore- and midbrain (Simeone et al., 1992; Boncinelli et al., 1993; Ang

et al., 1994). In the posterior parts its expression is switched off with the onset of Hoxa-1 and Hoxb-1 expression (Frohman et al., 1990; Murphy and Hill, 1991; Ang et al., 1994; Zhang et al., 1994). Treatment with retinoic acid does not only lead to an increased hindbrain compensated by a reduction in forebrain size in Xenopus (Durston et al., 1989), it also represses Otx2 and induces Hoxa-1 and Hoxb-1 expression. Retinoic acid is first synthesized in Hensen's node (*the node* in mice, *the primitive* node in humans; Hogan et al., 1992; Chen et al., 1992., Creech Kraft et al, 1994) and later in the notochord and the floor plate (Wagner et al., 1990, 1992), both of which are derivatives of Henson's node. Diffusion of retinoic acid from these structures could activate transcription of RA-responsive Hox genes and repression of Otx2 in the hindbrain and spinal cord, thereby generating two primary boundaries: a) the border between midbrain and hindbrain marked by the most posterior expression of Otx2 and b) the border between anterior and posterior hindbrain marked by the most anterior expression of the Hox 1 group (Conlon, 1995).

It seems worth mentioning the known teratogenic effects of retinoic acid in this context. Retinoic acid has been used for the treatment of severe acne for the last two decades (Retin-A® and Isotretinoin® in the UK). Since administration of large amounts of Vitamin A to pregnant animals leads to a number of malformations (Cohlan, 1953; Giroud and Martinet, 1959; Kochhar et al., 1984), the drug is labelled as teratogenic and must not be given during pregnancy. However, due to the significant overlap between the population dependent on acne medication and the population of woman of

childbearing age a number of pregnant woman have (inadvertently) overexposed their unborn children to Vitamin A. A study performed by Lammer and colleagues has shown that out of 56 foetuses who fell into this group, 12 aborted spontaneously and 21 were born with a range of anomalies, including absent or defected ears, absent or small jaws, cleft palate, and anomalies of the central nervous system (Lammer et al., 1985)

1.1.3.3. The role of Krox-20 in Hox gene regulation

Another homeobox gene implicated in hindbrain segmentation is Krox-20 (Gilardi et al., 1991). It was isolated in 1988 from a murine fibroblast cDNA library. The name is derived from its *Drosophila* relative, a zinc finger gene called Krüppel (Chavrier et al., 1988a/b). A zinc finger is a DNA binding domain featured by certain transcription factors. The amino acid chain forms a finger-like loop which is stabilised by a central zinc atom that binds two cysteine residues on one side of the loop and two histidine residues on the other side. The human homologue of Krox-20, early growth response gene (egr-2), which was isolated simultaneously, shares a 100% sequence identity in the zinc fingers and a 85% identity in the remaining region with the murine Krox-20 (Joseph et al., 1988, Chavrier et al., 1988). In the hindbrain, Krox-20 is first expressed in a small transverse stripe of tissue at day 8 and in a slightly more posterior, non-adjacent stripe at day 8.5, shortly before segmentation becomes visible (Wilkinson et al., 1989b; Wilkinson and Krumlauf, 1990). By day 9.5, these strips coincide with rhombomeres 3 and 5 (Fig. 1.2.3). It has been shown that Krox-20 directly activates the expression of Hoxa-2 (Nonchev et al., 1996) and Hoxb-2 (Sham

et al., 1993) in rhombomeres 3 and 5, suggesting that – like its *Drosophila* relative, Krüppel – it functions upstream of the Hox genes in the genetic cascade that regulates the patterning of the antero-posterior axis (see above).

Nevertheless, it has yet to be established how the expression of Krox-20 in r3 and r5 is regulated. An interesting insight is offered by a study by Graham and Lumsden: transplantation of r3 into the (depleted) r4 site of another embryo led to down-regulation of Krox-20 not only in the grafted but also in the neighbouring host r3. Culture explants of r3, freed from adhering tissue delivered the same result. On the other hand, r5 transposition or explantation did not affect Krox-20 expression (Graham and Lumsden, 1996). This suggests that Krox-20 expression in r3 is dependent on influences from r4 whereas expression of the gene in r5 seems to be regulated intrinsically. Furthermore, it shows that rhombomeres are not fully autonomous as for instance the maintenance of Hox gene expression after ectopic transposition might suggest. Instead, there seems to be certain degree of interdependence between them.

Krox-20 null mutant mice die at birth and show significant defects in hindbrain development (Schneider-Manoury et al., 1993, Swiatek and Gridley, 1993). Although the regions destined to become rhombomeres 3 and 5 form normally at early stages in these embryos, they are not maintained and disappear completely, leaving segmentation in the rest of the hindbrain unaffected (Schneider- Manoury et al., 1997). Interestingly, although the deletion of r3 and r5 inevitably leads to the approximation of even-numbered

rhombomeres and cells originating in rhombomeres of the same identity can mix freely (see above; Guthrie and Lumsden, 1991; Guthrie et al, 1993), Schneider-Manoury and colleagues did not observe defects of boundary formation between these rhombomeres, at least not in the ventral half of the region. Also, the motor nucleus of the trigeminus nerve was reduced in size at 10.5 days post coitum (dpc), consistent with a loss of the branchiomotoneurons from r3. Peripheral pathfinding of the remaining trigeminus motoneurons was disturbed. Although their axons exited the neuroepithelium via the appropriate exit point in r2, they then fasciculated with axons of the facial nerve and terminated in the second rather than the first branchial arch. Observations at later developmental stages revealed that all of these misrouted trigeminal motoneurons died around 17.5 dpc which is within the period of naturally-occurring cell death in murine motoneurons (Lance Jones, 1982). These findings are mirrored by similar observations made by Warrilow and Guthrie in r3 reversals (see above; Warrilow and Guthrie, 1999) and could be explained by a lack of specific growth factors for trigeminus motoneurons in the second branchial arch. The abducens nucleus which in the mouse derives solely from r5 (Gilland and Baker, 1993), was missing completely. So were the visceromotoneurons of the facial nerve. However, the facial nucleus which contains the branchiomotor contingent of the facial nerve appeared normal in size and morphology. The authors speculate that a significant part of r5 branchiomotoneurons is generated in r4 and migrate caudally into r6. This is consistent with the fact that these neurons express the r4 marker Hoxb-1 (Marshall et al., 1992) and

with more recent findings of Jacob and Guthrie that the genu of the facial nerve in rodents and humans is produced by caudally-migrating neurons from r4 (see above; Jacob and Guthrie, 2000). In the absence of r5, these neurons might migrate completely into r6. The remaining motoneurons which are normally generated in r5 might have been substituted by r6 branchiomotoneurons who due to the proximity of the r4 exit point in the mutants would have wrongly joined the facial nerve rather than taking the appropriate route with the glossopharyngeal nerve.

1.1.3.4. LIM homeobox genes and motoneuron development

As has been outlined above, different subpopulations of brainstem (and spinal) motoneurons are generated during early development. These subpopulations are defined by phenotype, position, and target. The selection of specific axonal pathways by motoneuron subpopulations is dependent on local guidance cues inside the neural tube as well as in the periphery (see above; Tosney, 1991; Guthrie and Lumsden, 1992; Landmesser, 1992; Eisen, 1994; Lumsden and Krumlauf; 1996; Warrilow and Guthrie, 1999). Different motoneuron subpopulations respond to different cues. For example, spinal motoneurons innervating axial muscles seem to be guided by cues provided from within their target dermomyotome (Tosney, 1987, 1988) whereas limb-innervating motoneurons ignore the dermomyotomes and respond to cues from cells of the limb mesenchyme (Lance-Jones and Landmesser, 1980a, 1980b, 1981a, 1981b; Ferguson 1983, Tosney and Landmesser 1984). It is therefore plausible to suggest that selective responsiveness to guidance cues is dependent on intrinsic differences within the motoneuron population

(Tsuschida et al; 1994). Over the past decade, it has become increasingly evident that a group of homeobox genes is involved in determining motoneuron identity, the LIM gene family (Ericson et al, 1992; Yamada et al, 1993; Tsuschida et al., 1994; Lumsden, 1995). Members of this gene family encode transcription factors that have two features in common: a) a DNA-binding homeodomain and b) two tandem repeats of a cysteine-histidine-rich motif called the LIM domain which mediates protein-protein interactions (Way and Chalfie, 1988; Karlsson et al., 1990; Freyd et al., 1990; Arber and Caroni, 1996). Tsuchida and colleagues have shown that the segregation of spinal cord somato- and visceromotoneuron subclasses in different rostro-caudal columns (see above) is defined by combinatorial expression of 4 LIM homeobox genes (Tab.1.1.4).

Motoneuron Subclass	LIM Homeobox Genes	Pathway
MMC_m	Islet-1, Islet-2, Lim-3	dermomyotome
MMC_l	Islet-1, Islet2	ventral mesenchyme
LMC_m	Islet-1, Islet-2	ventral mesenchyme
LMC_l	Islet-2, Lim-1	dorsal mesenchyme
CT_v	Islet-1	sympathetic chain

Tab.1.1.4: Combinatorial expression of LIM homeobox genes in embryonic chick spinal motoneuron subclasses at HH35. *MMC_m*: medial motor column, medial division; *MMC_l*: medial motor column, lateral division; *LMC_m*: lateral motor column, medial division; *LMC_l*: lateral motor column, lateral division; *CT_v*: Column of Terni, ventral region. Modified after Tsuchida et al, 1994.

The co-expression of Lim-3 together with the two Islet genes defines the MMC_m motoneurons which respond to cues from the dermomyotome (for innervation patterns of spinal motoneurons see Chapter 1.2). MMC_l and

LMC_m motoneurons which follow a common pathway despite their different targets, express Islet genes only, and motoneurons of the LMC_l which project into the dorsal mesenchyme are characterized by expression of Lim-1. Expression of Islet-1 alone appears to define visceromotoneurons of the ventral portion of Terni's Column. Interestingly and most revealing, the authors report one exception to the general relationship between columnar topography and target specificity. A subset of motoneurons in the LMC_l innervate the rhomboid muscle which is an axial muscle (Straznicki and Tay, 1983; Hollyday and Jacobson, 1990) and should therefore be supplied by neurons of the MMC_m. These LMC_l motoneurons that "wrongly" innervate an axial muscle show the same LIM expression pattern as MMC_m neurons (Islet-1, Islet-2, and Lim-3 rather than Islet-1 and Islet-2 alone). Therefore, it can be deduced that LIM homeobox gene expression by motoneurons predicts their muscle targets independent of their columnar association. Furthermore, since both Islet genes are expressed by all somatic motoneuron subclasses (with the exception of most LMC_l neurons), the authors speculate that these two genes might be required to specify features common to the development of all motoneurons, whereas the expression of Lim-1 and Lim-3 might account for distinguishing features between subclasses (Tsuchida et al., 1994).

If these speculations are true, then a similar picture should emerge from brainstem motoneurons. As has been pointed out on several occasions above, the hindbrain contains an additional subpopulation of motoneurons: the branchiomotoneurons which innervate derivates from the branchial

(pharyngeal) arches. In chick embryos, the first LIM gene that can be detected by *in situ* hybridization is Islet-1 (Varela-Echavarría et al., 1996). At HH14 its expression is confined to a narrow strip adjacent to the floor plate from r2 to r8 and a small patch in the lower midbrain, representing the motoneurons of the future nuclei V to XII and the oculomotoneurons respectively. By HH17 Islet-1 expression can also be detected in r1, reflecting the developing trochlear nucleus (see Tab.1.1.5).

Motor Nucleus	Islet-1	Islet-2	Lim-3
Oculomotor	HH14	HH14	
Trochlear	HH17	HH23	
Trigeminus	HH14		
Abducens	HH14	HH19	HH20 [1]
Facial	HH14		
Vestibulocochlear	HH14	HH15 [2]	
Vagus	HH14		
Accessory	HH14		
Hypoglossus	HH14	HH19	HH20

Tab. 1.1.5: Differential LIM homeobox protein expression in cranial motoneurons. The stages of earliest detection are indicated; [1] expression in accessory abducens nucleus only; [2] down-regulated during migration (after Varela-Echavarría et al., 1996).

Again, Islet-1 is expressed by all motoneurons regardless of subpopulation and expression is maintained until at least HH29. Islet-2 appears first in the midbrain area occupied by oculomotoneurons at HH14. By HH25 its expression is restricted to the somatomotoneurons of the 3rd, 4th, 6th and 12th cranial nerves. Between HH15 and HH24 Islet-2 expression can

be seen in r4, corresponding to efferent vestibuloacoustic neurons. However, these neurons seem to down-regulate Islet-2 expression, once their somata migrate to the contralateral side (Varela-Echevarría et al., 1996). Islet-2 is also down-regulated by accessory abducens motoneurons during lateral migration. Both, the abducens and the accessory abducens neurons express Islet-2 in early stages while projecting their axons towards a muscle mass that will later divide into the extraocular lateral rectus muscle (innervated by the abducens nerve) and the pyramidalis-quadratus complex (innervated by the accessory abducens nerve; Wahl et al., 1994). From HH21 onwards the nerve roots of these two nuclei diverge and the somata of the accessory abducens start migrating laterally and become successively Islet-2-negative. It should be noted that the pyramidalis and the quadratus are muscles of the nictitating membrane, a third eye-lid which can be found in reptiles, birds and a range of mammals (e.g. Romer and Parsons, 1991) but does not exist in humans who therefore lack the accessory abducens nerve.

Lim-3 which in the spinal cord is expressed in the MMC_m, is restricted to the hypoglossus nucleus (and the avian accessory abducens nucleus). This finding is consistent with two observations: a) the hypoglossus nucleus is a continuation of the ventral grey motor column of the spinal cord which includes the Lim-3 expressing MMC_m, and b) the target musculature of the hypoglossus nerve derives from occipital somites rather than head mesoderm (Noden, 1983; Couly, et al., 1993). A number of non-motoneuronal cells also express Lim-3 but their exact identity has not yet been established. They might include cells of the raphe nucleus and the reticular formation

(Zhadanov et al., 1995). Lim-1 and Lim-2 are not expressed in brainstem motoneurons.

These findings lend further support to the hypothesis that specific LIM codes determine the phenotypic identity of motoneurons and the responsiveness of their axons to selective guidance cues (Tsuchida et al., 1994; Varela-Echavarría et al., 1996). Islet-1 which is expressed in all brainstem and spinal motoneurons, might define the motor phenotype in general; not so Islet-2 as suggested by Tsuchida and colleagues (see above, Tsuchida et al., 1994), since it is not expressed by branchiomotor and visceromotoneurons. This view is supported by the observation that targeted deletion of Islet-1 in mice leads to the absence of motoneurons along the entire axis of brainstem and spinal cord. Instead, there is a markedly increased incidence of apoptotic cell death in neuroepithelial progenitor cells at the time of motoneuron generation (Pfaff et al., 1996).

On the basis of these observations, Varela-Echevarría and colleagues argue that LIM homeobox transcription factors might regulate genes whose protein products mediate various guidance cues responsible for axonal pathfinding and soma migration. For instance, it has been shown in explant cultures as well as *in vivo* that motoneuron axons are repelled by signals emanating from floor plate cells. These signals may polarize initial axon outgrowth away from the midline and towards the lateral exit points (Guthrie and Pini, 1995). One protein that may act as a chemorepellent is Netrin-1 which is secreted by floor plate cells and has been shown to repulse axons

from trochlear and all dorsally projecting motoneurons in culture (Colamarino and Tessier-Lavigne, 1995; Varela-Echavarría et al., 1997). In contrast, Netrin-1 seems to act as a chemoattractant for commissural axons which outgrow from neurons located in the dorsal spinal cord and turn ventrally towards the floor plate before crossing the midline and ascending on the contralateral side (Tessier-Lavigne et al, 1988, Plazcek et al., 1990; Kennedy et al., 1994; Serafini et al., 1994; reviewed by Davies, 1994). The LIM homeobox genes might have a role in this process by regulating the expression of membrane receptors (or other cell proteins) which mediate the response to Netrin-1 and other chemoattractants and –repellents such as members of the semaphorin family (Varela-Echevarría, 1996).

Further evidence fo the role of Lim homeobox genes in axon guidance of motoneurons has emerged from studies of mice with a combined null mutation for Lhx3 (Lim-3) and the highly related gene Lhx4. Both genes are expressed by motoneurons of the MMC_m innervating axial muscles. Their deletion leads to dorsal migration of spinal cord motoneurons and to the total absence of a ventral root. Instead the axons of the displaced motoneurons seem to exit the neural tube via a lateral exit point similar to those of the branchiomotor neurons of the spinal accessory nerve (Sharma et al., 1998). Also, a recent study by Helmbacher and colleagues has shown that the absence of EphA4, a tyrosine kinase receptor for a family of transmembrane and GPI-anchored molecules, called ephrins, led to a misprojection of LMC_l motor axons in the hindlimb. These axons are normally prevented from assuming a ventral path into the flexor department of the hindlimb, possibly

via interactions between the Eph4 recpetor and two of its ligands, ephrin-A2 and ephrin-A5. Knocking out the Eph4 gene led to a ventral projection of axons from the LMC_l population of motoneurons (Helmbacher et al., 2000). This is of particular interest since LMC_l motoneurons express Lim-1 and that hindlimb motor axons of the LMC_l randomly choose their path into either the flexor or the extensor department (Kania et al., 2000). Helmbacher and colleagues suggest that Lim-1 might be required not only for Eph4 expression of LMC_l motoneurons which prevents their axons to project into the extensor department but also for a putative second signalling system which promotes this pathway.

1.1.4. Development of the substantia nigra

1.1.4.1. General development of the midbrain

The midbrain or mesencephalon is the most rostral and smallest part of the brainstem. At a mere rostro-caudal length of 1.5 cm in humans, it connects the diencephalon with the pons. Its ventral surface is characterised by the two cerebral peduncles which contain several long motor tracts (see above). On the dorsal surface two conspicuous swellings can be seen on either side, the superior and inferior colliculi which contain cells that are part of the visual and auditory pathways, respectively. The centre of the midbrain, the tegmentum, contains nuclei involved in the modulation of movement, namely the substantia nigra and the red nucleus. It also contains the oculomotor nucleus and its accessory nucleus, the Edinger-Westphal nucleus (see above). Most anatomy textbooks also list the trochlear nucleus

as part of the midbrain. However, since the trochlear motoneurons originate from the first rhombomere of the metencephalon, they will not be considered here.

Transverse sections through the midbrain area during early development show the same pattern as discussed above for the hindbrain and spinal cord. The basal plates contain the somatic efferent neurons of the oculomotor nucleus and the general viscero-efferent neurons of the Edinger-Westphal nucleus which innervate the pupillary sphincter muscle of the eye. The marginal layer around the basal plates will enlarge to form the crus cerebri. The alar plate gives rise to cells of the future superior and inferior colliculi.

The midbrain lies beyond the rostral limit of Hox gene expression and unlike the hindbrain is not subdivided into apparent segments. There has been increasing evidence in recent years that patterning of mesencephalic neurons depends on signals from midbrain-hindbrain-junction (MHJ). The MHJ develops from an expanded area within the neural plate which coincides with the territory of the future hindbrain and midbrain. Until mid-gestation its size decreases to a small strip of constricted neuroepithelium, the isthmus which demarcates the border between the two parts of the developing brainstem. This region seems to act as an organiser for metencephalic and mesencephalic structures. Transplantation of the MHJ to other regions leads to ectopic specification of these structures (reviewed in Le Douarin, 1993; Alvarado-Mallart, 1993). Most interestingly, if the MHJ is transplanted into

the diencephalon, the local cells, on induction form mesencephalic structures (Alvarado-Mallart, 1993; Marín and Puelles, 1994). In contrast, transplantation of the MHJ into the hindbrain leads to the specification of cerebellar structures (Martínez et al., 1995). Other structures like the ventral thalamus and the telencephalon and the basal plate of the rhombencephalon do not change their fate in response to the ectopic MHJ (Martínez et al., 1995). This suggests some level of specificity in response depending on the brain region. Furthermore, signalling seems to be restricted to the rhombomere or prosomere that the MHJ tissue has been transplanted into, suggesting that the signals are propagated through the neuroepithelium and that segmental borders block this propagation (Marín and Puelles, 1994; Martínez et al., 1995).

Several genes that have been implicated in midbrain patterning are either expressed by MHJ cells or have expression borders that terminate in the MHJ: Wnt1, the engrailed genes En1 and En2, three members of the paired-box containing gene family (Pax2, Pax5, and Pax8), Otx, and FGF8, a member of the Fibroblast Growth Factor (FGF) family. In the rat brain, the first gene to be expressed in the MHJ is the transcription factor Pax2, followed slightly later at the 1 somite stage by Wnt1 (Rowitch and McMahon, 1995). All of these genes are expressed in overlapping domains. Whereas En1 extends into both metencephalic and mesencephalic regions, Wnt1 is solely expressed in the midbrain. At the 5-6 somite stage, FGF8 is expressed throughout the Pax2 expression domain (Reifers et al., 1998), but later restricted to the area surrounding the isthmus.

Although the specific functions of these genes are still unclear, analysis of mutant mice has provided certain clues to the part they might play during midbrain and hindbrain development. In Pax5 mutant mice the posterior colliculi of the midbrain are partially deleted (Urbanek et al.; 1994). En1 and Wnt1 null mutant mice die at birth and show deletions of the cerebellum and midbrain structures (reviewed in Wurst et al., 1994). The changes in the Wnt1 mutant mice are particularly interesting. Although Wnt1 is not expressed in the hindbrain, the cerebellum is deleted. The deletion of the cerebellum is preceded by the loss of midbrain tissue and engrailed protein expression (McMahon et al., 1992). Thus, Wnt1 might be required to maintain engrailed expression which in turn is required for cerebellar development. On the other hand , the deletion of the midbrain including the MHJ organiser region in Wnt1 mutant mice might result in the loss of critical signals that direct the development of the cerebellum (Bally-Cuif et al., 1995). The cerebellum in En2 null mutants is reduced by a third and exhibits an abnormal folding pattern (Millen et al., 1994). The homeobox genes En1 and En2 have a similar expression pattern but show little homology outside the homeodomain (Joyner, 1996). Compound engrailed mutants (double engrailed mutants heterozygote for one of the genes) have a more severe phenotype than the respective single homozygote mutants, despite the fact that single engrailed heterozygotes appear normal, suggesting a dose dependence (Joyner, 1996).

Although the picture is still patchy, it emerges that these genes, like their homologues in *Drosophila* are part of a genetic cascade that in

vertebrates give rise to the tegmentum and the colliculi of the midbrain and the hindbrain-derived cerebellum (Chalepakis et al., 1993; Rowitch and McMahon, 1995; reviewed in Joyner, 1996).

1.1.4.2. Early development of dopaminergic neurons

The pars compacta of the substantia nigra (SNpc) and the ventral tegmental area (VTA) of Tsai belong to a system of neurons in the CNS that is characterised by its neurotransmitter dopamine. The monoamine dopamine is synthesized from L-Tyrosine via L-DOPA, a step catalysed by the enzyme tyrosine hydroxylase (TH; Fig.2.2.2; see "Materials and Methods"). There are 8 dopaminergic cell groups in the mammalian brain, most of which lie in the mesencephalon and diencephalon (Tab.1.1.6).

Cell Group	Location
A8	Retro-rubral nucleus
A9	Substantia nigra, pars compacta
A10	Ventral tegmental area
A11	Caudal hypothalamus
A12	Arcuate (infundibular) nucleus
A13	Zona incerta
A14	Medial rostral hypothalamus
A15	Olfactory tubercle
A16	Olfactory bulb
A17	Retina

Tab.1.1.6: Location of the dopaminergic cell groups in the central nervous system. A8 to A10 are mesencephalic, A11 to A14 diencephalic, and A15 telencephalic. The not listed groups A1 to A7 consist of noradrenergic cells in the lower brainstem

In the rat brain, the first dopaminergic cells, as detectable by TH immunohistochemistry, emerge at E12.5 (Specht et al., 1981a). While the earliest possible immunohistochemical labelling of tyrosine hydroxylase coincides with the detection of catecholamine by histofluorescence in mesencephalic neurons (Lauder and Bloom, 1974; Olson and Seiger, 1972), in other neurons detection of the enzyme precedes that of the neurotransmitter, in hypothalamic cells by a minimum of 5.5 days (Hyppa, 1969; Loizou, 1971; Olson and Seiger, 1972). A group of cells emerging in the ventral mesencephalon at E12.5 will in the following days extend in the rostro-caudal axis, become partially confluent in the midline, and eventually give rise to the dopaminergic cells of the retro-rubral nucleus (A8), the substantia nigra (A9), and the ventral tegmental area (A10). Another TH-positive cell group becomes visible in the prosencephalon at E12.5 and divides into a caudal and a rostral group by E13.5. This group represents the anlage for the dopaminergic cells of the hypothalamus (A11), the arcuate nucleus (A12), the zona incerta (A13), and the olfactory tubercle (A15; Specht et al., 1981a). The dopaminergic cells in the glomerular layer of the olfactory bulb only become detectable by TH immunohistochemistry at E21 (Specht et al., 1981b). This is consistent with the late perinatal generation of external granular neurons in the olfactory bulb (Hinds, 1968).

The dopaminergic neurons of the substantia nigra and the ventral tegmental area which in the rat can first be detected by their marker, tyrosine hydroxylase at E12.5, differentiate from progenitor cells in close location to the floor plate (Lauder and Bloom, 1974; Altman and Bayer, 1981; Specht et

al., 1981a; Marchand and Poirier, 1983; Voorn et al., 1988). Floor plate transplants can induce differentiation of dopaminergic cells in the dorsal midbrain and dorsal rostral forebrain (Hynes et al., 1995a) but not the caudal forebrain (Ye et al., 1998). Taken together with the observations that MHJ transplants can induce midbrain structures in ectopic locations along the ventral A-P axis but not in dorsal locations (see above), the following assumption has been made: Floor plate-derived signals control the position of dopaminergic neurons along the dorsoventral axis and MHJ-derived signals control their position along the anterior-posterior axis (Ye et al., 1998)

The effects of ectopic floor plate transplants can be mimicked by sonic hedgehog (SHH; Hynes et al, 1995b; Wang et al., 1995) and blocked by antibodies against it (Ye et al., 1998). Recombinant SHH can also induce ectopic dopaminergic neurons in the dorsal portion of the midbrain (Hynes et al., 1995; Wang et al., 1995) and the rostral forebrain but not the ventral forebrain (Ye et al., 1998). SHH is expressed along the floor plate (reviewed in Shimamura et al., 1995) and has been suggested to mediate its inductive effects (Chiang et al., 1996; Ericson et al., 1996., Tanabe and Jessell., 1996). These observations strongly support the view of SHH as a major floor plate-derived agent controlling specification along the dorso-ventral axis.

Another gene that has been found to induce dopaminergic neurons, is Fgf8. Its protein product fibroblast growth factor 8, is secreted by MHJ cells and the anterior neural ridge (ANR) of the ventral forebrain from E9

onwards. (Ye et al, 1998). Ectopic expression of Fgf8 induces midbrain structures in the diencephalon (Crossley et al., 1996), an area that does not generate endogenous dopaminergic neurons. On the other hand, the development of dopaminergic neurons in mid- and forebrain explants can be blocked by a soluble FGF8-receptor. Furthermore, Fgf8 deficient mice lack midbrain and forebrain dopaminergic neurons (Ye et al., 1998). Interestingly, neither FGF8 nor SHH can induce dopaminergic neurons in the dorsal diencephalon whereas the combination of the two can. This suggests that the co-expression and integration of the these two molecules is critical for the specification of dopaminergic neurons at their defined location. Whereas SHH appears to mediate the floor plate's control along the dorso-ventral axis, FGF8 seems to be the MHJ's and ANR's signal necessary for dopaminergic specification along the anterior-posterior axis (Ye et al., 1998).

1.1.4.3. Development of the substantia nigra

The exact origin and migration of substantia nigra neurons had for a long time been a controversial issue. An early account from Spatz suggested that the substantia nigra originated from the diencephalon (Spatz et al., 1923) A little later, Shaner and Cooper claimed that the substantia nigra arose from the basal plate of the midbrain (Shaner, 1932, 1936; Cooper, 1946). The 1969 edition of Langman's "Medical Embryology" suggested that the SN originated from the alar plate (Langman, 1969). The 1995 edition of the same textbook avoids the matter altogether (Sadler ed., 1995). In 1971, Hanaway and colleagues conducted an autoradiographic study of the production, migration and differentiation of neurons of the substantia nigra and the

ventral tegmental area in the rat. They claimed that both structures as well as the dopaminergic interpeduncular nucleus (IPN) derived from the middle third of the midbrain's basal plate. The neurons that would give rise to the substantia nigra were thought to migrate radially towards the ventral surface of the mantle layer through already existing cells in the tegmentum. Another stream, also originating from the medial third of the basal plate was moving ventrally towards the interpeduncular fossa. Once having reached the ventral surface a proportion of its cells was migrating laterally (Fig. 1.1.4). This stream which had the shape of an inverted fountain, was thought to give rise to the VTA and the interpeduncular nucleus (Hanaway et al., 1971).

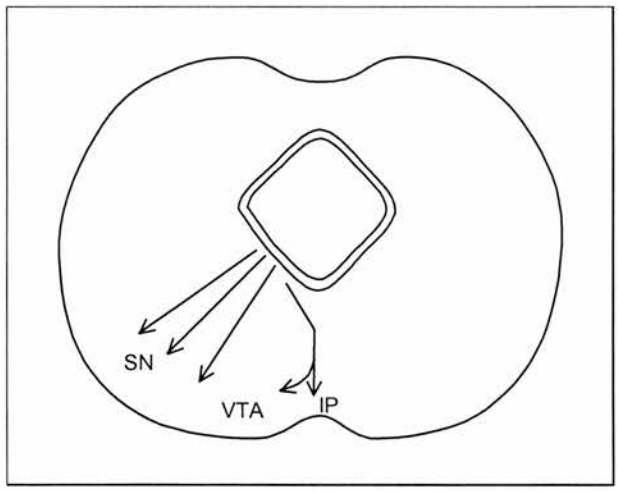

Fig. 1.1.4: Cell streams contributing to the genesis of the SN, VTA and IPN according to and adapted from Hanaway et al, 1971

These findings were challenged by Marchand and Poirier in 1983. They pointed out the weakness in Hanaway's and colleagues' work of solely using coronal sections to study migration pathways. Using [^{3}H]thymidine autoradiography, Marchand and Poirier analysed sagittal, horizontal and frontal sections of rat embryos between E11 and E18. They found that SN

neurons were born between E12 and E15 with a peak of neurogenesis at E13 and E14. They also noted a spatiotemporal gradient of origin. The first labelled cells appeared in the rostral part of the SN primordium and the last labelled cells were seen in the caudal part. Analysing the migration pathway of these neurons, they observed two streams of cells at E15, both of which were originating lateral to the floor plate in the rhombencephalic isthmus. Close to the floor plate, cells of the median stream (MSC) extended towards the ventral surface as well as heading rostrally into the midbrain area. The other more lateral stream (VLS) was less well outlined at E15. But on the following day its cells could be seen coursing through the tegmentum from the isthmic basal plate in a radial fashion towards the ventrolateral surface of the cephalic flexure. The MSC had in the meantime fused across the midline in its most rostral part which had proceeded to the level of the third ventricle (Fig. 1.1.5). In the intermediate part of the MSC, cells began spreading laterally across the ventral surface forming a wing-like structure. During E17 and E18, both streams increased in cell number and extended more rostrally with the MSC exhibiting prominent wings that at the streams rostral end appeared isolated from the median mainstream (Marchand and Poirier, 1983).

There are several differences in the findings of the two studies outlined above. Whereas Hanaway and colleagues believed SN and VTA neurons to originate from the midbrain, Marchand and Poirier found them to originate more caudally, in the isthmus. Although both studies revealed that the peak of neurogenesis lay at E13 and E14, only the later study showed a rostrocaudal gradient of neuronal birth with early born neurons settling in the

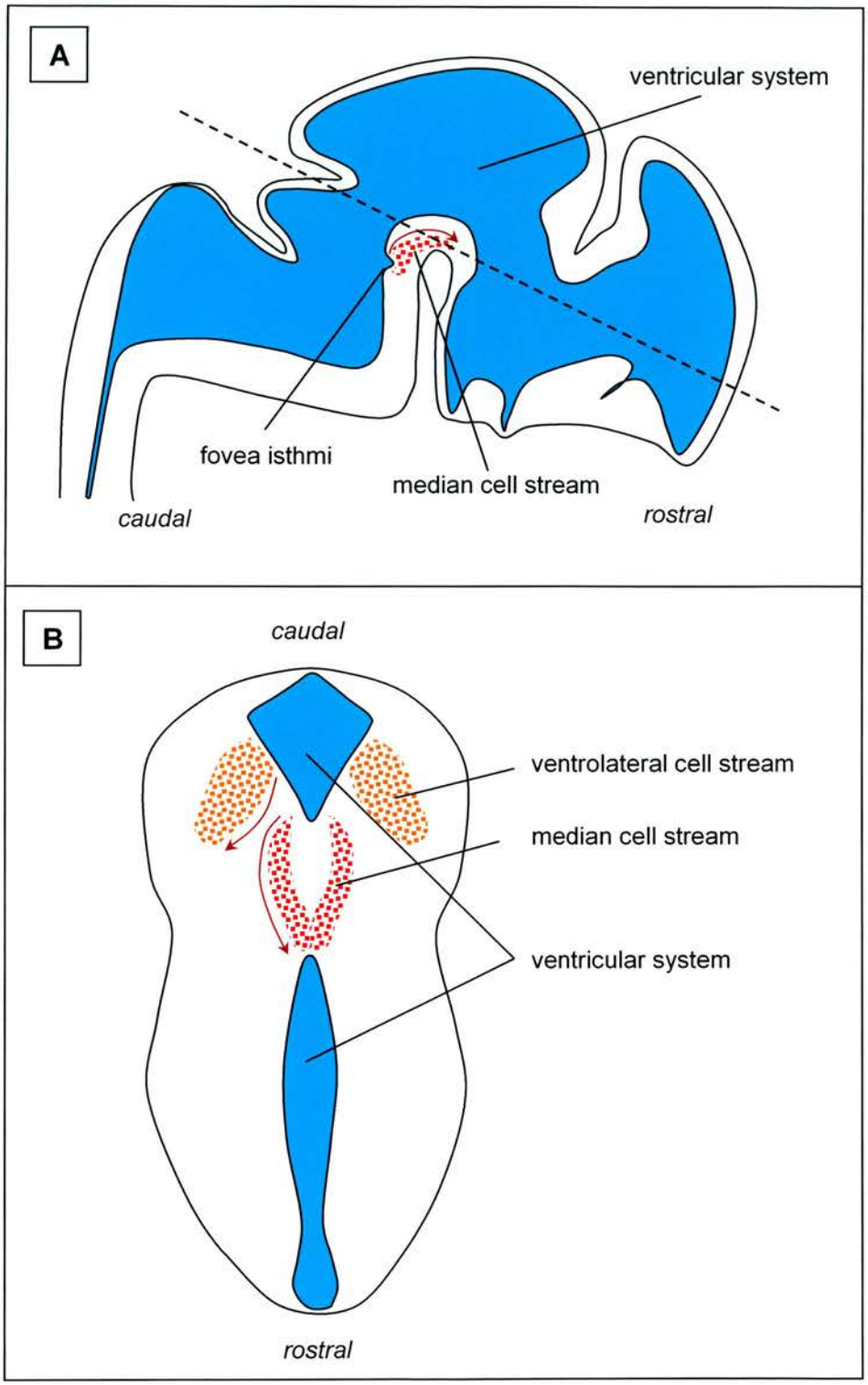

Fig. 1.1.5: The ventrolateral and median streams of cells in the developing rat midbrain at E16. **A:** median sagittal section; the dotted line indicating the approximate level of the section shown in B. **B:** horizontal section. Adapted from drawings and photos by Marchand and Poirier, 1983

rostral half of the SN and the late born neurons in the lower half. The three-dimensional analysis of the migration pathways revealed two streams, that extended not only towards the ventral surface but to a significant degree ascended rostrally. Marchand and Poirier claimed that both pathways significantly contributed to the SN. Comparing their own findings with a study by Tennyson et al., which had shown the existence of catecholamine-containing neurons in the same midventral proliferation area, they argued that the median portion of the MSC most likely contributed to the VTA and INP. The wing of the MSC would represent the zona compacta of the SN whereas the VLS would give rise to the zona reticulata. This is consistent with the fact that in Tennyson's study the area occupied by cells of the VLS didn't contain catecholaminergic neurons whereas the wing area did (Tennyson et al., 1973). Lastly, Marchand and Poirier strongly rejected Hanaway's claim that cells in the ventrolateral stream would migrate between existing cells in the tegmentum. Hanaway and colleagues had made that claim since their one-dimensional analysis did not detect the rostral movement of cells along the ventral surface. So, in order to explain how the neurons in the rostral parts of the midbrain could reach the ventral surface from the basal plate, they had to propose a scenario by which rostral basal plate cells would sneak their way through an already established marginal layer (Hanaway et al., 1971) to the ventral surface.

1.2.4.4. Neuronal cell death in the substantia nigra

Another controversial issue regarding the development of the substantia nigra is the occurrence of physiological cell death among its

dopaminergic neurons. The phenomenon of naturally-occurring cell death during development will be discussed in detail in the next chapter. However, while cell death has been known to be an integral part of the development of lower motoneurons since Hamburger's study in 1958 (see below), it has until very recently been unclear whether the dopaminergic neurons of the substantia nigra undergo the same process of developmental cell death. It therefore seems justified, with respect to the substantia nigra, to take this particular issue out of its general context and discuss it here.

During development, most neuronal populations undergo a sculpturing process, termed naturally-occurring cell death (Cowan et al., 1984; Oppenheim, 1991). This process which eliminates more than half of the members of a given neuronal population adjusts the number of neurons to its functional need (see below). Janec and Burke first showed that the dopaminergic neurons of the SNpc in the rat undergo this process during the first days of postnatal life (Janec and Burke, 1993). However, later studies questioned whether this event was unique to rats or could apply to mammals in general (Lieb et al., 1996; Blum 1998). The authors based their findings on counts of tyrosine hydroxylase (TH) positive neurons at various developmental stages in the mouse. Naturally-occurring cell death had until then been observed not only in different neuronal populations but also in a variety of different species (reviewed in Oppenheim, 1991). The studies undertaken by Blum as well as Lieb and colleagues however pointed towards some degree of phylogenetic divergence. This also would have had technical

implications for the way developmental neurobiological research is conducted and potentially could have shifted the cell death paradigm.

In 2000, Jackson-Lewis and colleagues reviewed the question of naturally-occurring cell death in the substantia nigra of the mouse. Using TH stains (see "Materials and Methods"), they noticed that during the first postnatal days, normal looking SNpc neurons intermingled with neurons that exhibited morphological signs of apoptosis (see next chapter). Only a fifth of these apoptotic neurons stained positive for tyrosine hydroxylase. About half of the neurons in the SNpc are known to be GABAergic (Dray,1979). But less than 15% of these neurons showed any signs of apoptosis in Jackson's study. They therefore concluded that a significant number of apoptotic neurons in the SNpc were dopaminergic but lost expression of tyrosine hydroxylase as a result of metabolic shutdown during the dying process. The authors therefore studied the time course of apoptosis in the murine SNpc showing two waves of cell death. The first wave started shortly before birth at E19, reached its peak at P2, and regressed over the next 8 days. A second wave resurged shortly afterwards and peaked at P14. No more apoptotic cells were observed after P32 (Jackson-Lewis et al, 2000).

Still, the question remained why these apoptotic waves didn't lead to a noticeable reduction in TH-positive neurons. Based on their own studies, the authors ruled out any late recruitment of neurons to the substantia nigra at this rather late stage in development. On the other hand, TH-expression and dopamine levels only reach their final maximum at 4 to 6 weeks after birth

(Coyle, 1977). Taken together with the finding that during development of the SNpc the number of Nissl-stained neurons increases significantly relative to the number of TH-positive neurons, they argued that the phenomenon could be explained by phenotypic maturation (Jackson et al., 2000). Put into simple terms that means, while some dopaminergic neurons shut down their metabolism during apoptosis (and therefore become TH-negative) a roughly similar amount of SNpc neurons upregulate their dopaminergic phenotype. As a result, the number of neurons as established by their expression of tyrosine hydroxylase would be more or less stable and cell death undetected.

To confirm their hypothesis , Jackson-Lewis et al. discussed the coincidence of the second wave of apoptosis with the peak of synapse formation between the dopaminergic neurons of the SNpc with their target cells in the striatum between P12 and P17 (Hattori and McGeer, 1973). Since naturally-occurring cell death is in many neuronal populations a process regulated by the target field (see below), the temporal coincidence of these two events would confirm the findings of Jackson-Lewis and colleagues. In fact, lesioning striatal neurons with excitotoxin QA (which does not affect the synaptic terminals of the SN neurons) shortly before the peak of synaptogenesis, led to a seven-fold increase in apoptotic neurons in the substantia nigra (Jackson-Lewis et al., 2000).

It can therefore be assumed that cell death takes place among dopaminergic neurons of the murine substantia nigra during the first two weeks postnatally. As shown in many other neuronal populations, the extent

of this process is regulated by the target field of these neurons, in this case the striatum.

1.2. Developmental Cell Death and Survival of Motoneurons

"The initial development of the lateral motor column in its qualitative and quantative aspects is determined by intrinsic factors, and all fibers grow out irrespective of peripheral conditions. The quantative relationship between the number of motoneurons and the size of the peripheral field of innervation is established by a selective milieu, and the degeneration of all others."

(Victor Hamburger, 1958)

1.2.1. Naturally-occurring *cell death*

1.2.1.1. Historical Overview

Perhaps one of the most important events in developmental neurobiology in the last century has been the discovery of naturally-occurring cell death (aka *programmed, epigenetic, histogenetic, probabilistic, developmental, or physiological cell death*). Although the concept of generating an initial surplus of neurons that will be decimated according to functional demand at later stages is now one that has become commonplace amongst developmental neuroscientists, it hasn't always been an obvious one. At the beginning of the 20th century, Shorey noticed a severe depletion of spinal motoneurons and sensory ganglion cells after removing limb buds of early chick and amphibian embryos (Shorey, 1909). In contrast, transplantation of limb buds to ectopic regions led to local hyperplasia of sensory and motoneurons (May, 1933, Detwiler, 1936). Furthermore, Hamburger demonstrated that when surgery was incomplete, there was a proportional relationship between the amount of remaining limb musculature

and the extent of spinal cord hypoplasia (Hamburger, 1939a, b). These and similar observations by other authors led to the recognition of interactions between the periphery and the nervous system. The obvious question that arose from these studies was by what means the observed numerical changes in neurons was controlled. In the early Thirties, Carpenter proposed what then became to be known as the *recruitment hypothesis*: following observations made on salamander spinal ganglia after limb transplantation, he deduced that an increase in the peripheral demand led to further proliferation and differentiation of yet undifferentiated cells into additional sensory neurons (Carpenter, 1932, 1933). Hamburger and Keefe proposed that pioneer nerve fibres which established the first contact with their target tissue acted as mediators between the periphery and the nervous tissue by releasing putative growth agents within the spinal cord which in turn would lead to the recruitment of neighbouring cells (Hamburger and Keefe, 1944). However, they denied that the periphery had any direct influence on proliferation, as they found that the decrease in motoneuron number after limb bud removal seemed to be balanced by an increase in other, non-motor cells. Instead they concluded that peripheral targets controlled the recruitment or the differentiation of neurons from an already established pool of totipotent cells rather than cell proliferation itself.

Five years later, Hamburger published a paper together with Rita Levi-Montalcini that changed the paradigm of developmental neurobiology. Studying spinal ganglia in chick embryos, the authors found a significant loss of sensory ganglion cells in non-limb-innervating segments during

normal development (Hamburger and Levi-Montalcini, 1949). This paper which became a classic in the history of developmental neurobiology, demonstrated for the first time that massive cell loss was a physiological feature of the developing vertebrate nervous system. Differentiated spinal ganglion cells were generated in abundance, without prior "knowledge" of peripheral demand, and a substantial amount of these neurons would subsequently be sacrificed. This was in stark contrast to the "recruitment-hypothesis" which didn't conceive that nature would indulge in the apparent luxury of generating an enormous surplus of cells in the first place and later adjust the number according to peripheral demand. Revisiting the motor system after these findings, Hamburger found that the same applied to spinal motoneurons (Hamburger, 1958). In fairness to other scientists who seem to have been forgotten after the 1949 paper by Hamburger and Levi-Montalcini, it should be pointed out that there had been earlier but largely ignored or rejected accounts of naturally-occurring *cell death* (see Collin, 1906; Ernst, 1926 for example).

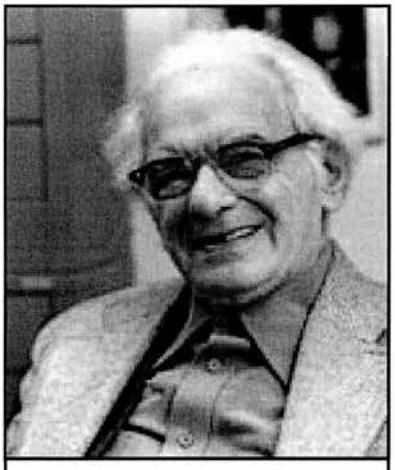

Victor Hamburger
1900 - 2001

However, one question still remained: if cell loss was part of a normal developmental program, and if the loss of target tissue increased the demise of cells whereas a peripheral overload attenuated the process, *how* did the periphery control the final number of functional neurons? The question did not remain unanswered for very long. The events that started with a

publication of one of Hamburger's students (Bueker, 1948) and finally led to the discovery of *Nerve Growth Factor* have become legendary and are well publicised. A very readable account of the discovery can be found in Levi-Montalcini, 1975, which also contains an unforgettable scene about the dual purpose of the egg as an object of scientific study as well as nutrition in war-torn Italy. Levi-Montalcini and colleagues found that spinal ganglia and sympathetic neurons were rescued from cell death by the means of a diffusible factor synthesized and released by their target tissue (Levi-Montalcini and Hamburger, 1951; Levi-Montalcini, 1952; Cohen, et al., 1954; Cohen and Levi-Montalcini, 1956). They initially called this factor "Nerve Growth-Stimulating Factor" and later shortened it to "Nerve Growth Factor" or "NGF".

Rita Levi-Montalcini, born 1909

In the following decades, naturally-occurring cell death was detected in an ever increasing number of neuronal populations and in a wide variety of different species (see for example: Hughes, 1961; Prestige, 1967; Cowan and Wenger, 1967, 1968; Harris, 1969; Larramendi, 1969; Cantino and Sisto-Daneo, 1972; Rogers and Cowan, 1973; Zilles and Wingert, 1973). Out of this wealth of reports, two studies are notable since they showed that naturally-occurring cell death and cell death due to target removal occur around the same time, implying a common underlying mechanism (Cowan and Wenger, 1967; Prestige, 1967). The question of whether natural cell death occurs in *all* developing neurons still remains unanswered.

Nevertheless, given the wealth of neuronal populations that have been shown to undergo naturally-occurring cell death, the problem of solving this question seems to be a methodological one. For instance, until very recently it was thought that the dopaminergic neurons of the murine substantia nigra do not undergo cell death (Jackson et al., 2000). This conclusion was reached on the basis of cell counts of tyrosine hydroxylase- positive neurons at various developmental stages. Since it is conceivable that some dopaminergic neurons still haven't reached full metabolic maturity including the expression of tyrosine hydroxylase while other neurons of the group are in the process of down-regulating the same protein due to programmed cell death, cell counts relying purely on the expression of tyrosine hydroxylase cannot be relied on fully (see below). Indeed, TUNEL stains of the substantia nigra have revealed two waves of postnatal apoptotic cell death in these neurons (Jackson et al., 2000; see above).

1.2.1.2. Neuronal differentiation and axonal outgrowth prior to cell death

Hamburger and Levi-Montalcini had shown that spinal ganglion cells and motoneurons in the chick embryo seemed to differentiate normally following limb bud removal (Hamburger and Levi-Montalcini, 1949; Hamburger, 1958). Furthermore, Hamburger found that cell numbers in the ventral horn of the operated side were equal to those on the control side *prior* to the onset of normally occurring cell death. The target-deprived motoneurons developed axons that seemed to grow out towards the body wall close to the site where the limb was removed, and formed a neuroma-like

tangle of nerve endings (Hamburger, 1958). Therefore, it could be deduced that target removal did not affect cell proliferation and migration but the maintenance of fully-differentiated neurons.

However, in later years electron microscopic studies revealed ultrastructural differences in chick ciliary ganglion cells deprived of their target and those undergoing naturally-occurring cell death (Landmesser and Pilar, 1976). Neurons on the control side developed a well-organised rough endoplasmic reticulum (RER) as well as polyribosomes coinciding with the onset of synapse formation, whereas target deprived neurons did not. As a result, those cells on the control side that underwent naturally-occurring cell death showed dilation of the RER and disruption of the cytoplasm prior to nuclear changes. In contrast, ganglion cells that were subjected to induced cell death by target removal merely exhibited nuclear changes. RER dilation in control neurons could be explained as a result of protein accumulation in those neurons that established initial synaptic contact which induced protein synthesis, but did not maintain a functional connection with their target cells. Landmesser and Pilar speculated that since target-deprived neurons were prevented from establishing synaptic contacts in the first place, they were also deprived of a critical signal from the periphery that would induce protein synthesis as indicated by the development of a RER in control cells. As satisfying as this hypothesis might seem, other neuronal populations, e.g. the chick spinal motoneurons (Chu-Wang and Oppenheim, 1978a,b), the duck trochlear nucleus (Sohal et al., 1978), and the retinal ganglion cells in the chick (Hughes and McLoon, 1979) do not show these differences in

degeneration. To make things even more confusing, both types of degenerative changes can be found in chick spinal motoneurons, but they occur during induced as well as naturally-occurring cell death (Chu-Wang and Oppenheim, 1978a,b). Some motoneurons even degenerate before any visible increase of their RER. The extent of differentiation prior to cell death obviously seems to vary among different neuronal populations and might be accounted for by intrinsic mechanisms or certain aspects of synaptogenesis.

Another, albeit related, question was of course whether those neurons that underwent naturally-occurring cell death actually grew axons in the first place, and if they did so, whether their axons established synaptic contacts with the target tissue. The first part of the question was addressed by Prestige and Wilson in 1972 who undertook electron microscopic counts of ventral root axons in the frog at different developmental stages. In all cases the axon number correlated to the number of cell somata in the ventral horn (Prestige and Wilson, 1972). These findings were confirmed for other populations in various species, e.g. the chick ciliary neurons (Landmesser and Pilar, 1976), and the duck trochlear nucleus (Sohal et al., 1978). The second part of the question owed its answer (or at least part of a solution) to a technique that was established in the seventies of the last century and that utilises the enzyme horseradish peroxidase (HRP). Exogenously-introduced HRP is readily taken up by nerve terminals and transported retrogradely to the cell body (reviewed in Heym and Forssmann, 1981). Clarke and Cowan injected HRP into the chick eye prior to the onset of naturally-occurring cell death in the isthmo-optic nucleus which innervates the eye, and demonstrated

that all of the nucleus' neurons were labelled, although 60 percent of them were destined to die later during the cell death period (Clarke and Cowan, 1976). These results were also confirmed for other neuronal populations such as lumbar spinal motoneurons (Chu-Wang and Oppenheim, 1978b). It is important to point out that the HRP technique by no means proves the existence of a functional synapse between an axon terminal and its target cell; it merely demonstrates that an axon has reached its target tissue.

1.2.1.3. Morphological modes of cell death

The occurrence of developmental cell death in the nervous system has now been widely accepted by the scientific community (for a "sermon in the desert" see Banker, 1982). However, some controversy still exists about the morphological modes of cell death. Kerr and Wyllie distinguished two forms of cell death: necrosis and apoptosis (Wyllie et al. 1980; Wyllie, 1981, Kerr et al, 1987). Necrosis is usually associated with a pathological process that leads to significant disturbances of the physiological status quo and is accompanied by the morphological signs of inflammation. Osmotic changes cause oedematous swelling of the cell and its internal compartments which in turn causes membrane rupture and leakage of cell content. Apoptosis – a term derived from ancient Greek for the autumnal drop of leaves – has been coined by Kerr and colleagues in 1972 to describe the morphological changes that they observed in hepatocytes subjected to the physiological cell turnover in the liver (Kerr et al., 1972). In contrast to the morphological changes seen during necrosis, apoptosis is characterised by the condensation of a cell's nuclear and cytoplasmic contents, break-up of the DNA into oligosomal

fragments, followed by breakdown of the nuclear membrane and fragmentation of the whole cell into small membrane bound vesicles ("membrane blebbing") that are rapidly phagocytosed by neighbouring cells, e.g. macrophages (see Fig. 1.2.1).

Apoptosis has also been recognised as the underlying mechanism of other forms of ontogenetic cell death. The most obvious and dramatic form of developmental cell death is probably that seen during metamorphosis, e.g. the tadpole's loss of it's tail. Amphibian metamorphosis which is generally regarded as preparing an aquatic organism for a terrestrial existence, is controlled by thyroid hormones and involves apoptosis of striated tail muscle fibres (Kerr et al., 1974; Sachs et al., 1997a,b). Another form of apoptotic degeneration occurs during the formation of digits. The difference between a chicken's foot and that of a duck is determined by the presence or absence of cell death in the interdigital spaces (Saunders et al., 1962; Saunders and Fallon, 1966). Although these spaces are for historical reasons often referred to as interdigital necrotic zones, their cells die by apoptosis, and show the typical fragmentation of DNA (Mori et al., 1995).

Although apoptotic cell death is widespread during development, several authors have argued for greater diversity of morphological modes of natural cellular demise. In 1973, Schweichel and Merker observed two other modes of cell death in developing tissues: a) degeneration due to endogenous lysosomal activity (autophagocytosis or autophagy), and b) cell death without apparent lysosomal involvement (Schweichel and Merker, 1973).

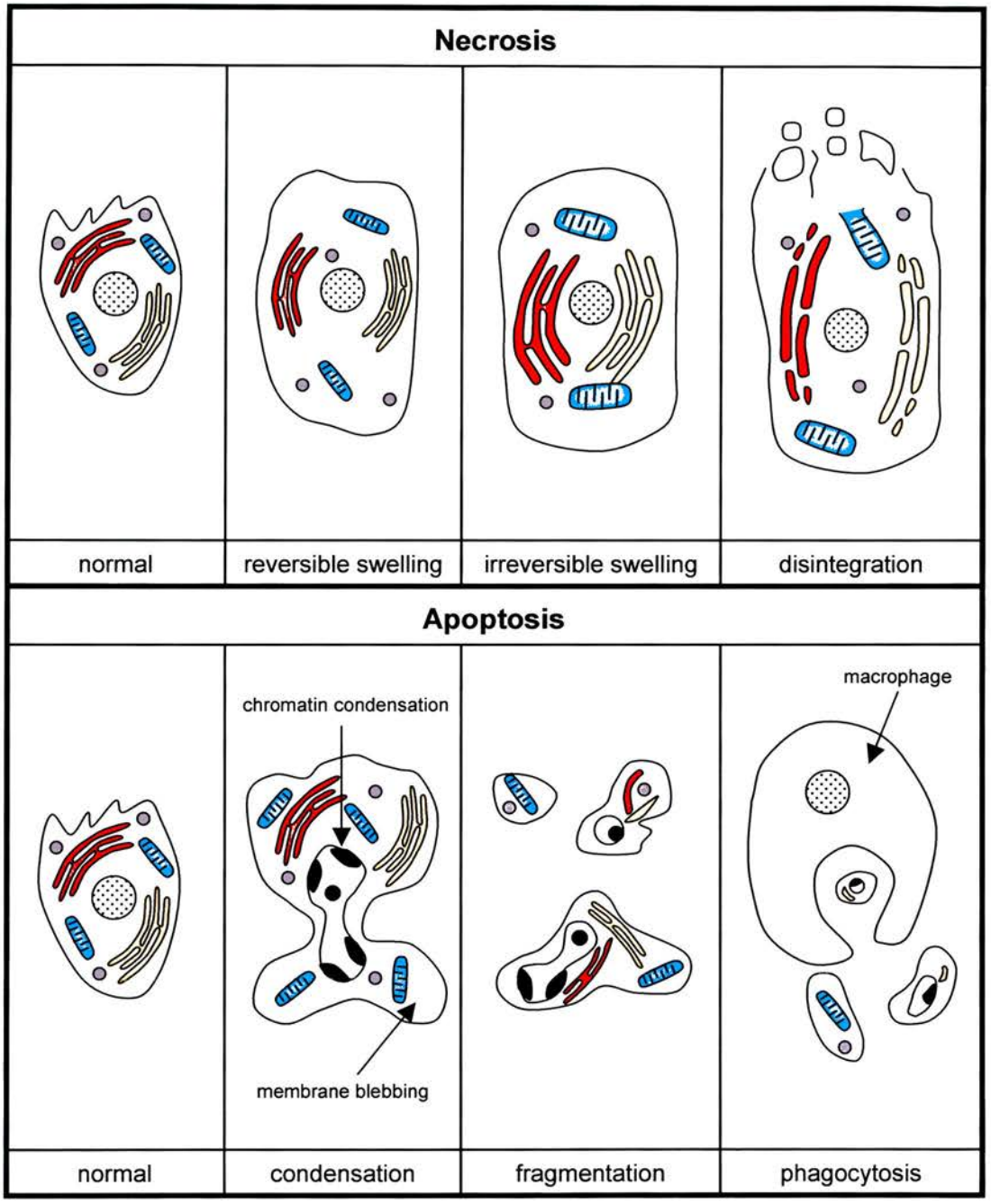

Fig.1.2.1: Morphological features of necrosis and apoptosis

More recently, autophagy has been reported in sympathetic neurons, albeit activated by signalling mechanisms that also cause apoptosis (Xue et al., 1999). In how far these modes of cell death are entities in their own right or merely variations on a common theme remains to be seen.

1.2.1.4. Biochemistry of apoptosis

The central biochemical event in apoptosis is the activation of a group of specific proteases called caspases. The term is a condensation of cysteinyl aspartate-specific proteinases, highlighting the enzymes' characteristic feature of cleaving their substrates after aspartic acid residues. The morphological hallmarks of apoptosis, chromatin condensation, DNA fragmentation, and breakdown of the nuclear membrane (Fig. 1.2.1), are the direct consequence of caspase activity (Nicholson et al., 1997; Thornberry and Lazebnik, 1998). In humans, a heterodimeric protein, DNA fragmentation factor (DFF), has been isolated which mediates chromatin fragmentation and probably condensation (Liu et al, 1997, 1998). Cleavage of a 45 kDa subunit of DFF by caspases dissociates it from another, 40 kDa subunit, and induces oligomerisation of the latter into a protein complex with DNase activity (Liu et al., 1999).

So far, two main apoptotic pathways have been identified, both of which converge on caspase activation (Fig.1.2.2). One pathway involves certain trans-membrane proteins termed death receptors. Their ligands, like Fas or tumor necrosis factor (TNF; see below), induce trimerisation of the receptors. This event recruits special adaptor molecules such as Fas-

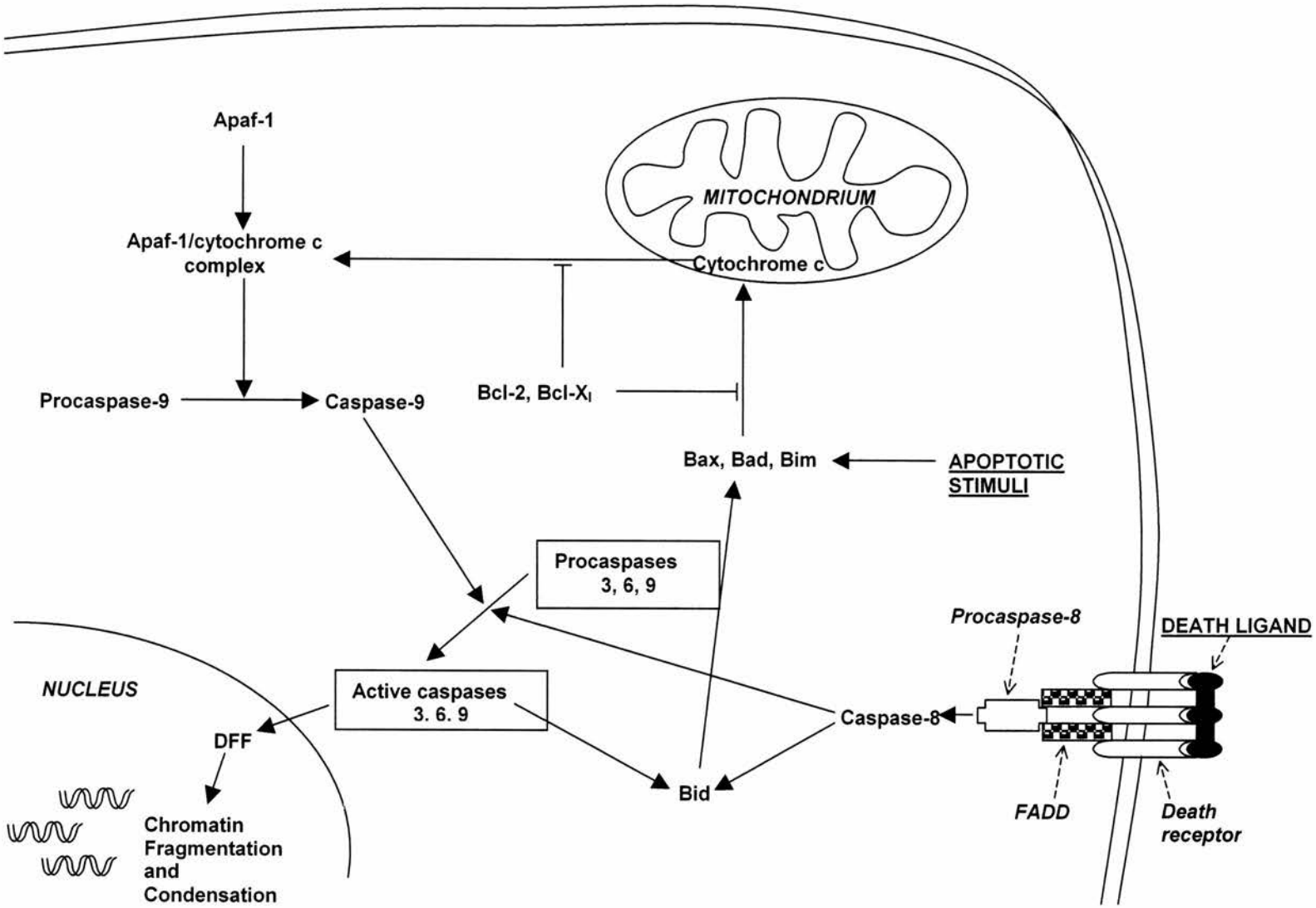

Fig. 1.2.2: Overview of apoptotic pathways

associating protein with death domain (FADD) to the intracellular domain of the death receptor. The adaptor molecules in turn bind Procaspase-8 and trigger its autocatalytic activation (Boldin et al., 1995, 1996; Chinnaiyan et al., 1995; Muzio et al., 1996; Srinivasula et al., 1996; Nagata, 1997). Caspase-8 then activates other caspases like caspase-3, 6, and 7, which mediate apoptosis.

The second apoptotic pathway involves the release of the electron transfer protein cytochrome c from its mitochondrial inter-membrane location into the cytoplasm (Liu et al., 1996). Although the exact mechanism of this release is still unknown, there has been mounting evidence in recent years that it is regulated by members of the Bcl-2 family of proteins (Adams and Cory, 1998). Members of this family, of which fifteen have been identified so far in mammals, are related to the CED proteins in C. elegans. They include pro-apoptotic proteins such as Bak, Bim, Bad, and Bax, and members with anti-apoptotic activity like Bcl-2 and Bcl-X_l. Bax, Bak, and Bid have been reported to directly cause the release of cytochrome c from mitochondria (Jurgensmeier et al., 1998; Kuwana et al., 1998; Li et al.,1998). In contrast, Bcl-2 and Bcl-X_l are able to block cytochrome c release (Kim et al., Kluck et al., Yang et al., 1997). Extra- and intracellular death signals may translocate and activate pro-apoptotic members of the Bcl-2 family to the mitochondria and facilitate the release of cytochrome c. On the other hand, survival signals can inhibit apoptosis via the phosphotidylinositol-3 kinase (PI-3K)/ Akt pathway (see below) by phosphorylation of the pro-apoptotic protein Bad which subsequently binds a protein called the 14-3-3

protein and is sequestered in the cytoplasm (Zha et al., 1996). Upon release into the cytoplasm, cytochrome c forms a multimeric complex with Apaf-1 (Li et al., 1997, Zou et al., 1997), a 130 kDa protein with a caspase recruitment domain (Zou et al., 1997). This protein complex activates pro-caspase-9 which in turn activates caspases 3, 6, and 9 (the same set of enzymes activated by the death receptor pathway).

1.2.2. Prevention of naturally-occurring cell death

1.2.2.1. Survival factors for motoneurons

Since the discovery of NGF by Levi-Montalcini and Cohen, an ever increasing list of factors that prevent naturally-occurring cell death in neurons has been identified and characterised on a molecular level. These so-called neurotrophic factors are a rather diverse group of polypeptides that serve different biological roles and are not confined to nervous tissue (Henderson, 1995; Henderson et al., 1998). For instance, Macrophage stimulating protein (MSP) which was the object of one of the studies included in this thesis, was originally identified as a factor that stimulated motility of residential peritoneal macrophages (Leonard and Skeel, 1978). Further studies have shown that this protein has a wealth of diverse biological functions (Banu et al, 1996; Wang et al., 1996; Broxmeyer et al, 1996; Kurihara et al., 1998; Schmidt et al, 2002).

At present, a dozen or so factors and their receptors that promote survival in motoneurons have been identified. They belong to 5 different protein families and include 3 factors that are related to NGF (reviewed by

Barde, 1990). Whereas NGF does not support survival in motoneurons, the other 3 members of this family – called neurotrophins – do (Sendtner et al., 1992; Hughes et al., 1993; Henderson et al, 1993). An overview of factors known to be involved in motoneuron survival is given in Tab.1.2.1.

Most of these factors have been identified by culturing purified embryonic chick and rat motoneurons (Bloch-Gallego et al., 1991; Henderson et al., 1995) in defined media and assessing the effects of putative survival factors *in vitro*. The method has certain shortcomings, such as a small time-window allowing purification (see Materials and Methods) and the creation of a somewhat artificial environment that applies to all in-vitro examinations. But it has the advantage of requiring any studied molecule to have a direct effect on its assumed target cells to qualify as a survival factor. Furthermore, these effects can be easily and precisely quantified. Also, in most cases *in vitro* observations have been confirmed by *in vivo* studies, either during the time span of naturally-occurring cell death or following axotomy in neonatal animals or in mutant mice (Henderson et al., 1998).

However, in some cases different approaches applied to the study of a certain putative motoneuron survival factor resulted in different findings that furthered the understanding of the mechanism of naturally-occurring cell death. For instance, Insulin-like growth factors IGF-I and IGF-II have been shown to promote survival of cultured embryonic rat spinal motoneurons but seem to have had only limited trophic effects on chick spinal motoneurons (Arakawa et al., 1990; Hughes et al., 1993; Neff et al., 1993).

Family	Factor	Receptor on motoneurons
Neurotrophins	Brain-derived neurotrophic factor (BDNF)	$p75^{NTR}$, trk-B
	Neurotrophin-3 (NT-3)	$p75^{NTR}$, trk-C
	Neurotrophin-4/5 (NT-4/5)	$p75^{NTR}$, trk-B
CNTF/LIF family	Ciliary neurotrophic factor (CNTF)	CNTFRα, LIFRβ, gp130
	Leukemia inhibitory factor (LIF)	LIFRβ, gp130
	Cardiotrophin-1 (CT-1)	?, LIFRβ, gp130
	Cardiotrophin-1-like cytokine (CLC)	?, LIFRβ, gp130
Kringle-protein family	Hepatocyte growth factor/scatter factor (HGF/SF)	c-met
	Macrophage-stimulating protein (MSP) [1)]	RON
Insulin-like growth factors	Insulin-like growth factor-I (IGF-I)	IGFR-1
	Insulin-like growth factor-II (IGF-II)	IGFR-1, mannose-6P receptor
Glial-derived neurotrophic factor and related factors	Glial-derived neurotrophic factor (GDNF)	GFRα1, c-ret
	Neurturin (NTR)	GFRα2, c-ret
	Persephin (PSP)	GFRα4, c-ret
	Artemin	GFRα3, c-ret

Tab.1.2.1: Neurotrophic factors for motoneurons and their receptors.

Nevertheless, the combination of IGFs with Ciliary neurotrophic factor (CNTF) in chick motoneuron cultures led to survival rates higher than for each factor alone (Arakawa et al., 1990). This was a significant finding since it showed that neurotrophic factors can potentiate each other's effects and that *in vivo* survival of motoneurons seemed to depend on a complex cooperation of several factors. Moreover, synergistic action of two molecules that completely lack neurotrophic activity on their own, can result in a neurotrophic effect, e.g. GDNF and TGF-β (reviewed by Unsicker and Krieglstein, 2000). "*The concept of a single 'motoneuron growth factor (MNGF)' was a useful simplification as long as the active molecule involved had not been identified. Now that nearly ten factors have been described as enhancing motoneuron survival, the important question is probably not which of them is the 'true' MNGF, but how the actions of each are coordinated in time (development) and space (interactions of the motoneuron with different cell types) so as to allow correct and stable formation of a neuromuscular junction.*" (Henderson et al., 1993).

The next important step was the observation that a single factor might support the survival of only subclasses of motoneurons rather than the entire motor population. Hepatocyte growth factor (HGF), a member of the kringle protein family (Stoker et al., 1987; Nakamura et al., 1989) rescues E5 chick lumbar motoneurons from cell death in culture but not motoneurons from thoracic or cervical levels (Novak et al., 2000). This is consistent with the fact that c-met tyrosine kinase, the receptor for HGF, is expressed in lumbar motoneurons but not at more cranial spinal cord levels. Similar observations

have been made for GDNF and NTN, both of which have strong survival promoting effects on motoneurons *in vitro* and *in vivo* (Henderson et al, 1994; Oppenheim et al, 1995; Yan et al, 1995; Klein et al, 1997). These factors mediate their actions through a receptor complex made up of the tyrosine kinase receptor RET and a ligand-binding glycosyl-phophatidylinositol (GPI)-linked protein (GFRα) which serves as co-receptor (Fig.1.2.3). The GFRα family consists of four receptors. GFRα1 and GFRα2 are thought to be generally favoured by GDNF and NTN, respectively (reviewed by Airaksinen et al, 1999). Both co-receptors are restricted to certain subpopulations of spinal motoneurons (Garcès et al, 2000). Most motoneurons purified from GFRα1 null mutant mice could not be rescued from cell death by GDNF, and spinal cord dissections at E15.5 revealed the loss of several motoneuron subpopulations at brachial and lumbar levels. Surprisingly, motoneurons purified from these mice were also less responsive to NTN, whereas motoneurons from GFRα2$^{-/-}$ mice retained their responsiveness to both GDNF and NTN *in vitro*. This suggests that survival in these motoneuron subpopulations is dependent on GFRα1 but not GFRα2 expression. However, the authors cautioned that there might be a subset of GFRα2-dependent motoneurons that could have evaded the *in vitro* survival assay as well as *in vivo* observations on mutants because their total cell number was too small (Garcès, 2000). Analysis of GDNF-deficient mice revealed the loss of about a third of motoneurons on all three spinal levels with most of the cell loss occurring in the rostral two thirds of the lumbar spinal cord. In the brainstem, motoneuron losses were observed in the

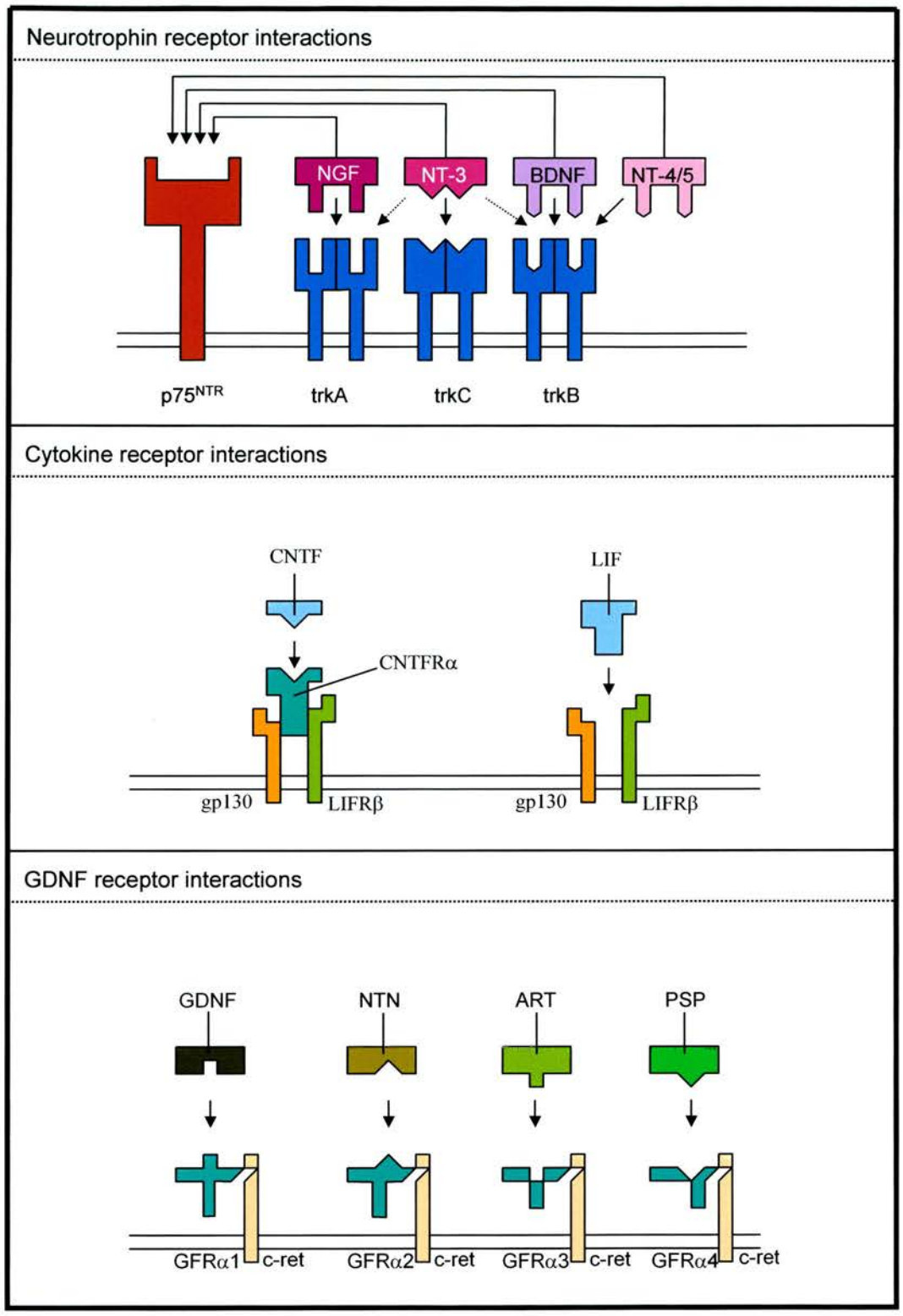

Fig.1.2.3: Neurotrophic Factors and their receptors. Preferred interactions are indicated by arrows (modified after Reichardt and Farinas, 1997; Rosenthal, 1999)

trigeminal, hypoglossal, and facial nuclei, but not in the oculomotor and abducens nuclei (Oppenheim et al., 2000).

1.2.2.2. Neurotrophic factors and intracellular signalling pathways

How do neurotrophic factors promote cell survival? The best studied family of neurotrophic factors are the neurotrophins (for reviews, see Segal and Greenberg, 1996; Lewin and Barde, 1996, Reichardt and Fariñas, 1997; Huang and Reichardt, 2001). Thus they will be used here to give an overview of the mechanisms involved in mediating neuronal survival. In mammals, four neurotrophins have been identified so far: Nerve Growth Factor (NGF), Brain-derived neurotrophic factor (BDNF), Neurotrophin-3 (NT-3), Neurotrophin-4 (NT-4, a.k.a. NT-4/5). Two other genes (NT-6 and NT-7) have been isolated in fish and are believed to have no orthologues in mammals or birds (Gotz et al., 1994, Nilsson, 1998). BDNF, NT-3, and NT-4/5 are known to promote survival of motoneurons. The neurotrophins interact with two major receptor classes (reviewed by Reichardt and Fariñas, 1997). The main signal-transducing receptors are the tyrosine kinases trkA, trkB, and trkC (Fig.1.2.3). In neurons and neuronal precursors, tyrosine kinases regulate signalling pathways that mediate proliferation, survival, axonal and dendritic growth, membrane trafficking, and synapse formation and function (reviewed in Huang and Reichardt, 2001). Members of other neurotrophic factor families such the GDNF related factors and the cytokine family also activate tyrosine kinases, all of which regulate many of the same intracellular signalling pathways (see Reichardt and Fariñas, 1997). Activation by neurotrophins induces homodimerisation of the respective trk

receptor and subsequent phosphorylation of the receptor's cytoplasmic domain which in turn activates intracellular signalling pathways by recruitment of certain adapter proteins to the receptor (reviewed in Pawson and Nash, 2000).

Three distinct signalling cascades activated by trk-receptors have been identified so far: the Ras/MAP-kinase pathway, the phosphatidylinositol-3-kinase (PI-3 kinase)/Akt kinase pathway, and the phospholipase C (PLC)-γ1 pathway. The Ras/MAPK pathway which has been shown to be involved in promoting neuronal survival and neurite outgrowth is linked to trk-signalling by the Shc adapter proteins. Several forms of Shc have been identified in neurons: ShcA, ShcB, and ShcC/N-Shc (Cattaneo and Pelicci, 1998). One interesting phenomenon worth pointing out, is the ratio of ShcA and ShcC expression. Whereas ShcA is widely expressed in all types of cells, ShcC seems to be neuron-specific (Nakamura et al., 1996). Conti and colleagues reported that as ShcC becomes upregulated in the brain, ShcA is downregulated. This coincides with the developmental stage at which these neurons become postmitotic and some of them, including motoneurons become dependent on neurotrophic factors (Conti et al, 1997).

Shc also couples the trk receptors to the PI-3 kinase pathway which leads to the activation of Akt (Baxter et al., 1995; Greene and Kaplan., 1995, Datta et al., 1997). Akt, a serine/threonine kinase with a broad spectrum of substrates has been shown to phosphorylate the pro-apoptotic protein BAD (Datta et al., 1997). This is important because it links a neurotrophin-

mediated signalling pathway directly to an apoptotic pathway. As mentioned above, phosphorylated BAD binds to the 14-3-3 protein and is subsequently sequestered in the cytoplasm which prevents it from mediating the release of cytochrome c from mitochondria, a point of no return in apoptosis (Zha et al., 1996). Akt also phosphorylates caspase-9 which is directly involved in the activation of DFFs (see above).

Activation of the PLCγ1 pathway leads to an increased release of intracellularly stored Ca^{2+} which activates the GTP-binding protein RAP1 and subsequently B-Raf (Grewal et al., 2000), the latter being expressed at relatively high levels during the time of naturally-occurring cell death in motoneurons (Sendtner et al., 2000). Rafs seem to play an important role in the activation of the MAPK pathway and also as effector kinases for the anti-apoptotic Bcl-2 protein. Bcl-2 can target Raf-1 to mitochondrial membranes, allowing it to phosphorylate and thereby inactivate the pro-apoptotic protein BAD (Wang et al., 1994, 1996). Again, this demonstrates how a neurotrophic factor might promote survival by activating an intracellular signalling cascade that is interlinked with an apoptotic pathway. Nevertheless, it has to be pointed out that the signalling cascades outlined above are vastly complex and that foregone conclusions based on rather oversimplified reviews like this should be avoided at all costs! For a comprehensive review of the neurotrophin-mediated signalling pathways, see Huang and Reichardt, 2001.

Each of the neurotrophins also binds to the low-affinity receptor $p75^{NTR}$, a member of the tumor necrosis factor receptor subfamily

(Rodriguez-Tebar et al., 1991; Chao, 1994; Bothwell, 1995; Frade and Barde, 1999). This receptor which was actually discovered prior to the trk receptors, has been found to serve several functions. Firstly, *in vitro* studies have shown that $p75^{NTR}$ is able to potentiate the activation of trkA by sub-optimal doses of NGF but not the activation of the other trk receptors (Davies et al., 1993; Mahadeo et al., 1994; Verdi et al., 1994). Secondly, it seems to reduce the responsiveness of trk receptors to noncognate ligands i.e. a neurotrophin that is not the preferred ligand for a certain trk receptor (Benedetti et al, 1993; Clary and Reichartd, 1994; Lee et al., 1994b). This has been supported by the finding that NT-3, whose preferred receptor is trkC, is able to promote the survival of TrkA-expressing neurons more effectively in the absence of $p75^{NTR}$ (Lee et al., 1994; Brennan et al., 1999). NGF and BDNF are also able to promote the survival of sensory neurons lacking functional TrkC receptors by activating TrkA and TrkB, respectively (Davies et al., 1995). Thirdly, $p75^{NTR}$ promotes retrograde transport of several neurotrophins (Curtis et al., 1995; Harrison et al, 2000). Fourthly, in the absence of trk receptors, $p75^{NTR}$ promotes cell death rather than survival (Chao et al., 1998; Friedman and Greene, 1999; reviewed by Frade and Barde, 1998). And finally, axon growth and target innervation are impaired in the absence of $p75^{NTR}$ (Lee et al., 1994a; Walsh et al, 1999a,b; Bentley and Lee, 2000).

Having been the first receptor to be discovered for a neurotrophic factor (NGF), the probably most striking feature about the p75 receptor is its ability to promote cell death rather than survival under certain conditions. p75 null mutant mice show reduced cell death in the retina, and in a

subpopulation of spinal interneurons (Frade and Barde, 1999). The fact that similar changes have been observed in NGF null mutant mice suggests that cell death in these cases is induced by NGF/p75 signalling (Frade and Barde, 1999). NGF also induces cell death in certain motoneurons via a p75-dependent mechanism (Sendtner et al., 1992; Wiese et al., 1999; Sedel et al., 1999). It is not yet understood how the presence or absence of the trkA receptor determines whether p75 acts as a survival receptor or as a mediator of death.

Another member of the tumor necrosis factor receptor subfamily acting as a death receptor is Fas. Both, Fas and Fas ligand are expressed in early motoneurons and have been found to promote death in cultured motoneurons from E12.5 murine embryos (Raoul et al., 1999). Studies on non-neuronal cells have revealed that the activated Fas receptor can form a complex with an adaptor protein called FADD that triggers activation of pro-caspase-8, a key molecule in apoptotic signalling (see above and Fig. 1.x; Irmler et al., 1997; Yeh et al., 1998; reviewed by Raoul et al., 2000). It is conceivable that this death pathway which is initiated during the early stages of neuronal development, might be prevented once neurons make contact with their target, Indeed, it has been demonstrated that neurotrophic factors can interfere with Fas signalling by different mechanisms: a) the prevention of Fas ligand upregulation, b) upregulation of an intracellular decoy called FLIP which competes with FADD for pro-caspase-8 (Irmler et al., 1997), and c) further downstream, by tilting the balance towards anti-apoptotic

signalling at the level of the Bcl-2 family (see above). For a critical discussion see Raoul et al., 2000.

1.2.2.3. Prevention of cell death by non-target-derived sources

So far, naturally-occurring cell death and its prevention has been described merely as a phenomenon which depends on the interactions between a neuron's axon and its target. However, anatomically speaking, a nerve cell is not solely defined by the cell it innervates but also by its afferent connections. Several studies have dealt with the question of what part afferents play in the natural demise of developing neurons. The earliest reports on this issue stem from observations made by Rita Levi-Montalcini and Victor Hamburger: transection of the spinal cord, performed before the longitudinal tracts reach the ventral horn motoneurons, did not affect motoneuron numbers (Levi-Montalcini, 1945; Hamburger, 1946). A more detailed study of the effects of afferent deprivation on spinal motoneurons by Wenger produced similar results (Wenger, 1950). But again, these observations are by no means true for all types of neurons: the chick auditory nuclei show increased cell death after the removal of their peripheral afferents (Levi-Montalcini, 1949; Parks, 1979). The removal of afferents to the chick ciliary ganglion even leads to the complete loss of those neurons (Levi-Montalcini, 1947).

More recently, *in vitro* studies have been performed which mimic afferent influences on neurons by creating depolarising culture conditions with elevated potassium concentrations or by adding glutamate receptor

agonists. Again, these studies have shown that various neuronal populations differ in their responsiveness to afferent influences. Whereas potassium levels of 35 mM supported the survival of E10 chick sympathetic neurons it had no effect on E5 or E6 chick motoneurons (Wakade et al., 1983; Sendtner et al., 2000). Interestingly, the survival of chick nodose neurons seems to depend on the maintenance of intracellular calcium levels. Depolarising conditions only have a survival-enhancing effect once these neurons have started to express L-type Ca^{2+} channels which facilitate depolarisation-dependent Ca^{2+} influx (Larmet et al, 1992).

Also, N-methyl-$_D$-aspartic acid (NMDA) or glutamate exposure which strongly enhanced survival effect of BDNF on purified retinal ganglion cells (Meyer-Franke et al., 1995), did not potentiate the effects of BDNF or other neurotrophic factors on motoneurons. However glutamate treatment led to specific and reversible inhibition of dendritic outgrowth but not axon outgrowth, suggesting that it is involved in plasticity of dendritic growth and formation of synapses between motoneurons and other neuronal cell types within the spinal cord (Sendtner et al., 2000).

In a previous sub-chapter it has been mentioned that laminin, an extracellular matrix protein, might be a factor that contributes to the guidance of axons along inter-rhombomeric boundaries. It has also been known for some time that laminin potentiates the survival effects of neurotrophic factors (Edgar et al., 1984). E6 chick motoneurons, cultured in the presence of laminin show a 55% survival after one week with CNTF

(Arakawa et al., 1990). The survival-promoting effect of CNTF drops significantly when the culture dishes are coated with laminin in a concentration of 1 μg/ml rather than 10 μg/ml. Sendtner and colleagues have shown that the same is true for FGF-2, and CNTF and FGF-2 combined (Sendtner et al., 1991).

Another molecule that can provide a short-term survival signal on its own and also potentiates the effects of neurotrophic factors on long-term survival in motoneurons is cyclic adenosine mono-phosphate (cAMP). cAMP has for a long time been known as a second messenger linking cell surface receptors and their ligands to intracellular signalling pathways, but has only recently been implicated in survival mediation (Meyer-Franke et al., 1998). cAMP is generated from Adenosine Tri-Phosphate (ATP) by adenylate cyclase. This enzyme is coupled to cell membrane receptors by Guanosine Tri-Phosphate (GTP)-binding protein (G-protein). Many neurotransmitters act via G-protein-coupled receptors. This might provide a mechanism by which neurotrophic factor-mediated survival of motoneurons is enhanced by afferent synaptic activity. Meyer-Franke and colleagues have shown that elevated cytoplasmic cAMP levels can increase the recruitment of trkB to the plasma membrane of retinal ganglion cells. This is of particular interest, since it has been demonstrated that BDNF exposure down-regulates trkB expression on the cell surface (Carter et al., 1995), which is consistent with the finding that administration of high BDNF concentrations after facial nerve transection has only transient rescue effects on facial motoneurons.

The view of the target as the major regulator for neuronal survival has also been challenged recently by the finding that mice deficient for the glial growth factor (GGF) receptor erb-B3 exhibited a significant loss of Schwann cells which in turn led to a 79% reduction in motoneurons (Riethmacher et al., 1997). Moreover, several groups have shown that massive cell death of a subgroup of motoneurons in the ventral cervical spinal cord occurs in the chick embryo around E4, prior to the onset of the cell death usually observed in chick motoneurons between E5 and E10 (Levi-Montalcini, 1950, O'Connor and Wyttenbach, 1974, Oppenheim et al., 1989). Yaginuma and colleagues have demonstrated that this type of cell death is target-independent and might be the result of a cell-autonomous program (Yaginuma et al., 1996). At the same time, Schwann cell and muscle cell (target) derived factors can act in unison to rescue motoneurons from cell death. GDNF which is synthesised by Schwann cells and myotube-derived CT-1 have been shown to synergistically rescue E14.5 rat spinal neurons from cell death *in vitro* (Arce et al., 1990).

1.2.3 Summary

Several deductions can be made from the observations listed above: Naturally-occurring cell death is a process that adjusts the number of available neurons to functional requirements. According to the neurotrophic hypothesis, a surplus of generated neurons compete for a variety of trophic agents derived from various sources, e.g. their target field. The mere fact that cell death in a given neuronal population or subpopulation occurs over a long

stretch of time or in several waves during development makes it conceivable that a neuron's trophic requirements change depending on its developmental stage. The idea of a solely target-derived neurotrophic factor that decides over death or survival of a certain neuronal population no longer holds true. The evidence that has been gathered in recent years points towards a highly complex and interactive process of survival management. From the moment a neuron is born, its success depends on how well it is equipped to respond to a wealth of environmental influences, none of which act on their own but in an integrated and time-dependent manner. In this scenario, the extracellular matrix surrounding a neuron's cell soma plays as an important role in the cell's quest for survival as the Schwann cell that myelinates its axon, the organ targeted for innervation or the afferent neuron making synaptic contact.

Both death and survival of a neuron are mediated by complex intracellular signalling pathways that interact with each other. The activation of these pathways is at least in part dependent on ligand/receptor-mediated induction. The expression of a given set of receptors, and therefore the neuron's ability to respond to environmental influences is dynamic and depends on its phenotype as well as its developmental stage.

1.3 Aims of thesis

The aim of this thesis was to study the effects of Macrophage Stimulating Protein (MSP) and γ-synuclein on brainstem motor systems. The objectives were:

1.) To purify hypoglossal motoneurons from chick embryos for *in vitro* studies.

2.) To investigate the effects of MSP on the survival of these neurons.

3.) To evaluate whether MSP had any effects on neurite outgrowth of these neurons.

4.) To investigate whether MSP was expressed in the embryonic tongue, the target for hypoglossal motoneurons.

5.) To study the effects of knocking out the γ-synuclein gene on the murine substantia nigra.

6.) To study the effects of knocking out the γ-syuclein gene on cranial somato- and branchiomotor neurons in the mouse brain.

7.) To study the expression pattern of γ-synuclein during development and in adult mouse brains on the protein level.

CHAPTER 2

Materials and Methods

2.1 Purification and Culture of Chick Hypoglossal Motoneurons

2.1.1 Dissection of the hypoglossal nucleus

The purification of hypoglossal motoneurons from chick embryos was made possible by two features: a) the nucleus' anatomical location and b) its expression of the cell surface antigen, SC1. During early development, motoneurons of the hypoglossal nucleus are located at the level of the 8th rhombomere (Lumsden and Keynes, 1989). This location is shared with the motoneurons of the dorsal vagus nerve. Both populations transiently express SC1 (Guthrie and Lumsden, 1992; Chang et al., 1992). However by E5.5 (the age used for the studies presented in this thesis) two important changes have occurred: the rhombomeric boundaries have disappeared, and the branchio- and viscero-motoneurons of the vagus nerve have migrated to their lateral position (Simon et al., 1994). As discussed above, the branchio- and viscero-motoneurons of the hindbrain downregulate SC1 on their cell somas once they start migrating to their lateral position, whereas the medially located somato-motoneurons retain the antigen up until E7. This leaves the hypoglossal neurons as the only SC1-positive cell population at this level apart from the floor plate cells which can be removed by dissection (see below).

Since the rhombomeric boundaries have disappeared by E5.5, an SC1 wholemount immunostaining was performed on an E5.5 hindbrain which could then be used as template for dissection. The hypoglossal nucleus could

easily be detected in the lower third of the hindbrain. The caudal tip of the hindbrain cone demarcates the border between hindbrain and cervical spinal cord. The next SC1-positive motoneuron population cranial to the hypoglossal nucleus is represented by the abducens nucleus which is located at the level of the former rhombomeres 5 and 6, leaving the territory of the former rhombomere 7 as a "safety margin" for dissection.

Using fine dissection forceps, the hindbrain was removed in from the embryo, the pia mater detached and the cranial two thirds discarded. At this stage in development, the pia mater comes off the neural tissue easily. It can be picked up with a pair dissection forceps and peeled off while fixing the neural tissue with a second pair of forceps to the dissection dish. The lower third of the hindbrain was divided into two halves using an electrolytically sharpened tungsten needle. A cut was made between the floor and the basal plate on one side, leaving the floor plate attached to the other half (Fig. 2.1.1). The half to which the floor plate remained attached was discarded. The other half was cut into three pieces and the fragments transferred to a 10 ml plastic tube containing 1 ml of calcium-, magnesium-free phosphate-buffered saline (CMF-PBS; Gibco-BRL).

2.1.2. Motoneuron purification and its troubles

The culturing of motoneurons is a notoriously difficult enterprise. The first objective that needs to be addressed is one of purity. Unlike sensory neurons which are assembled in clearly confined structures (dorsal root

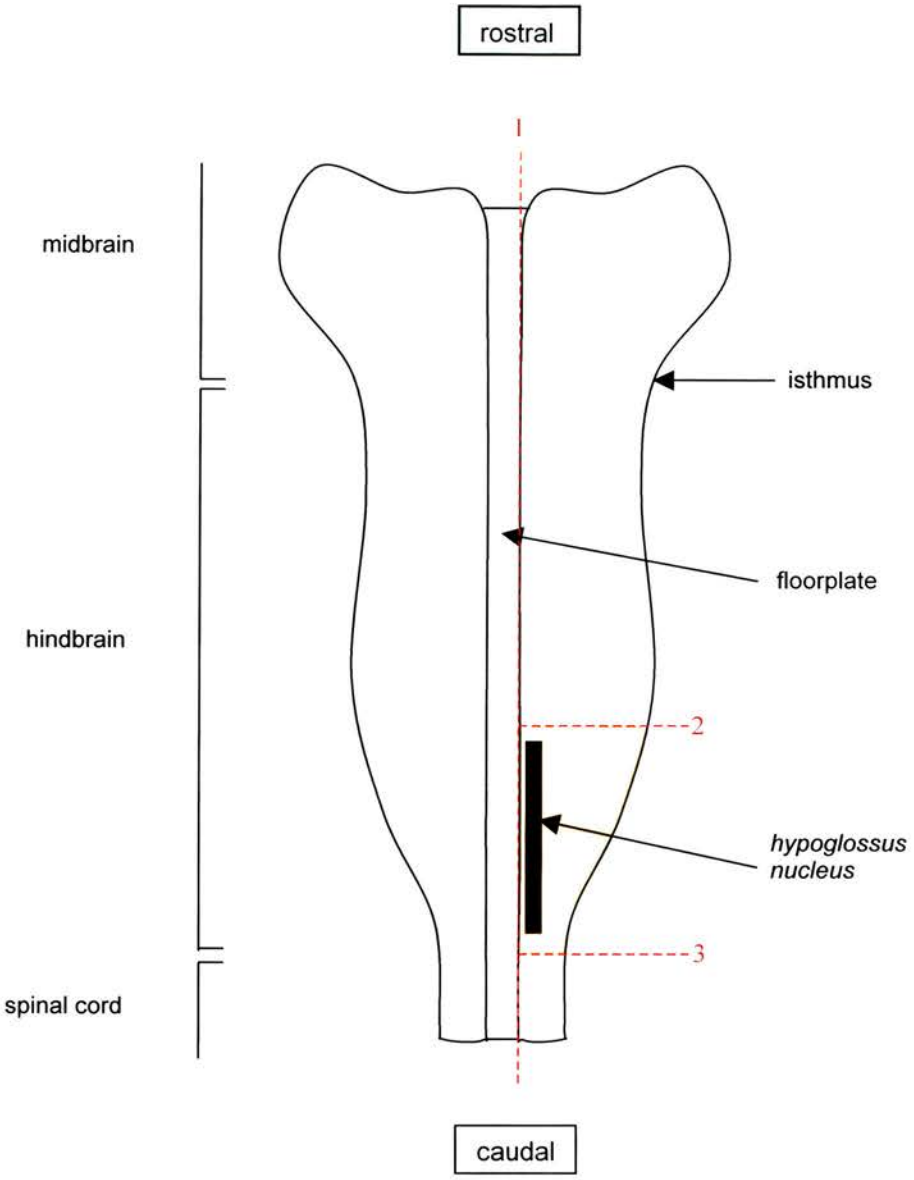

Fig. 2.1.1: Hindbrain dissection. The diagram shows a frontal open-book view of a hindbrain removed from a E5.5 chicken embryo and the sequence of dissection steps. The first cut – using a sharpened Tungsten needle – is made longitudinally along the border between one side of the neural tissue and the floor plate (1). The contralateral side with the floor plate still attached is discarded. The detached half of the hindbrain (right side in diagram) is further dissected along lines 2 and 3 to isolate the lower third (yellow shaded area) which contains the *hypoglossal nucleus*.

ganglia) in the peripheral nervous system, motoneurons are embedded in a heterogeneous cell assembly inside the central nervous system. A purification technique that solely relies on targeted dissection, however meticulous, will inevitably result in cultures that consist of an array of different celltypes. This is undesirable for two main reasons: Firstly, in order to obtain reliable cell counts, a strategy would have to be devised to distinguish the motoneurons from the other cells in the culture dish. Secondly, the unwanted cells might release substances into the culture medium that could exert unknown and uncontrolled influences onto the motoneurons. Such influences potentially skew any observations made on the survival as well as the neurite outgrowth of the cultured motoneurons (which were the main objectives of this study).

To overcome these obstacles, Henderson and colleagues developed a technique to purify chick (and rat) motoneurons by immunological means in combination with a density gradient (Bloch-Gallego, 1991; Henderson et al., 1995). This technique makes use of a) the size of motoneurons and b) SC1, a surface antigen transiently expressed by all chick motoneurons (as well as floor plate cells) during development (see above; Tanaka and Obata, 1984). The following paragraphs describe the original technique which I used to conduct the initial trial runs of E5.5 chick motoneuron cultures.

Using fine dissection forceps the area of interest (e.g. spinal cord, hindbrain) was removed in total from the embryo. The floor plate was removed and the nervous tissue cut into several fragments, which were

transferred into a 10 ml tube containing 1 ml of calcium-, magnesium-free phosphate-buffered saline (CMF-PBS; Gibco-BRL). Only calcium- and magnesium free PBS was used throughout the entire procedure in order not to mask the antibody-binding domains of the SC1 antigen with these ions. Trypsin (Gibco-BRL) was added to a final dilution of 0.05%, and the tissue incubated at 37°C for 15 min. The supernatant was then removed and the tissue transferred to 1 ml of defined L-15 medium (Gibco-BRL) containing 0.4% bovine serum albumin (BSA, Sigma-Aldrich), 10% DNase (Sigma-Aldrich), and 20mM glucose (Sigma-Aldrich). The tissue fragments were gently triturated by passing them approximately twelve times through a 1 ml blue Gilson pipette tip. Remaining fragments were allowed to settle and the supernatant pooled in a 15 ml tube. Another 1 ml of BSA-, DNase-, and glucose-containing L-15 was added to the remaining fragments which were again gently triturated until no more tissue residues were detectable. The cell suspension was then added to the previously pooled supernatant, diluted 1 in 4 in L-15, layered onto a 1 ml cushion of 4% BSA in L-15 and centrifuged at 300g for 10 minutes to remove debris. The supernatant was removed and the pellet resuspended in 1 ml culture medium.

The first step towards purifying the motoneurons from the cell suspension was achieved by metrizamide density gradient centrifugation. The main objective of this step was to rid the cell suspension from floor plate cells (which also express the SC1 antigen) and smaller neurons (e.g. interneurons). According to Henderson and colleagues, application of this technique alone results in quite pure cultures with 90% of the neurons

yielded expressing SC1 (Henderson et al, 1995). However, this technique has a couple of shortcomings which will be discussed further.

For density gradient centrifugation, the cell suspension was split into two fractions of 0.5 ml which were then processed in parallel. Each fraction was diluted in 8 ml of L-15 and carefully layered on top of 2 ml of 6.8% metrizamide in L-15 in a centrifuge tube. The cells were then centrifuged at 500g for 15 minutes resulting in a pellet of small cells at the bottom of the tube and a turbid band of large cells (mostly motoneurons) at the medium-metrizamide interphase (Fig. 2.1.2). Much care had to be taken when layering the cell suspension on top of the metrizamide cushion, so that a sharp interface was maintained. Even small disruptions of this interface usually resulted in a significant loss of motoneurons which would be diffusely suspended inside the cushion. After centrifugation the clear medium above the cell band was removed and the turbid band at the interface (approximately 1 ml) collected with a Gilson pipette. The suspension was diluted with 3 ml of L-15 and centrifuged through a BSA cushion (300g for 10 minutes) to remove remnants of metrizamide and possible debris. The supernatant was removed and the cell pellet resuspended in 1 ml of culture medium (L-15 plus supplement; Tab. 2.1.1).

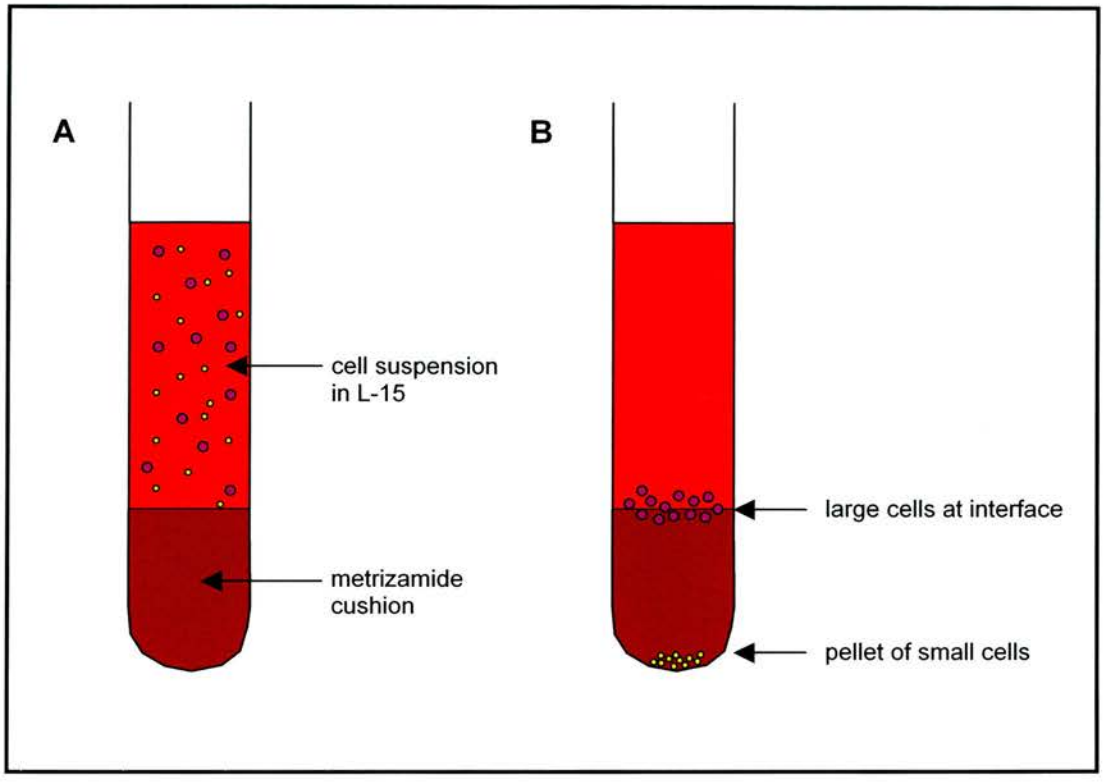

Fig. 2.1.2: Cell separation with metrizamide cushion. **A:** a suspension of mixed cells in L-15 medium is layered on top of a cushion containing metrizamide dissolved in L-15 and then centrifuged. **B:** state after centrifugation: due to the higher density of the metrizamide cushion only small cells are sedimented to the bottom of the dish. The larger cells (large motoneurons) are hindered from penetrating the cushion and assemble at the interface between medium and cushion. They form a turbid band which can easily be collected with a Gilson blue tip pipette.
Note: rather than layering the cell suspension on top of the metrizamide cushion it is easier to add it to the tube first and then gently undermine it with the metrizamide solution using a fine glass Pasteur pipette.

Ingredient	Stock concentration	Amount
L-15		45.4 ml
Glucose	72 mg/ml in L-15	2.5 ml
Penicillin-streptomycin	10,000 U/ml	0.5 ml
Progesterone	2×10^{-5} M	0.05 ml
IPCS mix*		1.55 ml
Sodium bicarbonate	7.5% (w/v) in H^20	1.0 ml
Horse serum		1.0 ml

Tab. 2.1.1.: Composition of culture medium used in initial trials of motoneuron cultures. *IPCS mix: 500 µl insulin (stock: 500 µg/ml), 500 µl putrescine (stock: 10^{-2} M), 500 µl conalbumin (stock: 10 mg/ml), 50 µl sodium selenite (stock: 3×10^{-5} M), all reagents from Sigma; table modified after Henderson et al., 1995

The cells were now ready for immuno-purification. A 90 mm polystyrene bacteriological Petri dishes was prepared for immuno-panning ahead of the purification. The dish was first incubated with 20 µg of affinity purified goat anti-mouse Ig antibody (Cappel) in 13 ml of Tris-buffer (0.05 M, pH 9.5) at 4°C for 24 h. After three gentle washes with 4 ml of CMF-PBS, 10 ml of SC1 supernatant (diluted 1:10 in CMF-PBS) were added and the dish incubated at 4°C for 48 hours (Fig. 2.1.3).

The dishes were then washed 3 times with 4 ml CMF-PBS. 1 ml of the density gradient-purified cell suspension was diluted in 10ml of L-15 and added to the dish. After swirling the dish to allow an even distribution of cells, it was allowed to stand for a minimum of 40 minutes or until a significant number of cells had bound to the SC1 antibody. The unbound cells were then discarded and the dish washed three times with 4 ml L-15

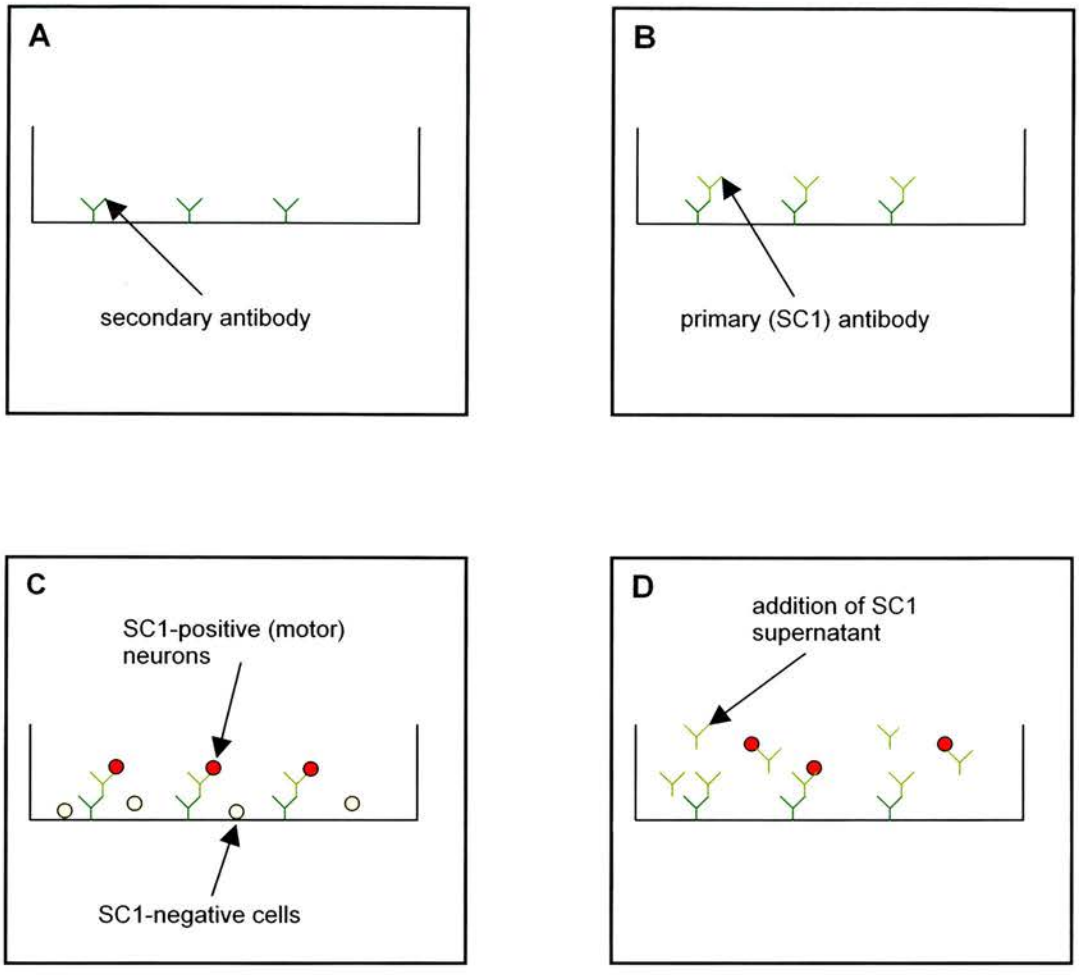

Fig. 2.1.3: Immunopanning method. **A:** A (secondary) antibody capable of binding the Fc-domain of the SC1-antibody (primary antibody) is added to a culture dish. **B:** The SC1-antibody (SC1 supernatant) is added, binding to the secondary antibody anchored to the dish. **C:** The cell suspension containing SC1-positive motoneurons and other SC1-negative cells is added to the dish. The SC1-positive cells bind to the antibody complex and are anchored to the dish. The dish is then washed several times to remove the unbound cells. **D:** SC1-antibody containing supernatant is added to the dish (which competes with the anchored SC1-antibodies for the SC1-antigens on the motoneurons) Agitation of the panning dish resuspends the motoneurons which are now ready for collection.

(Fig. 2.1.3). After pouring off the last wash, 3 ml of undiluted SC1 hybridoma supernatant was added. The dish was then vigorously tapped against a firm surface to dislodge the bound cells. The cell-containing supernatant was collected and the dish washed with a gentle streams of 3 x 1ml of L-15. The medium was pooled with the first eluate. The collected cells were then centrifuged through a BSA cushion (see above), the supernatant discarded, and the cell pellet resuspended in 1 ml culture medium. A small sample of the suspension was transferred to a counting chamber to evaluate the number of yielded cells. The suspension was diluted with culture medium depending on the number of cells required per dish and transferred to 35 mm poly-ornithine/ laminin-coated culture dishes (Greiner) in quantities of 1 ml per dish.

Initial trials were performed on spinal rather than hindbrain motoneurons, mainly because a far greater number of motoneurons can be yielded from the spinal cord. This reduces the number of required embryos and shortens dissection time. The Henderson protocol was followed as closely as possible. All materials, media and reagents were purchased from the companies stated in the published protocol. Nevertheless, the results were unsatisfactory and did not improve with routine over time. Four main problems were identified:

A) The neurons did not thrive well in culture. Dendritic outgrowth was retarded. The vast majority of neurons grew only plump and short processes (Fig. 2.1.4) and died during the first 24 hours.

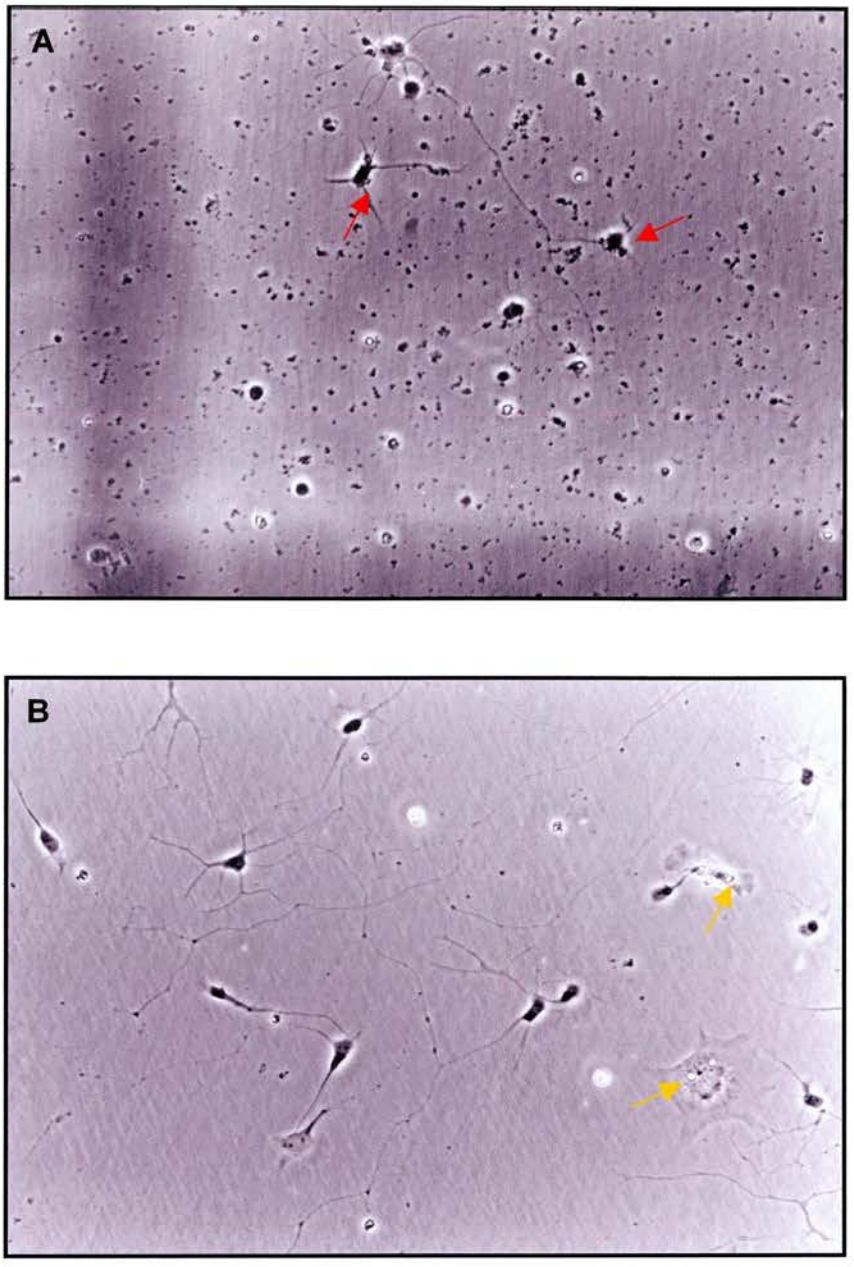

Fig. 2.1.4: Two examples of unsatisfactory motoneuron cultures. **A:** The culture dish is littered with debris. The neurons thrive poorly. Most of them have no or only short and plump processes (red arrows). **B:** An overcrowded motoneuron culture contaminated with non-neuronal cells (yellow arrows).

B) Despite repeated centrifugations through BSA cushions during purification, the cultures were often littered with debris.

C) The purity of the cultures was well below standard. Purity of 90% and more as stated in the Henderson protocol was never achieved (Fig. 2.1.4).

D) Cell dissociation was unsatisfactory and aggregates of cells were a common occurrence in the cultures.

These observations are partially inter-related: For instance, a large amount of debris can have potentially harmful effects on the cultured neurons, thus shortening their lifespan. Insufficient cell dissociation is to blame for low purity as unwanted cells "hitchhike" with the motoneurons through the purification process. Cell aggregates posed a problem for a substantial amount of time. The addition of more DNase to the cell suspension as suggested by Henderson et al. did not improve dissociation. Neither did prolonged and more forceful trituration eliminate the occurrence of cell clumps. Instead, as expected, it destroyed more cells during the purification process. The problem could finally be solved by doubling the concentration of trypsin to 0.1%. Cell aggregates vanished completely from the cultures. Furthermore, the use of DNase became obsolete and it was thus deleted from the protocol. An incubation time of 10 rather than 15 minutes proved sufficient with the increased concentration of trypsin.

However, the cultured cells contrived to grow poorly, and cell death was accelerated. In a first attempt to solve this problem, the metrizamide density gradient was omitted. The metrizamide density gradient poses two problems: Firstly, metrizamide has a known toxic effect on cultured neurons. Secondly, the density gradient selects for large cells. Small motoneurons pass through the metrizamide cushion, and the cultures only contain a subpopulation of motoneurons (Henderson et al., 1995). Omission of the metrizamide step therefore reduces the hazardousness of the purification procedure and allows all motoneurons to appear in the cultures. Alas, it also increases the potential of contamination with floor plate cells. As mentioned above, floor plate cells express SC-1, and are therefore co-purified by immuno-panning. However, meticulousness and a steady hand during dissection can reduce floor plate contamination to a negligible amount (it is always better to lose a few motoneurons than allowing floor-plate contamination!). The motoneuron cultures used for the data presented in this thesis typically contained less than 6% of floor plate cells (see below). Given the fact that all of these cultures were low density cultures (see below), the possible effect of the few present floor plate cells on the survival of the motoneurons could be neglected.

Although the omission of the metrizamide density gradient led to better thriving motoneurons (i.e. improved dendritic outgrowth) on average, the quality of the cultures still varied and cell damage during the purification process was still extensive. Several other hazardous factors were subsequently identified:

1.) Media and reagents used during purification were often at room temperature. This was changed to using cold media (4°C). The rationale behind this was that the low temperature would slow down the motoneurons' metabolism and prevent the possible activation of death pathways that might be switched on by the removal of the cells from their physiological environment.

2.) Impurities of the BSA used during purification can cause toxic effects on neurons. As suggested by the Henderson protocol in this case, the dissolved BSA (4% in L-15) was subsequently dialysed against PBS for 48h and subsequently L-15 for 24h before usage.

3.) The practice of vigorously hitting the panning dish to dislodge bound cells for harvesting creates shear forces that might lead to cell damage. Also, often the immuno-panning technique did not result in the purities desired, and neurons other than motoneurons appeared in the cultures. This problem was solved by abandoning the immuno-panning technique described above and introducing a novel technique using immuno-magnetic beads instead (see below).

4.) The supplemented L-15 medium used for the cultures (Tab. 2.1.1) seemed to have been sub-optimal. Upon suggestion by C. Henderson (verbal communication), the cells were subsequently cultured in Neurobasal medium (Gibco-BRL), supplemented with 0.5 nM glutamine, 25 mM mercapto-ethanol, and 20 μl/ml B27 supplement (Gibco-BRL).

5.) The original protocol advised to add antibiotics (Penicillin/ Streptomycin) to the culture medium. The use of antibiotics has two main drawbacks. Firstly, they are potentially damaging to cells, and secondly, their routine use creates resistant bacterial strains. Since bacterial contamination of cell cultures can be avoided by a clean working technique, the use of antibiotics is not essential, and was therefore abandoned.

These measures finally led to reproducible cultures of thriving motoneurons and to a high degree of purity. Also, cell aggregates and debris were no longer observed.

2.1.3 Immuno-purification with magnetic beads

This immuno-purification technique is based on the same principles as the immuno-panning technique above, i.e. making use of the SC1 surface antigen. The main difference is that here the Fc region of the secondary antibody is not bound to a culture dish but covalently linked to a microscopic magnetic bead. This "magnetic antibody" binds to the SC1 antibody opsonising the motoneurons. The whole cell suspension is subsequently loaded onto a specially designed column (Miltenyi Biotech) which is sitting inside a magnet, thereby retaining the magnetically labelled motoneurons. These are then harvested by removing the column from the magnet and washing it with PBS (Fig. 2.1.5). The protocol used is as follows:

After cell dissociation (see above), the cell suspension was centrifuged through a BSA cushion, the cell pellet gently triturated and

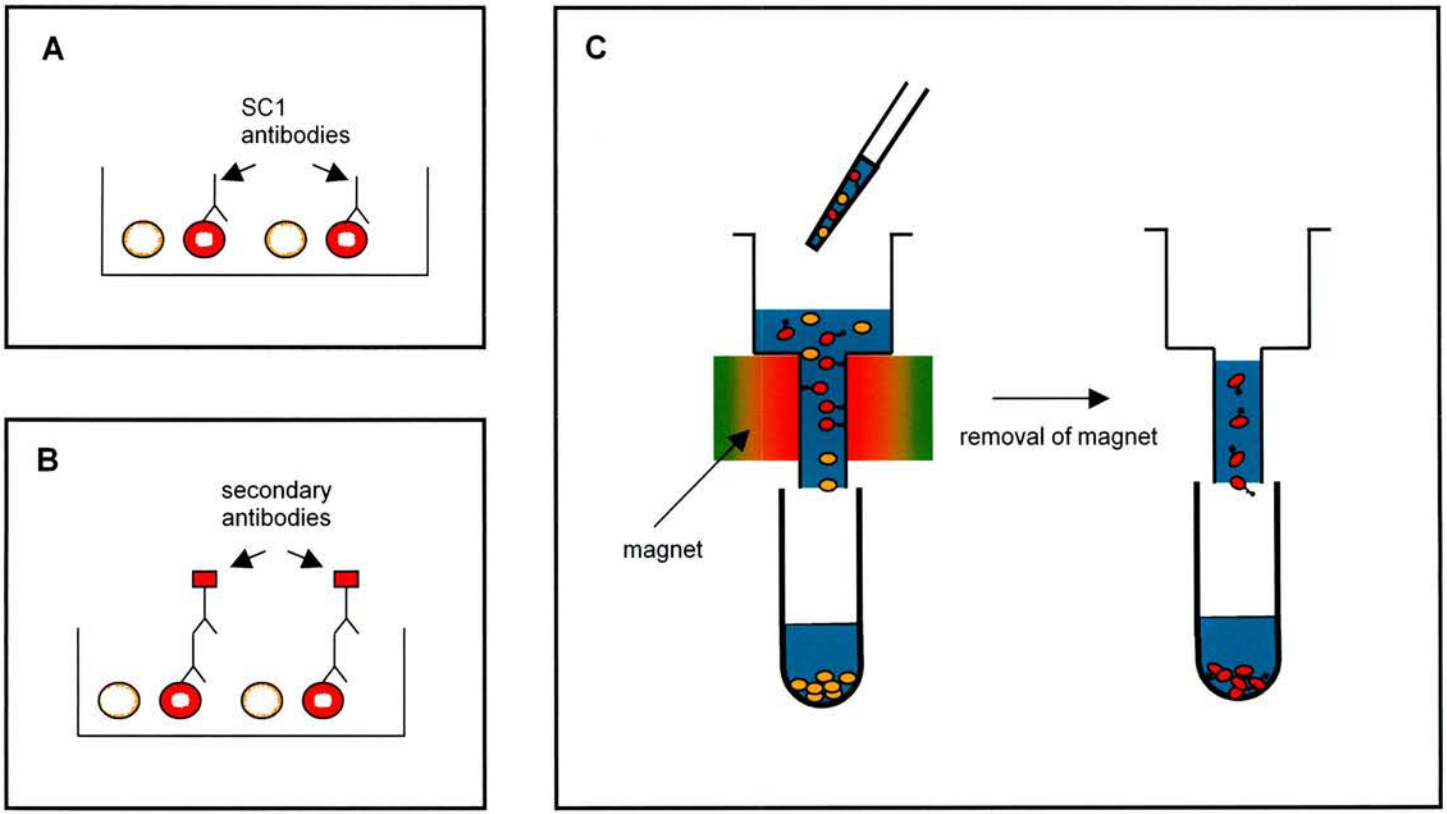

Fig. 2.1.5: Magnetic immunopurification of motoneurons. **A:** The SC1 antibody supernatant is added to the mixed cell suspension. The antibody binds to the SC1 antigen on the motoneurons. **B:** The secondary antibody tagged with a microscopic magnetic bead is added to the cell suspension specifically targeting the SC1 antibody. **C:** The mixed cell suspension is added to a column placed in a magnet. The magnetically tagged (SC1-positive) motoneurons are retained in the column by the magnetic forces, whereas the untagged cells pass through the column (assisted by several washes). The column is then removed from the magnet to release the motoneurons.

incubated with 50 μl BSA/PBS (4% BSA in L-15, diluted 1 in 8 with PBS) and 50 μl SC1 hybridoma supernatant for 10 minutes at 4°C. After washing in 10 ml BSA/PBS, the cells were pelleted by centrifugation and resuspended in 80 μl BSA/PBS plus 20 μl goat anti-mouse IgG magnetic microbead suspension (Miltenyi Biotech). After 15 minutes incubation at 4°C, the cells were again washed with 10 ml BSA/PBS, centrifuged at 400g, resuspended in 500 μl BSA/PBS and loaded onto the separation column placed in a MiniMacs magnet (Miltenyi Biotech). The column was then rinsed four times with 500 μl BSA/PBS to remove non-labelled cells. Thereafter the column was removed from the magnet, and the SC1-positive, magnetically labelled cells flushed out with 1 ml BSA/PBS. The collected cells were washed with 10 ml L-15 medium, centrifuged at 400g for 7 minutes and ready for culture.

Note: the magnetically labelled antibodies remain attached to the motoneurons in culture. However, the magnetic beads are of such small size that it is not possible to observe them under a light microscope.

2.1.4 Culture of motoneurons and assessment of survival and growth rates

The purified motoneurons were suspended in culture medium (supplemented Neurobasal medium, see above). After repeated gentle titration they were plated at a low density of approximately 1,000 cells per dish, in 35 mm tissue culture dishes (Greiner), coated with poly-ornithine and laminin (Davies et al., 1993). The reason that neurons were plated at a low density is to avoid possible paracrine influences between the

motoneurons that might influence their thriving and survival. Also, the practice of adding serum to the culture medium was abandoned here to prevent possible undefined trophic influences from substances in the serum.

Neurotrophic factors were added to the culture medium at the time of plating. Purified recombinant human MSP was purchased from R & D Systems and purified recombinant human CNTF was a gift of Dave Shelton, Genentech Inc. The neurons were incubated overnight at 37°C before an initial cell count was conducted. The reasons for delaying the first cell count were twofold:

1.) Immediately after the cells are seeded into the culture dish, their morphology is indistinguishable. All cells, regardless of their type, appear as smooth circular (spherical) objects. It is therefore impossible to recognize floor plate cell contamination, and these cells would have been unwittingly included in the initial count.

2.) A varying number of motoneurons are damaged beyond recovery during the purification process. These cells either die prematurely or fail to thrive (Fig. 2.1.4). Again, there is no certain way to distinguish these damaged cells from healthy motoneurons until they are well established.

Typically, about 20% of the plated cells were lost during the course of the first night, even in the presence of known growth factors like CNTF. This is a higher loss then can be observed over the following two 24h periods

which is most likely due to premature death of neurons severely damaged by the purification process.

The initial cell count was conducted first thing in the morning, about 16 hours after plating. For each dish, the count included all cells lying within the confinements of the counting grid that had been carved into the bottom (outer side) of the dish (Fig. 2.1.6). The centred grid which consisted of 5 rows and 5 columns covered about a third of the dish.

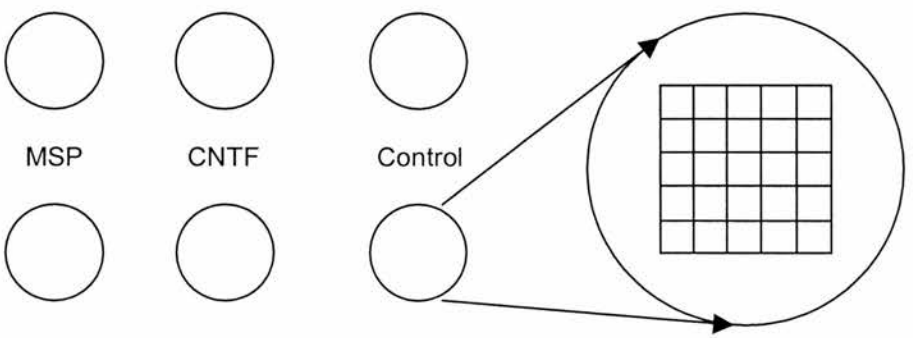

Fig. 2.1.6: Single experiment set-up: each neurotrophic factor (here MSP and CNTF) was tested in two culture dishes simultaneously. Grids had been carved at the back of the dishes' bottoms to facilitate counting.

Given an average total of about 1,500 initially plated cells and the loss of about 20% of these cells during the first night in culture, the number of cells counted ranged between 200 and 300 neurons. Two further counts were conducted at 24 hour intervals after the initial count, and the number of surviving neurons expressed as a percentage of the first count (Tab. 2.1.2).

Initial count (16 hours after plating)	24 hour count (40 hours after plating)	48 hour count (64 hours after plating)
256 cells = *100%*	234 cells = *91%*	216 cells = *84%*

Tab. 2.1.2: Example showing the counting results from one dish. The number of cells yielded in the 24 hour and 48 hour counts are expressed as a percentage of the motoneuron number obtained from the initial count which is taken as 100%.

Only healthy looking, well-established neurons were included in the counts. Living and dying neurons can be distinguished by morphological means. Healthy motoneurons have smooth, spherical, phase-bright cell bodies, and exhibit extensive neuritic outgrowth. In contrast, dying neurons are easily recognised by cytoplasmic vacuolisation, shrinkage and fragmentation of cell body and neurites (Allsopp et al., 1993a).

2.1.5 Measurement of neurite lengths

As there seems to be some confusion in the literature about the terminology of neuronal processes, I include a brief note to the reader, showing how the different terms should be used: *axon* refers to the neurons efferent branch, of which a typical neuron only has one (although collaterals are common). *Dendrite* refers to a neuron's afferent branches, of which there is usually a multitude (apart from unipolar, bipolar and pseudo-bipolar neurons). The term *neurite* is used to collectively refer to both axon and dendrites.

In order to measure the extent of the motoneurons' neuritic arbors, the neurons were grown for 48 hours in the presence of growth factors and in control conditions (see Chapter 3). This provided enough time for the neurons to grow sufficiently long neurites. Again, the cells were plated at low density to minimise overlap between the neurites of neighbouring cells which would have made the tracking of individual branches very difficult.

As there was no integrated, digital imaging system available at the time of the study, accurate hand-drawings of the cultured neurons had to be made. This was achieved with the aid of a camera lucida attached to the microscope. The camera lucida projects the image of any object placed underneath it (in this case a piece of drawing paper) into the microscope's eyepiece, so that both, the cell culture as well the as the drawing paper can be viewed at the same time. It is thus possible to draw the outlines of individual cells onto the paper.

The drawings were subsequently scanned into a computer, and the total neurite lengths of individual neurons determined using Scion Image for Windows (Scion Corporation). *Total neurite length* means that all processes (axon, dendrites and all of their visible branches) of an individual motoneuron would be measured and the length of each and every one summed up. For each experiment, 30 randomly picked cells were drawn per growth factor to be tested, and the average total neurite length calculated for the given culture.

2.1.6 Assessment of culture purity

If one were to dissociate and culture the caudal hindbrain of E5.5 chick embryos without purifying for a certain cell population, one would obtain a mixed culture containing 5 different types of cells: glial cells, floor-plate cells, sensory relay neurons, reticular neurons, and motoneurons. As demonstrated above, immuno-purification eliminates all cells apart from motoneurons and floor plate cells, the latter being removed by means of dissection. However, no purification technique is entirely reliable, and some degree of contamination is to be expected. Non-neuronal cells are readily detected due to their distinct morphology but it is nearly impossible to distinguish the three neuron types merely on morphological grounds. A specific marker is therefore needed. In this case, the cultures were immuno-stained with a monoclonal antibody against Islet-1, a transcription factor that is specifically expressed by embryonic motoneurons (see Introduction). Since it is neither feasible nor economical to perform an immuno-stain in parallel with every culture, purity checks were performed at four different times during the course of the study. This should be sufficient to ensure that standards necessary to obtain reliable results are maintained.

The anti-Islet-1 antibody was used in form of a diluted supernatant obtained from a hybridoma cell line (see next sub-chapter). Purification of the antibody was not necessary as the supernatant used in conjunction with the Vectastain ABC-kit (Vector Laboratories) resulted in a clear and reliable nuclear stain of the cultured motoneurons.

For the purity checks, motoneurons were grown for 24 hours as described above. Thereafter, the culture medium was removed and carefully replaced with 1 ml 100% methanol (-30˚C) for fixation. This is the most critical step in the protocol, for using methanol that is too warm or adding it too forcefully will inevitably detach the cells and render all subsequent efforts useless. It is of the utmost importance that fixation of the cells is achieved in an instant. After a few frustrating attempts, I found the right balance by slightly tilting the culture dish (no more than 10˚) and adding the ice-cold methanol swiftly but gently through a Gilson's blue-tip to the lowest point of the dish. The dish was then incubated at -30˚C for 10 minutes.

In order to quench endogenous peroxidase activity, the fixative was removed and the cultures incubated with 1% H_2O_2 in 100% methanol (4%) at room temperature for 20 minutes. Subsequently, the dishes were washed three times with phosphate-buffered saline (PBS, Oxoid). Again, this has to be done with the greatest care as cells still detach easily. It is a good idea in general to add all of the solution to the tangent of the dish and flood it rather than hosing down the entire culture with a jet stream from the pipette.

Since Islet-1 is not only an intracellular but a nuclear marker, antibody penetration had to be facilitated by incubating the cells with 50 mM lysine (Sigma Aldrich) and 0.1% Triton X-100 (Sigma Aldrich) in PBS for 15 minutes. The penetrating agent was then replaced with 2% horse serum and 2% BSA in PBS to prevent nonspecific binding of the antibody. The blocking agent was left for 30 minutes after which the supernatant was added

and the cells incubated at 4°C overnight. Two different supernatants (i.e., two antibodies, targeting different domains of the Islet-1 protein; see next sub-chapter) were used, each diluted 1:4 in PBS, 2% BSA, 2% horse serum and 0.1% Triton X-100.

The next day, the primary antibody was replaced with a biotinylated, affinity purified horse anti-mouse Ig antibody (Vector Laboratories). The ABC-kit makes use of the biotin/avidin system. Avidin is a glycoprotein that forms an essentially irreversible bond with the vitamin biotin. By conjugating horseradish peroxidase to avidin, the protein can act as a bridge between the enzyme and the biotinylated secondary antibody (Vector Laboratories Product Information). 3,3'-diaminobenzidine (DAB) in conjunction with Urea Hydrogen Peroxide is used as the chromogenic substrate:

Peroxidase + $2H_2O_2$ => O_2 + $2H_2O$

O_2 + **DAB => insoluble, brown-black precipitation** (Sigma Fast Product Information)

The cells were incubated with the secondary antibody at room temperature for one hour. They were then washed three times with 0.05 mM Tris-HCl, ph 7.6 (Sigma Aldrich) and incubated with the avidin/peroxidase reagent at room temperature for 30 minutes. After another three washes with Tris-HCl, the substrate (DAB plus Urea Hydrogen Peroxide, Sigma Aldrich) was added which produced a dark brown nuclear stain after about 10 minutes (Fig.2.1.7).

Fig. 2.1.7: Purity check of motoneuron culture. The cultured cells were stained with an antibody against the motoneuron-specific transcription factor Islet-1. Note the prominent stain of the cultured motoneurons' cell nuclei.

The four quality checks conducted throughout the course of this study demonstrated an average purity of more than 90% (92.34%). Thus, less than 10% of the cells in the cultures were non-motoneurons, of which most (about two thirds) were floor plate cells. This leaves a minute amount of reticular or sensory relay neurons (about 1%) which would have been included in the cell counts (due to their neuronal morphology). This is consistent with the fact that floor plate cells are the most likely contamination as they are not eliminated by the purification technique and only removed by means of dissection. As they are also easy to recognize due to their morphology, they can therefore be used as an indicator of the degree of contamination in routine cultures.

Moreover, at one stage a parallel immunostain was conducted with an SC1 antibody (i.e., an antibody against the very antigen that had been used for purifying hypoglossal motoneurons, (see above) which showed that 97.57% of the cultured neurons were positive for this marker. However, since SC1 is a surface antigen, it is not as easily detectable in culture as is Islet-1. It nevertheless produces a pronounced neuritic stain which was used here to distinguish non-SC1 expressing neurons from SC1-positive neurons.

In summary, these quality controls - even though performed at intervals - confirmed the magnetic bead technique as a reliable method to purify motoneurons.

2.1.7 Generation of monoclonal antibodies

Both monoclonal antibodies used in this study (SC1 and Islet-1) were derived from mouse hybridoma lines generated by Thomas M. Jessell. The SC1 hybridoma cells were a kind gift from Christopher E. Henderson, and the Islet 1 hybridoma cells were purchased from the Iowa Hybridoma Cell Bank. In the case of Islet 1 two different hybridoma cell lines were used simultaneously for better results: Islet 40.2D6 and Islet 39.4D5. Both antibodies recognise the C-terminal portion of Islet-1.

The hybridoma cells were rapidly thawed in a 37°C water bath for 1 minute and transferred to 5 ml of fresh culture medium (Iscove's Dulbecco's Modified Eagles Medium, Gibco-BRL for Islet hybridomas and RPMI, Gibco-BRL for SC1 hybridomas) and centrifuged at 125 g for 10 minutes. This was necessary to remove the freezing additive (DMSO, Gibco-BRL). The cells were then resuspended and transferred to T-75 suspension culture flasks (Greiner) containing 20 ml of culture medium plus 20% Fetal Bovine Serum (FBS, Gibco-BRL), 200mM L-Glutamine (Sigma) and 50.000 units of Penicillin-Streptomycin (Gibco-BRL) and incubated at 37°C.

The hybridoma cells had an approximate doubling rate of 24 hours, and were split 1:4 every second day. The cells were spun down at 125 g for 3 minutes and resuspended in 20 ml of fresh culture medium plus additives (see above). The cell suspension was then split into four 5 ml portions. Each portion was added to 15 ml of fresh enriched culture medium in T75 flasks (see above). Some passages were used to harvest cells by centrifugation of

the cell suspension at 125 g for 3 min and resuspension in 4 ml of medium plus 0.5 ml DMSO and 0.5 ml Fetal Calf Serum (FCS, Gibco-BRL). They were then transferred into liquid nitrogen for long term storage.

For antibody generation, cells were grown to saturation level (2 to 3 days). The suspension was then centrifuged at 125 g for 10 minutes and the supernatant pooled. The cell pellet was resuspended in 1 ml of fresh culture medium and transferred to a T-75 flask containing 17 ml of supernatant plus 119 mg of HEPES and 200 mg glucose in 2 ml of fresh medium. The cell suspension was incubated at 37°C for a week after which it was again centrifuged and the supernatant stored in 1 ml aliquots at –40°C. Purification of the antibodies was not necessary for the procedures used in this study. Only diluted supernatant was used for immuno-purification as well as immunocytochemistry (see relevant subchapters).

2.2. Detection of MSP mRNA expression by RT-PCR

A semiquantative RT/PCR assay was used to determine the expression pattern of MSP mRNA in a variety of embryonic chicken tissues at E5.5. Total RNA was extracted (Chomczynski and Sacchi, 1987), treated with DNAse (Amersham Pharmaca Biotech Inc.), purified using an RNAID kit (BIO101 Inc.) and recovered in 100-1,000 ml (depending on the tissue size) of DEPC-treated H_2O. Quantitative, competitive RT/PCR was used to determine the amount of mRNA for the housekeeping L27 ribosomal protein in each RNA sample (Allsopp et al., 1993b). The RNA was reverse transcribed for 1 hour at 37°C with Bio/Gene MmuLV-RT, RNaseH-enzyme (Bio/Gene) in a 30 μl reaction containing the manufacturers' buffer supplemented with 0.5 mM dNTPs (MBI Fermentas Inc.) and 10 μM random hexanucleotides. A 5 μl aliquot of each reverse transcription reaction was then amplified in a 50 μl PCR reaction containing 1 x PC2 buffer (Helena BioSciences), 0.1 mM dNTPs, 0.85 units of Taq Supreme (Helena BioSciences) and 20 pmoles of primers. The forward assay primers for each cDNA were 5'-CGCACACCCTTTGACTACTG-3' for MSP and 5'-GGCTGTCATCGTGAAGAACATC-3' for L27. The reverse assay primers for each cDNA were 5'-CCACCACACGTTGCTTCTG-3' for MSP and 5'-CTTCGCTATCTTCTTCTTGCCC-3' for L27. The primers hybridise 100bp and 83 bp apart in the chick MSP and L27 cDNAs, respectively. MSP cDNA was amplified by cycling at 95°C for 30 seconds, followed by 30 seconds at 63°C, followed by 21 seconds at 68°C. L27 cDNA was amplified by cycling

at 95°C for 45 seconds, followed by 50 seconds at 50 °C, followed by 50 seconds at 68°C. The reactions were then completed with a 10 minute extension at 68°C.

To ascertain the reproducibility of the MSP results, each PCR was repeated twice for two different (27 and 29) number of cycles. The cycling conditions were optimal for the amplification of the MSP transcript to that the rate of reaction did not plateau. The PCR products were separated on 8% non-denaturing polyacrylamide gels. These gels were subsequently stained with SyberGold (Cambridge Biosciences), and the intensity of the RT-PCR products were determined using a gel documentation system (Biogene) with Phoretix software (Phoretix International).

2.3. Histology

2.3.1. Specimen collection

For the quantification of dopaminergic neurons in the substantia nigra, brains were collected from three different ages: P18, P5 and 3 months. To minimize variance between the specimens, brains for each study were usually collected together, and processed and embedded in parallel. For experimental design, see Chapter 5.

Adult and postnatal mice were killed by exposure to CO_2 gas in rising concentrations and decapitated immediately post-mortem. Embryos which are not sensitive to CO_2 gas were culled by swift decapitation. Entire brains were removed with the most rostral parts of the spinal cord attached. After scalping, the rostral cervical vertebrae were split along their laminae with a fine pair of dissection scissors. The cut was extended along the sagittal suture of the skull towards the frontal bone. Small transverse cuts were made to either side of the midline at eye level and through the occipital bone. The temporal and parietal bones could then be opened up with a pair of strong, curved forceps exposing the brain which was carefully lifted out of the base of skull severing the cranial nerves. Brains of E18 embryos were not removed from the skull due to their small size and the likelihood of damaging the nervous tissue during dissection. Since the skull is largely cartilaginous at this age, decalcification of the specimen prior to fixation is not required either.

The brains were fixed in Carnoy's fixative (60% ethanol, 30% chloroform, 10% glacial acetic acid) at 4°C overnight. The decision to use Carnoy's as a fixative was made after an optimisation trial run with three different fixatives: neutral buffered formalin (NBF), formalin/ alcohol/ acetic acid (FAA), and Carnoy's solution. Since it is not possible to know a priori which fixative works best with an antibody employed for staining, a trial run is obligatory. For instance, Carnoy's fixative significantly damages cell membranes, and antibodies directed against surface proteins often do not work with this fixative. On the other hand, formaldehyde-based fixatives cross-link cellular proteins and mask antigen sites. This makes it necessary to introduce some means of antigen retrieval prior to the actual stain. For the three antibodies used in these studies (anti-tyrosine hydroxylase, anti-γ-synuclein, anti-choline-acetyl transferase), Carnoy's fixative proved to deliver the best results.

2.3.2. Specimen processing, embedding and cutting

The fixative was washed out, and the brains dehydrated by means of a graded alcohol series (see Tab. 2.3.1). The alcohol was then replaced with chloroform which is miscible with paraffin wax. The specimens were immmersed in a 1:1 mixture of ethanol and chloroform for 30 minutes, transferred to pure chloroform for 1 hour and incubated in a second change of chloroform overnight, at room temperature.

96% ethanol	5 minutes
96% ethanol	5 minutes
96% ethanol	5 minutes
100% ethanol	10 minutes
100% ethanol	30 minutes

Tab. 2.3.1: Specimen processing: graded alcohol series

The next day, the specimens were passed through 3 changes of melted wax at 37°C and embedded in paraffin blocks. The paraffin blocks were allowed to harden at 4°C for a minimum of 24 hours. The rapid cooling of the wax at 4°C after embedding ensures a finer crystalline wax structure than would be achieved by leaving the wax to harden at room temperature.

The embedded brains were cut into 8μm sections, using a Leica microtome and floated on a water bath at 37°C, from where they could easily be transferred to slides. Typically, two strips of 5 sections each were placed onto polysine coated slides. Specimens destined for immunostaining were placed onto gold-coated slides. Gold-coated slides ensure greater adherence of specimen sections and therefore decrease the likelihood of detachment during the rather hazardous process of immunostaining. Sections destined to be used for γ-synuclein expression analysis were placed on alternating slides to allow for control stains with Haematoxylin/Eosin (see Fig. 2.3.1). The slides were allowed to dry at 37°C for at least 24 hours to ensure maximum adhesion.

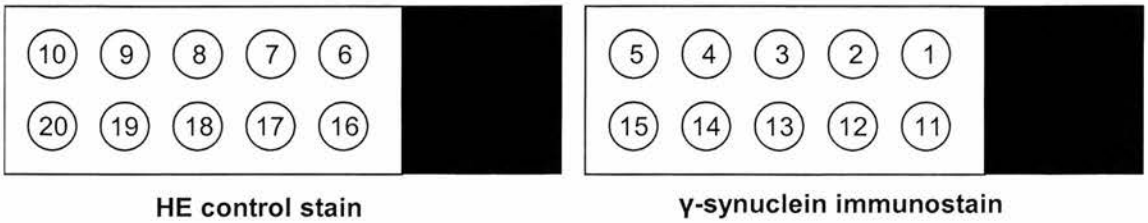

Fig 2.3.1: Placement of sections for γ-synuclein expression studies. The placing of strips of 5 sections each onto alternating slides ensures closer proximity between the structures depicted with the immunostain and those shown by the control stain.

2.3.3. Immunostaining of dopaminergic neurons

Dopaminergic neurons express Tyrosine Hydroxylase, the pace maker enzyme in the catecholamine synthesis pathway which converts L-Tyrosine to L-Dihydroxyphenylalanin (L-DOPA, Fig. 2.3.2). This enzyme is widely used as a marker for dopaminergic neurons. A monoclonal antibody against tyrosine hydroxylase was purchased from Novocastra Laboratories. For antibody detection a biotinylated antibody coupled with an avidin/peroxidase complex (Vectastain ABC-kit, Vector Laboratories, see above) and Diaminobenzidine/ Urea Peroxide (Sigma) were used.

The paraffin sections were cleared in two washes of xylene and rehydrated through a graded alcohol series (see Tab. 2.3.2).

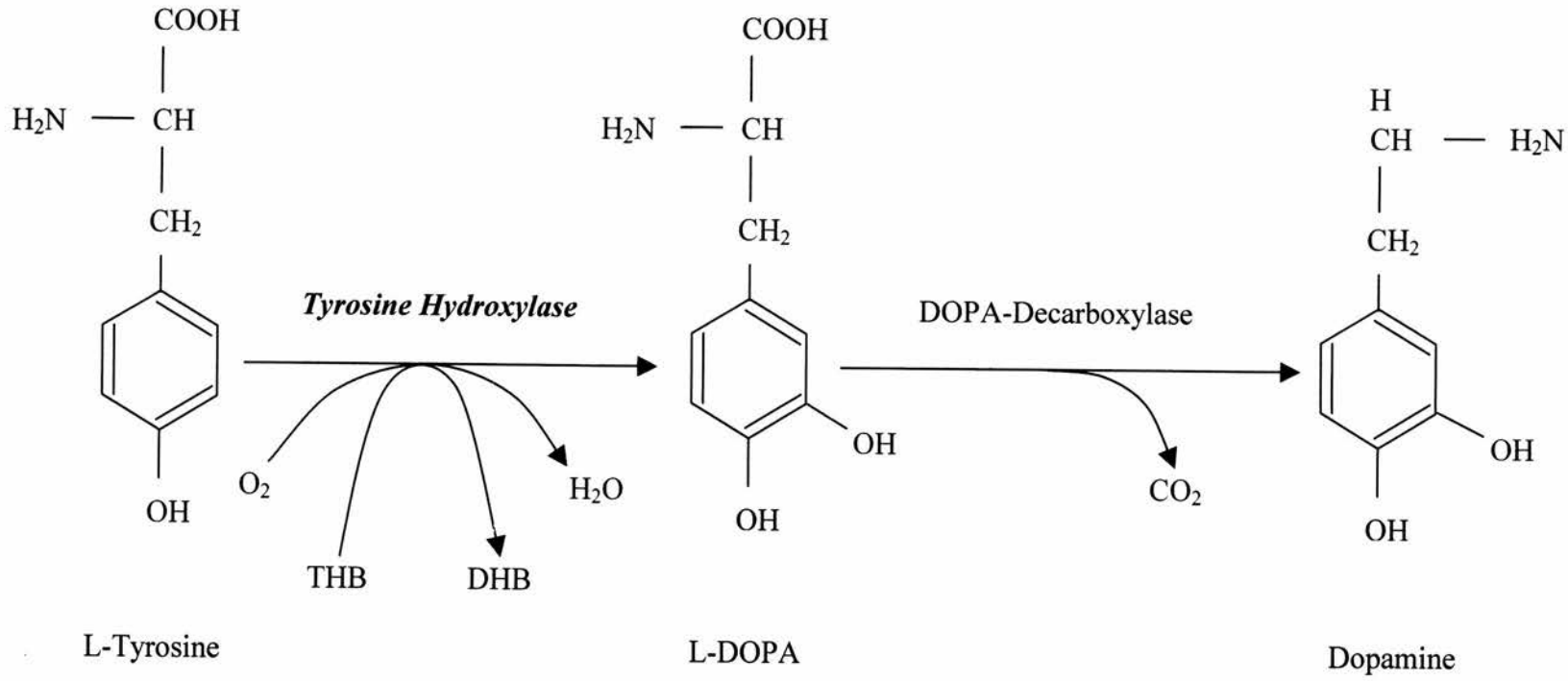

Fig. 2.3.2: Dopamine synthesis. Tyrosine hydroxylase catalyses the conversion of tyrosine to L-DOPA. DHB: dihydrobiopterin, THB: tetrahydrobiopterin.

Rehydration		Dehydration	
100% ethanol	3 minutes	H_2O	2 minutes
100% ethanol	3 minutes	70% ethanol	2 minutes
96% ethanol	2 minutes	96% ethanol	2 minutes
70% ethanol	2 minutes	100% alcohol	3 minutes
H_2O	2 minutes	100% alcohol	3 minutes

Tab. 2.3.2: Re- and dehydration of sections for immunostaining

Endogenous peroxidase activity was quenched by incubating the slides in 3% H_2O_2 in methanol for 20 minutes. After washing twice for 5 minutes with PBS the tissues were blocked in 10% horse serum and 0.4% Triton X in PBS for a minimum of 30 minutes. The Tyrosine Hydroxylase mouse monoclonal antibody was added at a working dilution of 1:40 and the sections incubated at 4°C overnight. Unbound antibody was then removed through two washes with PBS and an affinity purified horse anti-mouse IgG antibody (ABC-kit, Vector laboratories) added for 60 minutes at room temperature. Unbound antibody was washed off with PBS and the material incubated with the avidin/peroxidase complex from the ABC-kit for another 30 minutes (for the biochemistry of the ABC kit see above). Superfluous reagent was washed off and DAB and Urea H_2O_2 added. After about 3 to 5 minutes a clear dark brown stain could easily be detected with the naked eye in sections containing dopaminergic neurons. The sections were then dehydrated through an alcohol series, cleared with xylene for 2 times 5

minutes and mounted with DPX (BDH). Anti TH immunohistochemistry produced a dark brown cytoplasmic stain with a clear nucleus.

Essentially the same protocol was used for γ-synuclein and ChAT stains. Since the polyclonal anti-γ-synuclein antibody was generated by immunizing rabbits, a goat anti-rabbit secondary antibody was used and goat serum as a blocking agent.

The polyclonal anti-γ-synuclein antibody was generated in the lab of Vladimir Buchman by Natalia Ninkina and affinity-purified by Darren Robertson. The methodology for the generation of this antibody including Western blot analysis of its specificity has been published previously (Buchman et al., 1998)

2.3.4. Staining and identification of motoneurons

No *specific* marker exists to date to perform immunohistochemical stains on adult motoneurons. However, judging by the immunostains of cranial motoneurons with anti-choline acetyl transferase (anti-ChAT, see Chapter 4), one might be tempted to regard the use of this antibody as the ideal means for identifying motoneurons in cell counts. ChAT catalyses the synthesis of acetylcholine from acetyl coenzyme A (acetyl CoA) and choline. Acetylcholine is the neurotransmitter of several neuronal populations in the efferent nervous system: motoneurons, pre-and postganglionic parasympathetic neurons, and preganglionic sympathetic neurons. These populations are therefore known as *cholinergic neurons*. The enzyme is

synthesized in the cytoplasm and transported via axonal transport into the synaptic endings where it catalyses the synthesis of acetylcholine. Analogous to tyrosine hydroxylase in dopaminergic neurons (see above), it can therefore be detected in the cytoplasm, the axon and the nerve endings of cholinergic neurons. Since the exact location of cranial motoneurons can be easily established in histological sections by using an anatomical atlas, the expression of ChAT in sympathetic and parasympathetic neurons does not present a problem, and an anti-ChAT antibody could be regarded as relatively specific. However, Rodella and colleagues have shown that some interneurons which are scattered throughout most cranial motor nuclei, also express ChAT (Rodella et al., 1994). Although interneurons are small in size and most motoneurons are substantially larger, some motoneurons are of approximately the same size as interneurons. Given this predicament, the use of an anti-ChAT antibody presents no advantage to a basic histological stain such as cresyl-violet or neutral red. Taking the cost of antibodies and the extra time spent on immunostains (2 days compared to half a day for basic histological stains) into account, I decided to use a basic stain for the motoneuron counts. The choice of neutral red was made after deliberation with several histology technicians in the department.

Nevertheless, none of the three staining techniques mentioned above circumvents the problem of distinguishing small motoneurons (i.e. gamma motoneurons) from interneurons which are dispersed at random through a cranial motor nucleus. The decision to be made was whether to include a certain (and unaccounted) number of interneurons into the count or select for

the larger motoneurons. In order to be able to make the claim that the absence of γ-synuclein has an effect on the number of motoneurons in a given nucleus (or a subpopulation thereof), it was clear that the first option was not acceptable. I therefore decided to exclude all small neurons and count only large (~20 μm diameter) cells (Fig. 2.3.3). Given some experience this is not an unfeasible task!

Apart from motoneurons and interneurons every cranial motor nucleus contains glial cells (astrocytes and oligodendrocytes). In adult mice, these cells have a diameter of between 5 and 10 μm (Brophy, P., personal communication). Most of this space is occupied by the nucleus which is surrounded by a small cytoplasmic seam more or less invisible in neutral red stains (Fig. 2.3.3). These glial cells can easily be distinguished from neurons and don't pose a threat to motoneuron counts.

The staining protocol used for neutral red stains is straight forward. All brains were fixed in Carnoy's and processed, embedded and cut as described above for immunostains. As identification of motor nuclei was easy using Paxinos'and Franklin's mouse brain atlas (Paxinos and Franklin, 2001), and control stains (e.g. with anti-ChAT) were therefore unnecessary, sections were continuously placed in 2 strips of five sections onto polysine slides. The samples were rehydrated as described above and incubated in a 1% solution of neutral red in distilled water for 30 minutes. Dehydration was achieved by rapid progression through a graded alcohol series. The samples were then

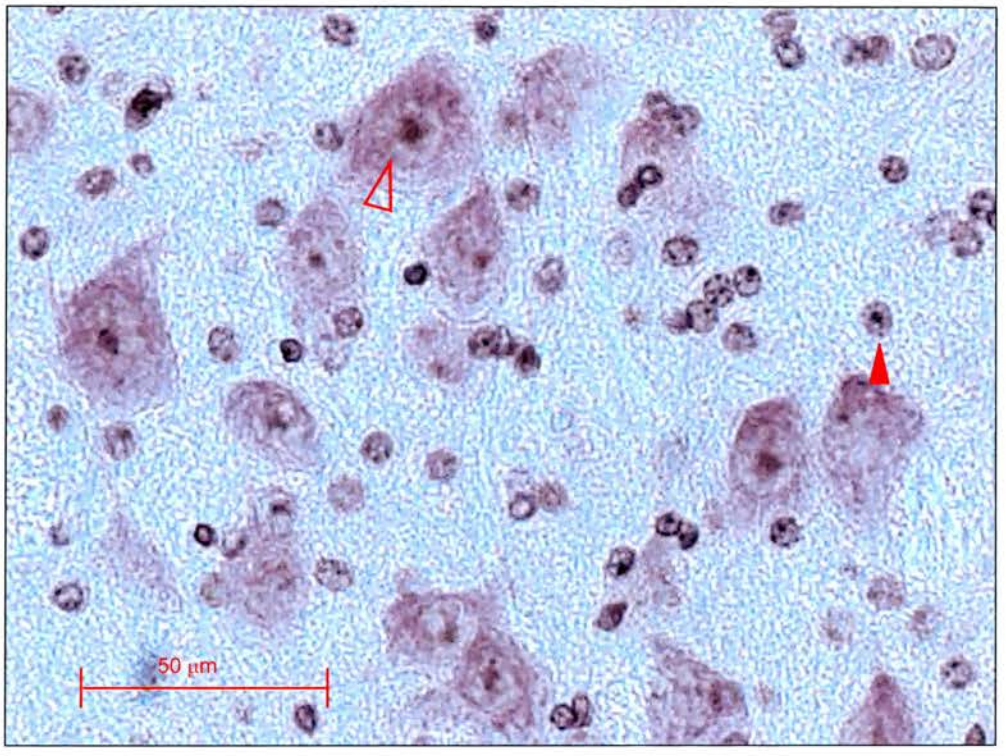

Fig. 2.3.3: High magnification image of the facial nucleus stained with Neutral Red. Interspersed between the large motoneurons (open arrowhead) are small glial cells with no or little cytoplasmic stain and a small nucleus (filled arrowhead).

taken through two changes of xylene (5 minutes each) and mounted with DPX.

2.3.5 Cell counts

To begin with, a note of caution for the reader: the term "nucleus" will be used with two different meanings in this sub-chapter. It either refers to the assembly of a certain population of motoneurons in the brainstem, i.e. a cranial motor nucleus, or to the DNA-containing nucleus of a single cell. In most cases I have taken care to specify which type of nucleus I am referring to by using terms like motor nucleus or cell nucleus but for stylistic reasons that could not be strictly adhered to.

All histological cell counts for this thesis were conducted employing a stereological method termed fractionator. Stereology is the histometrical technique by which quantative information on the volume, surface area, and/or particle numbers of objects within a two- or three-dimensional structure is obtained from one- or respectively two-dimensional data (Bancroft and Stevens et al., 1996). The fractionator method can be used if only total particle numbers - or as in this case, cell numbers – are required.First described by Gunderson in 1986, it delivers a direct estimate of particle number independent of the volume of the structure that the particles are part of (Gunderson, 1986). In terms of the studies presented here, it means that the total number of motoneurons in a cranial motor nucleus or the total number of dopaminergic neurons in the substantia nigra can be estimated without prior knowledge of the volume of the nucleus. The

beauty of this technique is that it is not affected by shrinkage. One of the biggest problems encountered in histometry (quantitative histology) is tissue shrinkage which can occur at all stages of specimen processing, e.g. fixation, processing, deparaffination, staining. Howard and Reed point out that the removal of paraffin from the specimen, prior to staining and mounting is known to cause a collapse of up to 60% of the sections' height (Howard and Reed, 1998). What's more, this shrinkage is variable and difficult to measure. Even though all care has been taken in the studies presented here to collect, fix, process and stain specimen in bulk and therefore subject them to identical conditions and timing, it is easy to see that not all specimens could have been collected at the same time as research progressed. For example, after preliminary data suggested that there might be a difference in neuronal numbers in the substantia nigra between γ-synuclein knockout and wild type mice, more specimens had to be collected to confirm these findings. Moreover, brains were taken from mice of different ages to establish the point in time where exaggerated cell death might occur during development. In this context, it is interesting to recall the findings of Haug and colleagues who "binned" 30 years of research efforts on the alleged loss of neurons in old people based on cell density studies by showing that young brains are subject to more shrinkage than old brains if fixed in formalin, thereby introducing a false positive bias (Haug et al., 1984).

If a stereological technique (e.g. the disector method) that depends on cell density rather than direct cell number estimates is employed, the reference volume, (i.e. the volume of a certain cranial motor nucleus) has to

be measured before an estimate of particle number can be made. However, cranial motor nuclei are not as clearly defined as spinal ganglia for instance. In order to obtain the precise volume of a structure in histology one has to be able to draw an exact outline of the structure in a section. The difficulty of employing this technique in cranial motor nuclei is illustrated in Fig. 2.3.4.

Bearing the problems outlined above in mind, I decided that the fractionator technique would be the most feasible method to obtain correct estimates of neuron numbers in my case. The principle of this technique is rather simple: a fraction of the whole object of interest is taken, e.g. a tenth. The *total* number of particles in this fraction is counted and then multiplied by the denominator of the fraction, in this case 10 (see Howard and Reed, 1998). Applied to the concrete case of counting motoneurons in a cranial motor nucleus, this translates into the following:

The whole brainstem was sectioned into sections of equal thickness (8 μm) to include all six motor nuclei of interest. The number of motoneurons in each motor nucleus was counted in total on every 5^{th} section. The motoneuron numbers obtained from these sections were summed up and the result multiplied by 5, giving an estimate of the total number of motoneurons contained in the motor nucleus. In general, this sampling technique can be expressed by the following formula:

$\mathbf{N_t = 1/f \times N_f}$, whereby N_t is the total number of neurons, N_f the number of neurons counted in the sampling fraction and f the sampling fraction. For example if the total number of neurons counted in every 5^{th} of 40 sections

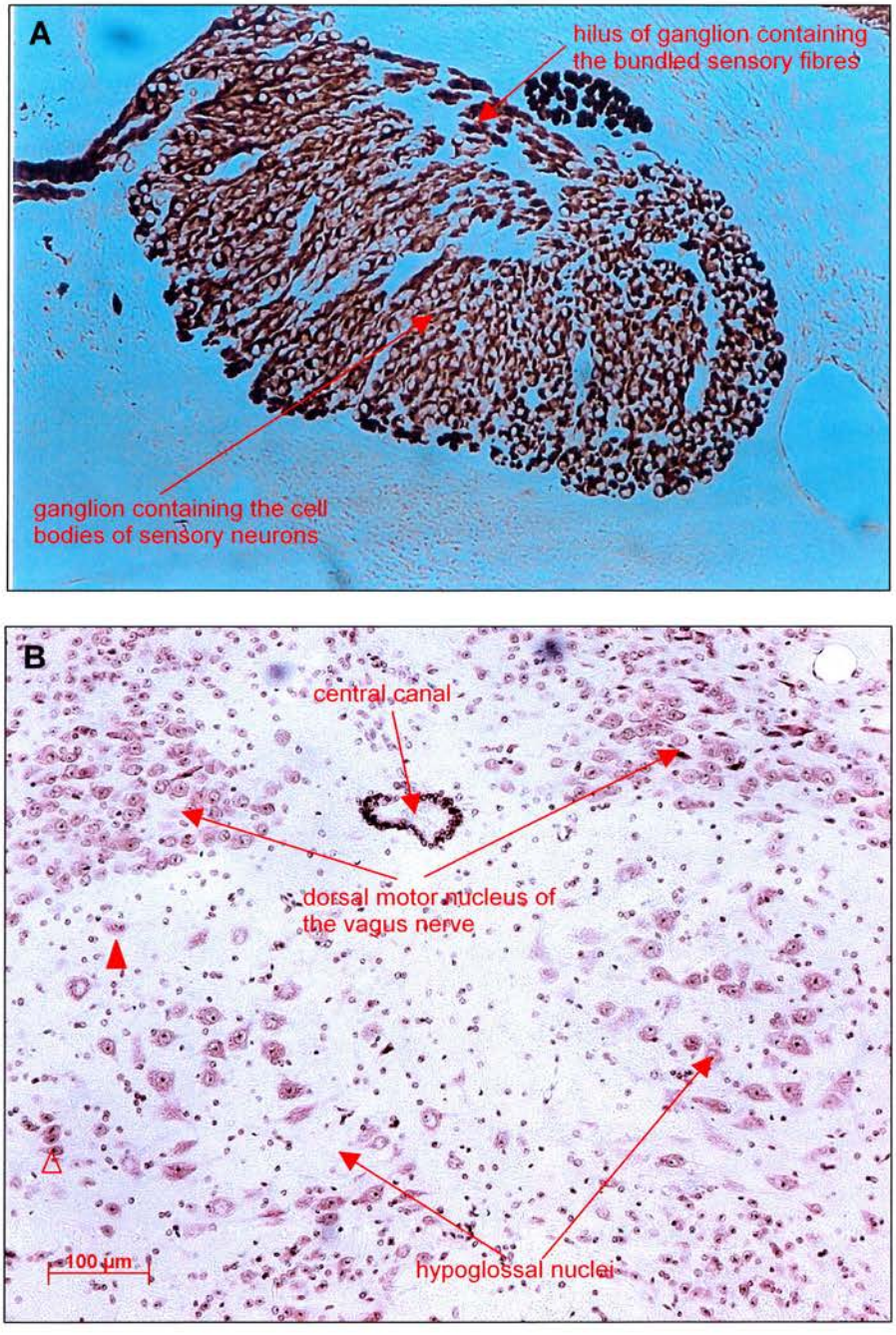

Fig. 2.3.4: Outlining neural structures. **A:** anti-neurofilament stain of a dorsal root ganglion. Note the tightly packed sensory neurons forming a clearly outlined structure (photo courtesy of G. Middleton). **B:** neutral red stain of the hypoglossus nucleus. Here the neurons are loosely arranged in an only vaguely confined area with small groups of neurons (open arrowhead) or single neurons (filled arrowhead) often assuming an eccentric position which makes outlining the structure a very ambiguous undertaking.

(the sampling fraction), was 188, then the total number of neurons would be:

1/1/5 x 188 = 5 x 188 = 940. (Fig. 2.3.5)

The same principle was applied to counts of dopaminergic neurons in the substantia nigra and the ventral tegmental area. It is clear, why this technique is not affected by tissue shrinkage. As shrinkage of the inter- and intra-cellular space would lead to an increase of cell number on the section level, this increase would be compensated by a decrease in size of the whole three-dimensional structure, i.e. the motor nucleus, thereby reducing the number of sections that hit the structure.

However, using a stereological method doesn't per se grant the absence of bias. As the structures studied in these studies were sufficiently small, it was not necessary to sample random blocks of tissue from within the region of interest. All motor nuclei as well as the SN/VTA could be studied as a whole as their entire transverse circumference was part of one section. It is easy to see why such an approach would be impossible if one were to count the glomeruli of a human kidney for instance (try to get a single slice of a human kidney onto a microscopy slide!). However, bias was potentially inherent to the technique employed at two stages: the choice of the first section to be counted (and thus the following sections) and the cell counting itself.

In the first case bias could be overcome by picking the first section to be included into the count by random. As every fifth section was counted in

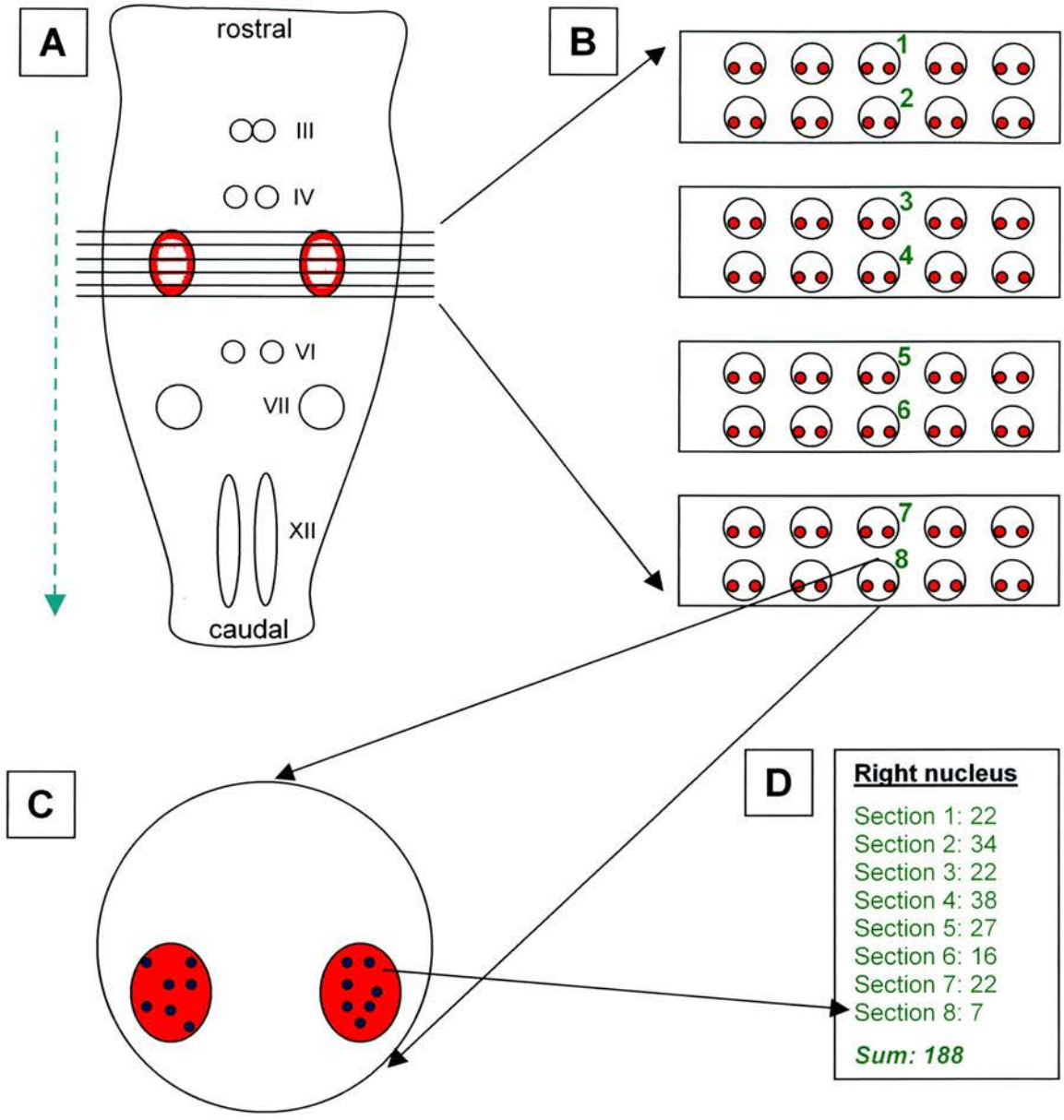

Fig. 2.3.5: Counting neurons with the *fractionator technique*. The *motor nucleus of the trigeminus nerve* is chosen as an example. **A:** schematic frontal view of the lower brainstem indicating the position of the motor nuclei (trigeminus motor nucleus in red). The whole brainstem is cut into sections of 8µm thickness in rostro-caudal direction as indicated by dashed arrow. **B:** transverse sections are transferred to slides in two strips of five sections per slide. The nucleus is hit by 40 sections in total. Every fifth section is counted (indicated by green numbers). The first section is picked by random (1) to exclude bias. **C:** The neurons of the left and the right nucleus are counted separately. For each of the two trigeminus nuclei the numbers of neurons counted in sections 1 to 8 are summed up and multiplied by the denominator of the fraction of sections counted (here 188 x 5 = 940 motoneurons for the right trigeminus nucleus).

the instance of motor nuclei and every tenth section in the case of the SN/VTA, the first section for counting was randomly chosen from the first five and respectively ten sections that included the structure of interest (Fig 2.3.5).

In the second case, bias would be inevitable if one were to count actual cells. This is due to the size as well as the shape of a neuron. The cell body of a typical adult cranial motoneuron measures between 20 and 40 μm in diameter. However, the thickness of one histological section (in this case) was only 8 μm. This means that the same cell is likely to appear on between 3 and 6 sections and would therefore be counted 3 to 6 times. This results in a falsely high number of cells in total. Moreover, a motoneuron is not spherical but irregularly shaped and can therefore make an appearance more than once in the same section. This would further skew the result towards a falsely high cell number (Fig. 2.3.6). There are several ways to overcome this problem. The most straight forward method (and the one applied here for motoneuron counts) is to count nucleoli. Typically, motoneurons have a single, central nucleolus. The rare occurrence of two nucleoli in one nucleus will be discussed below. A motoneuron nucleolus typically measures 1-2 μm and is significantly smaller than the section thickness. The assumption made here is that if the object appears in one section, it is so small that it would very seldom be seen in the next section. The problem of split nucleoli, i.e. a nucleolus appearing in two adjacent sections has been the subject of several studies (Jones, 1937, Møller et al., 1990). In the latter of the two studies referenced here the bias was estimated between 2 and 3%. Bearing in mind

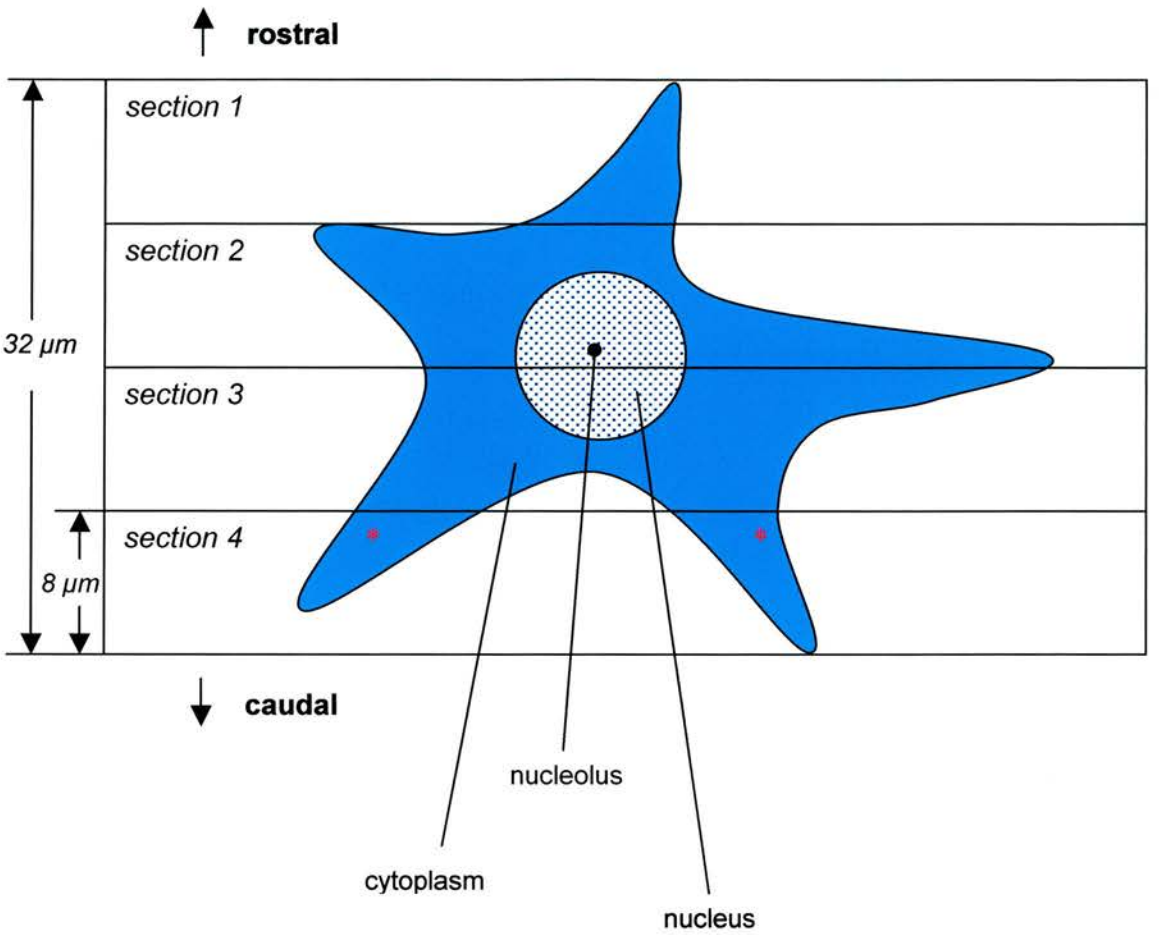

Fig. 2.3.6: Schematic representation of a sectioned motoneuron, illustrating the problem of over-counting. This cell which has a rostro-caudal length of 32 µm has been cut into sections of equal thickness. As each section has a thickness of 8 µm, the same cell would be encountered in at least 4 adjacent sections. Furthermore, the cell appears as two distinct objects in section 4 (*). Looking at section 4, there is know way of telling that the two objects are representing the same cell. This motoneuron would therefore be counted at least 5 times. A similar problem occurs if one were to choose the nucleus as a measure for counting cells. Although it is a spherical object that can not appear more than once in the same section, its diameter is larger than the section thickness (about 10 µm in this example), and would therefore appear in 2 to 3 adjacent sections. The only representative object significantly smaller than the section thickness is the nucleolus which would typically only appear in 1 section at a time (apart from the rare circumstances of "split nucleoli" (see main text).

that the same bias would occur in both counts of wild type and null mutant motoneurons, its effect on the end result is negligible. In this study, only neurons that contained a clear central nucleolus were included into the count.

In rare instances a nucleus can contain two nucleoli. In order to evaluate whether this might pose a problem for this study, the motor nuclei of a wild type and a knockout brain were scanned for the occurrence of nucleolus doublets. One hundred cells of each motor nucleus were studied in random sections. The entire thickness of each section was focused through in order to find the maximum possible number of cell nuclei containing more than one nucleolus (Tab. 2.3.3)

Nucleus	Wild type	γ-synuclein knockout
Oculomotor	3.41%	3.60%
Trochlear	2.50%	2.43%
Trigeminus	0.69%	0.88%
Abducens	1.41%	2.14%
Facial	1.50%	1.26%
Hypoglossus	3.50%	2.54%

Tab. 2.3.3: Occurrence of nucleolus doublets in cranial motor nuclei of wild type and γ-synuclein null mutant mice

These results show that the occurrence of two nucleoli in cranial motoneurons is a rare event, even given the fact that doublets will have been missed due to split nuclei. Furthermore, no obvious difference in the proportion of nucleolus doublets has been found between wild type and

knockout brains. Since the error occurred equally in both genotypes, it didn't affect the results.

To ensure that the counting of double nucleoli wasn't in itself inaccurate due to differences in cell nucleus sizes (either by nature between knockouts and wild types or due to varying degrees of tissue shrinkage), the average size of motoneuron cell nuclei was established for each cranial motor nucleus. The measurements were made on the eight Neutral Red-stained brains (four per genotype) that had been used for cell counts. The diameter of fifty cell nuclei per motor nucleus per brain were measured. The measurements were made on random sections. Since cell nuclei are not true spheres but of a somewhat ellipsoid shape, the largest diameter was measured in all cases. Measurements were made by means of a digital camera attached to the microscope and the Axiovision imaging program (Carl Zeiss Vision GmbH).

Two observations were made: firstly, none of the six studied motor nuclei displayed differences in nuclear diameters between wild types and knockouts. Secondly, variance of cell nucleus size in the same genotype was minimal, indicating that no technique-dependent bias had been introduced. The results are displayed in graphic mode in Chapter 4 (Fig. 4.2.3).

A different approach was taken for counting neurons of the substantia nigra. As the cells were stained with an antibody against tyrosine hydroxylase, the nucleus appeared as an empty structure surrounded by a

positively stained cytoplasm. Nucleoli do not show up with this stain. This left two options, either to counterstain the samples with a dye that stains nucleoli or to count nuclei instead and apply some means of correction. I decided to do the latter and adjust the numbers estimated using Abercrombie's correction. The problem of using cell nuclei for counting cells is explained in Fig. 2.3.6. Abercrombie devised the following formula to correct for the bias introduced by counting nuclei (or any spherical objects for that matter) in histological sections:

P = A x M / (L + M), whereby "**P**" is the actual number of nuclear points per section, "**A**" the crude count of number, "**M**" the thickness of the section, and "**L**" the nuclear diameter (Abercrombie, 1946).

The average diameter of the nuclei of dopaminergic neurons was established for every mouse brain included in this study by measuring the nuclei of 50 randomly picked dopaminergic neurons per brain. The nuclei were drawn onto a sheet of paper with the help of a camera lucida attached to the microscope as described further above. The drawings were subsequently scanned into a computer, and the diameters measured with Scion Image, an image analysis program that is freely available from Scion Corporation via their website at www.scioncorp.com.

It is important to point out that the mean nuclear diameter so obtained represents an underestimate since it is not possible to differentiate whole nuclei from smaller fragments. However, as Abercrombie points out, since

the section is of a finite thickness, the full diameter of the nucleus is frequently included. This and other mathematical considerations make this problem statistically negligible, especially when comparing two structures, since again (as was true for the bias in counting nucleoli) the error lies in the same direction for both genotypes (Abercrombie, 1946).

Final note: It will not have escaped the reader that measurements of cell nuclei in the cranial motor nuclei were made in a different (more up to date) fashion than those on dopaminergic neurons. This is due to the recent acquisition of a new imaging system and not based on methodological grounds!

2.3.6 Identification of cranial motor nuclei

Given some basic knowledge in vertebrate neuro-anatomy and a species-specific histological atlas, identification of the cranial motor nuclei is a fairly straight-forward matter. The position of the cranial motor nuclei in the rostrocaudal axis is more or less the same in all vertebrates, with the exception of the facial nucleus, whose position shows a fair extent of variability. In the mouse, it is located caudal to the abducens nucleus, whereas for instance, in the chicken hindbrain it lies rostral to it. This is the result of different embryological migration patterns of facial motoneurons between species and has been discussed in the introduction. Compared to humans where it also lies caudal to the abducens nucleus, the murine facial nucleus assumes a far more ventral position, almost reaching the ventral surface of the brainstem. In humans, strongly developed fibre-tracts (mostly

cortico-spinal fibres) make up the ventral part of the brainstem at this level (called the pons – lat.: bridge), forcing the facial nucleus into a more dorsal position. Figure 2.3.7 gives a schematic overview of the six cranial motor nuclei studied here in the mouse brainstem.

All cranial motor nuclei are more or less ellipsoid in shape with the larger diameter in the rostrocaudal direction. This means that the caps of each nucleus only contain a few neurons in a transverse section which makes it impossible to positively identify the nucleus. The approach taken here was to scan sections for the – most conspicuous – middle part of each given nucleus and then work from there in either direction until no more motoneurons could be identified in the field. I worked myself down from the middle to the caudal pole of a motor nucleus and then count every fifth section rostral from that position until I had reached the rostral cap.

The oculomotor nucleus (III):

The most rostral of the cranial motor nuclei, it is also one of the smallest. This seems surprising at first sight given the fact that it controls subtle eye movements. However, bearing in mind its intricate connections and the fact that it shares the control of eye movement with two more nuclei (the trochlear and abducens nuclei) puts its size into perspective. Being part of the midbrain, it is located on both sides of the ventral tip of the ventral grey which surrounds the fourth ventricle in a more or less triangular fashion. The bilateral nuclei are adjacent to the neurons of the Edinger-

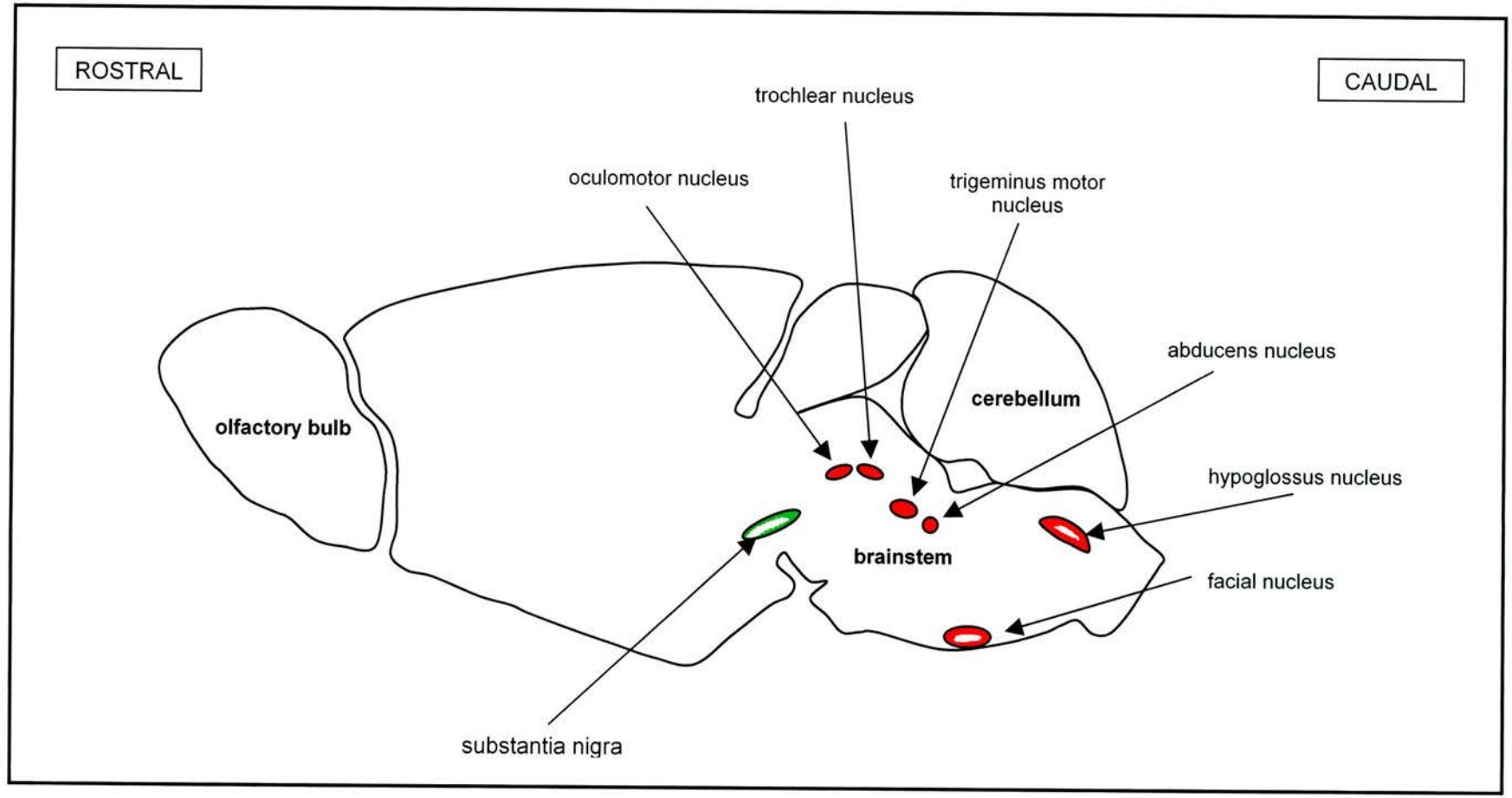

Fig. 2.3.7: Diagram depicting the location of the *cranial motor nuc*lei and the *substantia nigra* in the mouse brainstem. The diagram represents an idealized sagittal section trough the adult mouse brain showing the rostrocaudal and ventrodorsal positions of these structures. Note that the motor nuclei assume different positions in the coronal plane and can never be all seen together in the same sagittal plane in real-life sections. Here, they have been projected onto the same plane for reasons of simplicity.

Westphal nuclei which separate them in the midline. The neurons of the Edinger-Westphal nucleus are easily identified by their dorsoventral orientation (Fig. 2.3.8).

The trochlear nucleus (IV):

The trochlear nucleus lies in close proximity to the oculomotor nucleus. Put into the context of these studies its rostral pole was usually only one slide (80μm) away from the caudal pole of its neighbour. Like the oculomotor nucleus it is located close to the midline. This might make it seem difficult to distinguish from the former nucleus. Nevertheless, several features help to identify it. Firstly, it lies in a slightly more lateral position than the oculomotor nucleus does. Secondly, its cells appear less packed than those of the oculomotor nucleus. Thirdly, it is crossed in rostro-caudal direction by fibres of the medial lemniscus which is probably its most conspicuous landmark. And fourthly, its transverse circumference (unlike most other cranial motor nuclei) isn't rounded but assumes a fountain-like shape if taken together with the Edinger-Westphal nucleus which divides its bilateral instances (Fig. 2.3.9).

The motor nucleus of the trigeminus nerve (IV):

The motor nucleus of the trigeminus nerve is positioned between the upper two and the lower of the three ocular motor nuclei. Its middle part appears ellipsoid in shape in transverse sections. Being a branchiomotor

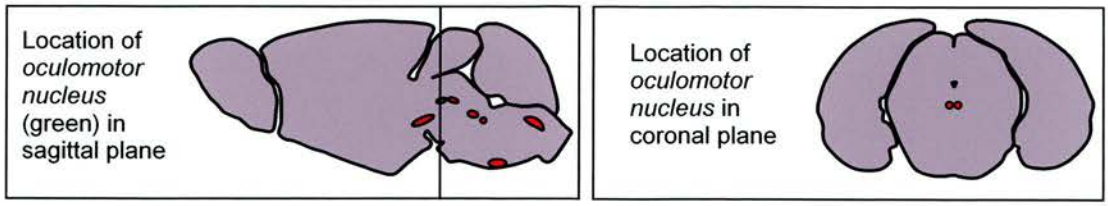
Location of *oculomotor nucleus* (green) in sagittal plane
Location of *oculomotor nucleus* in coronal plane

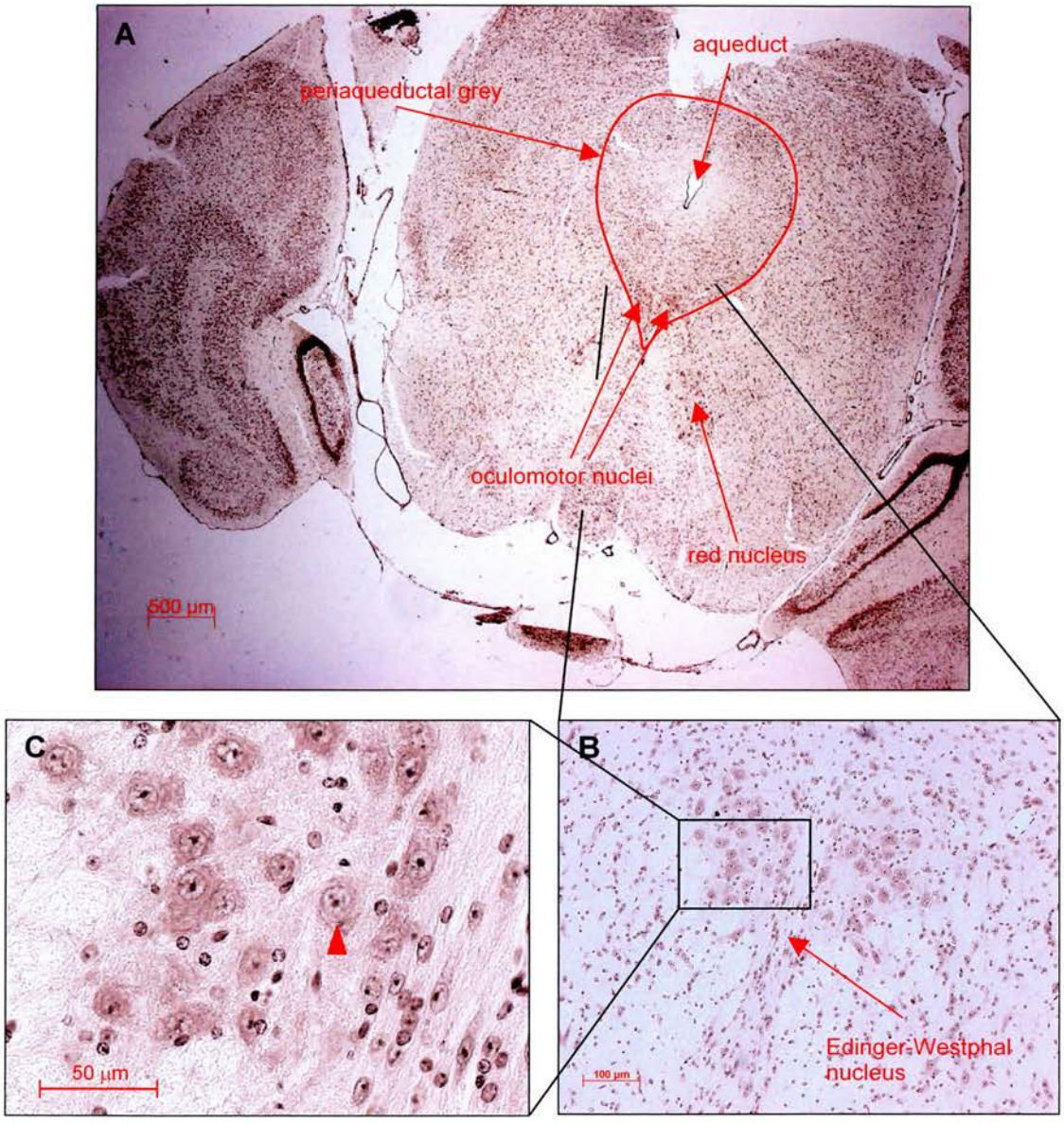
A
periaqueductal grey
aqueduct
oculomotor nuclei
red nucleus
500 µm
C
50 µm
B
100 µm
Edinger-Westphal nucleus

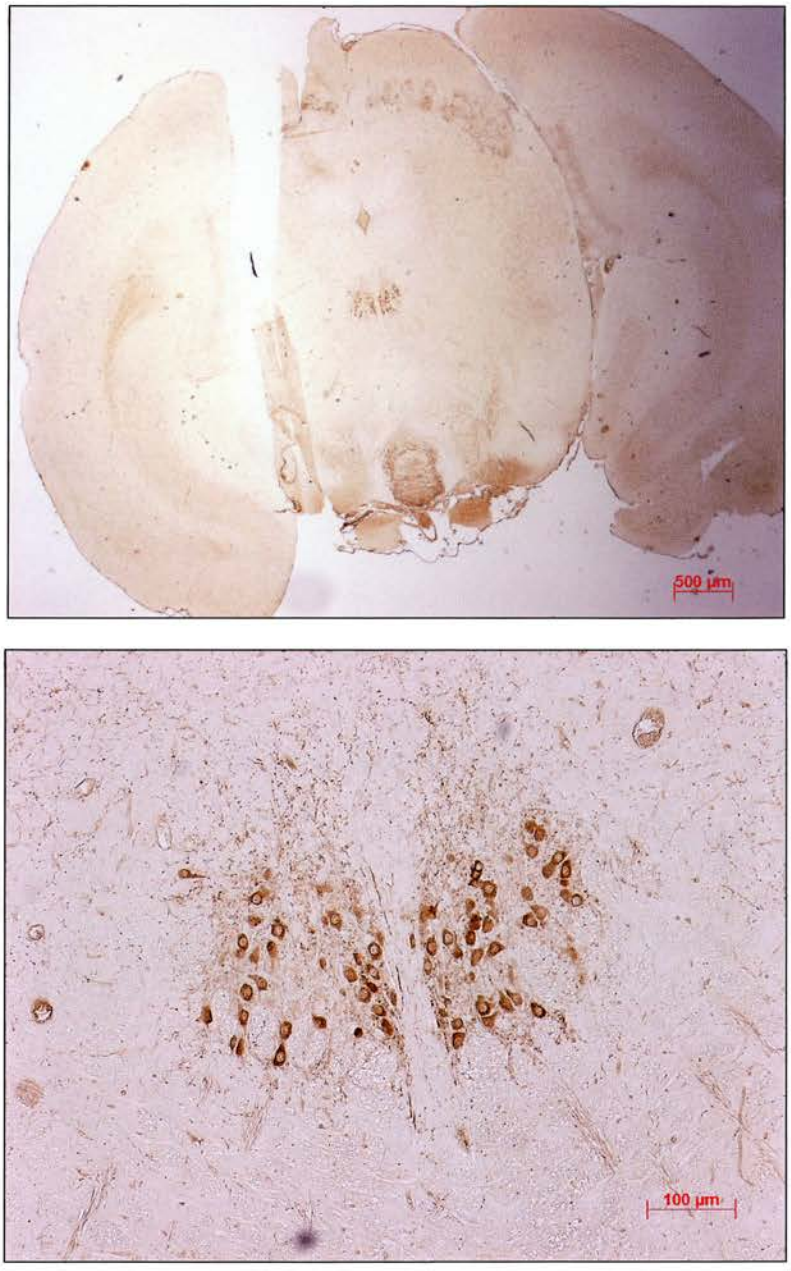

Fig. 2.3.8: Neutral Red (A-C) and anti-ChAT (D, E) stain of the murine *oculomotor nucleus*. **A:** coronal overview showing the location of the oculomotor nuclei at the ventral tip of the periaqueductal grey. **B:** higher magnification of A. Note the dorsoventrally aligned neurons of the Edinger-Westphal nucleus between the two oculomotor nuclei. **C:** individual oculomotor neurons (arrowhead). The neurons can easily be identified by their large size and the central nucleolus. **D, E:** anti-ChAT control stain.
Line through sagittal diagram shows level of coronal plane.

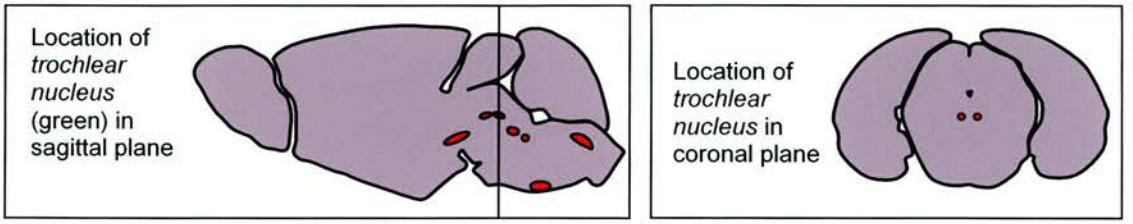
Location of *trochlear nucleus* (green) in sagittal plane
Location of *trochlear nucleus* in coronal plane

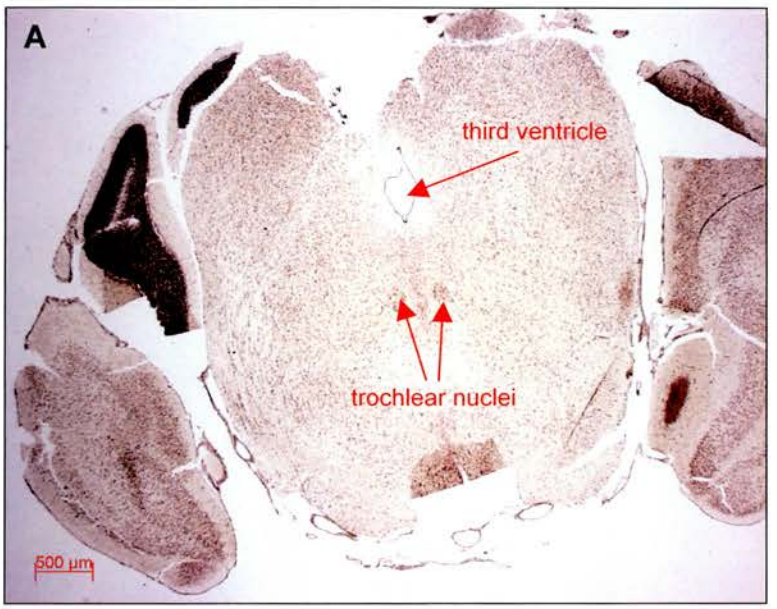
A
third ventricle
trochlear nuclei
500 µm

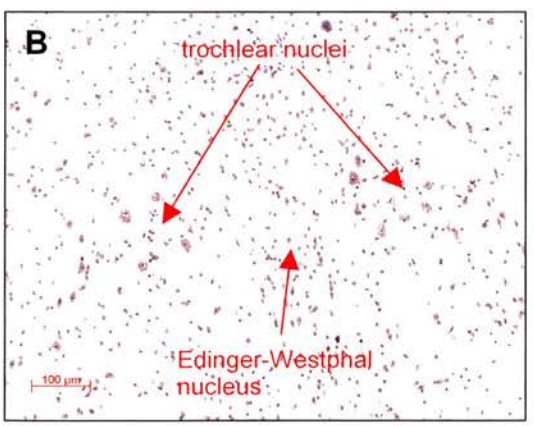
B
trochlear nuclei
Edinger-Westphal nucleus
100 µm

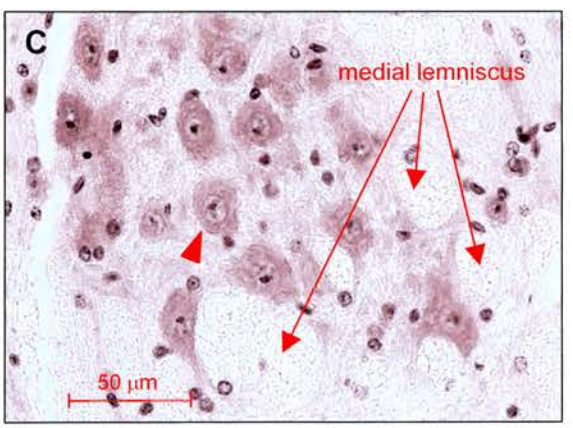
C
medial lemniscus
50 µm

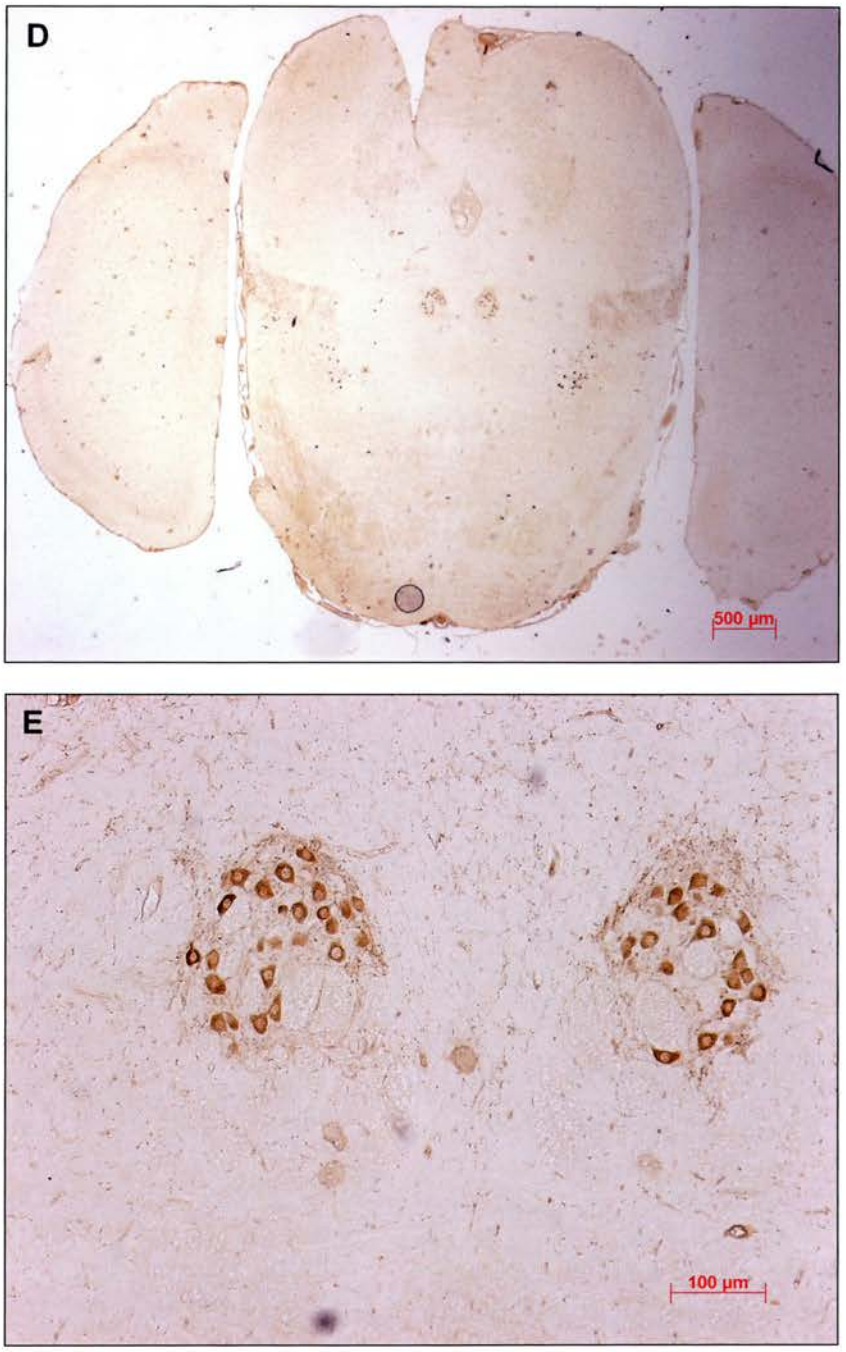

Fig. 2.3.9: Neutral Red (A-C) and anti-ChAT (D, E) stains of the murine *trochlear nucleus*. **A:** coronal overview showing the trochlear nuclei. **B:** higher magnification of A. Note the fountain-like (or "bunch-of-flowers") structure that the two trochlear nuclei form with the Edinger-Westphal nucleus which lies between them. **C:** individual trochlear motoneurons (arrowhead). Note the fibre-bundles of the medial lemniscus that cross the nucleus in rostro-caudal direction. **D, E:** anti-ChAT control stain.
The line through the sagittal diagram shows the level of the coronal plane.

nucleus it assumes a rather lateral position juxtaposed to the spinal tract of the trigeminal nerve (Fig. 2.3.10).

The abducens nucleus (VI):

As the other two ocular motor nuclei, the abducens nucleus assumes a very medial position. It is a small nucleus that can easily be missed but can be recognized by its proximity to the internal knee of the facial nerve. As mentioned above, in humans as well as in mice the facial nucleus lies caudal and ventral to the abducens nucleus. However, its nerve fibres leave the brainstem rostral to the abducens nerve (indicating the true embryological origin of the nucleus). As a result the facial nerve curves sharply around the abducens nucleus giving rise to the so called *genu internis* (lat.: inner knee) of the facial nerve (as opposed to the *genu externis* where the nerve fibres make another U-turn in the inner ear). The inner knee of the facial nerve is the most crucial landmark in identifying the abducens nucleus in the mouse (Fig. 2.3.11).

The facial nucleus (VII):

The facial nucleus is probably the most characteristic of all cranial motor nuclei in the mouse brain due to its horseshoe shape in transverse sections. It is also the only motor nucleus that reaches the ventral surface of the brainstem. Controlling almost all facial muscles, it is not surprising that it is the largest of all cranial motor nuclei, more than twice as wide as the

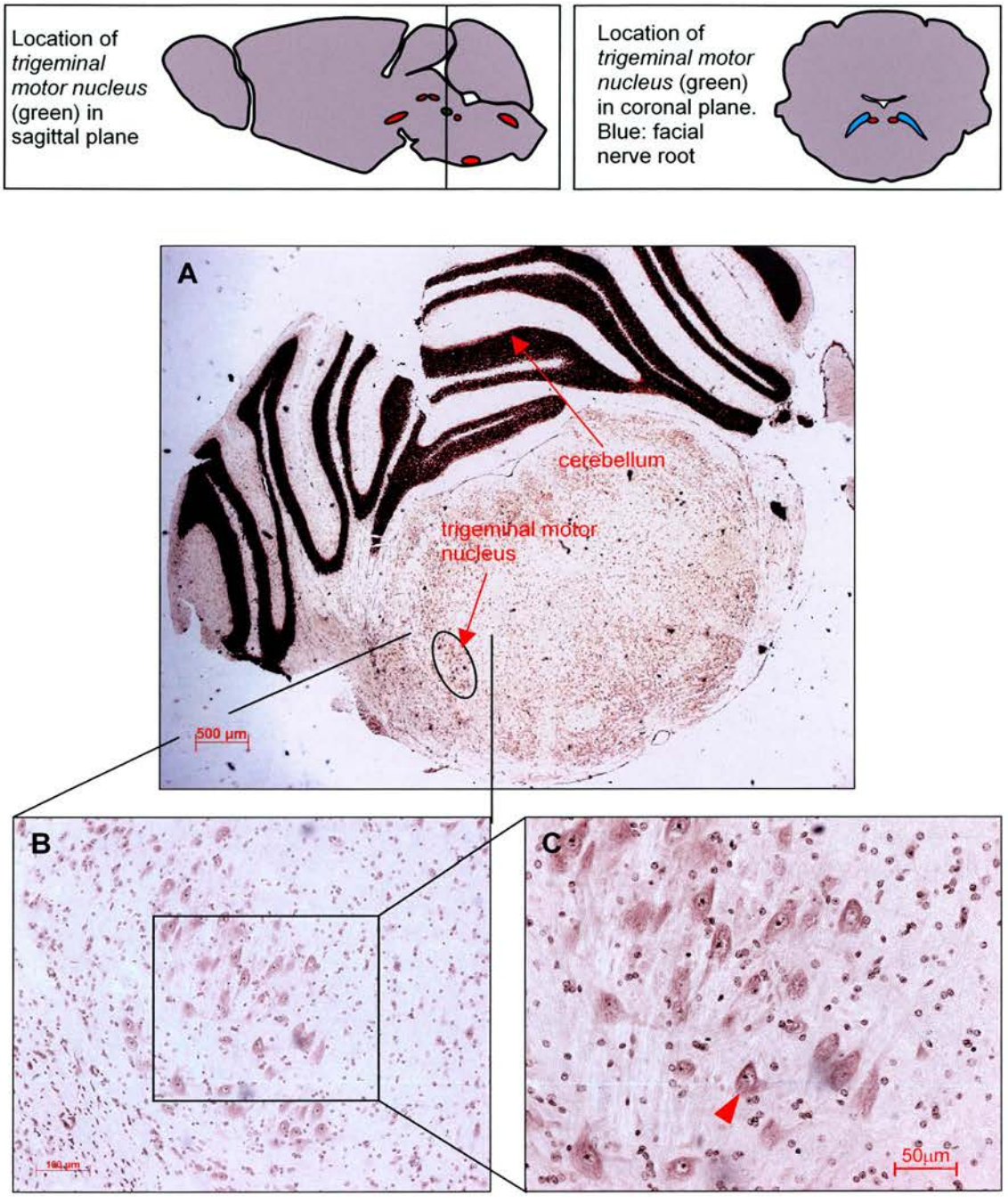
Location of *trigeminal motor nucleus* (green) in sagittal plane
Location of *trigeminal motor nucleus* (green) in coronal plane. Blue: facial nerve root
A
cerebellum
trigeminal motor nucleus
500 µm
B
100 µm
C
50µm

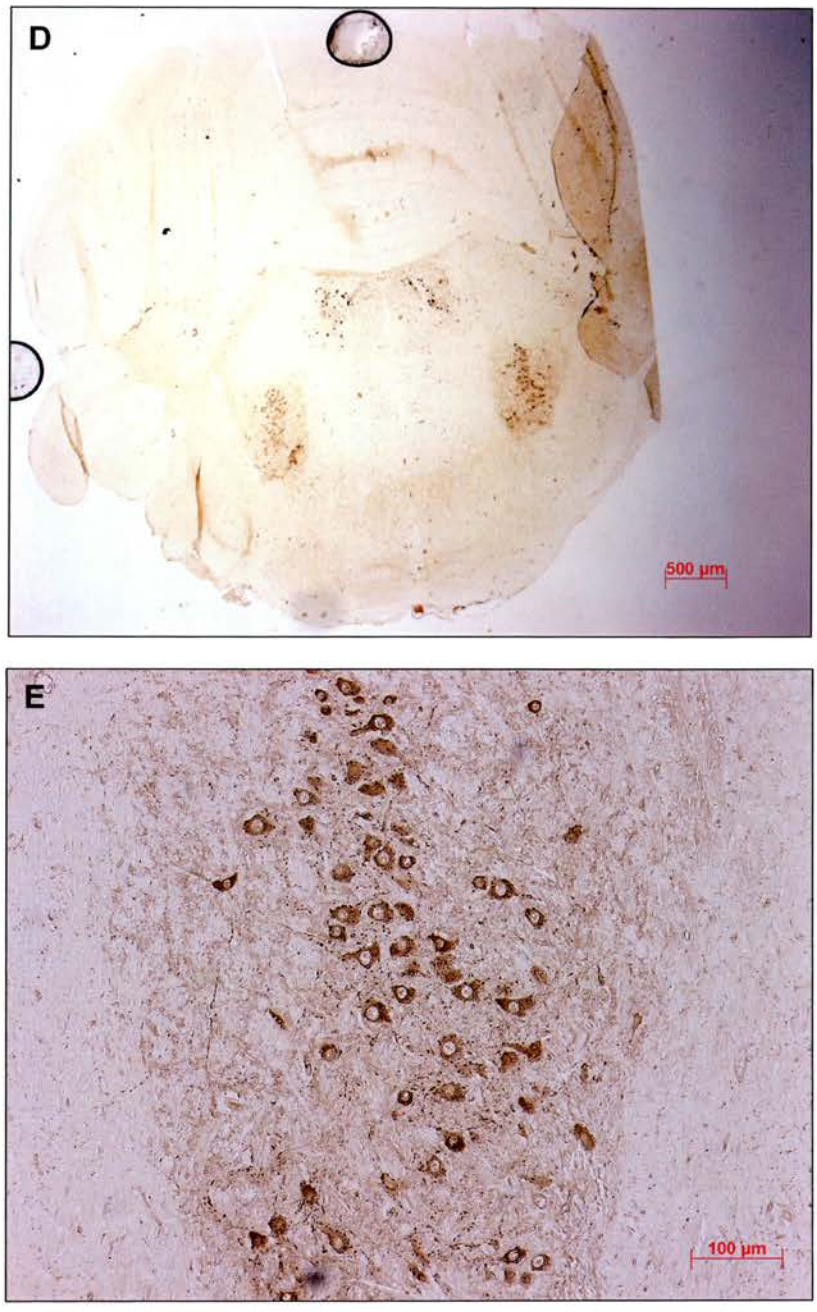

Fig. 2.3.10: Neutral Red (A-C) and anti-ChAT (D, E) stains of the murine *trigeminal motor nucleus*. **A:** coronal overview showing the left trigeminal motor nucleus. The right nucleus is not apparent as the section is not strictly symmetrical. **B:** higher magnification of A. **C:** individual trigeminal motoneurons (arrowhead). **D, E:** anti-ChAT control stain.
Note: line through sagittal diagram shows level of coronal section.

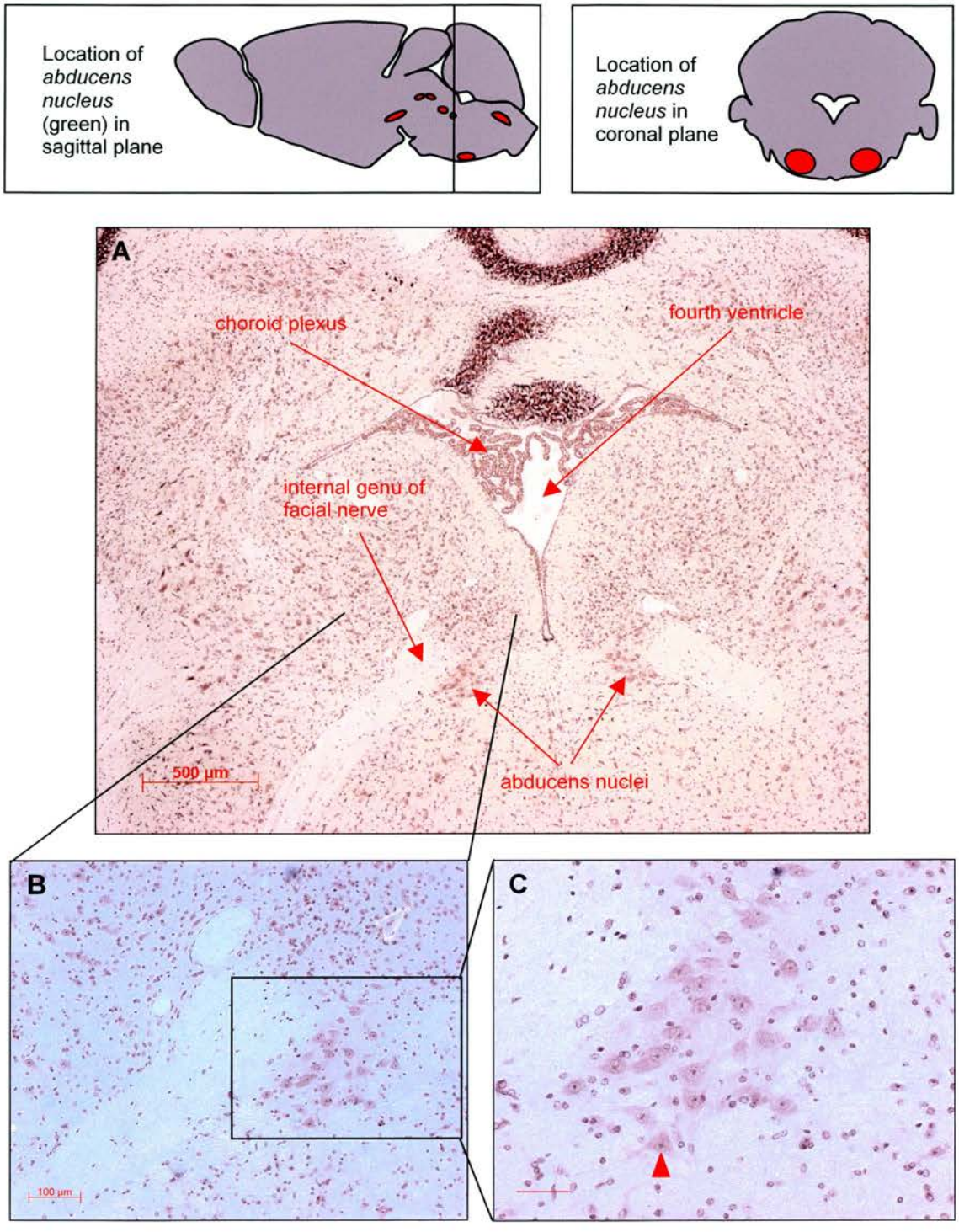
Location of *abducens nucleus* (green) in sagittal plane
Location of *abducens nucleus* in coronal plane
A
choroid plexus
fourth ventricle
internal genu of facial nerve
500 µm
abducens nuclei
B
100 µm
C

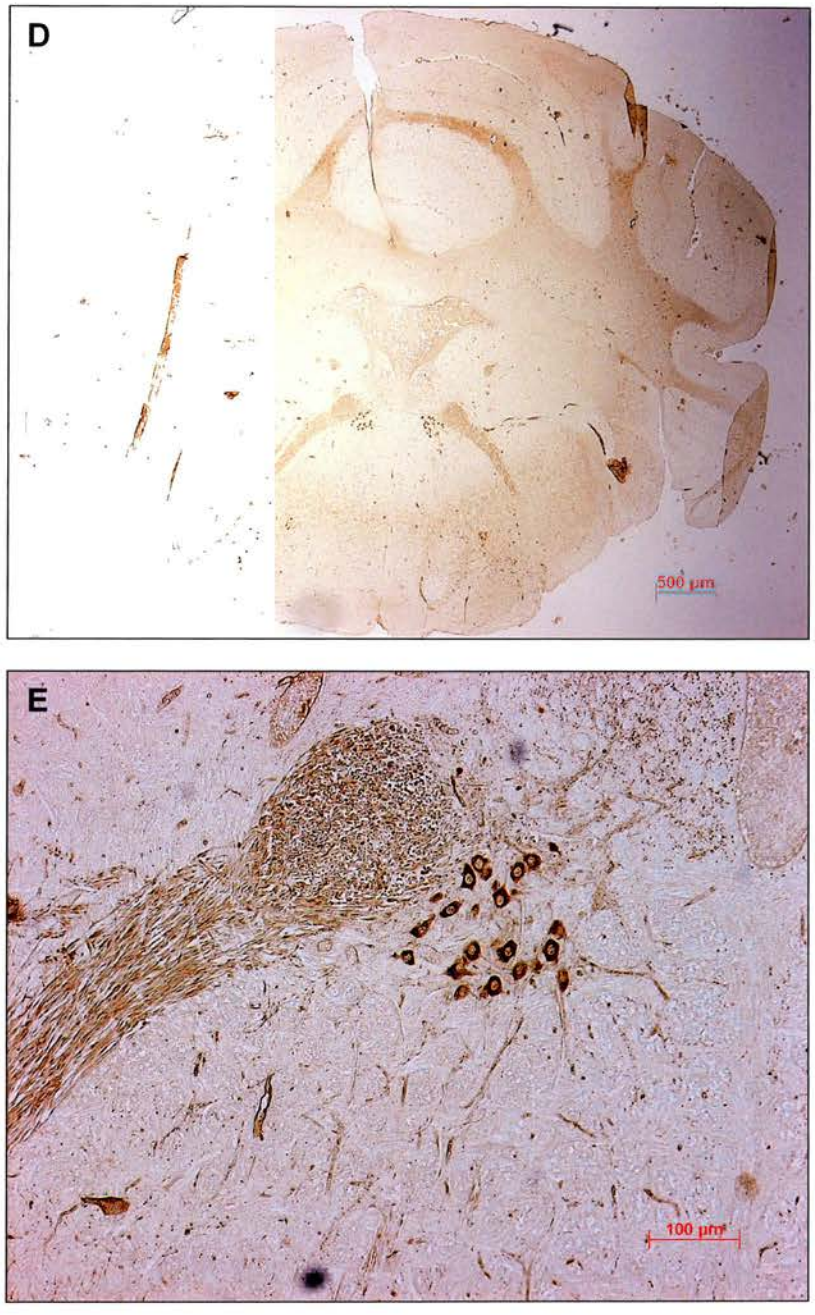

Fig. 2.3.11: Neutral Red (A-C) and anti-ChAT (D, E) stains of the murine *abducens nucleus*. **A:** coronal overview showing both abducens nuclei ventro-adjacent to the internal genu (lat.: knee) of the facial nerve. **B:** the left abducens nucleus in higher magnification. **C:** individual motoneurons (arrowhead). **D, E:** anti-ChAT control stain.
Note: line through sagittal diagram shows level of coronal plane.

hypoglossus nucleus. Of all motor nuclei in the murine brainstem, this is without doubt the easiest to identify (Fig. 2.3.12).

The hypoglossus nucleus (XII):

The hypoglossus nucleus is the longest (in rostro-caudal direction) of all cranial motor nuclei. In the transverse plane, it lies just ventral to the central canal, with a curved ventral border and a somewhat straight interface that marks the dorsal boundary between it and the dorsal nucleus of the vagus nerve. The dorsal nucleus of the vagus nerve is an important landmark to identify the hypoglossus nucleus. In transverse sections the preganglionic neurons of the vagus nerve appear as an assembly of tightly packed cells that are orientated in a medio-lateral fashion and thus easily distinguished from the more loosely positioned hypoglossal motoneurons (Fig. 2.3.13).

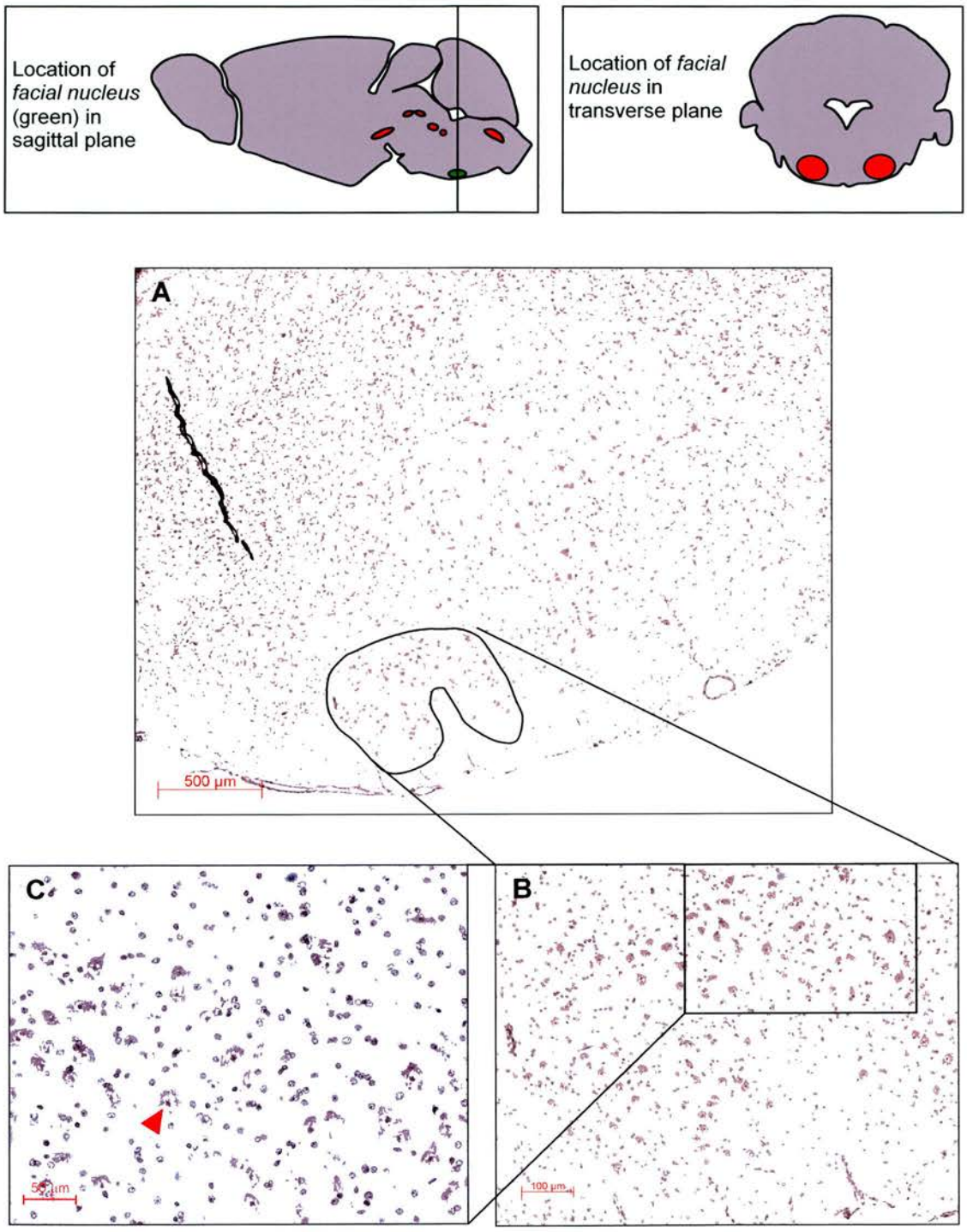
Location of *facial nucleus* (green) in sagittal plane
Location of *facial nucleus* in transverse plane
A
500 µm
C
50 µm
B
100 µm

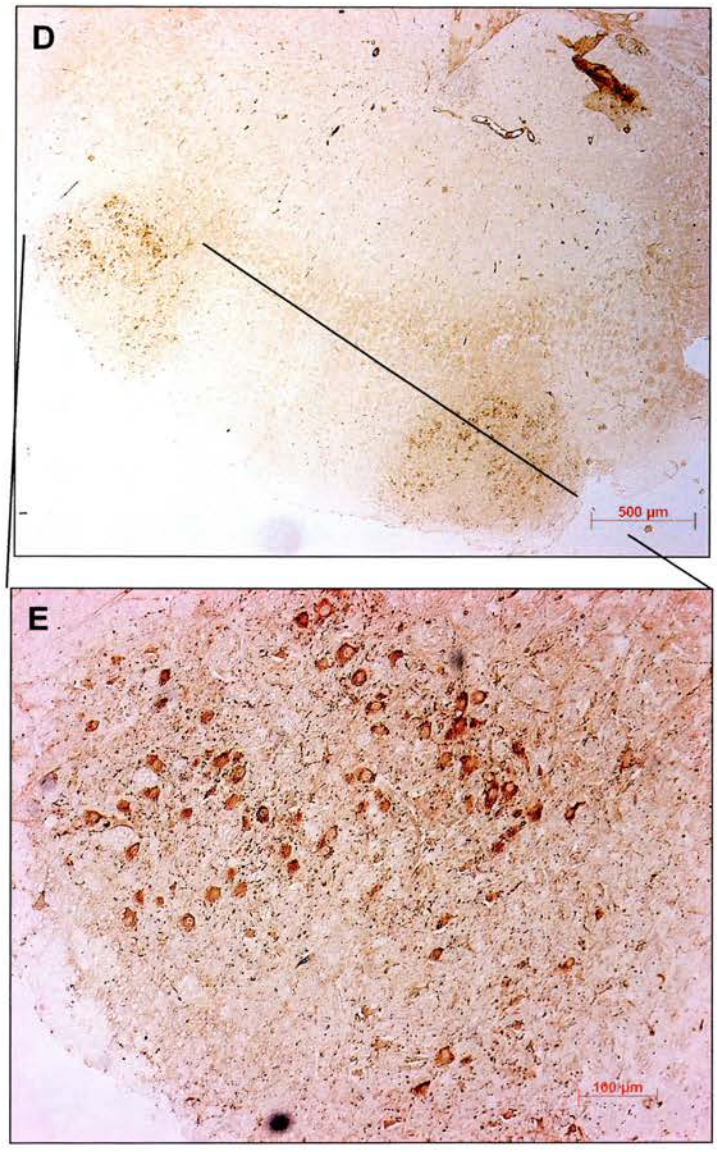

Fig. 2.3.12: Neutral Red (A-C) and anti-ChAT (D, E) staining of the murine *facial nucleus*. **A:** coronal overview showing the ventrolateral position of the left facial nucleus in the lower brainstem. **B:** higher magnification of A. Note the typical horseshoe shape (as outlined in A). **C:** individual facial motoneurons. Note the large size and the clear central nucleolus (arrowhead). **D,E:** anti-ChAT control stain.
Line through sagittal diagram shows level of coronal plane.

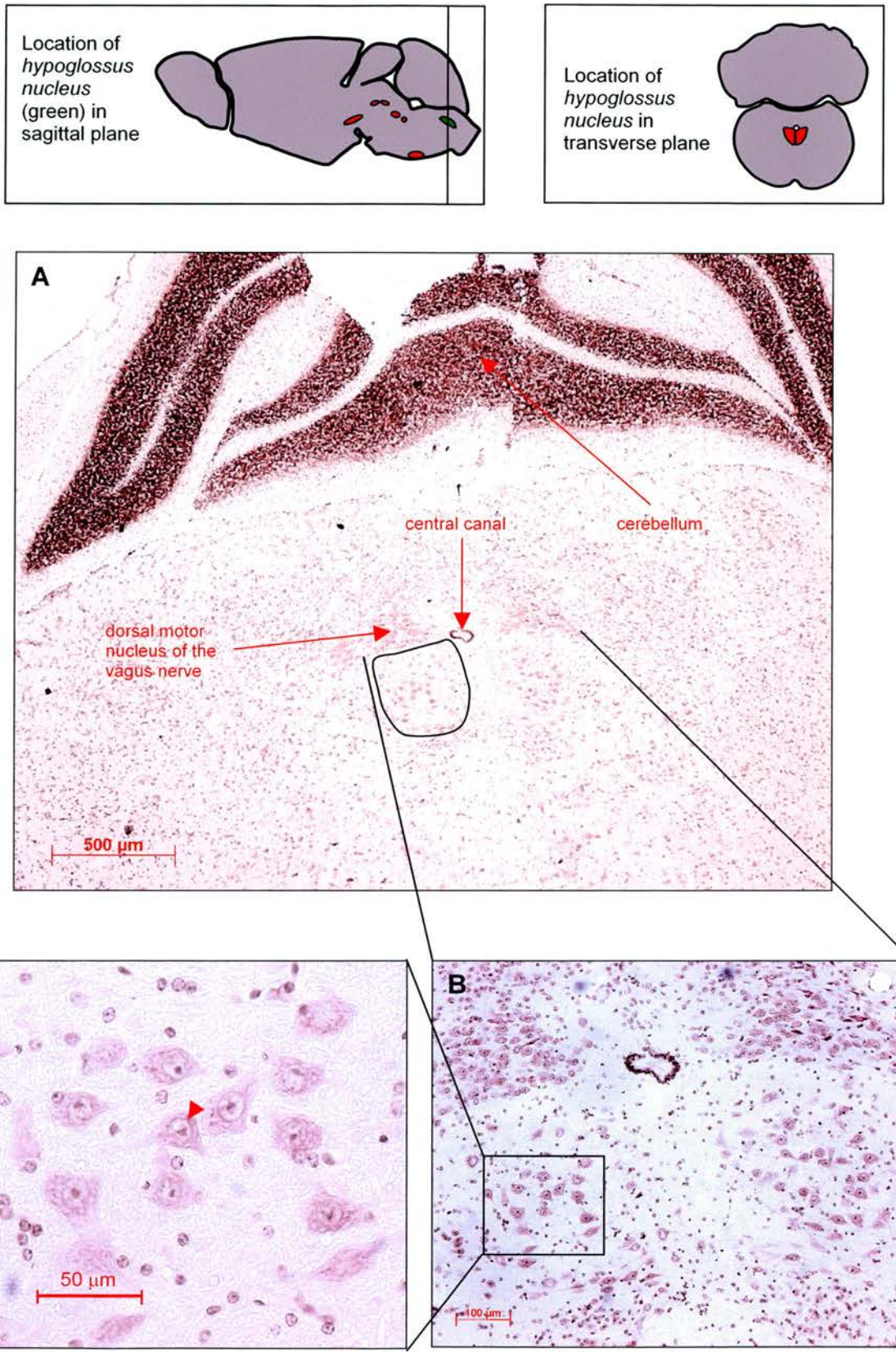
Location of *hypoglossus nucleus* (green) in sagittal plane
Location of *hypoglossus nucleus* in transverse plane
A
central canal
cerebellum
dorsal motor nucleus of the vagus nerve
500 µm
C
50 µm
B
100 µm

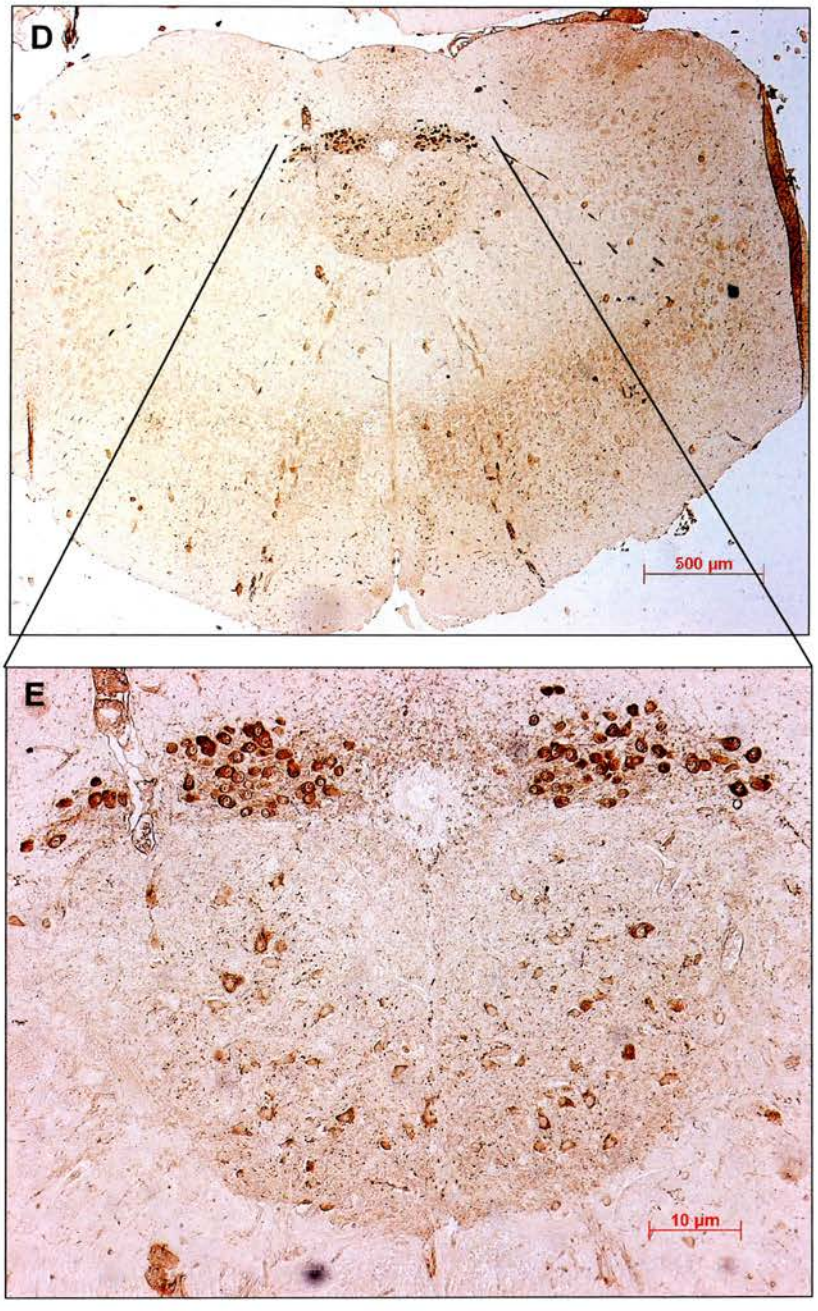

Fig. 2.3.13: Neutral Red (A-C) and anti-ChAT (D, E) stainings of the murine *hypoglossal nucleus*. **A:** coronal overview showing the location of the hypoglossal nucleus in the coronal plane. Note the close proximity to the central canal and the tightly packed neurons of the dorsal motor nucleus of the vagus nerve dorso-adjacent to the hypoglossal nucleus. **B:** higher magnification of A. **C:** individual motoneurons of the left hypoglossal nucleus, conspicuous by their large size and the clear, central nucleolus (arrow). **D, E:** anti-ChAT control stain.
Line through sagittal diagram shows level of coronal plane.

CHAPTER 3

Macrophage Stimulating Protein is a Neurotrophic Factor for Embryonic Chicken Hypoglossal Motoneurons

3.1. Introduction

Macrophage Stimulating Protein (MSP) is a 78 kDa, heterodimeric, secreted protein (Leonard and Skeel, 1978) that belongs to the kringle protein family (Yoshimuro et al., 1993). This family includes plasminogen (Sottrup-Jensen et al., 1975) and Hepatocyte Growth Factor/ Scatter Factor (HGF; Stoker et al., 1987; Nakamura et al., 1989). MSP was originally isolated as a serum protein that stimulates the motility of mouse peritoneal macrophages and makes them responsive to the complement-derived chemoattractant C5a and ingest C3bi-coated erythrocytes (Leonard and Skeel, 1978; Skeel et al., 1991, Skeel and Leonard, 1994). Several functional studies have revealed a variety of other activities. MSP induces interleukin-6 production and differentiation of megakaryocytes (Banu et al., 1996), suppresses the proliferation of myeloid precursor cells (Broxmeyer et al., 1996) and stimulates osteoclast activity (Kurihara et al., 1998). It also stimulates the proliferation and migration of keratinocytes *in vitro* (Wang et al., 1996).

MSP and HGF are closely related and highly conserved proteins. Their human forms show a 45% sequence homology (Yoshimura et al., 1993). Both, the avian (chick) and mammalian (mouse, human) forms of MSP and HGF have the following features in common: they are disulfide-linked heterodimers with an N-terminal domain that contains four cysteine residues

forming a hair loop, four kringle domains and an inactive serine protease domain (Théry et al., 1995). HGF, a pleiotropic factor that is required for the development of placenta, liver and skeletal muscle of the limbs and trunk (Bladt et al., 1995; Schmidt et al.,1995; Uehara et al., 1995; Maina et al., 1996) is also widely expressed in the nervous system (Honda et al., 1995). It has been shown to enhance the survival of several different kinds of neurons and promote the growth of their axons during development (Ebens et al., 1996; Hamanoue et al., 1996; Maina et al., 1997, 1998; Yamamoto et al., 1997; Wong et al., 1997; Yang et al., 1998; Okura et al., 1999; Caton et al., 2000; Davey et al., 2000; Novak et al., 2000). Interestingly, both proteins are expressed in all hindbrain rhombomere boundaries at stage 23 in chick embryos (Théry et al., 1995). Rhombomere boundaries may serve as conduits for outgrowing axons (see above).

MSP and HGF exert their actions on responsive cells by binding to structurally related receptor tyrosine kinases RON and Met, respectively (Bottaro et al., 1991; Naldini et al., 1991; Gaudino et al., 1994; Wang et al., 1994). The receptors are members of a RTK subfamily that comprises RON, Met, and SEA, the avian orthologue of RON (Huff et al., 1993; Ronsin et al., 1993; Bardelli et al., 1994). Iwama and colleagues have shown that MSP activated RON is able to mediate both, apoptotic and growth signals via a multifunctional, intracellular docking site which is highly conserved in the HGF receptor subfamily (Iwama et al., 1996). Depending on the cell type, MSP either induces a growth signalling pathway or activates two different pathways, i.e. growth and apoptosis. The latter seems to involve the delayed

and sustained activation of the JNK pathway which may overcome the co-active mitogenic signals.

During development of the mouse embryo RON mRNA is expressed in a variety of tissues (Table 3.1.1; Gaudino et al., 1994, 1995; Quantin et al., 1995; Thery et al., 1995). Cell lines derived from these tissues respond to MSP *in vitro*. MSP shows strong mitogenic effects on the neuroendocrine PC12 cell line while NGF halts growth and induces morphological differentiation in these cells (Gaudino et al., 1995)

Nervous System	**Other tissues**
Hypoglossus nucleus	Liver
Trigeminal ganglion	Lung
Spinal cord and ganglia	Kidney
	Medulla of adrenal glands
	Epithelium of gastrointestinal tract
	Skin
	Bone marrow

Table 3.1.1: RON mRNA expression in and outside the nervous system

In the developing brain stem, RON expression is restricted to the trigeminal nucleus and the hypoglossus nucleus. These findings suggest that MSP might act as a neurotrophic factor for distinct populations of developing neurons. This study shows that MSP is capable of enhancing survival and growth of an anatomically discrete population of motoneurons, and that its

mRNA is expressed in the developing tongue, the target tissue for hypoglossus neurons.

3.2. Results

3.2.1. MSP promotes the survival of embryonic hypoglossal motoneurons

To investigate if MSP is capable of enhancing the survival of hypoglossal motoneurons, these cells were purified by an immuno-magnetic bead method developed by Henderson and colleagues (personal communication) which is a modification of their own previously published motoneuron purification method (Henderson et al., 1995, Bloch-Gallego, 1991). This technique uses a monoclonal antibody that recognises the SC1 epitope which in the caudal hindbrain of chick embryos at E5.5 is uniquely expressed on hypoglossal neurons and floor plate cells (see "Materials and Methods"). To confirm the effectiveness of the purification procedure, cultures of purified neurons were stained with a monoclonal antibody that recognises the motoneuron-specific transcription factor Islet 1 (Ericson et al.,1992). Typically, over 90% of viable cells in these cultures were Islet-1 positive (see Materials and Methods, Fig. 2.1.7 on page 124). Cells were grown at low densities to minimise possible homotrophic effects between the neurons themselves.

In dissociated cultures of purified hypoglossal neurons, half of the neurons died within 24 hours in defined, serum-free medium without added neurotrophic factors (Fig. 3.2.1). The addition of MSP to the culture medium enhanced the survival of these neurons by a further 30%, which was comparable with the survival enhancing effect of CNTF, a neurotrophic

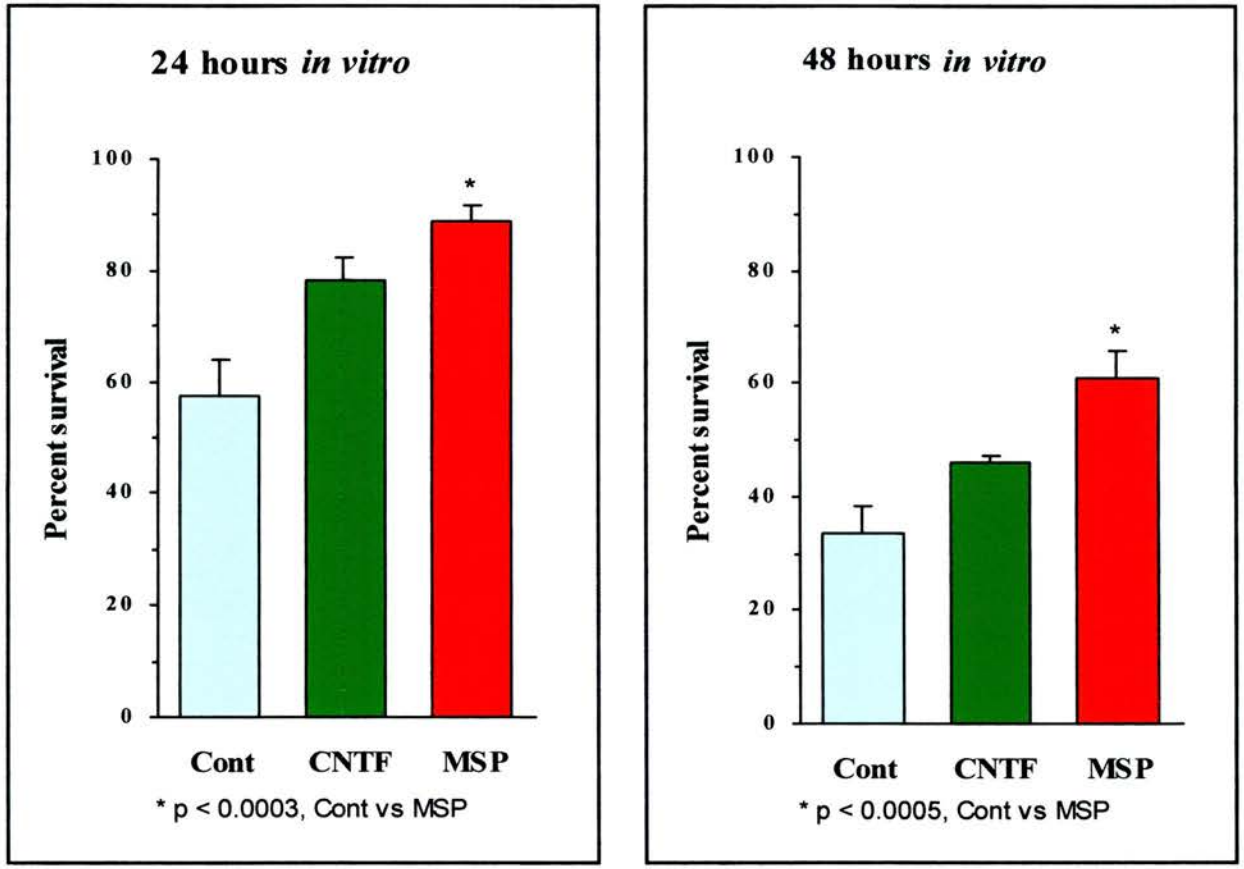

Fig. 3.2.1: Survival of embryonic chick hypoglossal motoneurons in defined medium alone (Cont) and in the presence of CNTF and MSP after 24 and 48 h incubation; n (experiments) = 6

factor that has previously been shown to promote the survival of spinal motoneurons in culture (Arakawa et al., 1990). By 48 hours incubation, more neurons had died in control cultures, but survival in the presence of MSP was still much higher (approximately double that in control cultures; Fig. 3.2.1). The combination of MSP plus CNTF did not result in higher survival than with either MSP or CNTF alone (data not shown).

Dose response analysis of the survival-enhancing effects of MSP on hypoglossal motoneurons revealed that 10 ng/ml was maximally effective; higher concentrations did not further enhance survival (Fig. 3.2.2). These results suggest that MSP enhances the survival of hypoglossal motoneurons in the developing chick embryo.

3.2.2. MSP promotes neurite outgrowth from embryonic hypoglossal motoneurons

To investigate if MSP affects the growth of neurites emanating from hypoglossal motoneurons, camera lucida drawings were made of the neurite arbors of neurons grown in defined medium for 48 hours, alone or in medium supplemented with either MSP or CNTF. The total length of each neurite arbor was measured by digitising the drawings and using a graphics program to make the measurements (see "Materials and Methods"). To avoid any confusion about which neurites emanated from which cell body, the neurons were grown at very low density so that overlapping of arbors was kept to a minimum. Figure 3.2.3 shows that neurite outgrowth of motoneurons cultured in the presence of MSP was significantly enhanced compared with

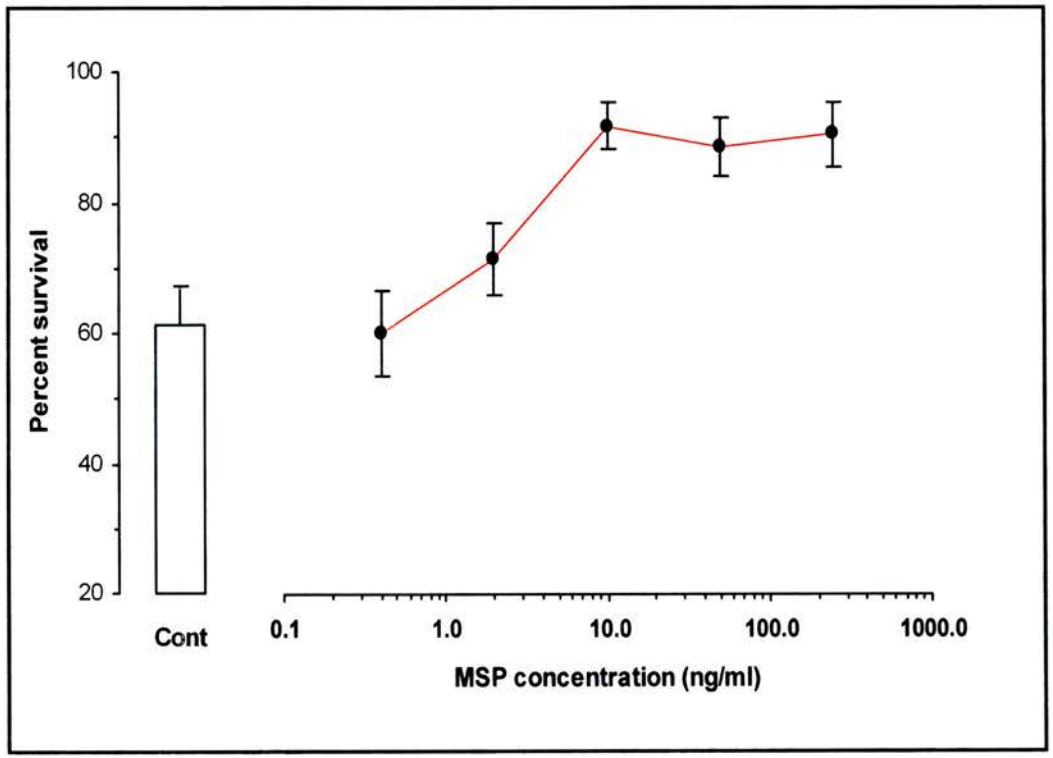

Fig. 3.2.2: Survival of embryonic chick hypoglossal motoneurons with concentrations of MSP ranging from 0.4 to 250 ng/ml after 24 h incubation. n (experiments) = 3

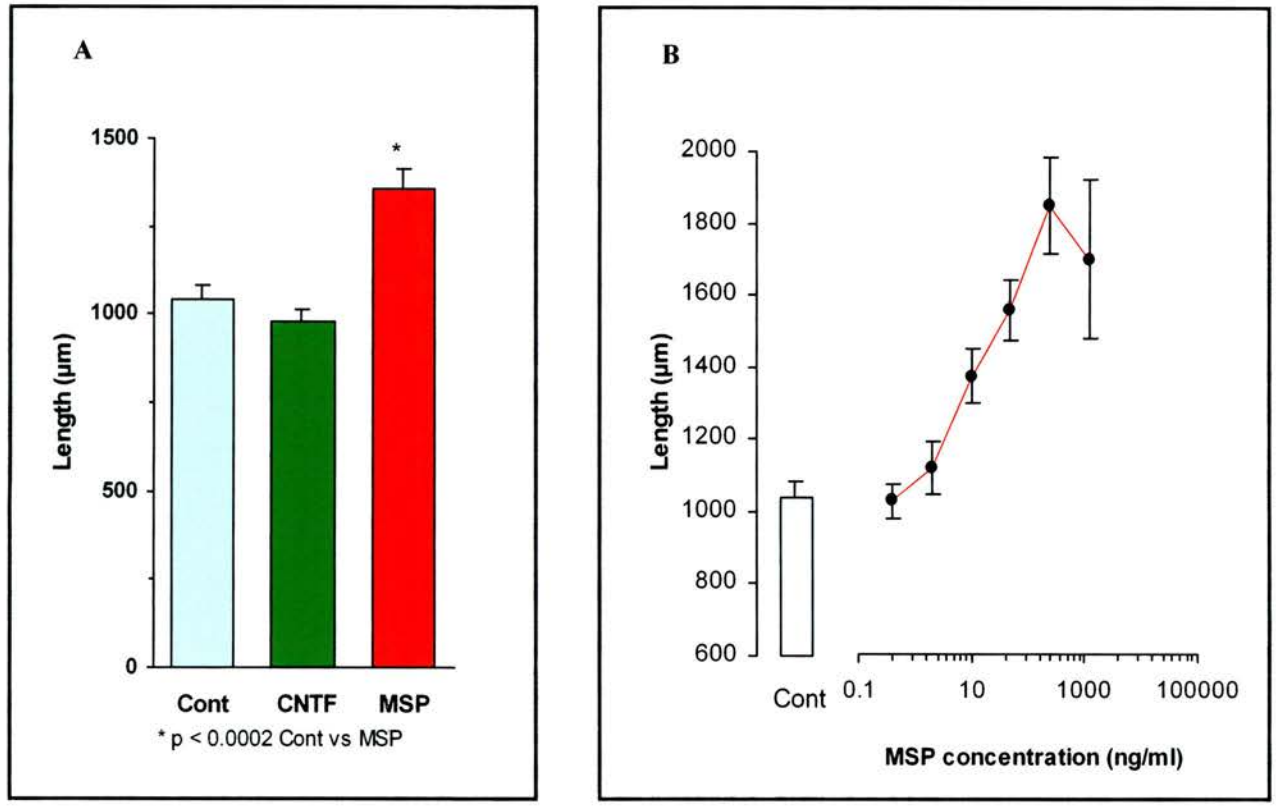

Fig. 3.2.3: A: Total lengths of the neurites of embryonic chick hypoglossal motoneurons grown for 48 h in defined medium alone (Cont) and in the presence of 10 ng/ml CNTF and 10 ng/ml MSP; n (neurons per growth factor) = 100. **B:** Total lengths of the neurite arbors of embryonic chick hypoglossal motoneurons grown for 48 h with MSP concentrations ranging from 0.4 to 1250 ng/ml; n (experiments) = 3

that of neurons in un-supplemented medium ($p<0.0002$, two-tailed, unpaired T-Test). Interestingly, although CNTF enhanced the survival of hypoglossal neurons, it did not increase the lengths of their neurite arbors compared with control cultures ($p> 0.05$, two-tailed, unpaired T-Test).

Dose response analysis of the neurite growth-promoting effects of MSP on hypoglossal neurons (Fig. 3.2.3) revealed that MSP was maximally effective at a concentration of 250 ng/ml. At this concentration, the total neurite arbor length was almost two-fold higher compared with control cultures. This contrasts with the survival dose response of hypoglossal motoneurons to MSP in which maximal survival was observed at much lower concentrations (Fig 3.2.2). These findings discount the possibility that the mean increase in the length of motoneuron arbors in MSP-supplemented cultures is secondary to the survival of an MSP-dependent subset of neurons that has intrinsically faster neurite growth than those neurons that survive in control cultures. At concentrations of higher than 10 ng/ml, there was no increase in the number of surviving neurons, yet there were further substantial increases in neurite length with concentration in essentially the same population of neurons. These results indicate that MSP significantly enhances neurite growth from embryonic hypoglossal motoneurons.

To ascertain whether, in addition to enhancing neurite growth, MSP also increases the number and branching of hypoglossal motoneuron neurites, the number of neurites emerging from the cell bodies of the neurons (first order branches) and the number of branches in their neurite arbors (second

and third order branches) were counted. Figure 3.2.4 shows that the number of first order branches of motoneurons grown in the presence of MSP was no greater than the number of those emerging from cell bodies grown in control cultures. Counts of second and third order branches reveal the same picture; no difference between motoneurons grown in MSP-supplemented medium and defined medium only could be observed. CNTF also did not affect the number of first order branches or branching points either (Fig. 3.2.4).

The camera lucida drawings of representative motoneurons growing with and without MSP illustrate the typical appearance of neurite arbors under these different experimental conditions (Fig. 3.2.5). It appears that MSP mostly affects the growth of one neurite of most of the neurons more than others. While it is tempting to assume that these prominent processes represent axons, additional studies using immunocytochemical markers that distinguish axons from dendrites will be required to support such a hypothesis. Taken together, these results suggest that MSP enhances the elongation of hypoglossal motoneuron neurites but does not affect the number of processes emanating from the cell bodies nor further branching.

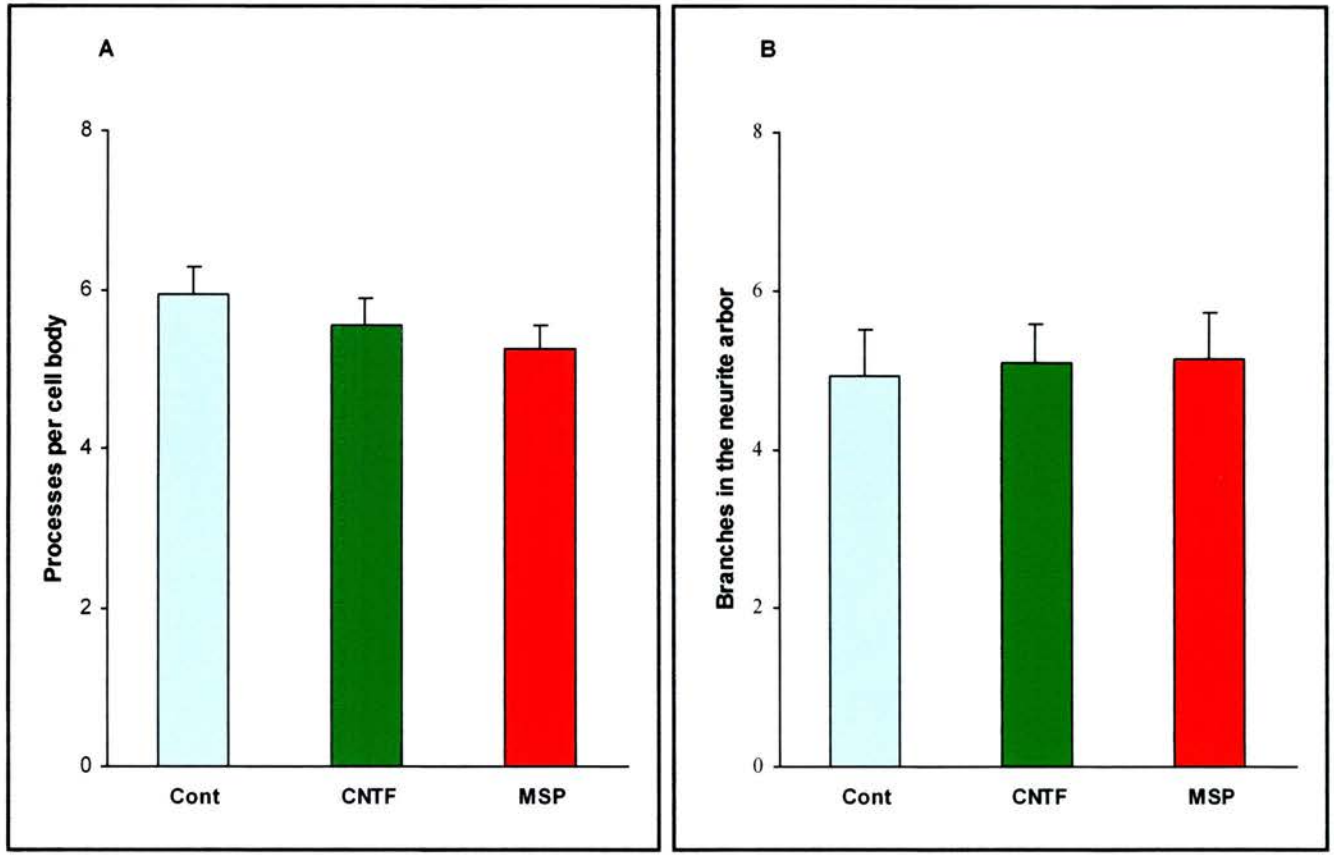

Fig. 3.2.4: A: numbers of neurites emerging from the cell bodies of embryonic chick hypoglossal motoneurons. **B:** numbers of branch points in the neurite arbors. Neurons grown for 48 h in defined medium alone (Cont) and in the presence of 10 ng/ml CNTF and 10 ng/ml MSP; n (neurons per growth factor) = 100

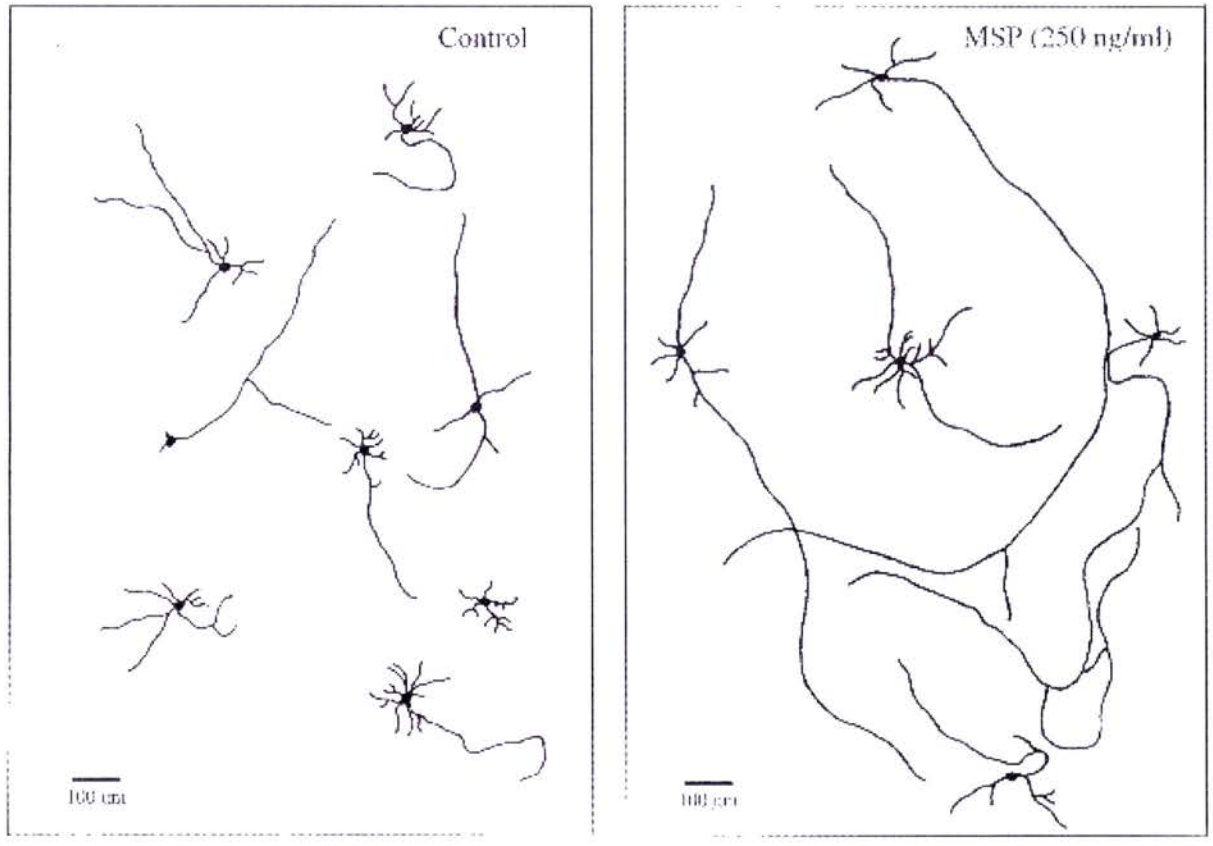

Fig. 3.2.5: Camera lucida drawings of typical neurite arbors of embryonic chick hypoglossal motoneurons grown for 48 h in defined medium alone (Control), and in the presence of 250 ng/ml MSP.

3.2.3. MSP is expressed in the target of hypoglossal motoneurons

Semiquantative RT/PCR was used to determine if MSP mRNA is expressed in the target tissue of hypoglossal motoneurons, the tongue, at E5.5 when naturally-occurring cell death is taking place. For comparison, the relative levels of MSP mRNA were also measured in two other tissues, the liver and the forebrain. Figure 3.2.6 shows that MSP mRNA was clearly detectable in the tongue and at higher levels in the liver. Although MSP mRNA was also present in the forebrain it was barely detectable. No MSP product was detectable when the reverse transcription step was omitted from samples of RNA extracted from the tongue, indicating that there was no contamination by genomic DNA. These results show that MSP mRNA is present in the target tissue of hypoglossal neurons during the period of naturally-occurring cell death, suggesting that MSP is a target-derived neurotrophic factor for these neurons.

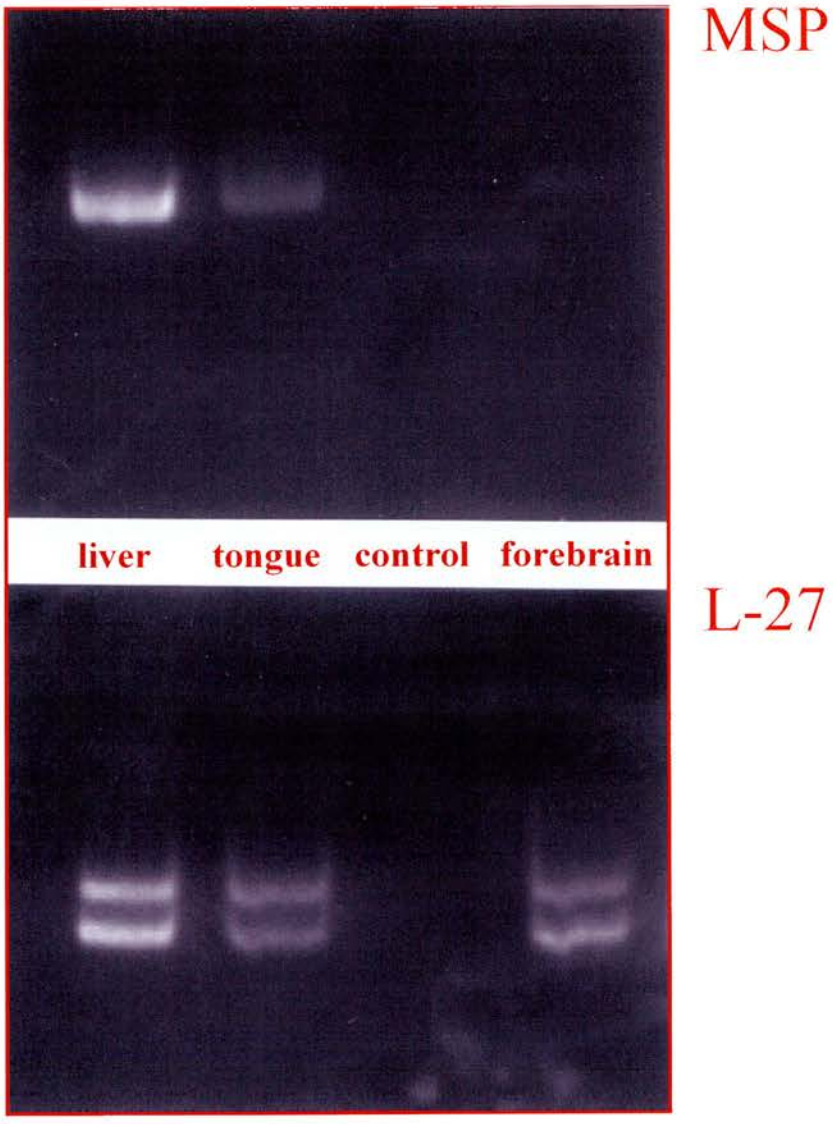

Fig. 3.1.6: MSP Expression in the tongue and control tissues of chick embryos at E5.5.
Corresponding gels of the RT-PCR products for MSP mRNA (upper gel) and L-27 mRNA (lower gel). Control Control reactions for MSP and L-27 mRNA from which the reverse transcriptase step was omitted show no detectable contamination by genomic DNA.

3.3. Discussion

This study has shown that MSP is a neurotrophic factor for embryonic hypoglossal motoneurons. MSP promotes the survival of these neurons and enhances the rate at which neurites extend from these neurons. While previous studies have shown that the MSP receptor RON is expressed in several locations in the central nervous system, including the hypoglossal nucleus (Gaudino et al., 1995; Quantin et al., 1995; Thery et al., 1995), this study provides evidence that MSP has a role in promoting neuronal survival in the developing brain. It is known that MSP has a variety of effects on cells derived from different tissues, including the regulation of cell proliferation, migration and differentiation (Skeel and Leonard, 1994; Banu et al., 1996; Broxmeyer et al., 1996; Wang et al., 1996; Kurihara et al., 1998). This study reveals for the first time that MSP promotes cell survival in an anatomically discrete population of motoneurons in the developing brainstem. It has recently been reported that exogenous MSP sustains cholinergic acetyltransferase expression in hypoglossal neurons in adult mice following axotomy, showing that these neurons are also sensitive to MSP *in vivo* in the mature central nervous system (Stella et al., 2001).

Showing that MSP promotes the survival of hypoglossal motoneurons during a stage in development when programmed cell death is taking place within populations of motoneurons (Lance-Jones, 1982), adds another factor to the ever growing list of neurotrophic factors capable of promoting the

survival of developing motoneurons (Oppenheim, 1996). However, it has been increasingly apparent in recent years that motoneurons are heterogeneous with regard to their functional characteristics and neurotrophic requirements. Hypoglossal neurons are the only brainstem motoneurons that express the MSP receptor RON during development.

HGF, a pleiotropic factor that is structurally related to MSP, has a well established neurotrophic role in the developing vertebrate nervous system (Ebens et al., 1996; Hamanoue et al., 1996, Maina et al., 1997, 1998; Yamamoto et al., 1997; Wong et al., 1997; Yang et al., 1998; Okura et al., 1999; Caton et al., 2000; Davey et al., 2000; Novak et al., 2000). However, the neurotrophic actions of MSP on hypoglossal motoneurons differ in a number of respects from the known neurotrophic actions of HGF on motor- and other neurons. In many cases, HGF does not enhance the survival of neurons on its own, but exerts its neurotrophic effect only in the presence of other neurotrophic factors. For example, HGF does not promote the survival of sensory or parasympathetic neurons alone, but synergises with Nerve Growth Factor (NGF) in promoting the survival of nociceptive sensory neurons and also with CNTF in increasing the survival of proprioceptive and parasympathetic neurons (Maina et al., 1997; Davey et al., 2000). In contrast, this study has shown that MSP enhances survival of purified hypoglossal motoneurons grown in low density cultures in the absence of other neurotrophic factors, suggesting that MSP has a direct trophic effect on these neurons on its own. Where HGF has been shown to have a direct survival-promoting effect on cultured neurons – as is the case with spinal

motoneurons (Ebens et al., 1996; Wong et al., 1997; Novak et al 2000) - its activity is enhanced by the presence of CNTF (Wong et al., 1997). This additive effect could not be shown for MSP. Although both, MSP and CNTF promote the survival of hypoglossal motoneurons on their own, combining the two factors did not increase the effect they have on their own.

The effects of MSP on neurite growth also differ in several aspects from those of HGF. Although HGF promotes growth of motoneuron neurites in dissociated culture (Wong et al., 1997), it does not enhance the growth of processes from sensory, sympathetic or parasympathetic neurons unless either NGF or CNTF are present (Maina et al., 1997, 1998; Davey et al., 2000). Moreover, whereas HGF increases both length and branching in the presence of these factors, this study has shown that MSP only increases the length of hypoglossal motoneurons, not their branching. An interesting finding is that the hypoglossal nerve is truncated in mice with targeted disruption of the HGF gene and also in mice null mutant for the HGF receptor, Met (Caton et al., 2000). HGF is known to be expressed along the pathway and is also required for the correct migration of tongue myoblasts (Bladt et al, 1995). Caton and colleagues speculate that the loss of synaptic targets might be responsibe for the observed defect in the hypoglossal nerve (Caton et al., 2000). Given the findings presented here, MSP might be the target-derived factor responsible for the outgrowth defect. Interestingly, the authors note that the delay in hypoglossal outgrowth is compensated at later developmental stages which could be due to a different guidance system. Unfortunately, they do not mention whether the tongue is absent in these null

mutant mice or whether its formation is delayed. A delayed or even partially formed tongue might be the reason for the later compensation of hypoglossal outgrowth. To elucidate whether MSP might be the missing link, valuable information could be obtained from studying the hypoglossal nerve in $MSP^{-/-}$ /$HGF^{-/-}$ double knockout mice.

In summary, this study has provided the first evidence that MSP can function as a neurotrophic factor for a subset of neurons in the developing brain. However, its effects on motoneuron survival and neurite growth differ in a number of aspects from the structurally-related factor HGF. In future work it will be important to determine not only the physiological relevance of these *in vitro* observations by studying the consequences of targeted deletion of either the MSP or RON genes but also to focus on motoneuron populations that do not express RON. Since the purification of anatomically distinct populations of cranial motoneurons still proves to be difficult due to the lack of specific markers cell counts in transgenic mice might be a way of showing the specificity of MSP.

CHAPTER 4

Effects of γ-Synuclein on dopaminergic midbrain neurons and cranial motoneurons

4.1 Introduction

The synucleins are a recently discovered family of small, heat-stable and soluble proteins (Nakajo et al., 1990; George et al., 1995) which are abundant in the nervous system. The name is a contraction of *synapse* and *nucleus* reflecting the initial finding of localization in both synapse and nuclear envelope (Maroteaux et al., 1988). However, nuclear localization has not been consistently observed in subsequent studies (Jakes et al., 1994; George et al., 1995; Iwai et al., 1995). Synucleins are between 120-140 amino acids long and contain an acidic stretch towards the C terminus. Characteristic is a hydrophobic stretch of 5 to 6 highly conserved , imperfect KTKEGVLYVGS repeats within the first 93 residues of the protein's N-terminal region(Maroteaux et al., 1988; Nakajo et al., 1990; George et al., 1995; Iwai et al., 1995).

The first member of this family was purified from cholinergic synaptic vesicles of the Torpedo californica (electric ray) electromotor nucleus (Maroteaux et al., 1988). In humans, 3 members of the family have been identified so far: α-, β-, and γ-synuclein (Jakes et al., 1994; Ji et al., 1997). Little is known about the physiological functions of these proteins. Most studies undertaken so far have focused on the association of synucleins with a range of neurological diseases, in particular with Alzheimer's and Parkinson's disease.

The first *human* synuclein was detected in brain samples of patients suffering from Alzheimer's disease (AD). The disease is characterized by the presence of proteinaceous deposits in certain cerebral structures known as amyloid plaques. The main components of these plaques are fibrils made up from variants of the β-amyloid protein (Aβ). Another fibrillar component of the amyloid plaque was identified in 1993 as a 35 amino acid proteolytic peptide, named non-Aβ component of AD amyloid (NAC; Ueda et al., 1993). It was found to be derived from a 15 kDA precursor protein, NACP (Iwai et al., 1995; Weinreb et al., 1996). In 1994, Jakes and colleagues cloned two similar but distinct human proteins, one of which was equivalent to NACP (Jakes et al., 1994). The other showed high similarity to an earlier purified brain-specific bovine protein named phosphoneurin-14-kDa (PNP-14; Nakajo et al., 1993). They named these two proteins α- and β-synuclein.

The third member of the synuclein family was identified by three different groups using subtractive cDNA cloning techniques (Akopian and Wood, 1995; Ji et al., 1997; Buchman et al., 1998a). It has therefore been tagged with three different names: peripheral synuclein-like protein; breast cancer specific gene 1 (BCSG 1); and persyn. To avoid confusion, Clayton and George suggested to rename the protein as γ-synuclein (Clayton and George, 1998). Notwithstanding close associations with one of the groups that have initially cloned the gene, the protein is referred to as γ-synuclein throughout this thesis. The gene which is located on chromosome 10q23, has

a 54% homology with α-synuclein and 56% homology with β-synuclein (Ji et al., 1997).

γ-synuclein is widely expressed throughout the central and the peripheral nervous system with a cytoplasmic and axonal localization on the cellular level. The particularities of γ-synuclein's expression pattern are the subject of Chapter 5. Consistent with the cytoplasmic localization in many neurons, Surgochov and colleagues have recently shown that γ-synuclein is associated with the centrosome (Surgochov et al., 2001). The centrosome is the major microtubule organizing centre of the cell. Adjacent to the cell nucleus, it determines the number, polarity and organization of microtubules during interphase and mitosis. In their study γ-synuclein co-localized with 3 centrosome proteins (γ-tubulin, centrin, CTR453) in retinoblastoma cells, astrocytes and melanoma cells. The fact that it remained connected to the centromere even after nocodazole-induced disassembly of microtubules suggest that it might be centromere-associated protein (Surgochov et al., 2001). Another intriguing aspect that might be of significance in the protein's involvement in malignant diseases like breast cancer (Ji et al., 1997; Ninkina et al., 1998) and ovarian cancer (Bruening et al., 2000), was the observation that γ-synuclein localized to the poles of mitotic spindles in dividing cells of the retinoblastoma cell line (Surgochov et al., 2001).

Alterations in the organization of the cell cytoskeleton are characteristic in both, neurodegenerative and malignant diseases. Disruption of the centrosome's function involving γ-synuclein might be a contributing

factor in the pathogenesis of these diseases (Surgochov et al., 2001). Buchman and colleagues have shown by means of immunostaining that overexpression of γ-synuclein by microinjection of an expression plasmid into cultured sensory neurons, dramatically decreased detection of the three neurofilament types (NF-H, NF-M, NF-L). In contrast, immunostaining for peripherin (another intermediate filament protein), microfilaments (actin), and microtubules (tubulin) did not change. Interestingly, calpeptin and leupeptin, inhibitors of calcium-dependent proteases that have been implicated in the degradation of neurofilaments after acute insults to neurons, were shown to suppress the effects of γ-synuclein overexpression. This might imply that the observed γ-synuclein-induced neurofilament degeneration is catalysed by calcium-dependent proteases (Buchman et al., 1998b).

Recent studies suggest that γ-synuclein – like α-synuclein – is involved in the pathogenesis of neurodegenerative diseases. Spheroid-like lesions that stain positive for γ-synuclein have been identified in the hippocampal region of brains from patients with Parkinson's disease as well as Dementia with Lewy bodies (Galvin et al., 1999). γ-synuclein immunoreactivity was also detected in axonal spheroids in the brains of patients suffering from Neurodegeneration with Brain Iron Accumulation (Hallervorden-Spatz syndrome; Galvin et al., 2000).

It is important to note that current knowledge of the functions of γ-synuclein is fragmentary and at least partially based on anecdotal evidence.

A whole range of approaches to gain knowledge about a protein's function are feasible, and some of them have been employed in the findings presented above. The very recently developed technique of "knocking out" single genes, and therefore eliminating the effects of the genes' protein products has become a widely used tool to study the function of particular proteins.

In the present study null mutant mice, lacking the γ-synuclein gene have been used to analyse brainstem structures involved in motor control. The mouse strains with a targeted deletion of the first three exons of the murine γ-synuclein gene (Fig. 4.1.1) were produced in the laboratory of Vladimir Buchman by Natalia Ninkina, Liz Delaney, and Vladimir Buchman. Two strains generated from independent ES cell clones were used in this study. Western blotting using an antibody specific to the C-terminal peptide of mouse γ-synuclein showed complete absence of the protein in all tissues of null mutant mice. Northern hybridisation of RNA from various tissues confirmed complete inactivation of γ–synuclein function in null mutant mice, which was not accompanied by compensatory increase of α- or β-synuclein mRNA levels (Fig. 4.1.1). Mice lacking the γ-synuclein gene were viable, fertile and did not show any obvious abnormalities in behaviour or gross morphology of the nervous system.

Since there is some evidence that γ-synuclein is implicated in the pathogenesis of Parkinson's disease (see above), it seemed interesting to investigate whether the lack of γ-synuclein would lead to changes in the substantia nigra, especially its content of dopaminergic neurons. Parkinson's

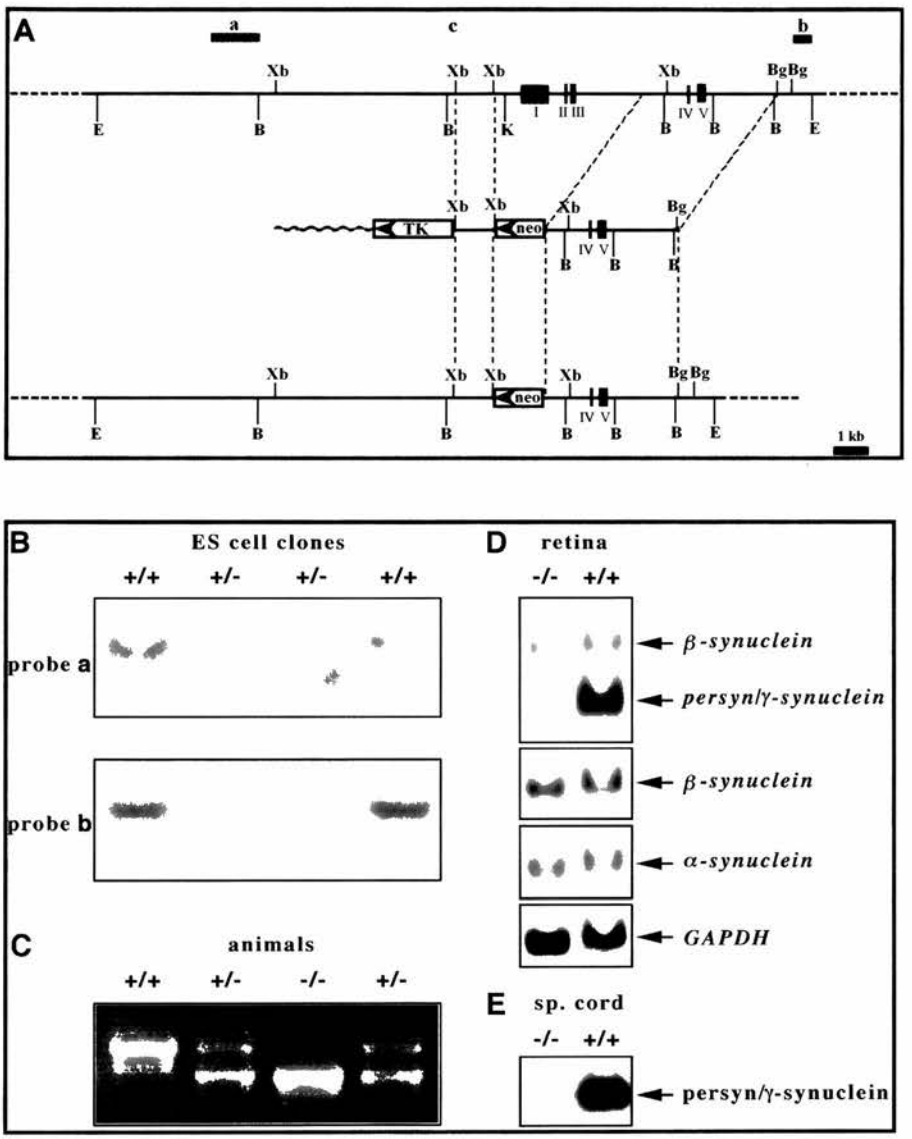

Fig. 4.1.1: Targeted inactivation of the murine γ-synuclein gene. **A:** Diagram showing deletion of exons I, II and III and promoter region of the γ-synuclein gene by homologous recombination. The organization of the wildtype genomic locus (top), targeting vector (middle) and resulting knockout locus (bottom) are shown. **B:** Examples of analysis of homologous recombination in ES cell lines by Southern hybridisation. **C:** Example of PCR-based genotyping of mice from a litter of two heterozygous parents. **D:** Expression of mRNA encoding members of the synuclein family in the retina of wildtype and γ-synuclein mice. Results of Northern hybridisation with full-length mouse γ-synuclein-specific cDNA probe, mouse β-synuclein–specific and α-synuclein-specific and GAPDH probe are shown. **E:** Western blot of 10 mg of total spinal cord proteins of wildtype and γ-synuclein null-mutant mice was probed with the mouse γ-synuclein-specific SK23 antibody. (Figure courtesy of Vladimir Buchman)

disease, the most common movement disorder and the second most common neurodegenerative disease after Alzheimer's disease, is characterized by a range of symptoms, mainly paucity and slowness of spontaneous movement, a resting tremor, increased muscle tone, shuffling gait, stooped posture, and a greasy, mask-like face devoid of expression. The majority of these symptoms is due to a substantive loss of dopaminergic neurons in the zona compacta of the substantia nigra (SNpc), a basal ganglion involved in the fine-tuning of movement.

Since expression of γ-synuclein mRNA had also been found in brainstem motor nuclei (Buchman et al., 1998b), it seemed feasible to include these nuclei into the study. This would provide clues as to whether possible changes in the substantia nigra of γ-synuclein null-mutant mice were specific or a more generalized phenomenon.

The brainstem contains three subpopulations of motoneurons which are arranged in anatomically distinct nuclei. Each of these three subpopulation is characterized by the position of their respective nuclei in the coronal plane, the exit points of their nerve roots, and their targets. The most medially located motor nuclei comprise the somatomotor (SM) neurons which innervate the muscles of the tongue and the external ocular muscles. In a slightly more lateral position to the discontinuous column of somatomotor nuclei lies the group of branchiomotor (BM) nuclei. Their motoneurons supply striated muscles that have derived from the mesoderm of the pharyngeal (branchial) arches. The most lateral group of cranial motor

nuclei comprises visceromotor (VM) neurons. These are presynaptic neurons that innervate parasympathetic ganglia.

The present study focuses on six cranial motor nuclei. They are the four SM nuclei (*oculomotor, trochlear, abducens*, and *hypoglossal nucleus*), and two nuclei from the BM group (*facial* and *trigeminal motor nucleus*).

4.2 Results

4.2.1 Lack of γ-synuclein leads to a loss of dopaminergic neurons in the substantia nigra and the ventral tegmental area

To investigate the number of dopaminergic midbrain neurons in wild type and γ-synuclein mice brains were taken from adult (6 month old) animals. The mice were bred from F5 parents both of which were heterozygous for the γ-synuclein gene. A total of 16 brains – either homozygous wild types or homozygous null mutants - were analysed. Brains used for optimisation of the staining procedure (see Materials and Methods) are not included in this number. Genotyping of the mice was done by a different investigator. Cell counts were therefore performed in a blind fashion.

Brain sizes and weights were essentially the same in the wild type and the γ-synuclein null mutant mice (Fig. 4.2.1). Morphological comparison of the SNpc in both genotypes revealed no gross differences. The average lengths in the rostrocaudal direction were almost the same; 770 μm for knockouts and 752 μm for wild types ($n=20$, $p> 0.7$). No differences in cell distribution were noted. Neither did the null mutant mice reveal any obvious defects in the substantia nigra. The dopaminergic neurons as outlined by the anti-TH-stain were of equal appearance in both groups (Fig. 4.2.2). As actual cell sizes are difficult to measure for a range of reasons, the nuclear diameters were measured. This was necessary anyway for the application of

A: wildtype brain

view from dorsal

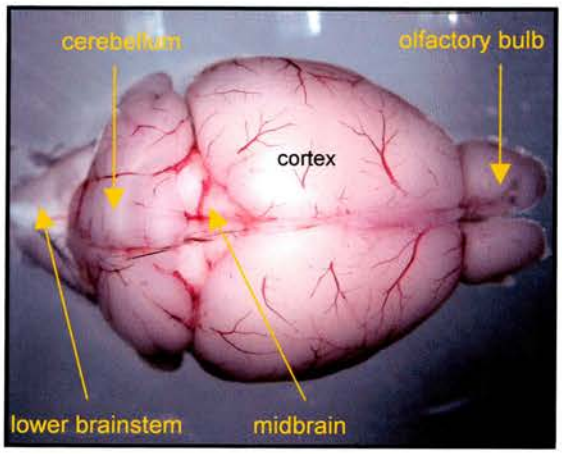

view from ventral

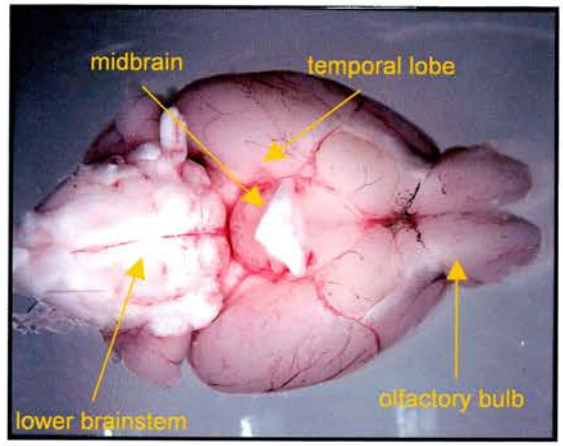

B: γ-synuclein knockout brain

view from dorsal

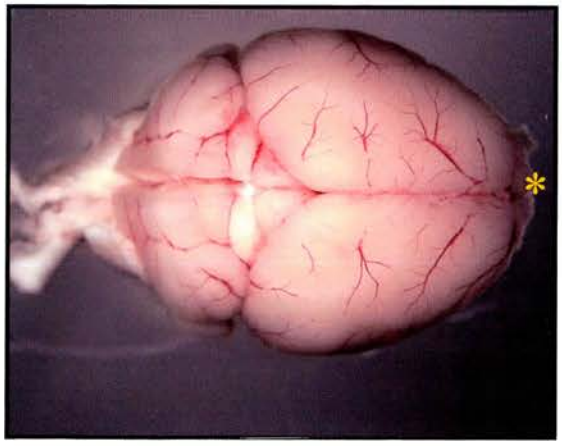

view from ventral

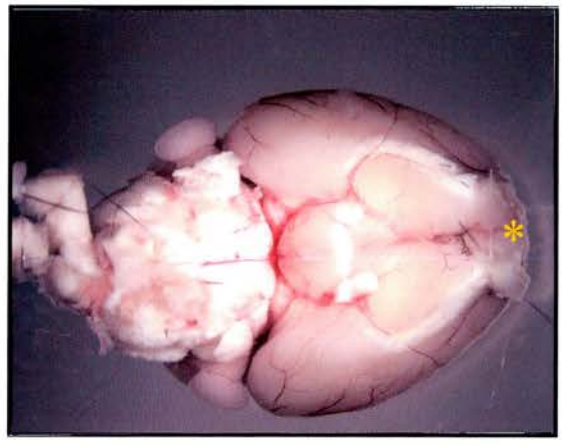

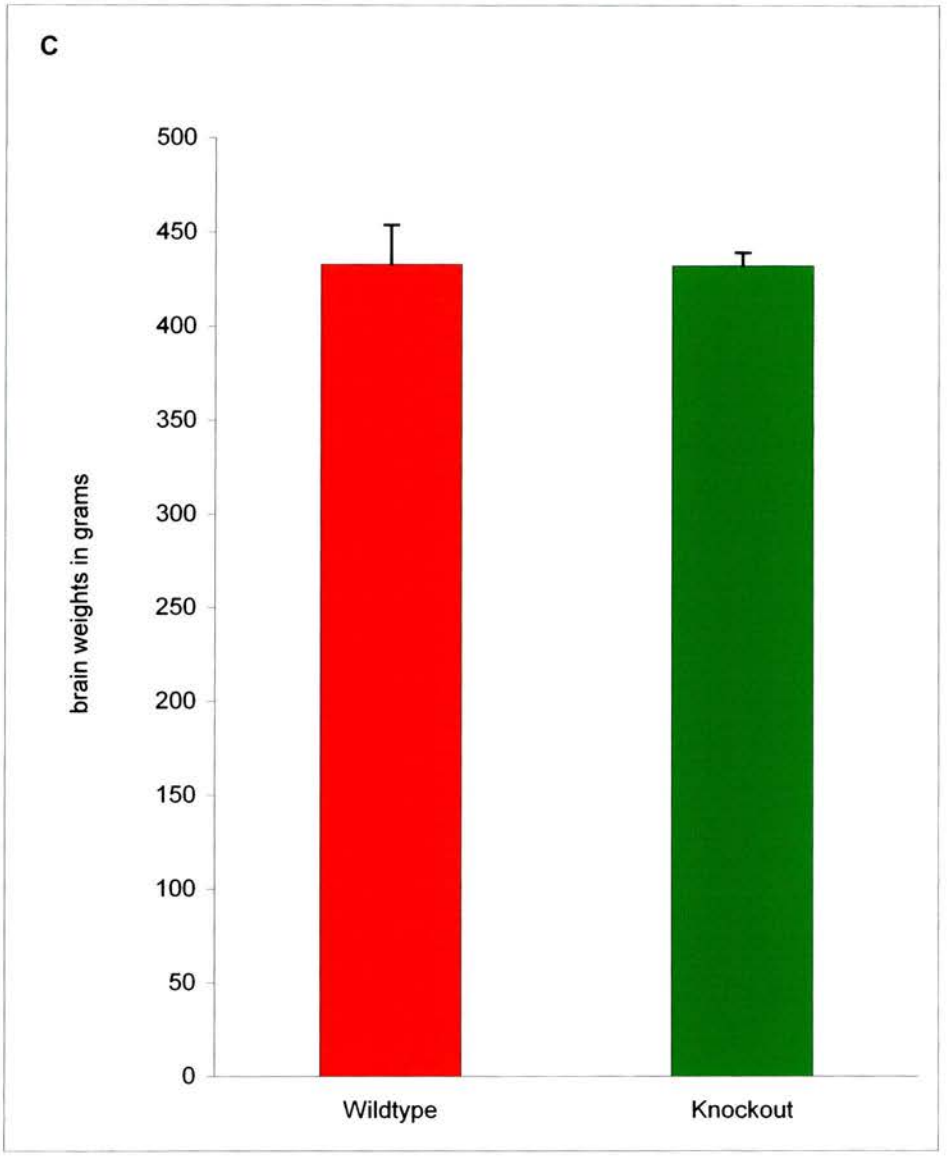

Fig. 4.2.1: Comparison of the gross brain anatomy from wildtype and γ-synuclein null-mutant mice. **A:** Freshly dissected, unfixed brain from a wildtype mouse. The most prominent brain structures are labelled. Note the superior and inferior colliculi of the midbrain in the gap between cerebellum and forebrain cortex. **B:** Freshly dissected, unfixed brain from a knockout mouse. All major structures of a normal brain are present. Also note the vascular pattern which is almost identical to the pattern shown in the wildtype brain. The star indicates the remains of the olfactory bulbs which were severed during dissection. **C:** Comparison of brain weights. No differences between wildtype and knockout brains were observed. n=8 (4 brains per genotype), $p>0.9$, two-tailed, unpaired Student's T-Test. Error bars show standard error of mean.

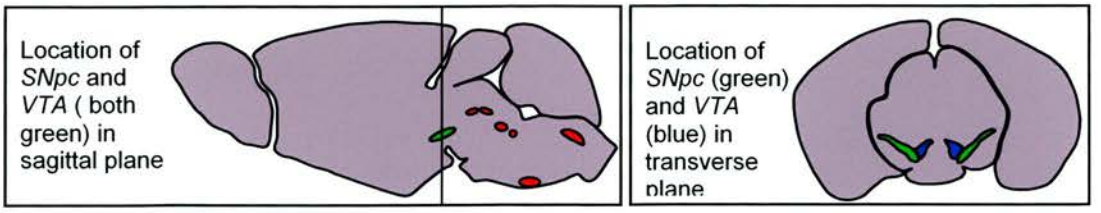
Location of *SNpc* and *VTA* (both green) in sagittal plane
Location of *SNpc* (green) and *VTA* (blue) in transverse plane

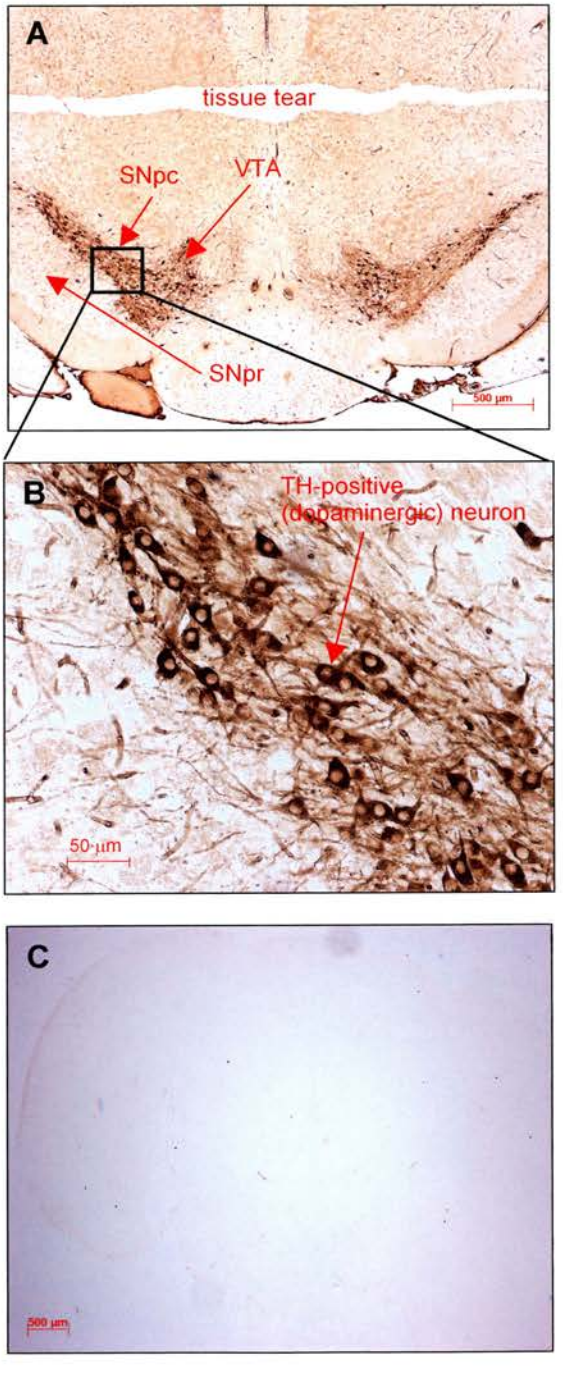
A
tissue tear
SNpc
VTA
SNpr
500 µm
B
TH-positive (dopaminergic) neuron
50-µm
C
500 µm

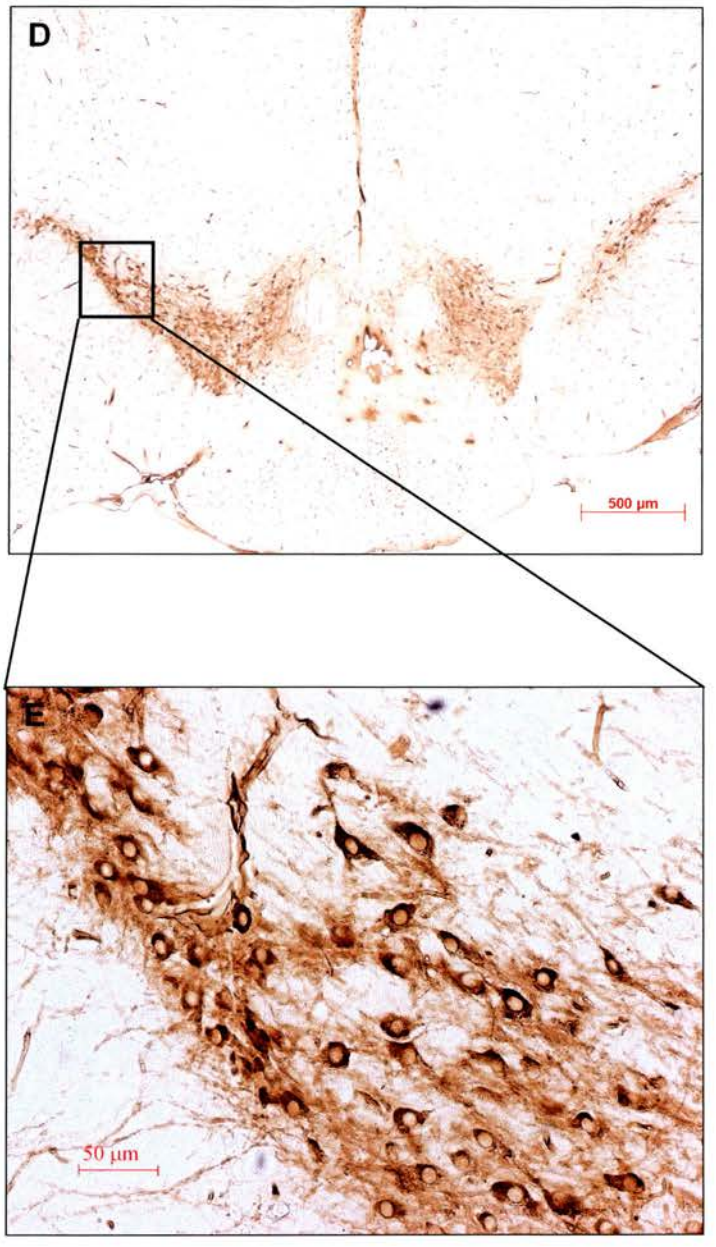

Fig. 4.2.2: Anti-tyrosine hydroxylase (TH) stains of the *substantia nigra, pars compacta (SNpc)* and the *ventral tegmental area (VTA)* in a wildtype and a γ-synuclein null-mutant mouse. **A:** transverse section through the middle part of the SN and VTA of a wildtype mouse at 25 fold magnification. **B:** higher magnification of A (200x) showing single dopaminergic neurons. **C:** Negative control: omission of the anti-TH antibody. **D, E:** similar section through the SN and VTA of a knockout mouse. The gross anatomical features of the SNpc and the VTA as well as the morphology of the dopaminergic neurons are preserved in the null-mutant mice. SNpr: substantia nigra, pars reticulata (unstained).

Abercrombie's correction to the cell count results (see Materials and Methods). No significance difference of cell nucleus diameters was observed (Fig. 4.2.3).

Cell counts were performed on dopaminergic neurons of the SNpc as well as the Ventral Tegmental Area (VTA). Although the latter is not part of the brain's motor control system (but belongs to the limbic system), its dopaminergic neurons were included in the study for two reasons: firstly to ascertain whether any possible differences observed in the substantia nigra could be seen in other dopaminergic system, and secondly, since the VTA lies on the same rostrocaudal level as the SN and its neurons were also TH-stained and therefore readily available for investigation. Ironically, as it turned out during further research on the subject, the decision to include the VTA would become a necessity rather than a luxury: At E18, it is impossible to draw a line between the SNpc and the VTA. Cell counts at that stage can therefore only be conducted on both structures together (see below).

A note on sample numbers: every brain contains two substantiae nigrae (1 per side) and two ventral tegmental areas. Therefore, the sample numbers (n) in the figures represent the number of structures not brains counted. The same applies to the motor nuclei below.

A significant reduction in the numbers of dopaminergic neurons was observed in the SNpc of the γ-synuclein null mutant mice (Fig. 4.2.4; $p<0.03$, two-tailed, unpaired Student's T-Test). The loss of cells accounted for about

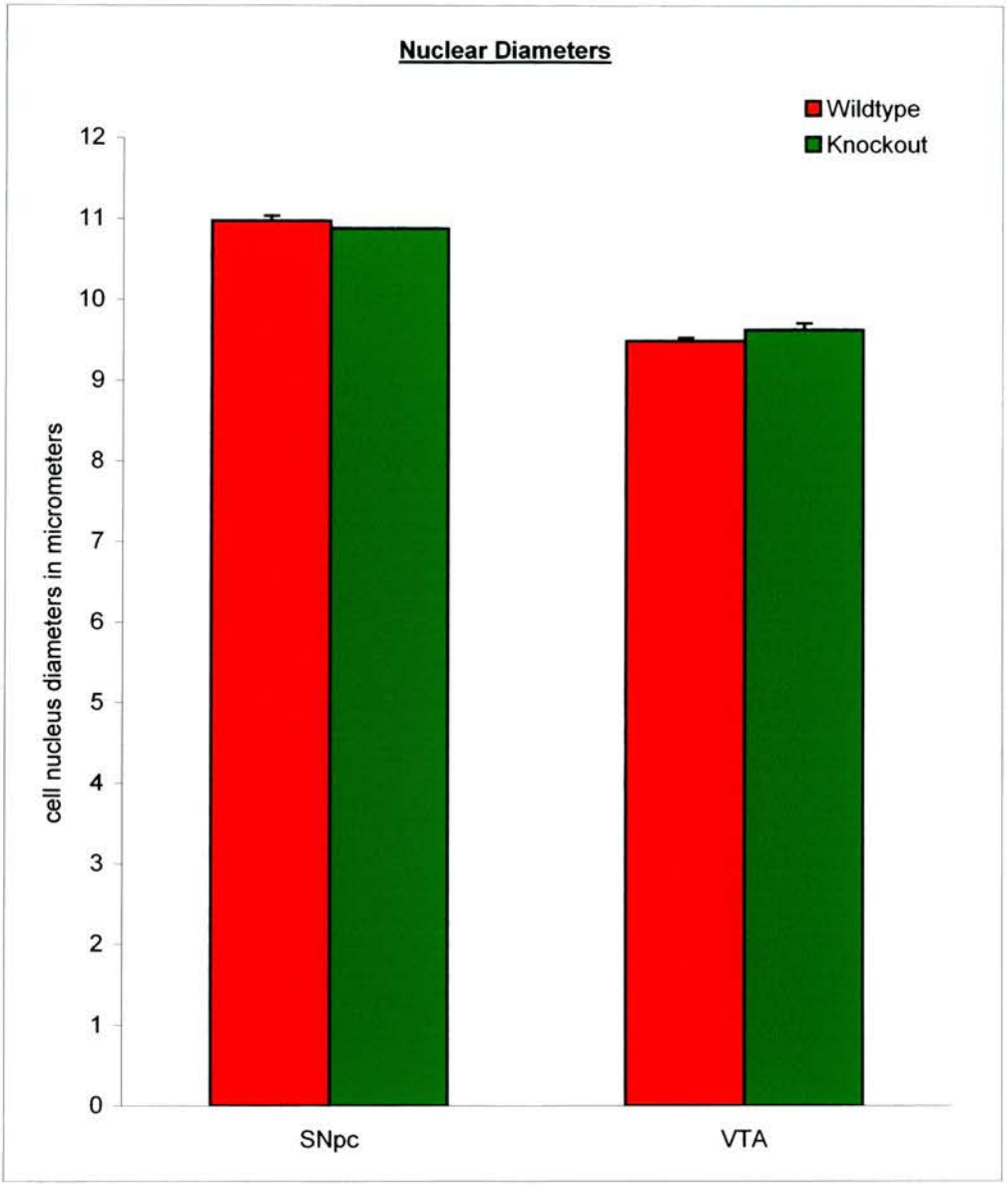

Fig. 4.2.3: Comparison of dopaminergic neuron cell nucleus diameters in the *substantia nigra, pars compacta (SNpc)* and the *ventral tegmental area (VTA)* of wildtype and γ-synuclein null-mutant mice. The nuclei in the VTA on average are smaller than those of the dopaminergic neurons of the SNpc in both wildtypes and knockouts. No significant differences between the genotypes in either structure were noted.

n=10 brains (5 per genotype) per structure. p(SNpc)>0.4; p(VTA)>0.4 (two-tailed, unpaired Student's T-Test). Error bars show the standard error of mean.

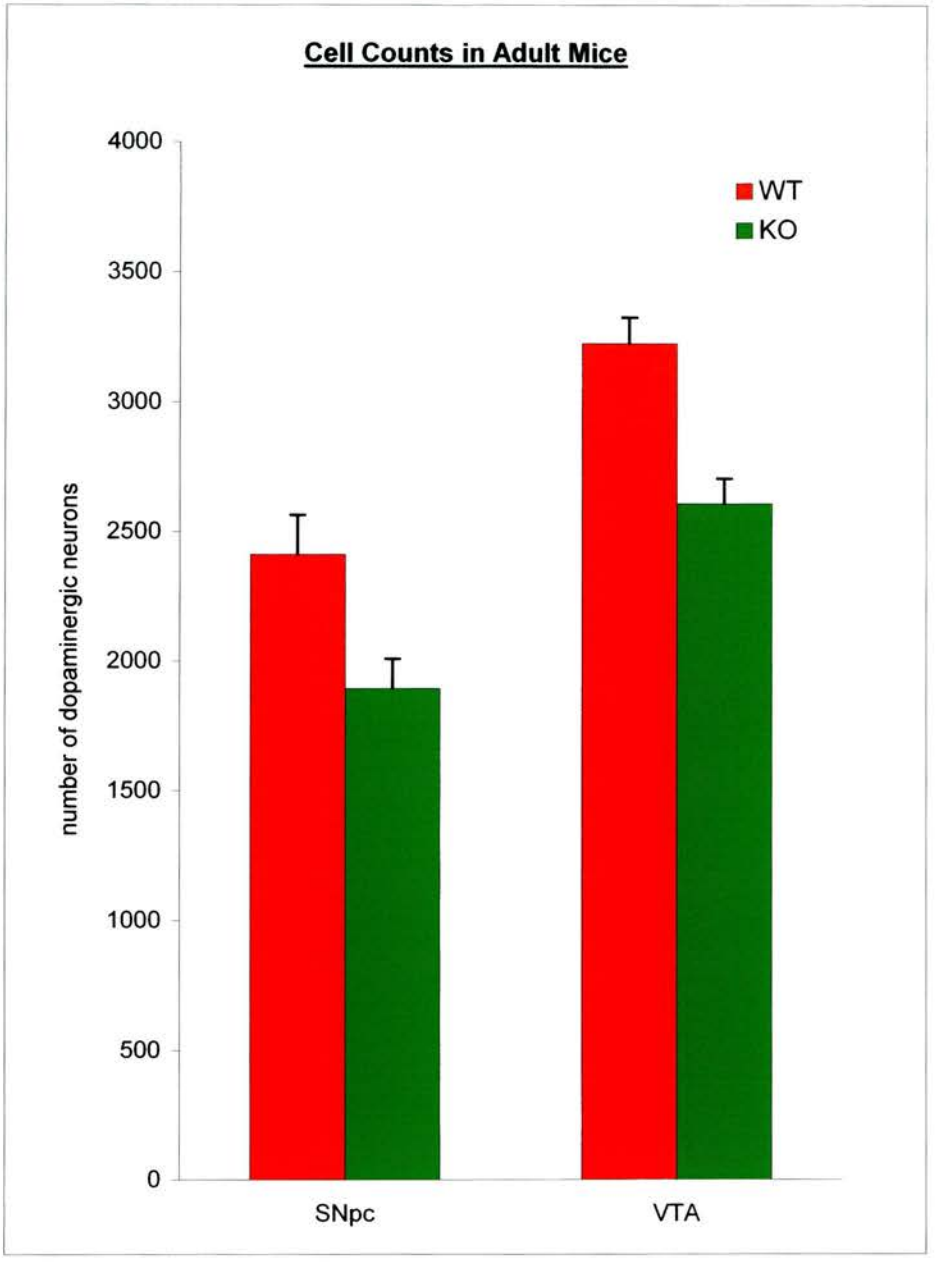

Fig. 4.2.4: Comparison of numbers of midbrain dopaminergic neurons in *adult, 6 months old* wildtype (WT) and γ-synuclein null-mutant (knockout, KO) mice. Results from cell counts conducted in the pars compacta of the *substantia nigra (SNpc)* and the *ventral tegmental area (VTA*) are presented. Both structures show a significant reduction in numbers of dopaminergic neurons in the knockout mice.
SNpc: n=20 (10 per genotype), $p<0.03$, two-tailed, unpaired Student's T-Test.
VTA: n=20 (10 per genotype); $p<0.0005$, two-tailed, unpaired Student's T-Test.
Cell numbers refer to results obtained from unilateral cell counts. Error bars show standard error of mean.

a quarter of all TH-positive neurons. As mentioned above, there were no obvious defects, suggesting that the loss of cells was not confined to a particular part of the SNpc but was more or less evenly spread throughout the nucleus. Interestingly, the same pattern of cell loss was observed in the VTA (Fig. 4.2.4; $p<0.005$, two-tailed, unpaired Student's T-Test). Again, about a quarter of TH-positive neurons was lost, and there was no obvious confinement to a particular area of the VTA.

The data just presented was obtained from male and female mice. This was necessary due to a shortage of specimens at the time. Moreover, cell counts were also conducted on very young animals and embryos (see below). At those stages it is very difficult to sex a mouse. However, one has to be aware of the problems that can arise when using mice of both sexes. Nervous structures (as any other physical parameters) might very well differ between male and female specimen. For this reason, the data was reanalysed according to the mice's sex. The results mirrored those seen in the mixed samples. (Fig. 4.2.5).

One of the obvious questions to emerge from these results was when these neurons were lost. Three possible scenarios to explain the loss of SN neurons in the mutants came to mind:

1. A reduced number of precursor cells had differentiated into dopaminergic midbrain neurons.

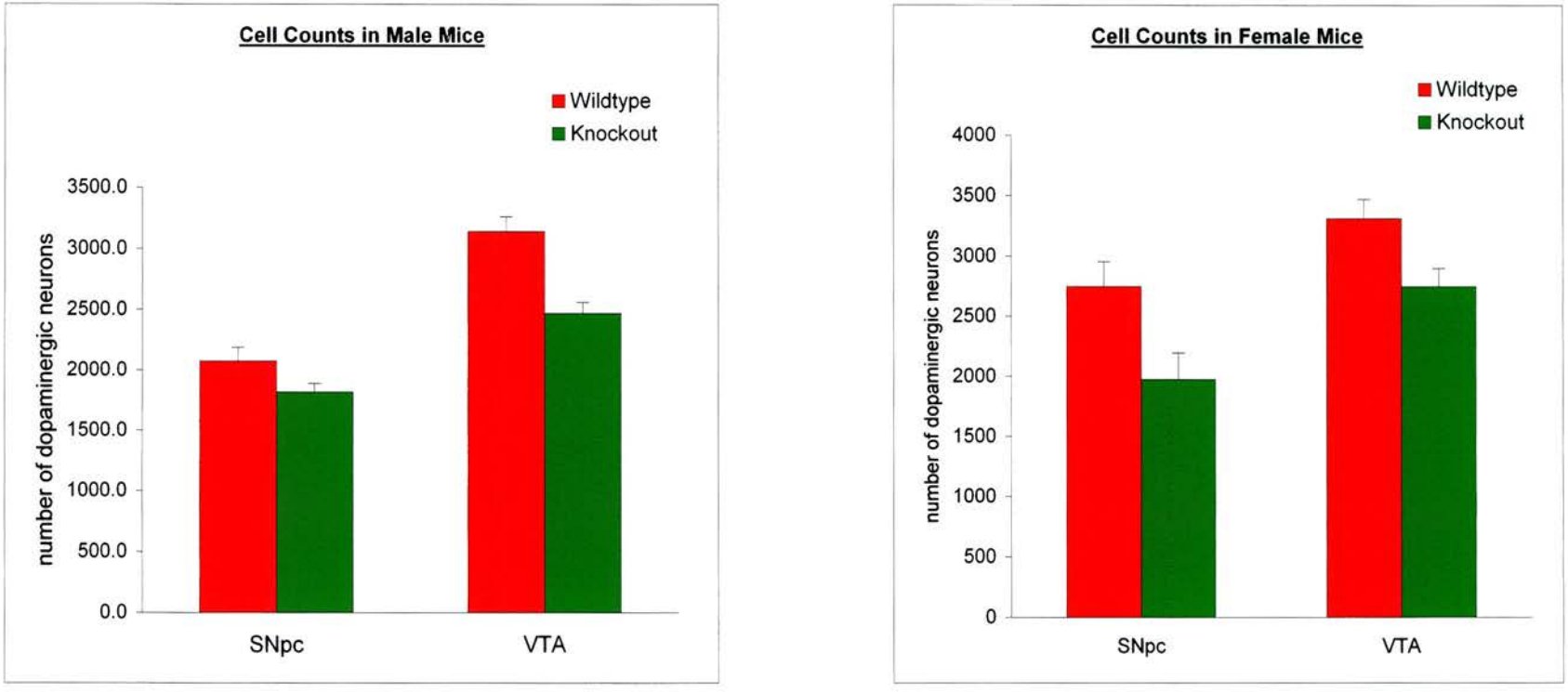

Fig. 4.2.5: Gender-specific comparison of numbers of midbrain dopaminergic neurons between adult wildtype and γ-synuclein null-mutant mice. The reduction of dopaminergic neurons in the *substantia nigra (SNpc)* and the *ventral tegmental area (VTA)* detected in mixed samples is independent of gender.

Substantia nigra		*Ventral tegmental area*	
Male	Female	Male	Female
n=10; p<0.09	n=10; p<0.04	n=10; p<0.004	n=10; p<0.04

Cell numbers refer to results obtained from unilateral cell counts. Error bars show standard error of mean.

2. An increased number of dopaminergic neurons had undergone physiological cell death or a particular, putative subpopulation of dopaminergic neurons had been eliminated during development.

3. The observed loss of cells had been due to a pathological process.

The first and the last scenario would have been hard to demonstrate, but some evidence for a possible increased physiological cell death could be gathered by performing cell counts on brains of different ages: Murine midbrain dopaminergic neurons undergo two distinct wave of postnatal developmental cell death, the first and more pronounced of which begins at E19 and peaks at 2 days post partum (see above). I therefore immunostained brains from E18 mouse embryos (just before cell death commences) and P5 (towards the end of the first cell death period). The mice were taken from the same colony as the adult mice above. Two litters of P5 mice were used with a total of 4 knockout and 4 wild type brains. And for E18 counts 6 knockout and 6 wild type embryos were taken from 2 litters. Immunohistochemistry was performed in the same fashion as with adult mice.

At P5, as was the case in the adult brains, a significant reduction of dopaminergic midbrain neurons was observed in the γ-synuclein null mutant mice. Again, the reduction amounted to about a quarter of all dopaminergic neurons in both the SNpc and the VTA (Fig. 4.2.6; $p<0.005$ and $p<0.0005$ respectively, two-tailed, unpaired Student's T-Test).

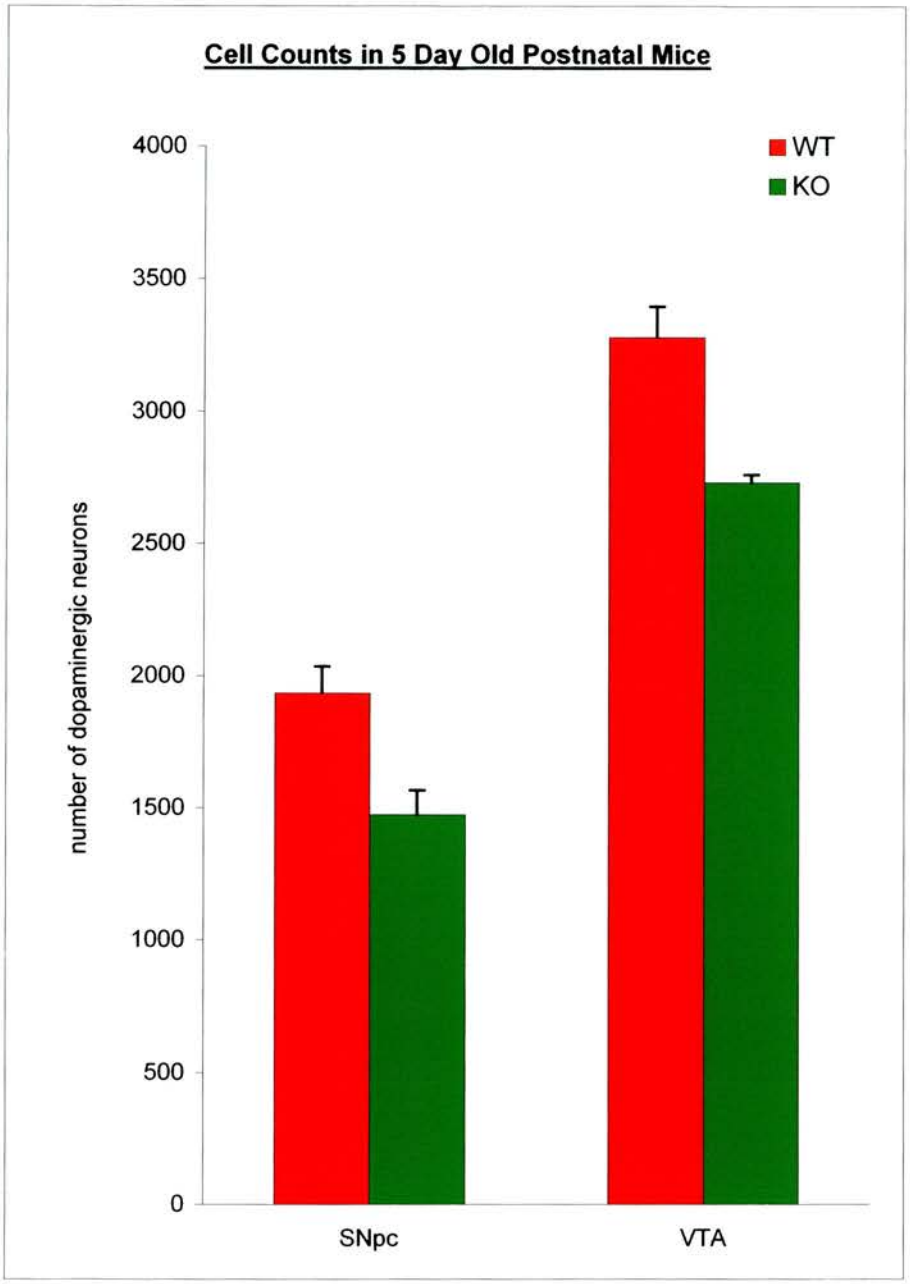

Fig. 4.2.6: Comparison of numbers of midbrain dopaminergic neurons in *5 day old* wildtype (WT) and γ-synuclein null-mutant (knockout, KO) mice. Results from cell counts conducted in the pars compacta of the *substantia nigra (SNpc)* and the *ventral tegmental area (VTA)* are presented. Both structures show a significant reduction in numbers of dopaminergic neurons in the knockout mice, comparable to the one seen in adult mice.
SNpc: n=16 (8 per genotype), $p<0.005$, two-tailed, unpaired Student's T-Test.
VTA: n=16 (8 per genotype); $p<0.0005$, two-tailed, unpaired Student's T-Test.
Cell numbers refer to results obtained from unilateral cell counts. Error bars show standard error of mean.

Analysis of the E18 brains posed a problem already hinted at above. Even in more mature brains, it can be rather difficult to draw a distinction between neurons of the SNpc and those of the VTA in their rostral parts. At E18, it is impossible to mark the boundary between the two structures (Fig. 4.2.7). I therefore decided to count the dopaminergic neurons of both structures in their entirety. Taken together, the total number of these neurons revealed no difference between wild type and null mutant mice (Fig. 4.2.8; $p>0.7$, two-tailed, unpaired Student's T-Test). As both, the SNpc and the VTA of γ-synuclein knockout mice are depleted of a quarter of their dopaminergic neurons at P5 and indeed in adulthood, the observations made at E18 suggest that the lack of γ-synuclein does not interfere with the production of dopaminergic midbrain neurons during embryogenesis but might be due to increased developmental cell death of these neurons between E19 and P5 (see discussion).

4.2.2. Lack of γ-synuclein leads to cell loss in some but not all cranial motor nuclei

Another question that arose from the observation of increased cell loss in the substantia nigra and the ventral tegmental area was whether this was a general phenomenon that affected the entire nervous system or whether it was more specific. A co-worker had at the same time observed cell losses in the cervical dorsal root ganglia (Gayle Middleton, personal communication). It seemed therefore reasonable to extend cell counts to other parts of the nervous system. I decided to investigate neuron numbers in the cranial somato-and branchiomotor nuclei. In situ hybridisation studies have shown

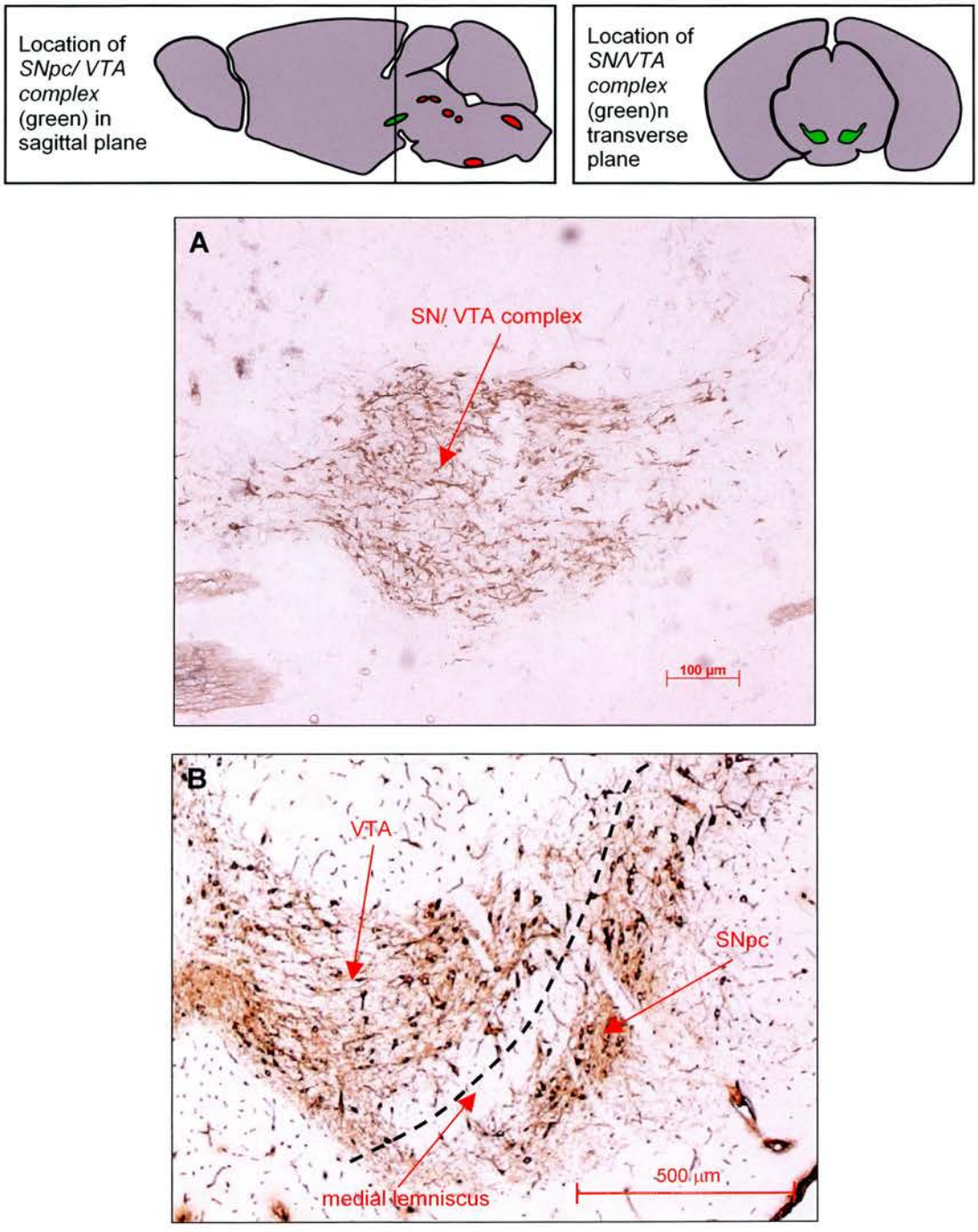

Fig. 4.2.7: Dopaminergic neurons of the right *substantia nigra, pars compacta (SNpc)* and *ventral tegmental area (VTA)* at E18 (A) and in the adult mouse (B). **A:** E18. The neurons of both structures form a somewhat united complex. **B:** adult brain. The two structures are separated (dotted line) by the fibre bundles of the medial lemniscus that run in rostrocaudal direction.

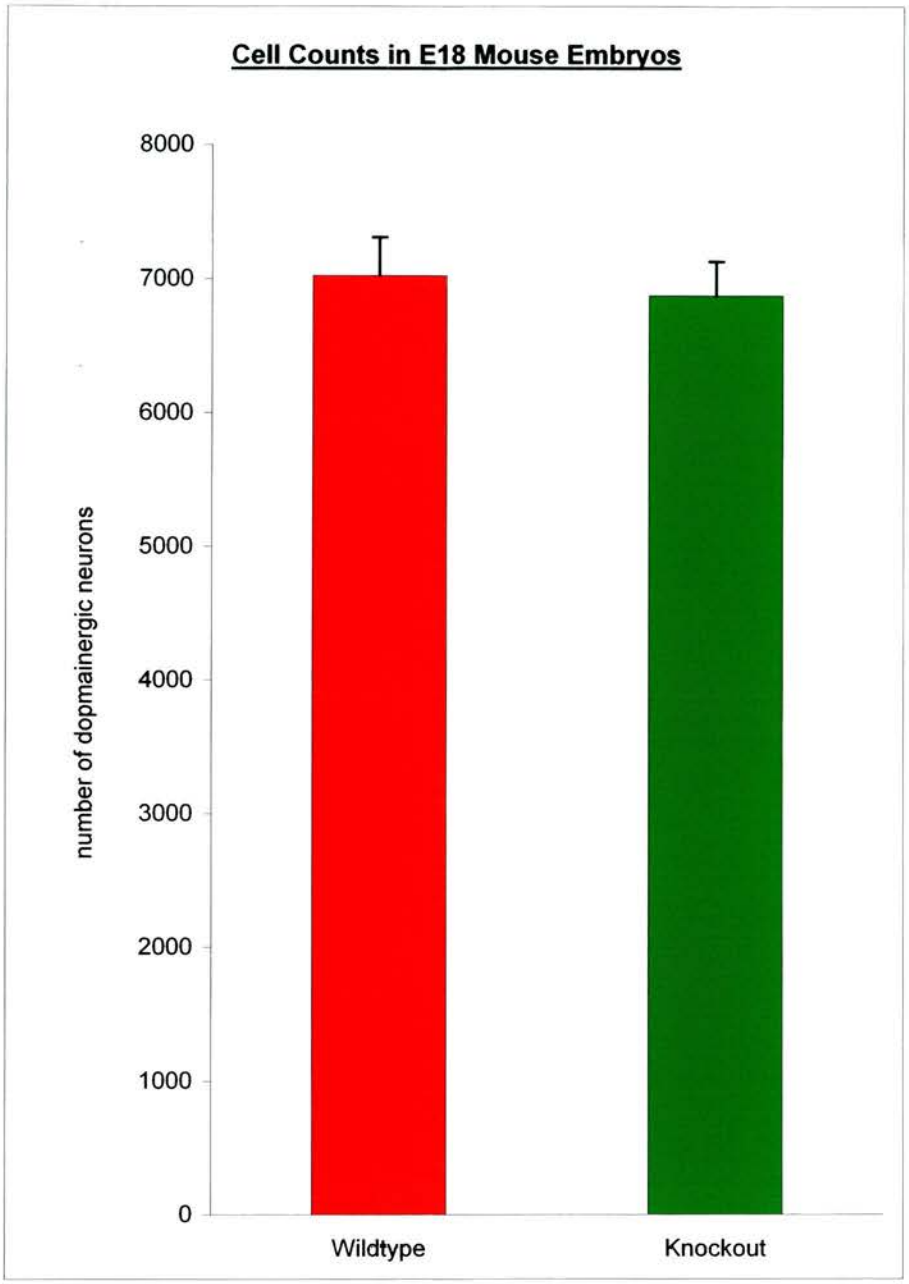

Fig. 4.2.8: Comparison of numbers of midbrain dopaminergic neurons in *18 day old embryos* of wildtype and γ-synuclein null-mutant (knockout) mice. Total cell numbers of both the *substantia nigra, pars compacta (SNpc)*, and the *ventral tegmental area (VTA)* are presented. No significant difference in the number of dopaminergic neurons in the *SNpc/VTA complex* was detected between wildtype and knockout mouse embryos. n=20 (10 per genotype), $p>0.7$, two-tailed, unpaired Student's T-Test.
Cell numbers refer to results obtained from unilateral cell counts. Error bars show standard error of mean.

that γ-synuclein is expressed in these nuclei (Buchman et al., 1998b; Putten, van der, personal communication).

Analogous to the approach for the midbrain dopaminergic neurons, brainstems from adult wild type and γ-synuclein null mutant mice were embedded in paraffin wax and sectioned at 8 μm. As no specific marker was available for the motoneurons (see Materials and Methods), the specimens were stained with Neutral Red. Counts were performed on 5 wild type and 5 knockout brainstems taken from two litters of the same colony of mice used to derive the SN/VTA counts.

No obvious morphological differences between corresponding motor nuclei were noted. As with the substantia nigra and the ventral tegmental area, the rostrocaudal lengths of all nuclei were calculated to check whether there were any significant differences in size. Most nuclei did not reveal any differences between genotypes. In the cases of the *hypoglossus* and the *trigeminus nucleus* average lengths seemed to be shorter in the knockouts but without statistical significance (Fig. 4.2.9). On the cellular level, motoneurons in the null mutants exhibited normal morphology with average cell nucleus diameters being of the same length as in the corresponding wild type neurons (Fig. 4.2.10).

As far as neuron numbers were concerned, there was a general tendency towards lower cell numbers in the null mutant mice, but only two of the six motor nuclei showed significant differences. Cell counts performed

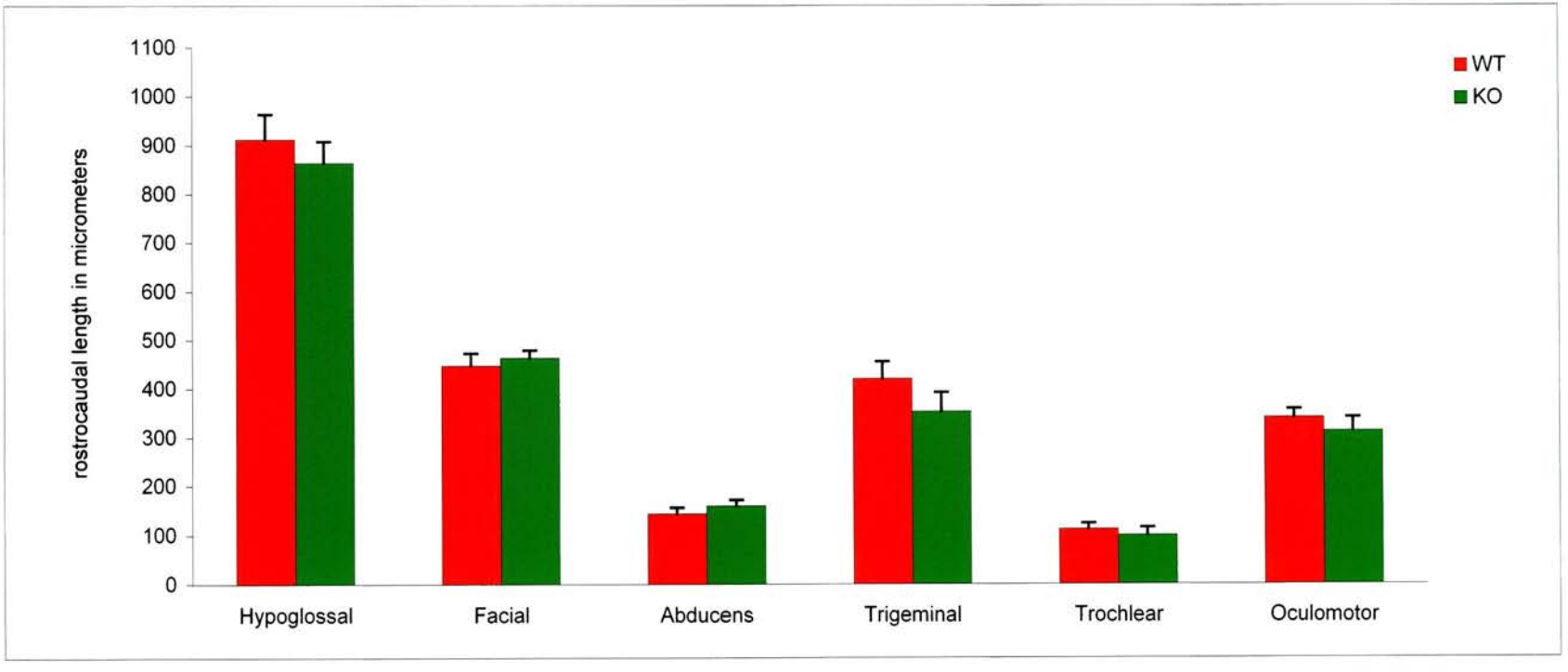

Fig. 4.2.9: Comparison of *rostrocaudal lengths of cranial motor nuclei* between wildtype and γ-synuclein null-mutant mice. None of the nuclei show a significant difference of length between genotypes.

n=8 (4 per genotype) per motor nucleus. Error bars show standard error of mean.

Significance tests (two-tailed, unpaired Student's T-Test):

Hypoglossal nucleus	Facial nucleus	Abducens nucleus	Trigeminal motor nucleus	Trochlear nucleus	Oculomotor nucleus
p>0.3	p>0.4	p>0.2	p>0.1	p>0.3	p>0.2

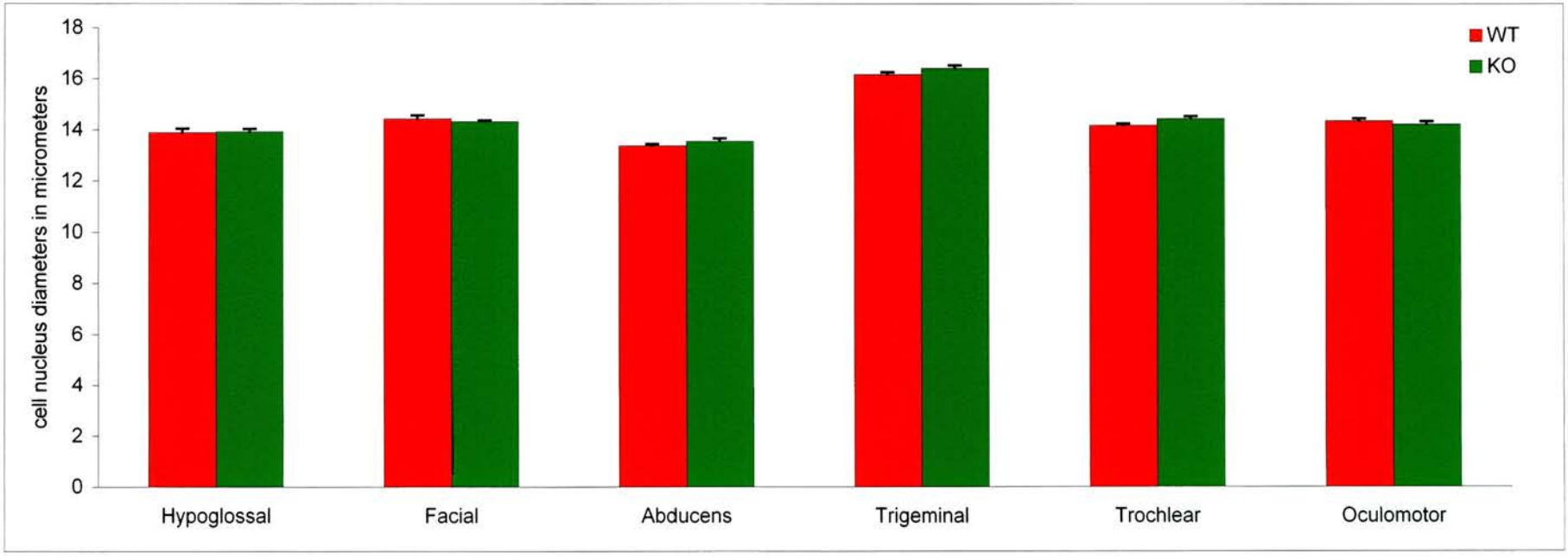

Fig. 4.2.10: Comparison of *motoneuron cell nucleus diameters* in the cranial somato- and branchiomotor nuclei of wildtype and γ-synuclein null-mutant mice. No differences in nuclear diameters in any given motor nucleus were detected between wildtype and knockout mice.

n=8 (4 per genotype) per motor nucleus. Error bars show standard error of mean.

Significance tests (two-tailed, unpaired Student's T-Test):

Hypoglossal nucleus	Facial nucleus	Abducens nucleus	Trigeminal motor nucleus	Trochlear nucleus	Oculomotor nucleus
p>0.8	p>0.4	p>0.2	p>0.1	p>0.1	p>0.3

on the *hypoglossal nuclei* led to almost identical results (Fig. 4.2.11; $p>0.8$, two-tailed, unpaired Student's T-Test). Cell numbers in the *facial nuclei* were slightly lower in the knockouts but the difference was not significant (Fig. 4.2.11; $p>0.4$). A similar picture was seen in two somatic motor nuclei, the *trochlear* and the *oculomotor*. Average cell numbers in the *oculomotor nuclei* were almost identical and the difference noted for the *trochlear nucleus* were subtle (Fig. 4.2.12; $p>0.4$ and $p>0.8$, respectively, two-tailed, unpaired Student's T-Test).

However, the situation was different in the case of the *trigeminal* and the *abducens nuclei*. Motoneuron numbers of both nuclei were reduced in the null mutants by approximately 20%, mirroring the findings in the substantia nigra and the ventral tegmental area. The differences were statistically significant in both nuclei (Fig. 4.2.13; $p<0.0005$ for the *abducens nucleus* and $p<0.05$ for the *trigeminus nucleus*, two-tailed, unpaired Student's T-Test).

These results show that the loss of neurons in γ-synuclein null mutant mice is not a generalized phenomenon indiscriminately affecting all neuronal populations in the nervous system but is confined to certain structures. Notably, in the case of the cranial motor nuclei, the effects of γ-synuclein - or more correctly its absence – did not abide by conventional classifications, like the distinction between somato- and branchiomotor neurons (see Introduction). Even more strikingly, of the three nuclei innervating the extra-ocular muscles, the oculomotor and the trochlear nuclei seemed unaffected

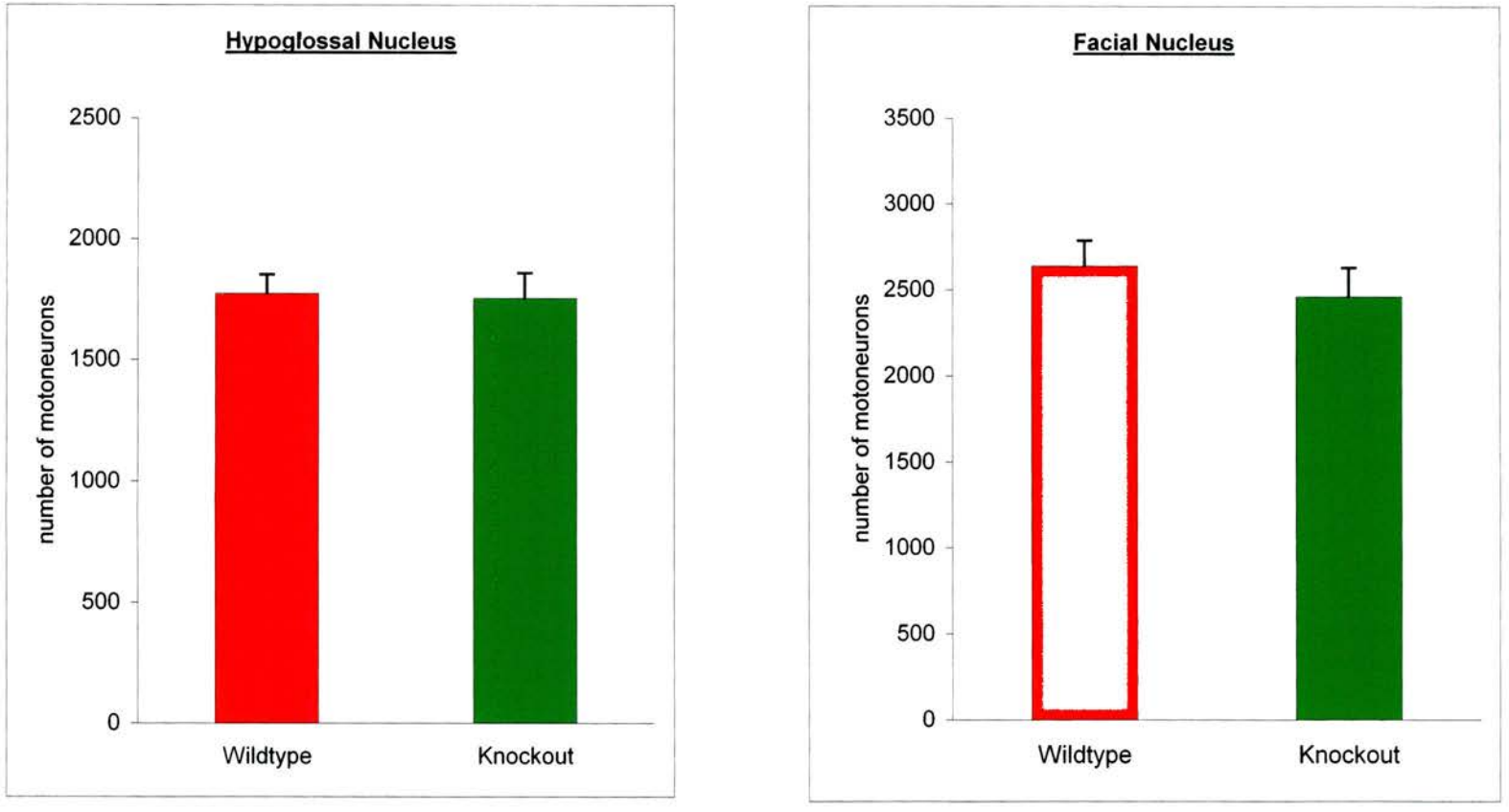

Fig. 4.2.11: Comparison of motoneuron numbers in the *hypoglossal* and *facial nucleus* between wildtype and γ-synuclein null-mutant mice. No differences in cell numbers were detected in either nucleus.

n=20 (10 per genotype) per motor nucleus. Hypoglossal nucleus: $p>0.8$; facial nucleus: $p>0.4$ (two-tailed, unpaired Student's T-Test).

Cell numbers refer to results obtained from unilateral cell counts. Error bars show standard error of mean.

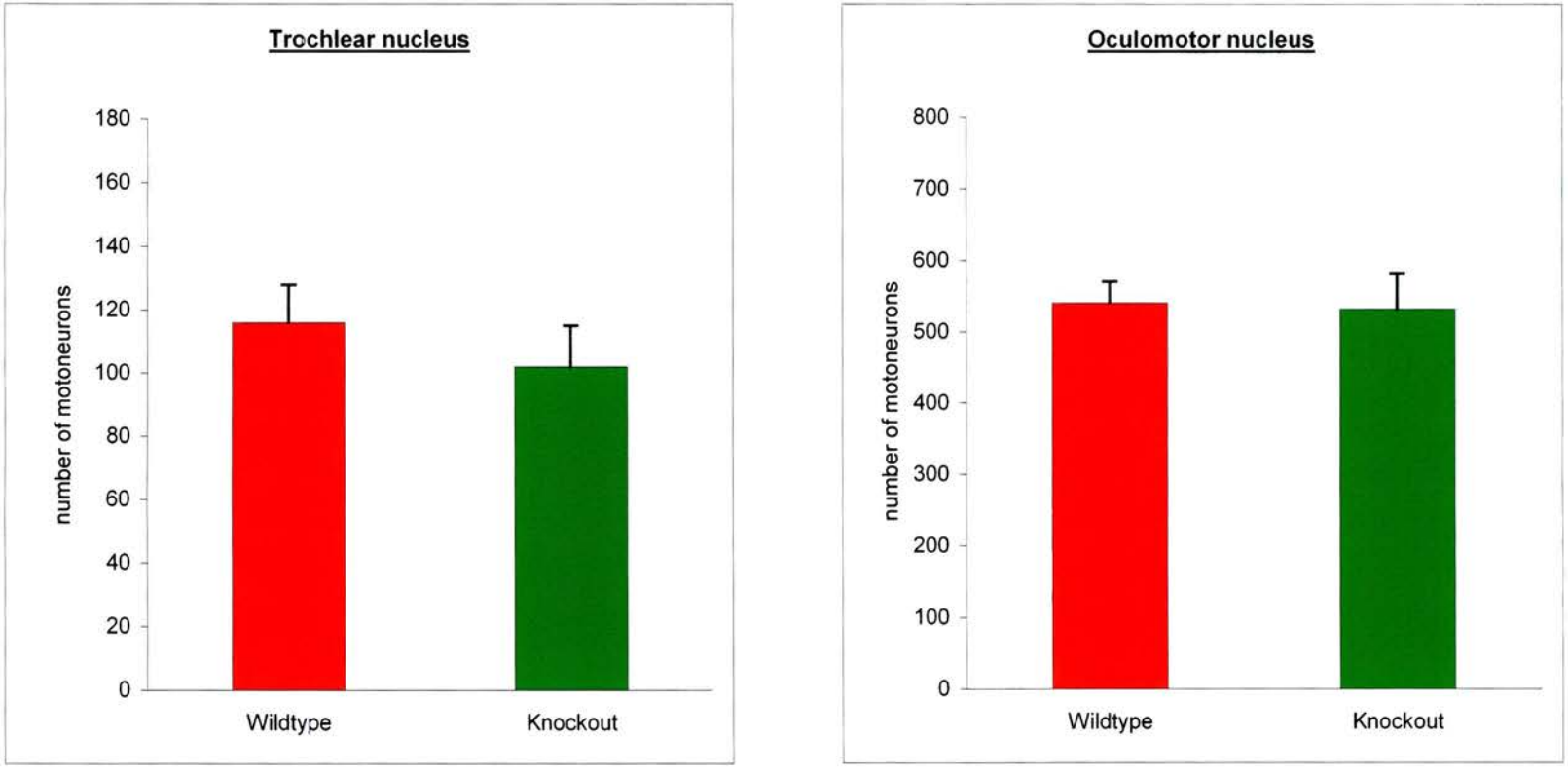

Fig. 4.1.12: Comparison of motoneuron numbers in the *trochlear* and *oculomotor nucleus* between wildtype and γ-synuclein null-mutant mice. No significant differences in cell numbers were detected in either nucleus.

n=20 (10 per genotype) per nucleus. Trochlear nucleus: $p>0.4$; oculomotor nucleus: $p>0.8$ (two-tailed, unpaired T-Test).

Cell numbers refer to results obtained from unilateral counts. Error bars show standard error of mean.

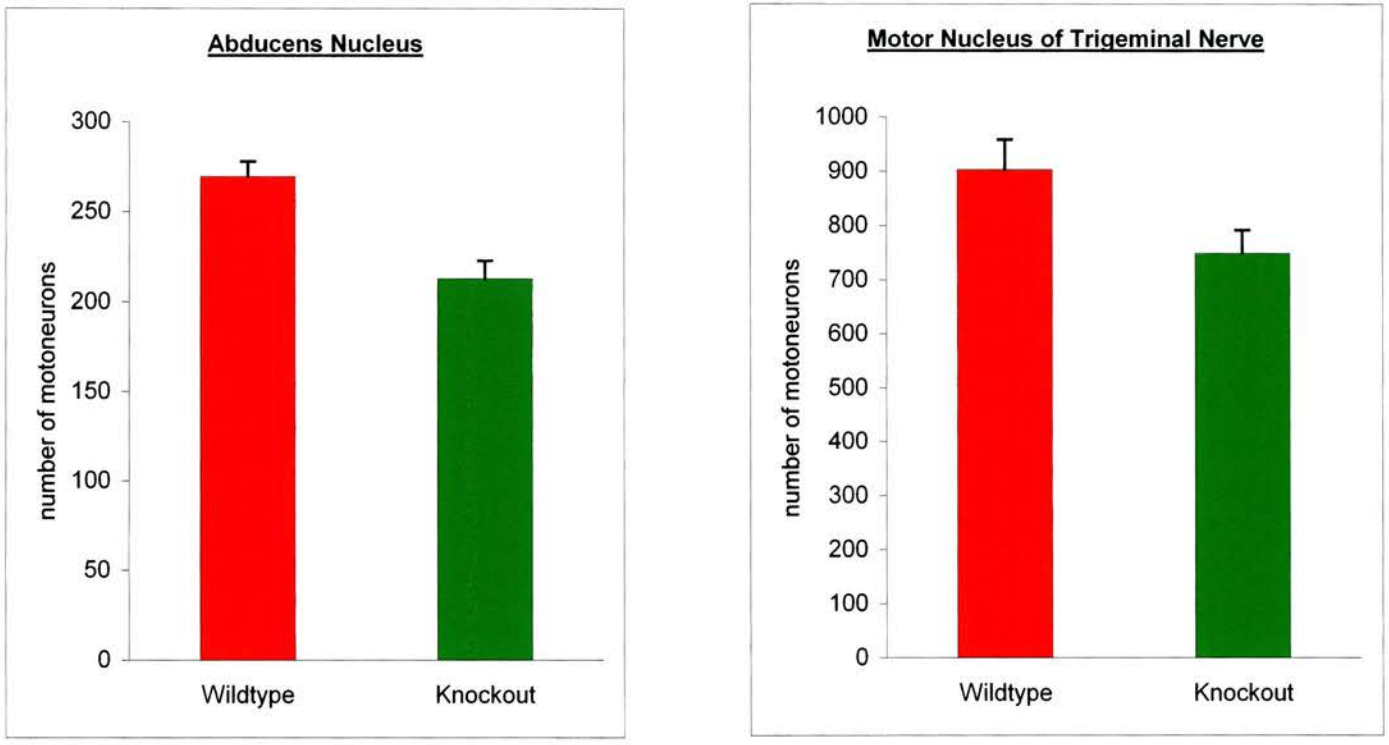

Fig. 4.2.13: Comparison of motoneuron numbers in the *abducens* and *trigeminal motor nucleus* between wildtype and γ-synuclein null-mutant mice. Both nuclei show a significant reduction of cell numbers in the knockout mice.

n=20 (10 per genotype). per motor nucleus. Abducens nucleus: $p<0.05$; trigeminus motor nucleus: $p<0.0005$ (two-tailed, unpaired Student's T-Test).

Cell numbers refer to results obtained from unilateral cell counts. Error bars show standard error of mean.

by the knocking out of the γ-synuclein gene, whereas the *abducens nucleus* suffered a significant loss of motoneurons.

4.3. Discussion

Given strong evidence that the synucleins are involved in neurodegenerative diseases, especially Parkinson's disease, the effects of knocking out the γ-synuclein gene on the dopaminergic neurons of the substantia nigra (and the ventral tegmental area) were analysed. While no obvious changes in the morphology of the basal ganglion were observed either on the macroscopical or on the cellular level, a significant lack of dopaminergic neurons in both structures was detected. About a quarter of all dopaminergic neurons in the SNpc and the VTA of γ-synuclein null mutant mice were lost. Cell counts performed at very young ages (P5 and E18) showed that the loss of these neurons seems to occur during the first few days of postnatal life, a period that coincides with the first and main wave of physiological cell death of SN and VTA dopaminergic neurons (see Introduction). The lack of these neurons in the γ-synuclein null mutant was of more or less the same ratio in the P5 pups as it was observed in 6 month old adult mice. This suggests that no more cells were lost either during the second wave of developmental cell death in the SN and the VTA (peak at P14; see Introduction) or by means of a later pathological process initiated by the lack of the protein.

The loss of neurons in γ-synuclein null mutant mice did not seem to be a generalized phenomenon affecting the entire nervous system as cell counts obtained from cranial motor nuclei have shown. In only two of the six motor

nuclei analysed, namely the *abducens* and the *trigeminal motor nucleus*, has the deficiency in γ-synuclein led to a reduction in neuronal numbers. No significant change of motoneuron numbers were observed in the *hypoglossal*, the *facial*, the *trochlear*, and the *oculomotor nucleus*. This suggests that only certain nervous structures are affected by the lack of γ-synuclein.

It is intriguing that of the three nuclei that supply the extra-ocular muscles, two (the *oculomotor* and the *trochlear nuclei*) showed no loss of motoneurons, whereas the third, the *abducens nucleus* did. Although all three nuclei are part of the somatomotor group and have their share in the same function, namely the movement of the eye, there are clear differences that separate them. Both, the *oculomotor* and the *trochlear nucleus* are adjacent midbrain nuclei, whereas the *abducens nucleus*, which lies caudal to the trigeminal motor nucleus, is part of the hindbrain. The former two are characterized by the expression of the homeodomain transcription factors, Phox2a and Phox2b (Valarche et al. 1993; Pattyn et al., 1997). A null mutation for Phox2a results in the total absence of these two nuclei but not of the *abducens nucleus* which does not express Phox2a (Pattyn et al., 1997; Morin et al., 1997).

Although the loss of the midbrain dopaminergic neurons coincided with the first phase of developmental cell death in this area, γ-synuclein certainly doesn't fulfil the requirements of a classical neurotrophic factor for example. For once, there is no evidence that the protein is secreted by its cells of origin. And secondly, during development, γ-synuclein appears

confined to the nervous system (Buchman et al., 1998a). The cranio-facial musculature, the target for cranial motoneurons does not express the protein. However, the old neurotrophic model of a target-derived factor that rescues competing neurons from physiological cell death by binding to a specific receptor expressed by these neurons, is a rather simplistic one (See Introduction and General Discussion). Cell survival is clearly a highly complex matter, and the requirements for a neuron to survive development and to become a fully functional part of a nervous structure are varied.

On the basis of γ-synuclein overexpression studies in sensory and sympathetic neurons, Buchman and colleagues have suggested that γ-synuclein influences neurofilament network integrity. Overexpression of the protein led to degradation of the heavy neurofilament NF-H possibly by calcium-dependent proteases (see above; Buchman et al 1998b). However, if one were to assume that the absence of γ-synuclein had a similarly detrimental effect on the neurofilament network and therefore on the survival of affected neurons, the question remains as to why only some nuclei showed cell losses. From a genetic point of view, it could be argued that the gene showed varying degree of penetrance. Thereby, the deleterious effects of its absence would be ameliorated by some counteracting mechanism. On a molecular level, this translates into the involvement of other factors equally involved in neurofilament network integrity. Furthermore, γ-synuclein might not be expressed in all of the dopaminergic neurons of the substantia nigra

for example but only in a certain subpopulation. Its absence would therefore only affect those neurons that actually express the gene.

Another and intriguing aspect that might assist in explaining the observed cell loss in the γ-synuclein null mutants can be derived from studies on the relative, α-synuclein: Overexpression of α-synuclein has been shown to exert a cytotoxic effect on a range of neurons in vitro and in vivo (van der Putten et al., 2000; Saha et al., 2000). In vitro studies on nodose neurons and sympathetic neurons from the superior cervical ganglion have shown that the anti-apoptotic protein, Bcl-x_L rescues these cells from the cytotoxic effects of α-synuclein overexpression whereas co-expression with the pro-apoptotic members of the Bcl family, Bad and Bax, enhances cell death. Sung and colleagues reported that α-synuclein as well as two mutant forms which are associated with a rare dominant form of Parkinson's disease, induce cell death in immortalized hippocampal H19-7 cells and primary cortical neurons in culture. The cytotoxic effect was dose-dependent. The authors also demonstrated that the addition of α-synuclein to the cultures increased the activity of several protein kinases involved in intracellular signalling, namely c-Jun N-terminal kinase (JNK), extracellular signal-regulated protein kinase (ERK), and p38 kinase. The upregulation of JNK in cultured neurons exposed to increasing doses of α-synuclein is especially interesting since there is strong evidence that inhibition of JNK rescues sensory neurons from α-synuclein induced cell death in vitro (Middleton G, personal communication). This suggests that the cytotoxic effect of α-synuclein

overexpression maybe mediated by the pro-apoptotic JNK signalling pathway. The interesting aspect here is that this JNK-dependent induction of apoptosis by overexpression of α-synuclein can be counteracted in turn by overexpression of γ-synuclein (Middleton G, personal communication). Furthermore, a recent study has shown that α-synuclein fibrillation which is a characteristic feature in Parkinson's disease can be inhibited by γ- (and β-) synuclein (Uversky et al., 2002).

A conceivable scenario would be that in certain neuronal populations, at certain developmental stages, an imbalance between α- and γ-synuclein could trigger apoptotic cell death. If α-synuclein had indeed a cytotoxic effect which requires certain factors downstream of cell death pathways to be active, and if γ-synuclein were able to ameliorate this effect, then this would explain the timing of cell loss observed in the SN and the VTA. α-synuclein could "take advantage" of the absence of its repressor and the highly activated intracellular death-promoting machinery during phases of developmental cell death. The cell losses seen in γ-synuclein null mutant mice would therefore be the consequence of a multifactorial process, requiring a certain constellation of factors at a certain time. Only if these requirements were met in a given neuronal population or subpopulation would cell loss ensue. A similar mechanism could be proposed to play a role in the pathogenesis of neurodegenerative disorders like Parkinson's disease. γ-synuclein might be involved in neurodegeneration not by accumulation in pathological structures that are readily detectable under the microscope but

by some means of under-activity which disturbs a critical balance between the members of the synuclein family. If an imbalance between α- and γ-synuclein was indeed responsible for the observed cell losses in the SN, the VTA, and the two cranial motor nuclei, then immunohistochemical analysis of these structures in α-/γ-synuclein double null mutant mice might provide valuable information.

However, care has to be taken not to over-interpret what is at hand. In order to conduct cell counts on dopaminergic neurons, midbrain sections had to be stained with an antibody against tyrosine hydroxylase to be able to recognize such neurons as dopaminergic. Strictly speaking, an antibody against tyrosine hydroxylase doesn't mark a neuron as dopaminergic but as tyrosine hydroxylase-positive. Therefore, any neurons that utilize tyrosine hydroxylase to synthesize a neurotransmitter that lies further downstream in the biochemical pathway, i.e., adrenaline or nor-adrenaline would also be stained . Fortunately, no such neurons exist in the SN and the VTA. Therefore, one can quite safely assume that the neurons visualized in an anti-tyrosine hydroxylase immunostain are indeed dopamine-synthesizing neurons. Furthermore, some antibodies used as neuronal markers tend to work only under most stringent conditions and might even then produce a weak or inadequate stain to perform reliable cell counts. It is therefore important to optimise the antibody for the right conditions (e.g. use of fixative, incubation time, concentration of antibody). Such optimisation trials were conducted with the anti-TH antibody and are discussed in the Materials and Methods chapter. The antibody from Novocastra (via Vector

Laboratories) used for the studies presented here is widely used and proved to be a reliable antibody which produced clear and adequate stains throughout the experiments. No stain-enhancing techniques (like nickel chloride) needed to be employed. For references on the anti-TH monoclonal antibody see Kitahama et al., 1988 and Berod et al., 1982.

It is also important to bear in mind that an antibody against an enzyme involved in the synthesis of a neurotransmitter or against the neurotransmitter itself is a metabolic marker. A cell can up- or downregulate its metabolites depending on conditions and requirements. It has been shown that the synthesis rate of tyrosine hydroxylase can be increased as well as decreased by a number of mechanisms (Tank et al., 1986a/b; Burke and Joh, 1988; Fossom et al., 1992). Although no reports could be found on a total down-regulation of TH, one still has to be aware that the non-detection of TH is not synonymous with the absence of the cell itself. Thus, strictly speaking when stating that a loss of dopaminergic neurons was observed, a careful mind should translate this into a reduction of TH synthesising neurons at the time of the animal's death.

As far as the question is concerned whether there is an active loss of dopaminergic neurons during the phase of physiological cell death a set of different approaches can be employed to confirm the assumption made on immunohistochemical grounds. One of the experiments planned for the immediate future is to specifically look for increased apoptotic cell death in the SN and VTA of γ-synuclein null mutant mice at P2. This can be done by

counting the appearance of pyknotic nuclei in the structures or performing TUNEL stains on the dopaminergic neurons. In a more functional approach, the dopamine content of the striatum, the target area of SN dopaminergic neurons, can be measured by biochemical means. Such experiments are currently undertaken by co-workers of mine in collaboration with another group. Lastly, the effects of α- and γ-synuclein on dopaminergic neurons could be studied in vitro. However, the latter possibility is not without significant difficulties since there is currently no technique available to obtain pure cultures of dopaminergic neurons.

CHAPTER 5

Expression Pattern of γ-Synuclein in Cranial Motor Nuclei and the Substantia Nigra

5.1 Introduction

γ-synuclein is widely expressed throughout the central and peripheral nervous system. During mouse development, γ-synuclein mRNA expression can be detected in the ventral horns of the spinal cord from as early as E10. From E11 onwards, it is also found in the dorsal root ganglia as well as cranial sensory ganglia and in parts of the hind- and midbrain. In the adult rat brain, γ-synuclein mRNA is strongly expressed in the motoneurons of the oculomotor and trigeminal motor nuclei as well as in the Purkinje and granular cell layer of the cerebellum, the thalamus, hypothalamus, olfactory bulbs, and the hippocampus (Buchman et al., 1998a). Expression has also been observed in the neuronal layers of the cortex. Interval expression studies in the developing trigeminus ganglion have shown that γ-synuclein mRNA and protein product are upregulated at a stage when the earliest axons are growing towards their targets between E10 and E12. Given some evidence that γ-synuclein plays a role in the regulation of neurofilament network integrity (Buchman, et al., 1998b), this might suggest that the protein could be involved in mechanisms influencing axonal growth and morphology.

In chicken embryos, γ-synuclein mRNA can be detected as early as E3 (Hamburger-Hamilton stage 14). In contrast to α- and β-synuclein, whose expression at this stage is restricted to mesencephalic and rhombencephalic

structures, γ-synuclein can be detected throughout the entire extent of the developing nervous system (Tiunova et al., 2000). By E10, Northern hybridization of sample tissues taken from various parts of the nervous system, shows a clear rostrocaudal gradient in γ-synuclein with lowest levels in the telencephalon and highest levels yielded from spinal cord material. This again sets γ-synuclein apart from its two relatives who, at this stage appear uniformly expressed throughout the mes- and rhombencephalon. Moreover, Western blotting and immunocytochemical investigations on sensory neurons have shown a different intracellular distribution for γ-synuclein. Whereas α- and β-synuclein are predominantly localized in synaptic terminals, γ-synuclein – in embryonic sensory neurons at least –is mainly distributed throughout the cytoplasm and the axons (Buchman 1998a/b).

To investigate the expression of γ-synuclein in more detail on the protein level, immunohistochemistry was performed on paraffin sections of adult and postnatal mouse brains (C57Bl6/J strain, Charles River) as well as mouse embryos of different developmental stages. A specific rabbit polyclonal antibody (SK23) which recognizes the C-terminal of mouse γ-synuclein was used in conjunction with a biotin/avidin detection kit (see Materials & Methods and Buchman et al., 1998b). To identify γ-synuclein-positive structures a range of tools was used. Parallel stains were conducted with Haematoxylin/Eosin (HE) for general orientation, with an antibody against cholin-acetyl-transferase (ChAT) to facilitate identification of motoneurons, and with an antibody against tyrosine hydroxylase (TH) for

identification of dopaminergic neurons (see Materials and Methods). In addition, a numer of anatomical atlases was utilized (Theiler, 1989; Kaufman, 1992; Altman and Bayer, 1995; Foster, 1998; Paxinos and Franklin, 2001). The personal assistance of Prof. M.H. Kaufman was also much appreciated.

The specimens were cut into sagittal as well as coronal sections. It has to be said though that in the case of whole embryo sections it is not possible to obtain true coronal sections throughout the entire CNS due to the curved position of the embryo.

5.2 Results

5.2.1 Adult brain

Immunostains of whole adult brains with anti-γ-synuclein revealed widespread expression in the central nervous system (Tab. 5.2.1). Strikingly, cytosolic staining was rare in any part of the brain which seemed to contrast with the findings of Buchman and colleagues (Buchman et al., 1998b). Instead, many structures were outlined in a pointillistic fashion which is suggestive of a synaptic protein localization. Where cell bodies were stained they appeared to be neuronal judged by their size and morphology. Typically, stained cell bodies were few and scattered in any given structure. The following table gives an overview of the extent of γ-synuclein expression in the adult central nervous system.

Among the cranial nuclei and the substantia nigra, only two of the structures revealed cytosolic localization of γ-synuclein: the facial nucleus and the substantia nigra. Inside the pars compacta of the substantia nigra a few neuronal cell bodies stained positive for the protein (Fig. 5.2.1). Their number was well below the number of neurons staining for tyrosine hydroxylase. The protein was also detected in neuronal processes throughout the pars compacta as well as the pars reticulata. Moreover, the ganglion's neuropil was dispersed with the dotted pattern seen in many other parts of the central nervous system (see above).

Structure	Cell soma stain	Neuropil stain	Fibre tract stain
Amygdala	-	++	NA
Area postrema	-	+++	NA
Brachium pontis	-	++	NA
Cerebellum, granular layer	-	+++	NA
Cerebellum, white layer	NA	NA	+++
Cochlear nucleus	-	++	NA
Cuneate nucleus	-	+++	NA
Dentate gyrus	-	+	NA
Diagonal band (Broca)	NA	NA	++
Dorsomedial spinal trigeminal nucleus	-	++	NA
Edinger-Westphal nucleus	++	++	NA
Facial nerve root	NA	NA	+++
Facial nucleus	+	+++	NA
Fasciculus retroflexus	NA	NA	+++
Hypoglossus nucleus	-	++	NA
Hypothalamic nuclei	+	++	NA
Inferior olive, principle nucleus	++	+++	NA
Intermediate nucleus of the lateral lemniscus	++	++	NA
Interpeduncular nuclei	-	+++	NA
Lateral habenular nucleus	-	++	NA
Lateral lemniscus	NA	NA	++
Lateral olfactory tract	NA	NA	+++
Lateral supramamillary nucleus	+	++	NA
Locus coeruleus	-	++	NA
Medial preoptic area	-	++	NA
Medial septal nuclei	-	++	NA
Medial terminal nucleus of the accessory optic tract plus tract	-	+++	+++
Medial vestibular nucleus	-	++	NA
Nigro-striatal tract	NA	NA	++
Nucleus ambiguus	++	+++	NA
Nucleus of the horizontal limb of diagonal band (Broca)	+	++	NA
Olfactory bulb	-	+	NA
Optic tract	NA	NA	+++
Periaquaeductal grey	-	+	NA
Peripyramidal nucleus	+	++	NA

Pontine nuclei	++	++	NA
Raphe nuclei	++	++	NA
Rubrospinal tract	NA	NA	+++
Solitary tract and nuclei	-	+++	+++
Spinal trigeminal tract	NA	NA	+++
Striatum	-	++	NA
Substantia nigra, zona compacta	+	++	NA
Superior colliculus	-	+++	NA
Supraoptic decussation	NA	NA	++
Tectospinal tract	N	NA	+
Trigeminus nerve, motor nucleus of	-	+	NA
Trigeminus nerve, motor root of	NA	NA	+++
Trochlear nerve root	NA	NA	++
Trochlear nucleus	-	+	NA
Vagus nerve, dorsal motor nucleus of	-	++	NA
Ventral spinocerebellar tract	NA	NA	++
Ventral spinocerebellar tract	NA	NA	+++
Ventral tegmental area	-	+	NA
Vestibulocochlear nerve, nerve root of	NA	NA	+++
Zona incerta	-	++	NA

Tab. 5.2.1: Localization of γ-synuclein in the adult central nervous system of the mouse as detected by anti-γ-synuclein immunohistochemistry. + weak stain, ++ intermediate stain, +++ strong stain.

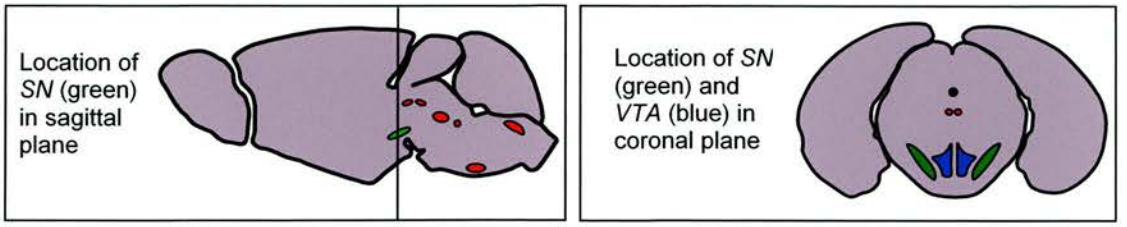
Location of *SN* (green) in sagittal plane
Location of *SN* (green) and *VTA* (blue) in coronal plane

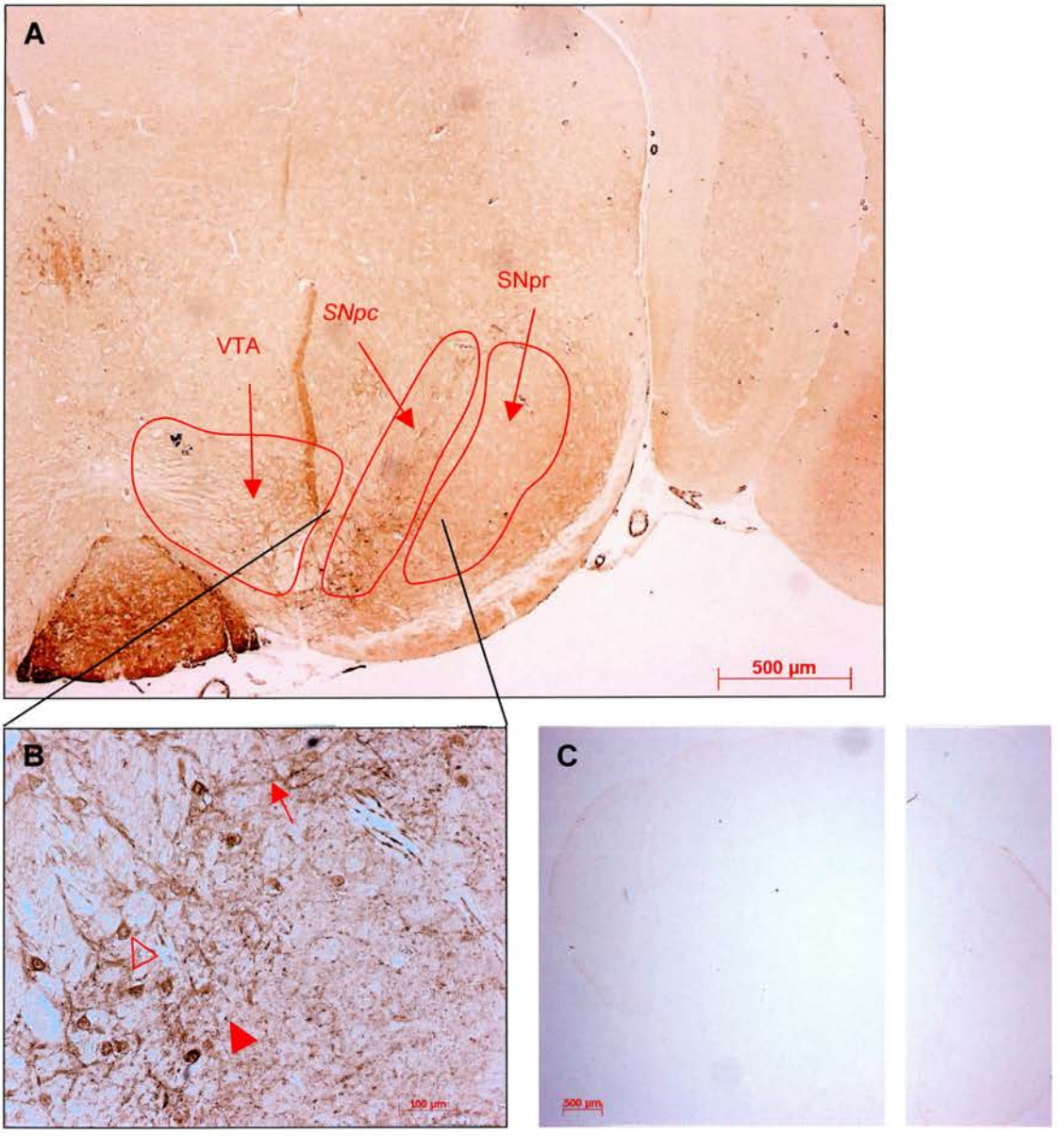
A
VTA
SNpc
SNpr
500 µm
B
100 µm
C
500 µm

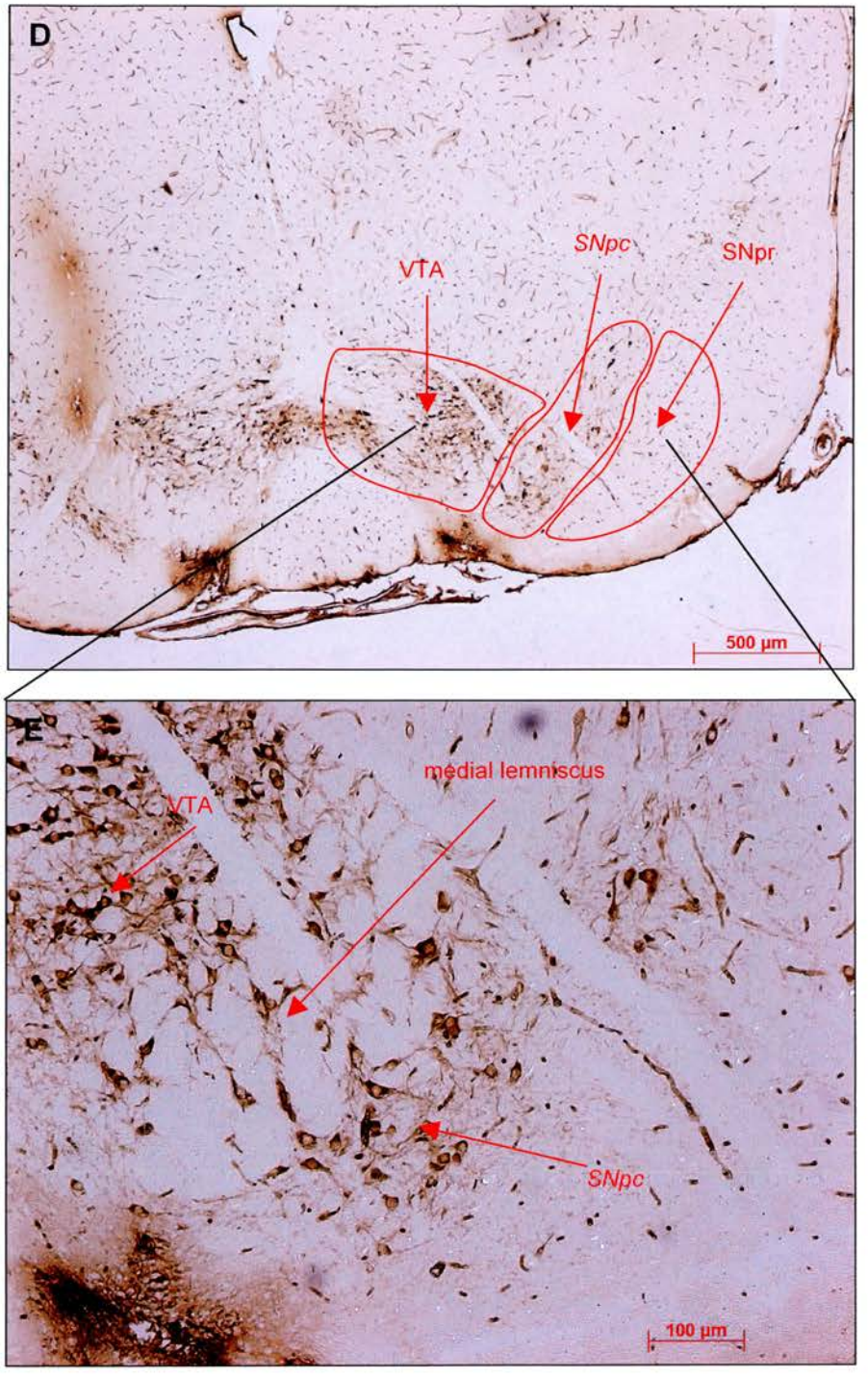

Fig. 5.2.1: Anti-γ-synuclein (A-C) and anti-TH (D, E) staining of the *substantia nigra* in the adult mouse. **A:** coronal overview showing diffuse staining in the substantia nigra and the ventral tegmental area. **B:** Higher magnification of A. Protein detection in the cytoplasm (open arrow) of a few individual neurons, nerve processes (arrow), and possibly synapses (filled arrowhead) inside the substantia nigra, pars compacta (SNpc). **C:** negative control, omission of anti-γ-synuclein antibody. **D, E:** control stain of an adjacent section of the same brain with anti-tyrosine hydroxylase antibody. SNpr: substantia nigra, pars reticulata, VTA: ventral tegmental area. Line through sagittal diagram shows level of coronal section.

Although the neurons that exhibited a cytosolic stain resembled those stained with anti-TH in size and morphology, it could not be taken for granted that they were dopaminergic neurons. The hope was that if the dopaminergic neurons indeed expressed γ-synuclein then it could be detected in the nigro-striatal tract. Therefore, brains of adult wild type mice of the same strain were cut into sagittal sections which were stained in an alternating fashion (see Material and Methods) with both anti-TH and anti-γ-synuclein antibodies. As Fig. 5.2.2. shows γ-synuclein was clearly detected in the nigro-striatal tract. Furthermore, the target of the dopaminergic neurons of the SN, the striatum exhibited a dotted stain (data not shown). This pattern was detected throughout the entire striatum and is therefore likely to represent a number of structures projecting onto the striatum.

γ-synuclein was also detected in the somato- and branchiomotor nuclei of the adult brainstem. However, the staining pattern varied between the nuclei. The dotted neuropil stain of γ-synuclein was only observed in four of the six nuclei (IV, V, VII, and XII).

Of the three nuclei of the *oculomotor complex (abducens, trochlear, and oculomotor nuclei*), only the trochlear nucleus showed a weak neuropil stain (Fig. 5.2.3). The area occupied by the abducens nucleus was void of any immunostaining (Fig. 5.2.4) and the oculomotor nuclei appeared like two holes on both sides of the γ-synuclein-positive Edinger-Westphal nucleus (Fig. 5.2.5). Nevertheless, the protein could be detected in the motoneuron

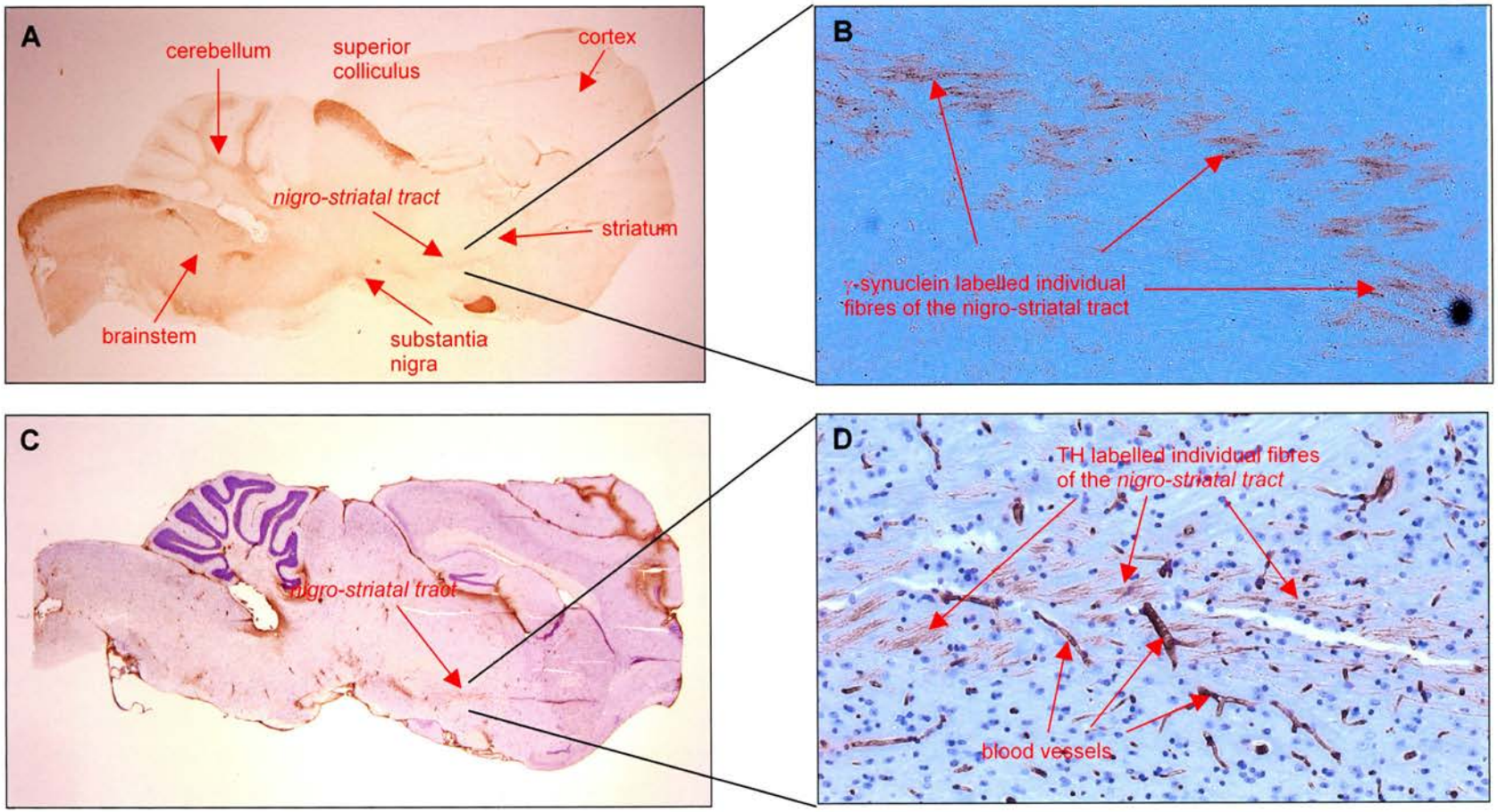

Fig. 5.2.2: Anti-γ-synuclein (A, B) and anti-TH/haematoxylin staining of the *nigro-striatal tract* in the adult mouse. **A:** sagittal overview of the whole brain showing localization of γ-synuclein in the nigro-striatal tract. **B:** higher magnification of A. **C, D:** control staining with anti-TH (tyrosine hydroxylase) and haematoxylin of an adjacent section of the same brain.

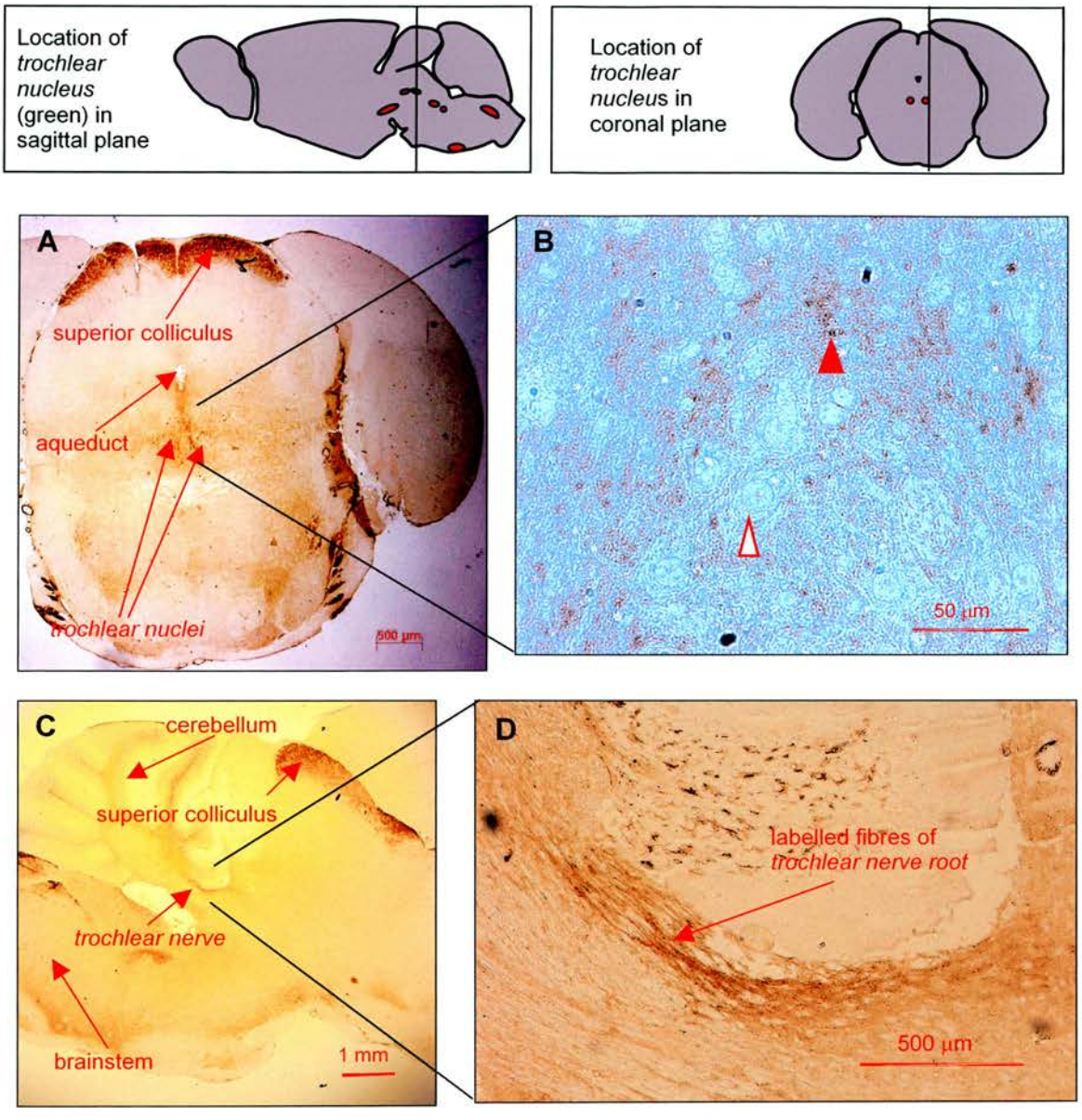
Location of *trochlear nucleus* (green) in sagittal plane
Location of *trochlear nucleus* in coronal plane
A
superior colliculus
aqueduct
trochlear nuclei
500 µm
B
50 µm
C
cerebellum
superior colliculus
trochlear nerve
brainstem
1 mm
D
labelled fibres of *trochlear nerve root*
500 µm

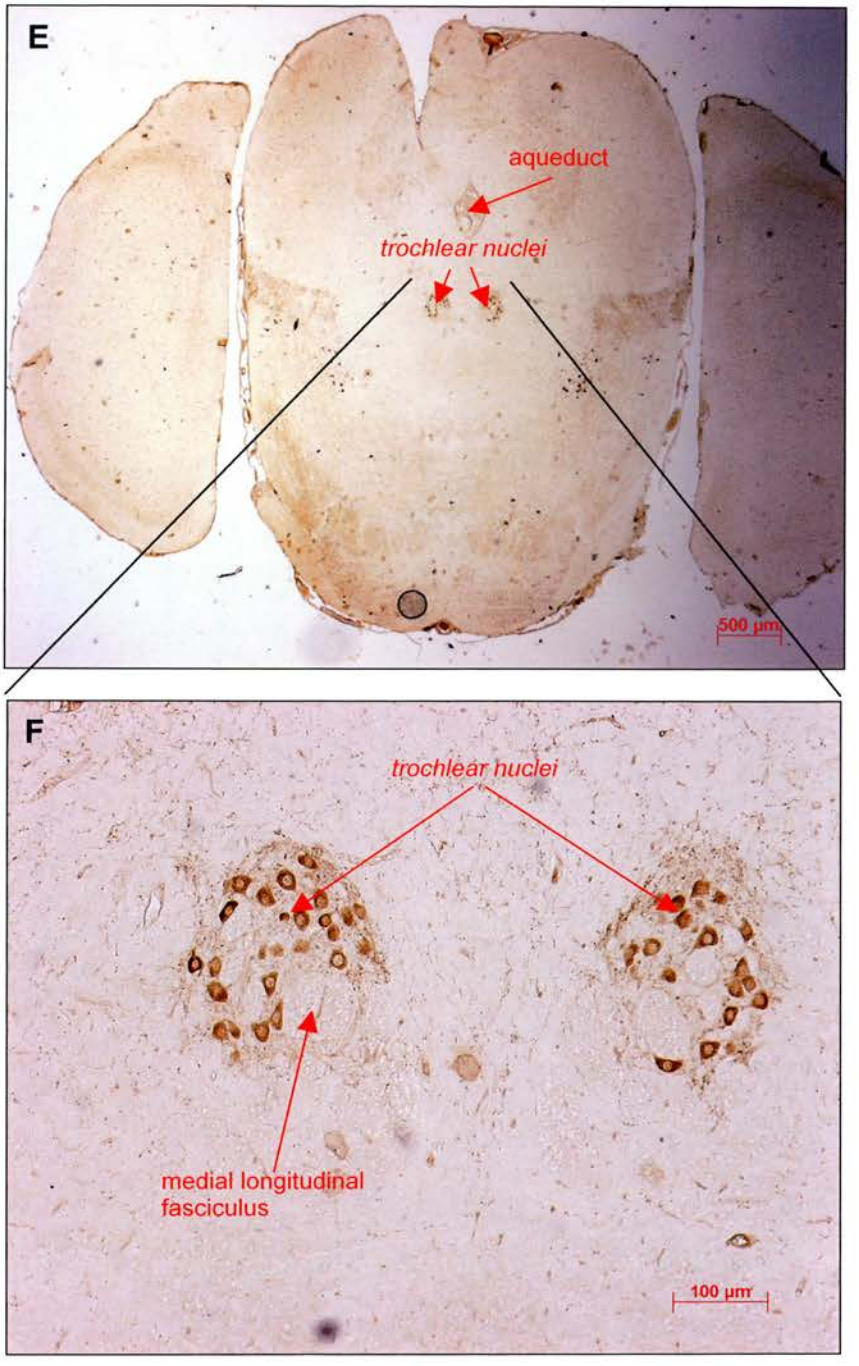

Fig. 5.2.3: Anti-γ-synuclein (A-C) and anti-ChAT (D, E) staining of the *trochlear nucleus* in the adult mouse. **A:** coronal overview showing weak labelling of the area occupied by the trochlear nuclei. **B:** high magnification of the right trochlear nucleus revealing a dotted neuropil stain (open arrowhead). The neurons appear as empty outlines embedded in the labelled neuropil (filled arrowhead). **C:** sagittal section showing the labelled trochlear nerve curving around the 2nd cerebellar lobule. The line through the coronal diagram (top) indicates the plane of this sagittal section. D: higher magnification of C. **E:** coronal overview of the ant-ChAT stained trochlear nuclei. **F:** higher magnification of E revealing labelled individual trochlear motoneurons. Line through sagittal diagram shows level of coronal section.

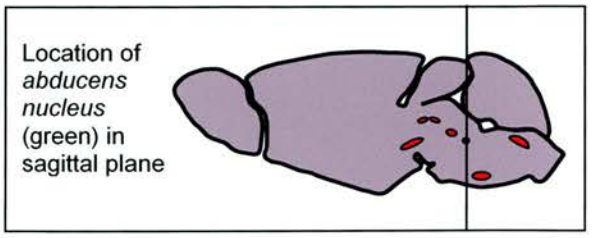
Location of *abducens nucleus* (green) in sagittal plane

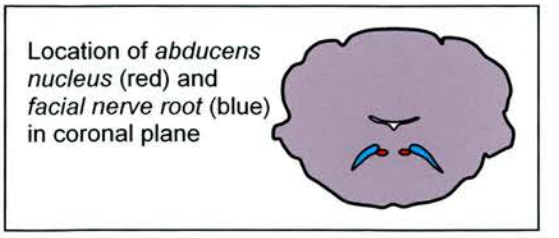
Location of *abducens nucleus* (red) and *facial nerve root* (blue) in coronal plane


A
500 µm

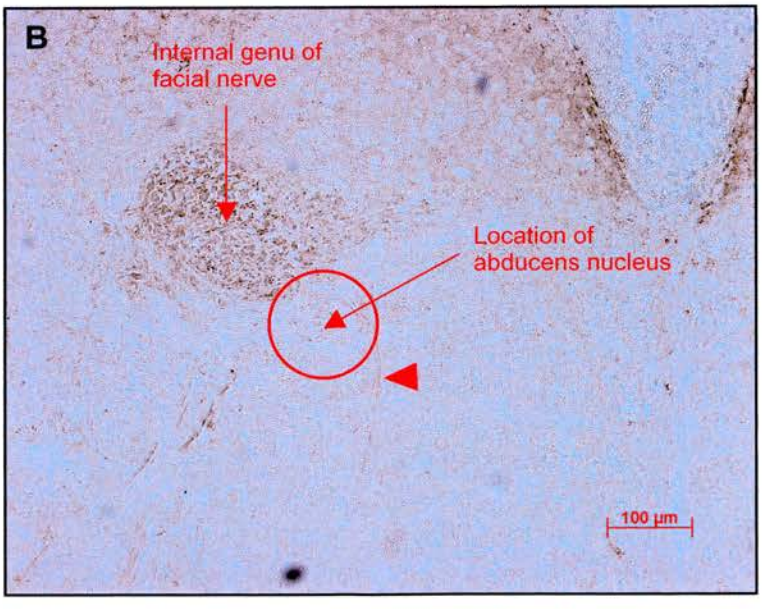
B
Internal genu of facial nerve
Location of abducens nucleus
100 µm

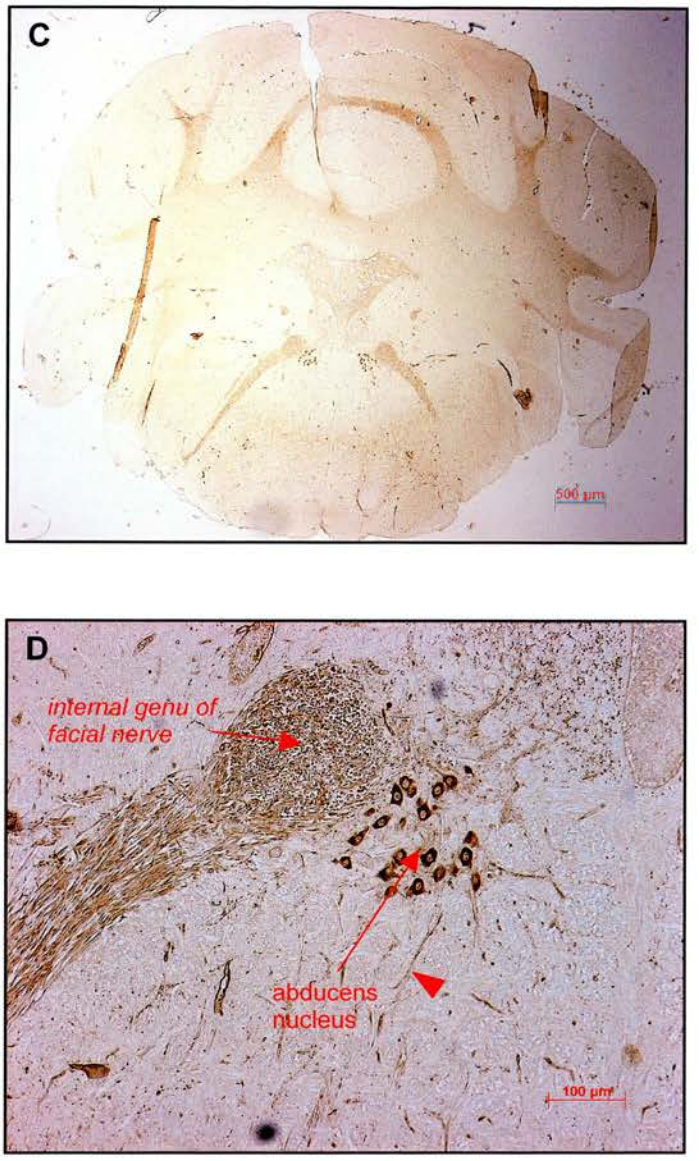

Fig. 5.2.4: Anti-γ-synuclein (A, B) and anti-ChAT (C, D) staining of the *abducens nucleus* in the adult mouse. **A:** coronal overview. The area occupied by the abducens nucleus just ventral to the *internal genu of the facial nerve* shows no obvious staining. However, small fibres emerging from the area are positively labelled (arrowheads) B: higher magnification. **C,D:** control immunostain with anti-ChAT antibody. The cell bodies of abducens motoneurons are labelled as well as emerging fibres (arrowhead).

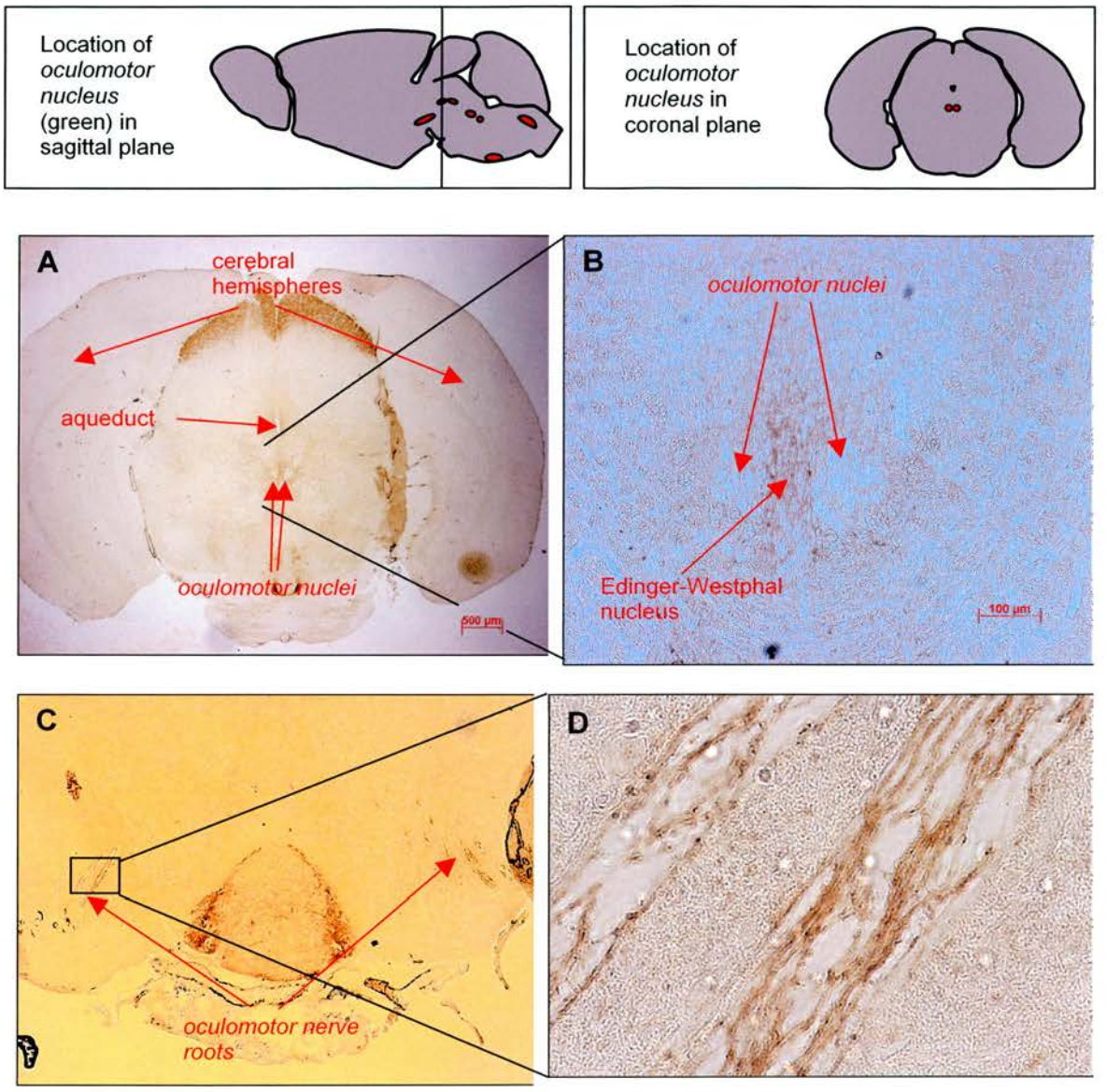
Location of *oculomotor nucleus* (green) in sagittal plane
Location of *oculomotor nucleus* in coronal plane
A
cerebral hemispheres
aqueduct
oculomotor nuclei
500 µm
B
oculomotor nuclei
Edinger-Westphal nucleus
100 µm
C
oculomotor nerve roots
D

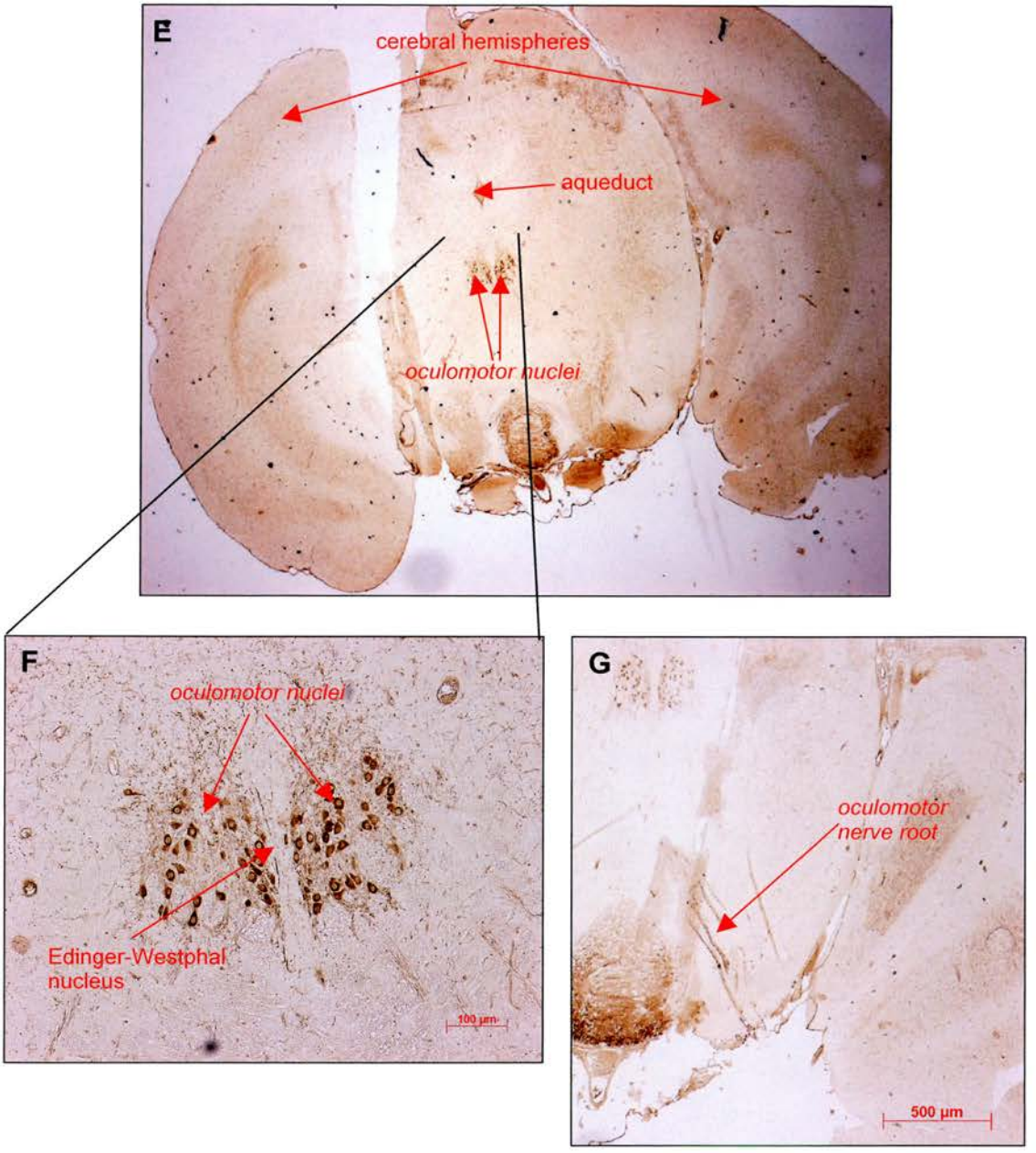

Fig. 5.2.5: Anti-γsynuclein (A-D) and anti-ChAT (E-G) staining of the *oculomotor nucleus and nerve root* in the adult mouse. **A:** coronal overview. The oculomotor nuclei appear like two holes bilateral to the median Edinger-Westphal nucleus. **B:** higher magnification of A. **C, D:** localization of γ-synuclein in roots of oculomotor nerve. **E:** anti-ChAT control staining of oculomotor nucleus. Note how the anti-ChAT stain results in an almost inverse picture of the anti-γ-synuclein stain with the oculomotor nuclei clearly labelled and an empty Edinger-Westphal nucleus. **F:** higher magnification of E showing individual motoneurons. **G:** ChAT labelled root of the oculomotor nerve.
Line through sagittal diagram shows level of coronal section.

axons of all three nuclei, indicating that all ocular motoneurons express γ-synuclein.

The *motor nucleus of the trigeminus nerv*e showed a clear neuropil stain (Fig. 5.2.6). No protein was detected in cell bodies. But its presence in the axons of the motor root of the trigeminus was evident.

As mentioned above, the *facial nucleus* was exceptional as it was the only cranial motor nucleus of the six nuclei studied that showed a cytosolic presence of γ-synuclein. Judging by their size and morphology, the cells exhibiting a cytosolic expression of the protein, were clearly facial motoneurons (Fig. 5.2.7). Mirroring the situation in the substantia nigra, the number of γ-synuclein-positive neurons represented only a fraction of the entire neuronal population of the structure. The nucleus itself was outlined by the familiar dotted neuropil stain. A clear stain was also detected in the fibres of the facial nerve root coursing dorsally and rostrally towards the abducens nucleus.

The *hypoglossal nucleus* showed extensive neuropil staining (Fig. 5.2.8). No cell bodies stained positive. The motoneurons appeared like stencilled negative images in a diffusely stained neuropil. However, the axons of the hypoglossal nerve root were clearly γ-synuclein-positive, indicating that the protein is present in the hypoglossal motoneurons.

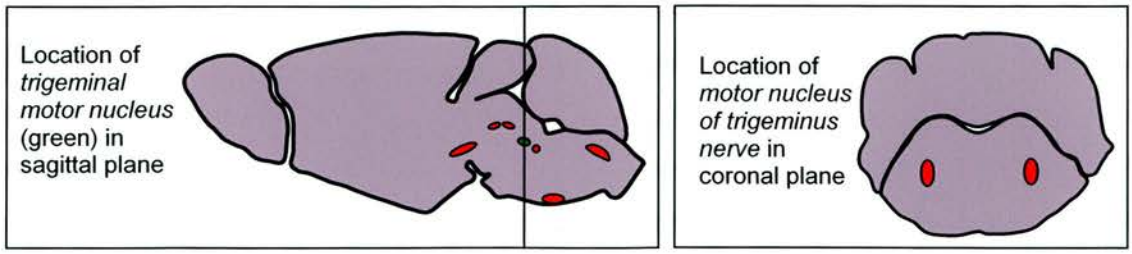
Location of *trigeminal motor nucleus* (green) in sagittal plane
Location of *motor nucleus of trigeminus nerve* in coronal plane

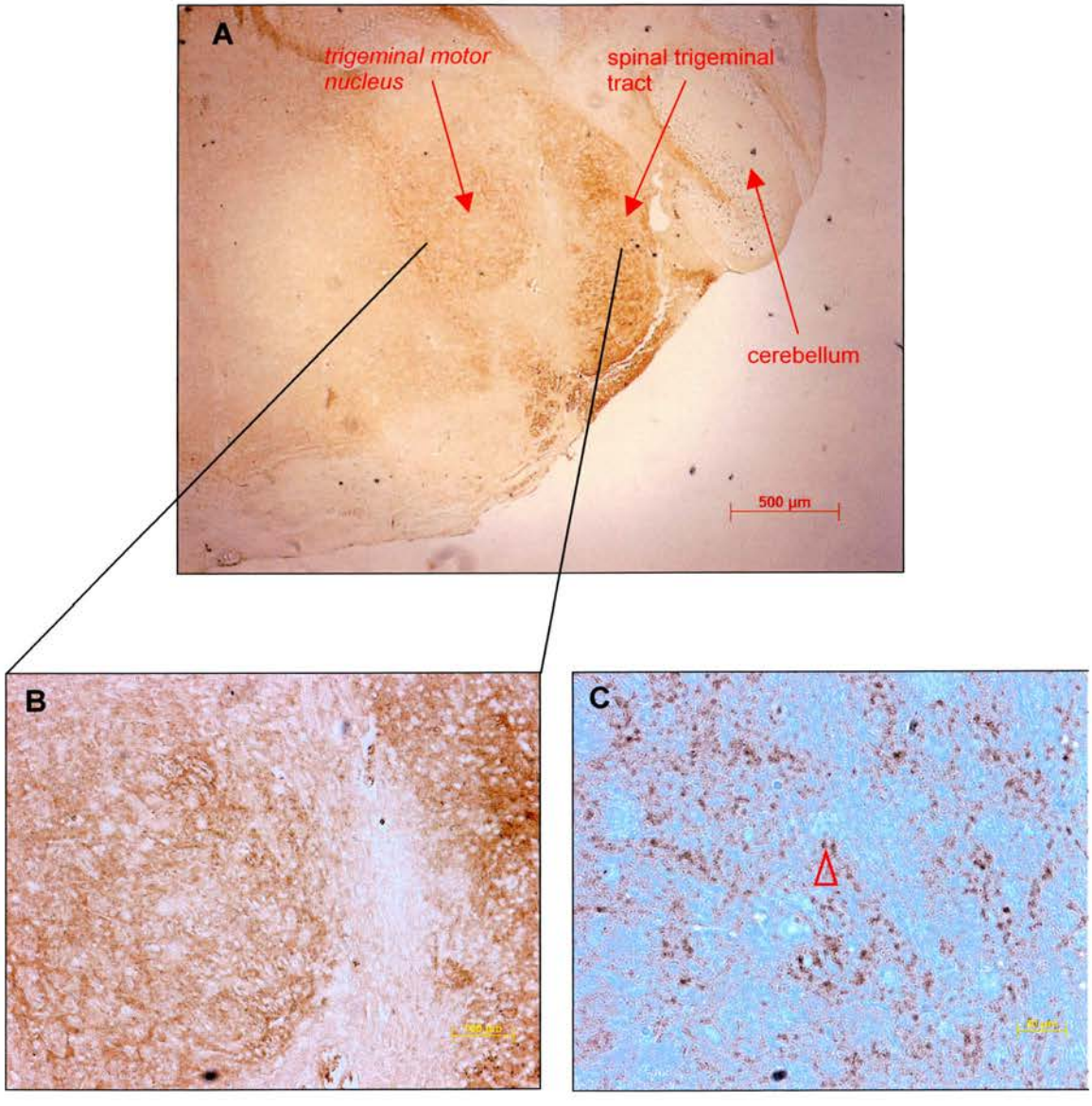
A
trigeminal motor nucleus
spinal trigeminal tract
cerebellum
500 µm
B
C

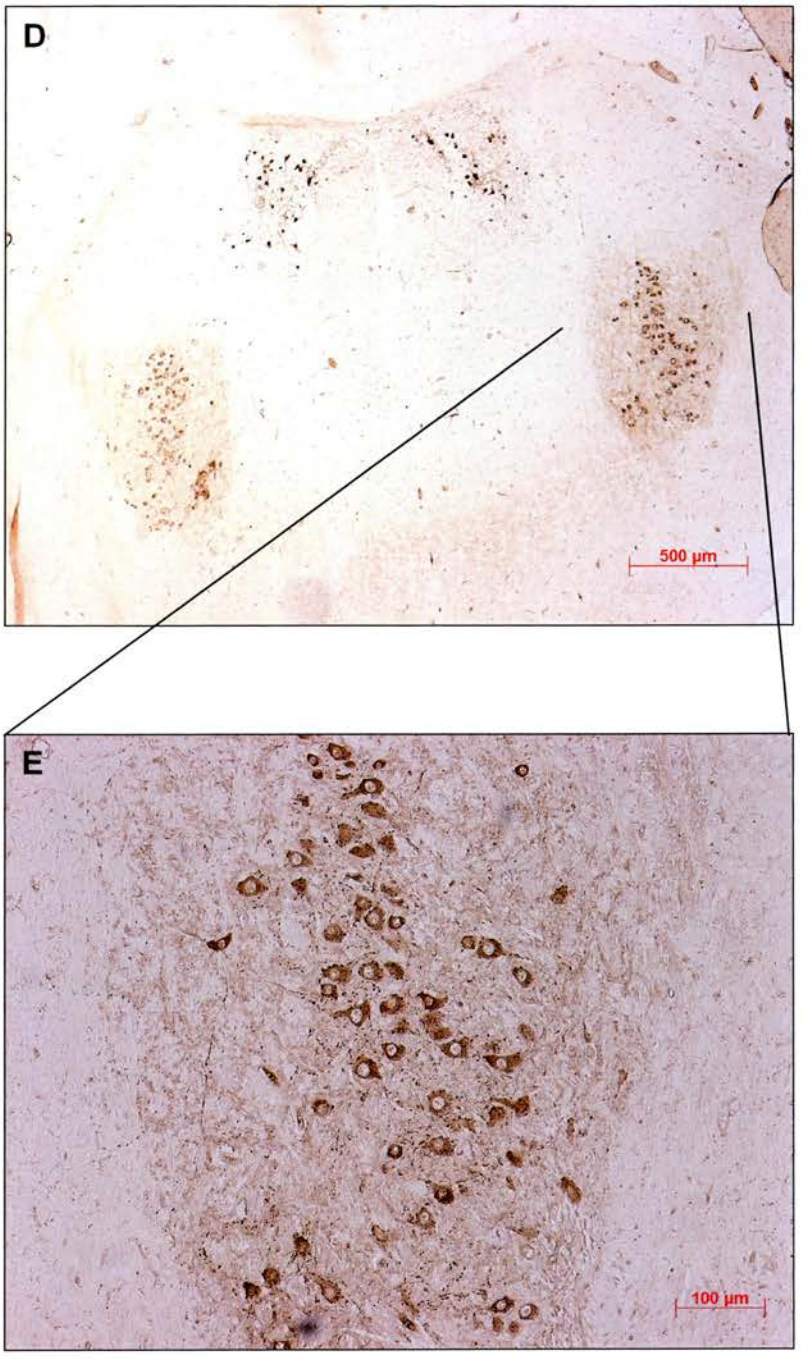

Fig. 5.2.6: Anti-γ-synuclein (A-B) and anti-ChAT (D, E) staining of the *trigeminal motor nucleus* in the adult mouse. **A:** coronal overview showing diffused labelling of the motor nucleus and the spinal trigeminal tract. **B, C:** higher magnifications of the nucleus. Note the dotted staining (open arrowhead) in C presumed to represent localization of γ-synuclein in axonal terminals. No cell somata are labelled. **D, E:** Anti-ChAT control stain; overview and at higher magnification showing individual trigeminal motor neurons.
Line through sagittal diagram shows level of coronal plane.

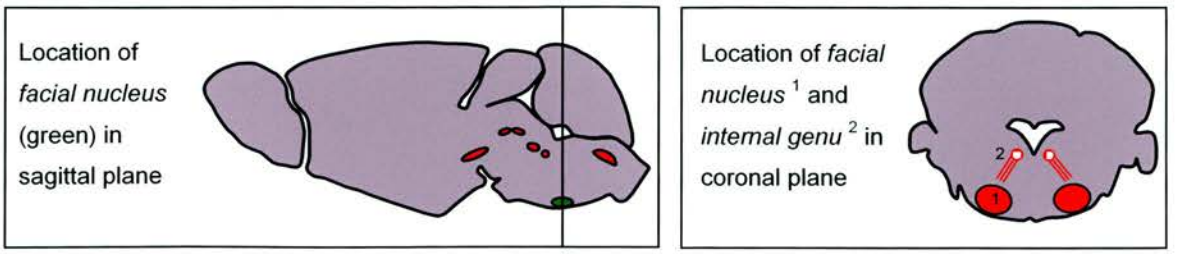
Location of *facial nucleus* (green) in sagittal plane
Location of *facial nucleus* [1] and *internal genu* [2] in coronal plane
2
1

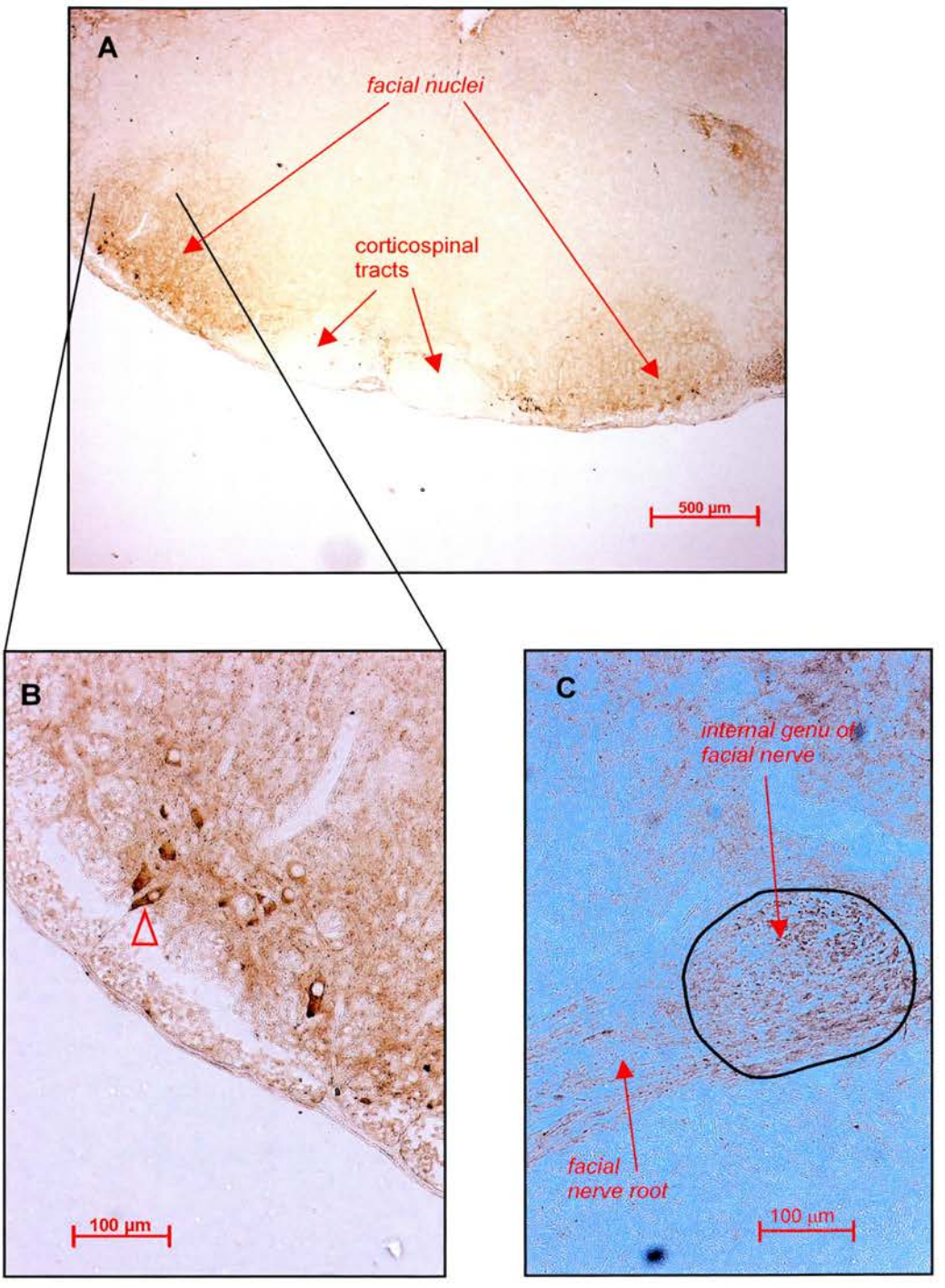
A
facial nuclei
corticospinal tracts
500 µm
B
100 µm
C
internal genu of facial nerve
facial nerve root
100 µm

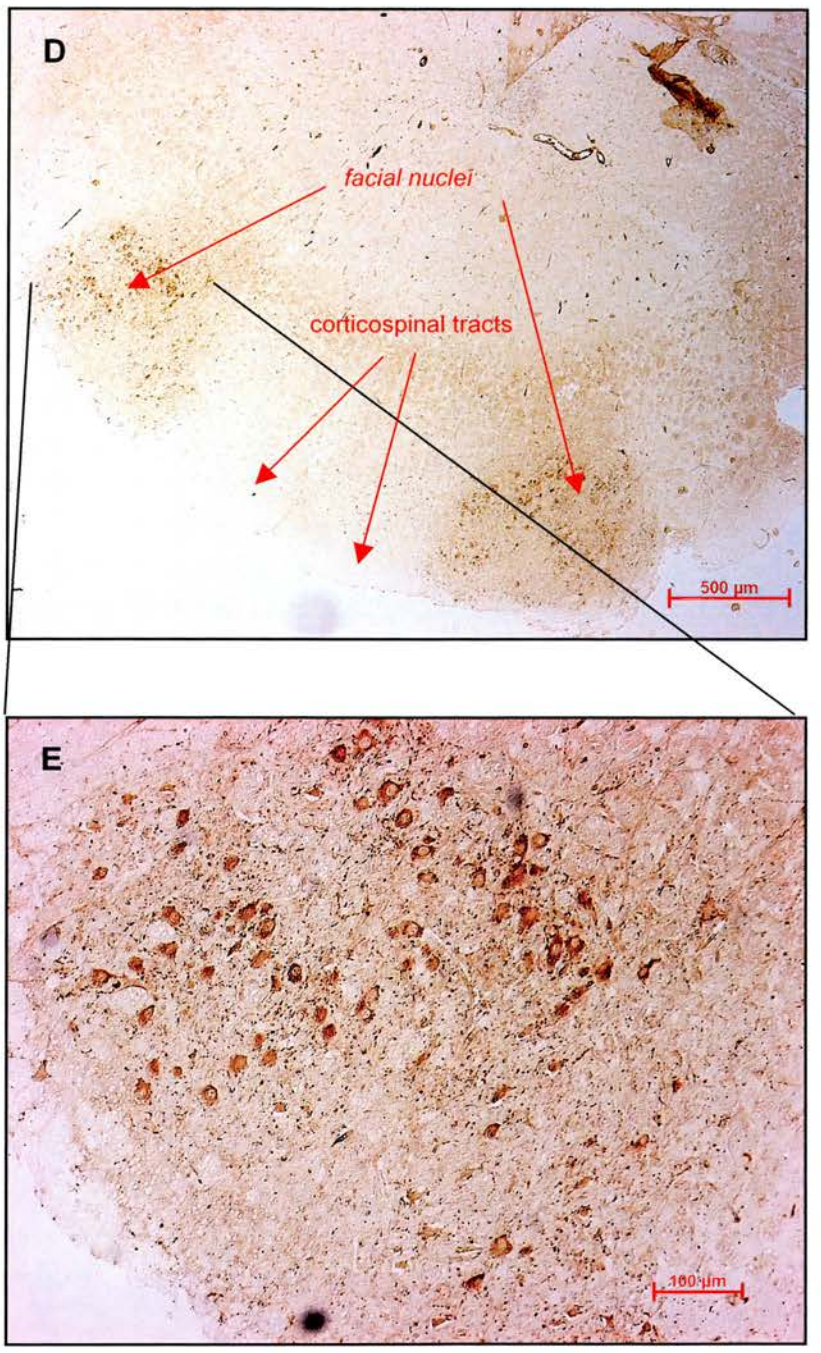

Fig. 5.2.7: Anti-γ-synuclein (A-C)and anti-ChAT (D-E) staining of the *facial nucleus* in the adult mouse. **A:** a diffuse marks the approximate outline of the left and right facial nucleus. **B:** higher magnification reveals detection of γ-synuclein in the cytoplasm of a few motoneurons (open arrowhead) which are easily recognizable by their size. Comparison with the ChAT stain at the same magnification (E) shows that only a small fraction of the cell bodies of facial motoneurons stain positive for γ-synuclein. **C:** detection of γ-synuclein in facial axons at the level of the internal genu (lat.: knee) of the facial nerve. **D:** low magnification anti-ChAT control stain of both facial nuclei. **E:** higher magnification of D showing the cell bodies of the facial motoneurons.
Note: The diagram at the top of the left page shows the outlines of both the nucleus and the internal genu in the same transverse plane. This was done for reasons of simplicity. In fact, the internal genu lies rostral to the facial nucleus. The line through the sagittal diagram shows the level of the coronal section.

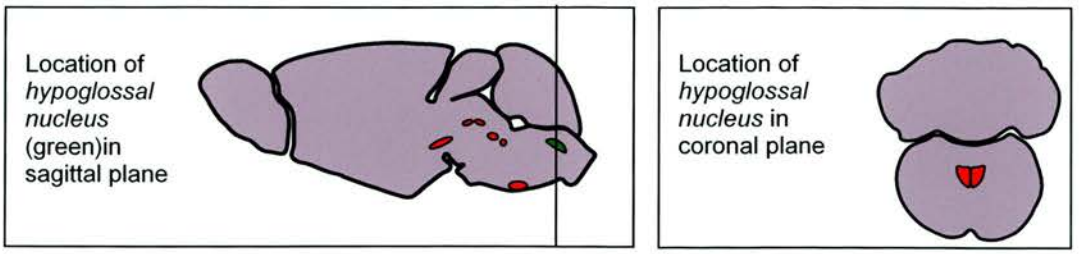
Location of *hypoglossal nucleus* (green)in sagittal plane
Location of *hypoglossal nucleus* in coronal plane

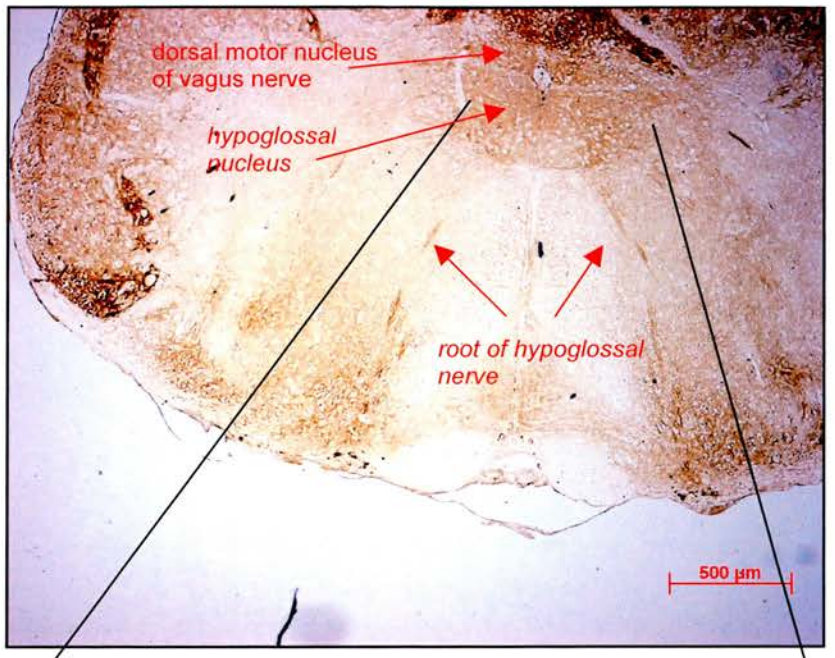
dorsal motor nucleus of vagus nerve
hypoglossal nucleus
root of hypoglossal nerve
500 µm

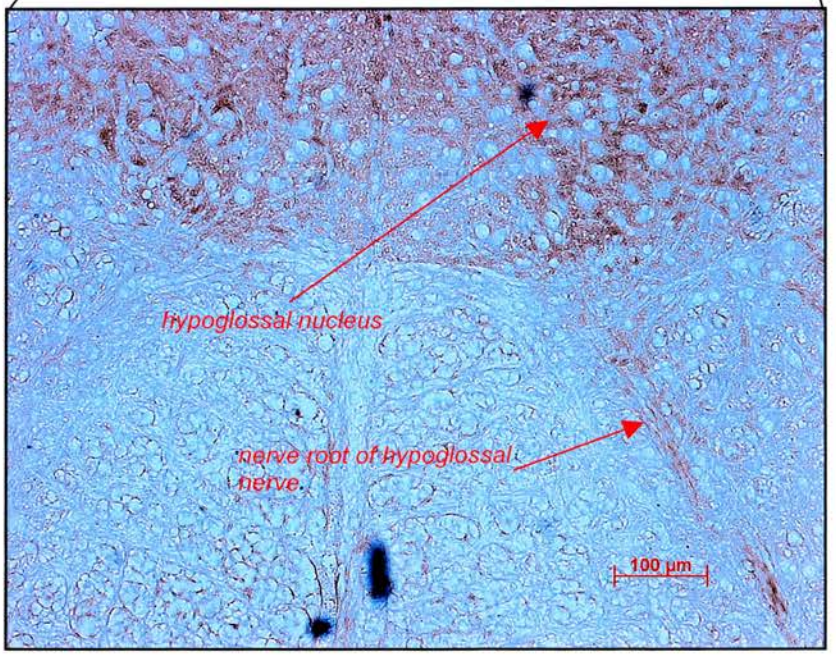
hypoglossal nucleus
nerve root of hypoglossal nerve.
100 µm

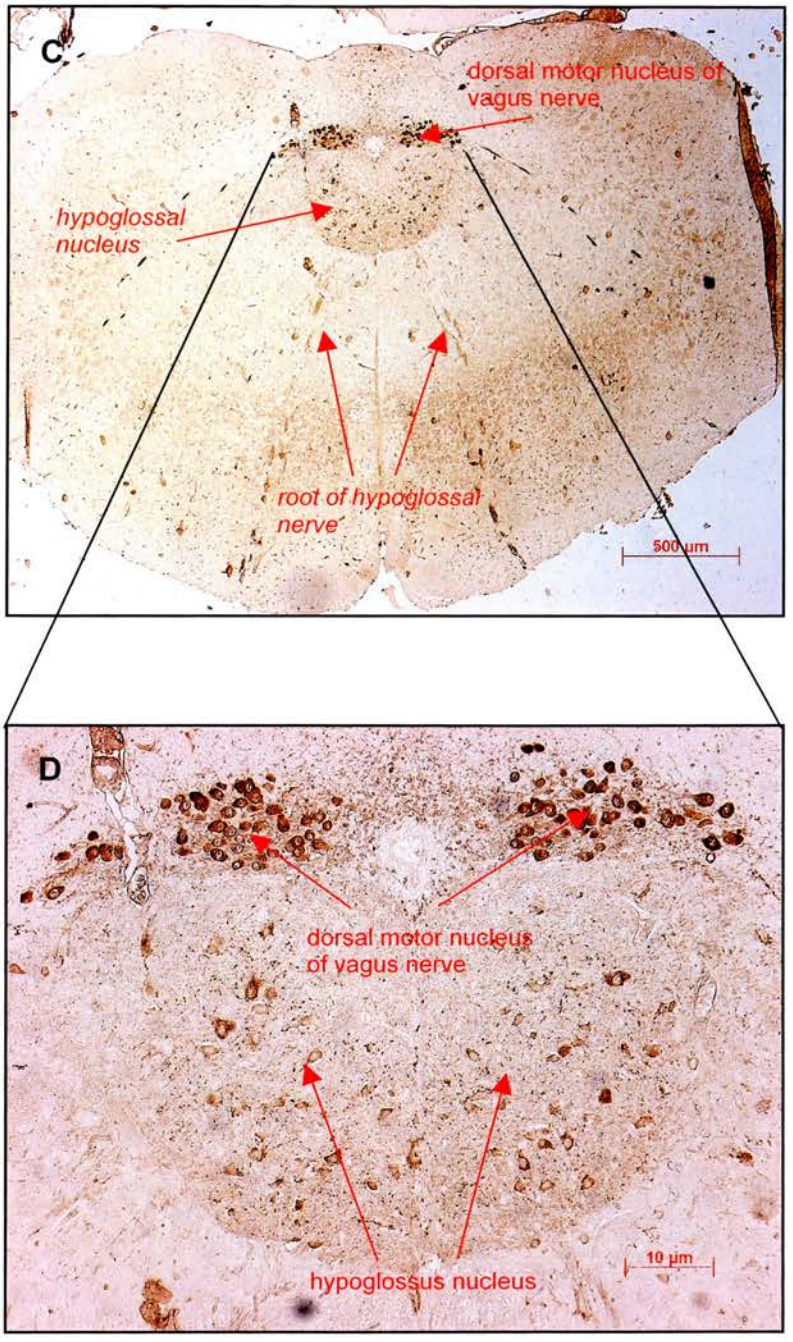

Fig. 5.2.8: Anti-γ-synuclein (A, B) and anti-ChAT (C, D) staining of the adult murine *hypoglossal nucleus* in the adult mouse. **A:** low-magnification view showing diffuse immunoreactivity in the hypoglossus and dorso-adjacent dorsal motor nucleus of the vagus nerve as well as the axons of the hypoglossal motoneurons. **B:** higher magnification view of the same stain. Note the empty appearance of the cell bodies and the positive stain of the nerve root emerging from the nucleus and heading towards the ventral surface of the brainstem to form the root of the hypoglossus nerve.
Line through sagittal diagram shows level of coronal plane.

As these findings appeared to contrast with the findings of Buchman and colleagues who had detected the protein in the cytoplasm of the embryonic trigeminal sensory neurons, the immunostaining was repeated on a brain fixed with a different, formalin-based fixative (FAA). However, the immunostaining performed on this brain confirmed the earlier findings. No significant differences were seen between the specimen.

To elucidate whether these observations would also hold true for embryonic material, immunohistochemistry was performed on mouse embryos from developmental stages E11, E12, E15.

5.2.2 Embryonic and early postnatal brains

In the mouse γ-synuclein mRNA become clearly detectable in various neuronal structures between E9.5 and E10. This coincides with the birth of the three types of cranial motoneurons (somatic, visceral and branchiomeric; Taber Pierce, 1973). The dopaminergic neurons of the substantia nigra and the ventral tegmental area have been reported to become postmitotic at E12.5 in the rat (Specht et al., 1981). Since there is general developmental delay of between one and three days in the rat with regard to the mouse it could be assumed that in these neurons completion of final mitosis and upregulation of γ-synuclein expression coincide as well.

Since γ-synuclein mRNA was shown to be upregulated around E10, I decided to perform earliest immunohistochemistry on E11 and E12 embryos.

This was done to allow for the protein to be produced in high enough quantities to be detectable by immunohistochemistry on paraffin sections. Immunostainings of E11 embryos showed a clear presence of γ-synuclein in the *basal plate* along its entire extent from the mesencephalon to the spinal cord (Fig. 5.2.9). Unlike the situation in the adult brain, γ-synuclein appeared clearly localized in the somata of the neurons. At E12, the protein could be detected in individual, newly forming cranial motor nuclei. It also appeared in the outgrowing motor nerve roots (Fig. 5.2.10). γ-synuclein was also detected in the cytoplasm of the migrating neurons of the *substantia nigra* and the *ventral tegmental area primordium* (Fig. 5.2.11).

At E15 all cranial motor nuclei have formed and can be found in the position that they assume in the adult brain. Even the lengthy migration of facial motoneurons from the territory derived from the 4th rhombomere to the former 6th rhombomere is completed and the outgrowing motor axons have formed a sling around the abducens nucleus (Auclair et al., 1996; Studer et al., 1996; Schneider-Manoury et al., 1997; Garel et al., 2000).

Motoneurons of the *oculomotor complex (oculomotor, trochlear and abducens nuclei)* were clearly labelled by the SK23 antibody. The protein could be detected in both cell bodies and axons (Fig. 5.2.12 to 5.2.14). The labelled cell bodies were densely packed giving the impression that γ-synuclein was expressed if not by all but by most of the eye muscle-innervating motoneurons. The same applied to the *trigeminal, facial and hypoglossal nuclei*. All of these motor nuclei presented as strongly labelled

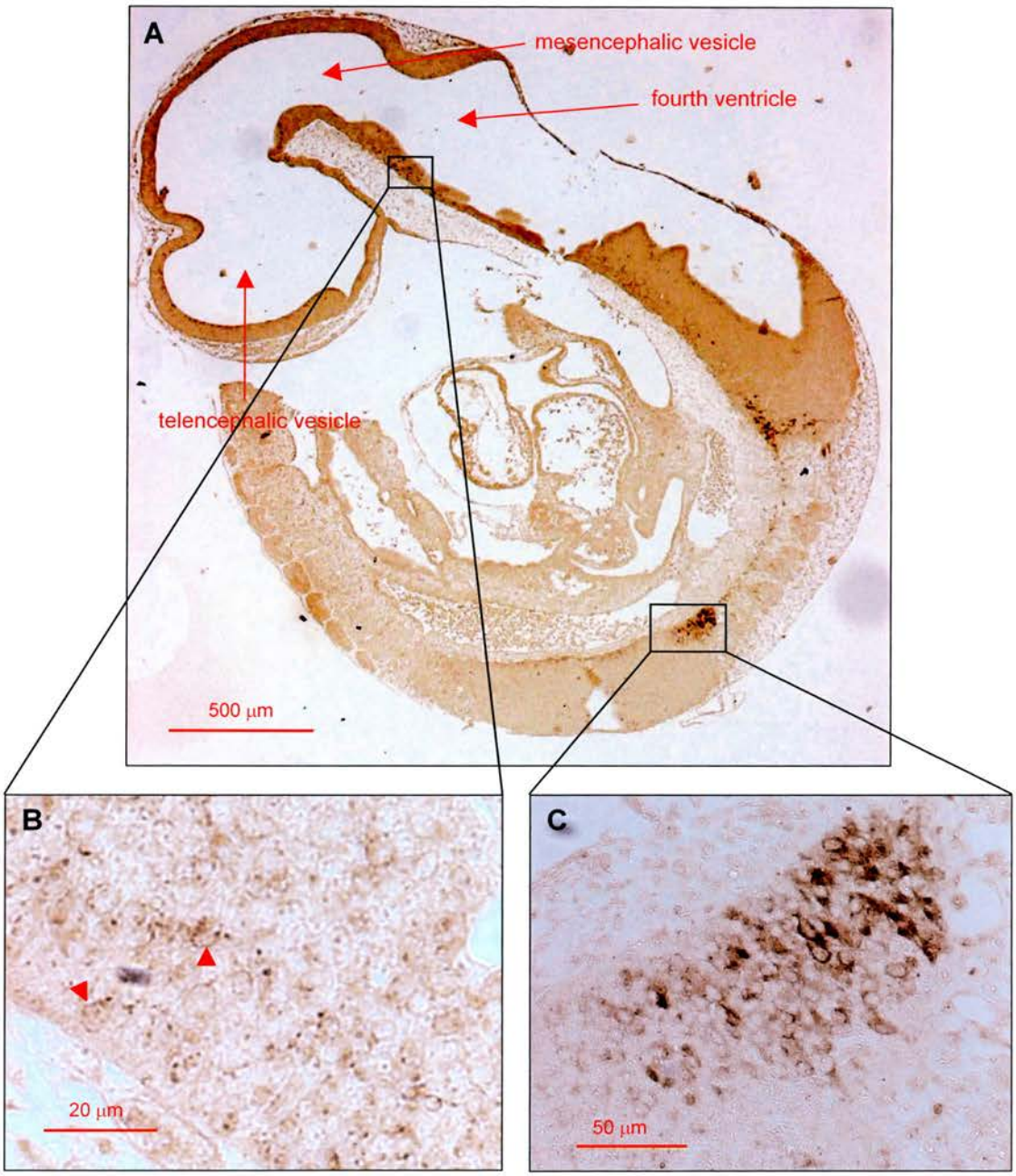

Fig. 5.2.9: Anti-γ-synuclein staining of a mouse embryo at E11. **A:** sagittal overview showing γ-synuclein in the basal plates of hindbrain and spinal cord. **B:** higher magnification of hindbrain region. Some cells are faintly outlined by a slim circle of cytoplasmic labelling (arrowheads). **C:** higher magnification of spinal cord region showing clear staining of cell somata.

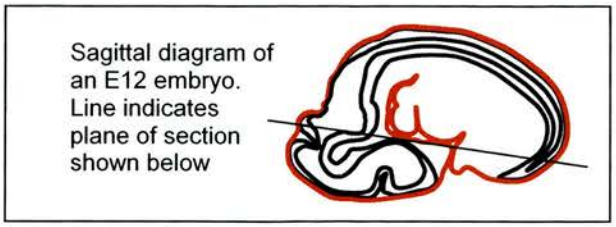

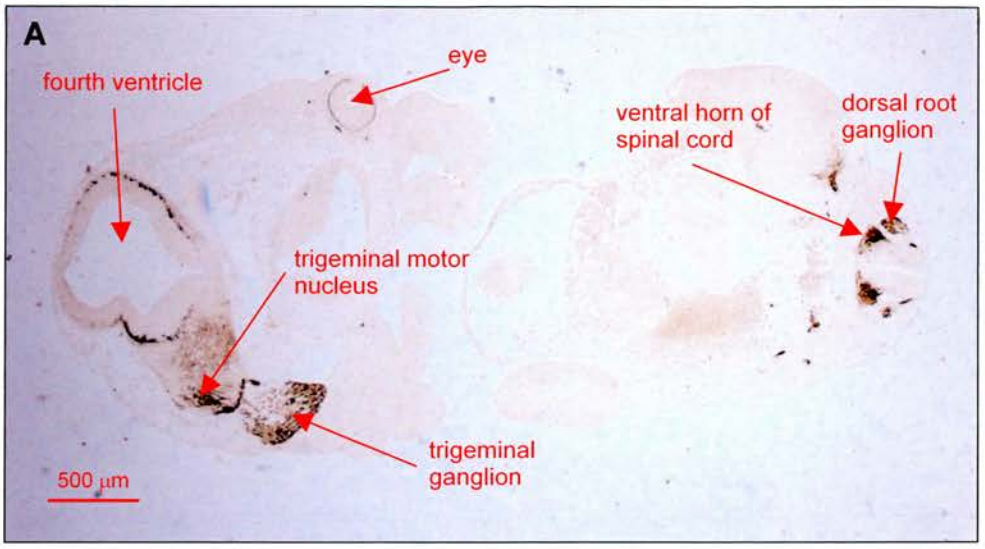

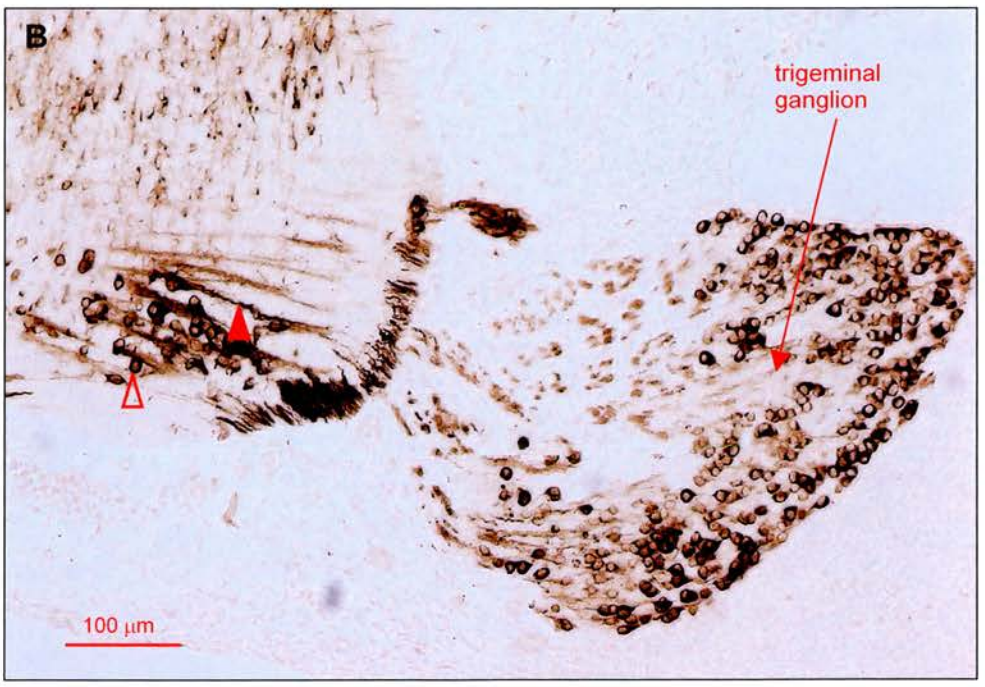

Fig. 5.2.10: Anti-γ-synuclein staining of the murine *trigeminal motor nucleus* at E12. **A:** overview showing the whole embryo. Note the localization of γ-synuclein in the developing trigeminal motor nucleus, the trigeminal ganglion (left side of picture) and in the ventral horn as well as the dorsal root ganglion (right side of picture). **B:** higher magnification of A. γ-synuclein can be detected in the cell bodies (open arrowhead) and the emerging axons (filled arrowhead) of the developing trigeminal motor nucleus.

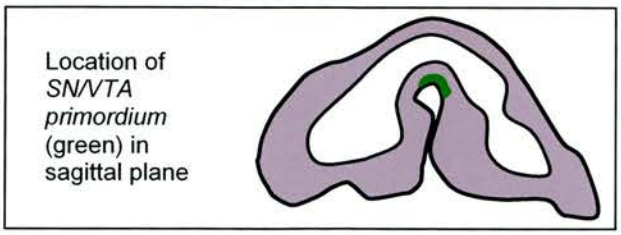

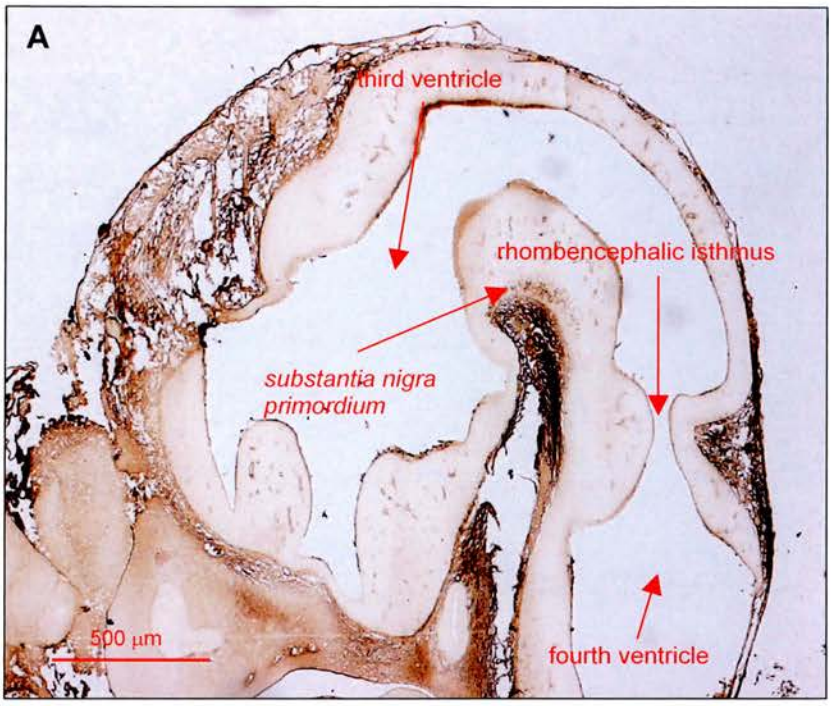

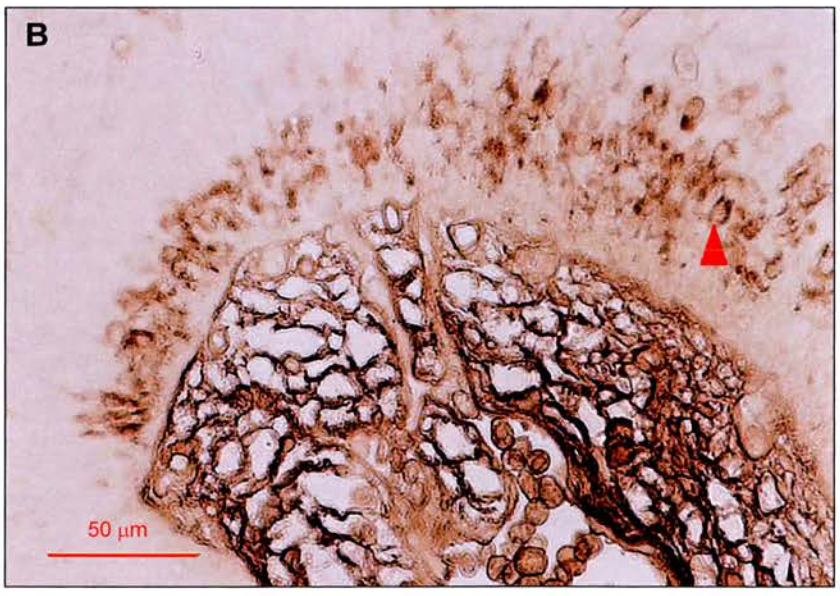

Fig. 5.2.11: Anti-γ-synuclein staining of the murine substantia nigra/ ventral tegmental area (SN/ VTA) primordium at E12. **A:** sagittal overview showing the labelled primordium of the SN/VTA. **B:** higher magnification of A revealing γ-synuclein localization in the cell bodies of individual neurons (arrowhead).

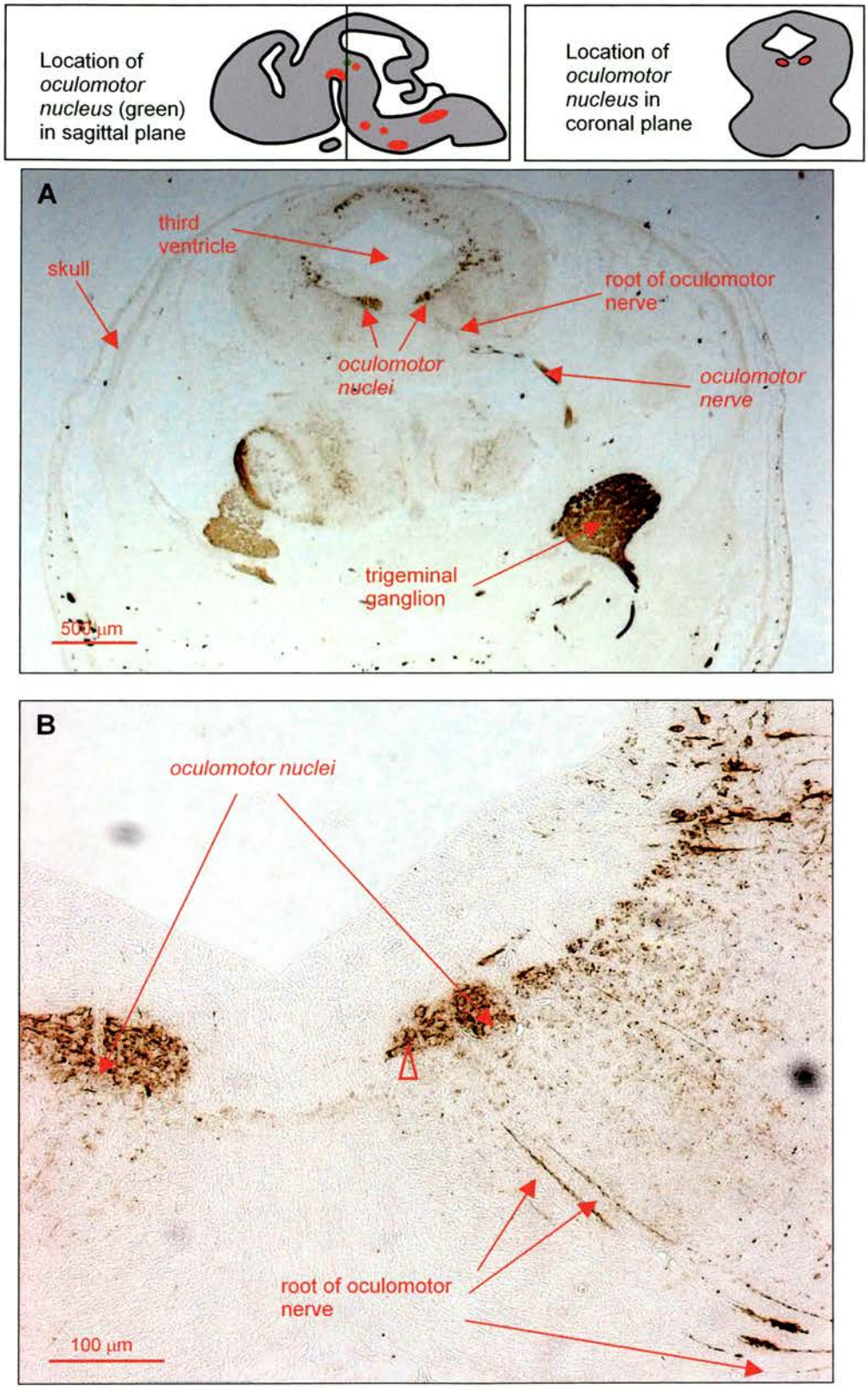

Fig. 5.2.12: Anti-γ-synuclein staining of the murine *oculomotor nucleus* at E15. **A:** coronal overview showing labelling of both oculomotor nuclei and nerve. **B:** higher magnification revealing localization of γ-synuclein in the cell bodies (open arrowhead) and in the nerve root.
Line through sagittal diagram shows level of coronal plane.

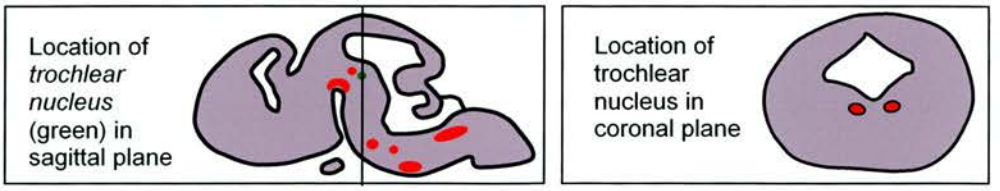

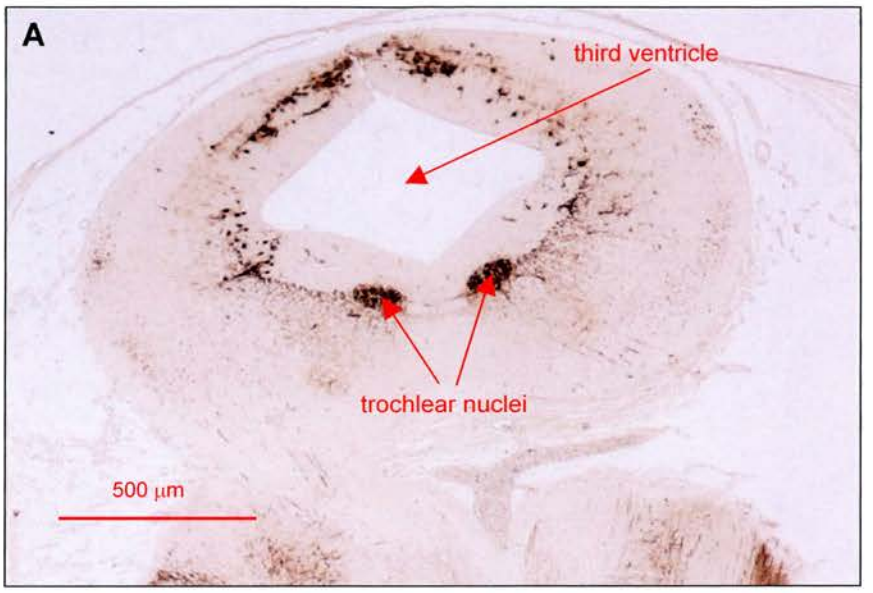

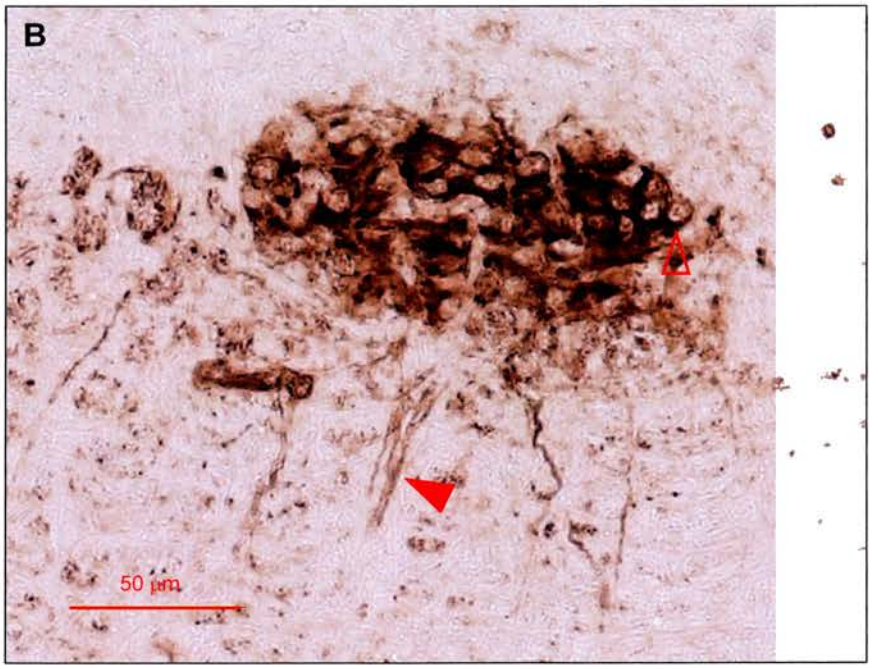

Fig. 5.2.13: Anti-γ-synuclein staining of the murine *trochlear nucleus* at E15. **A:** coronal overview. **B:** higher magnification of A showing localization of γ-synuclein in the cell bodies (open arrowhead) and in emerging fibres (filled arrowhead) of the left trochlear nucleus.
Line through sagittal diagram shows level of coronal plane.

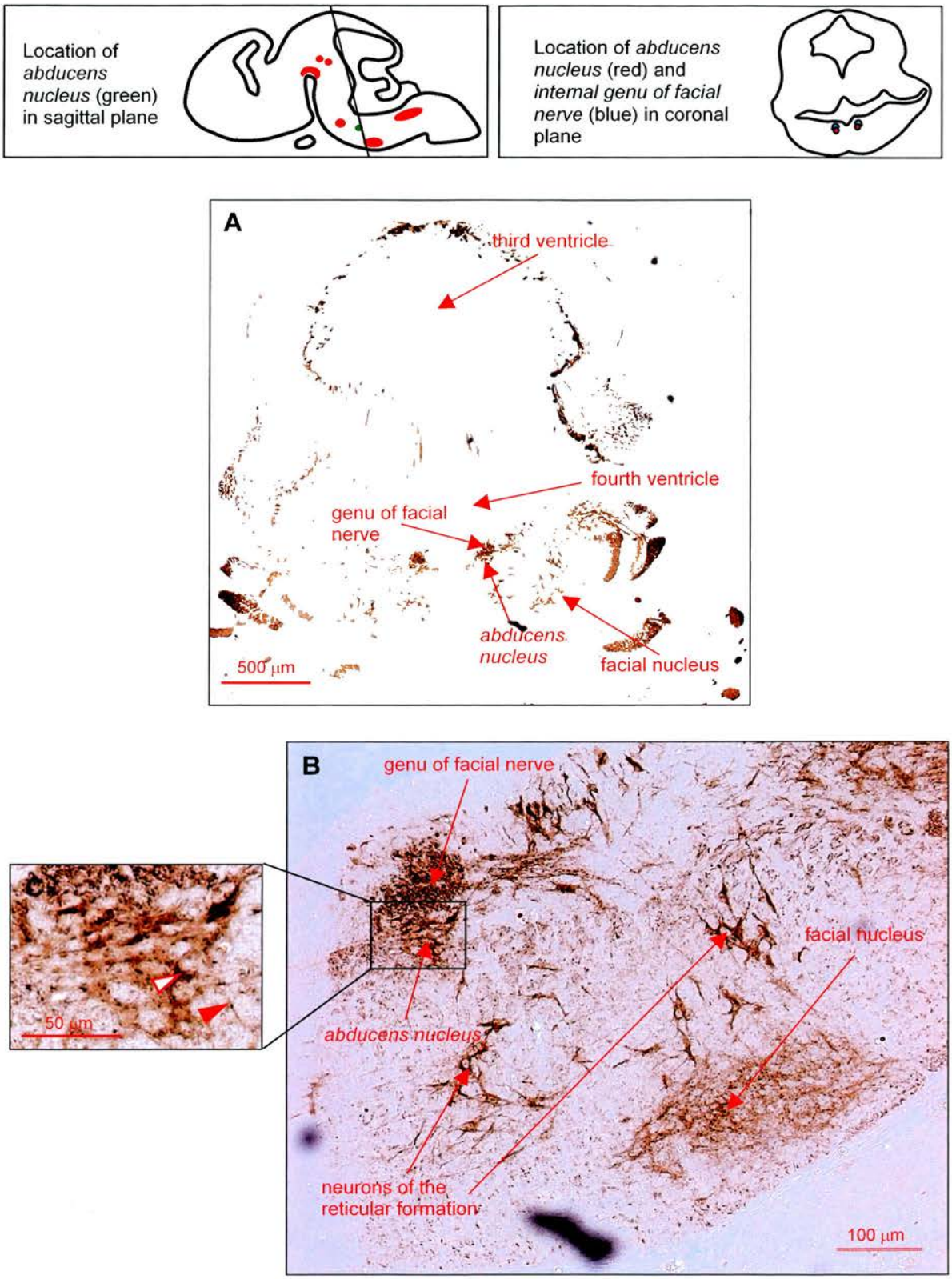

Fig. 5.2.14: Anti-γ-synuclein staining of the murine *abducens nucleus* at E15. **A, B:** coronal overviews showing labelling of the abducens nucleus and the adjacent internal genu of the facial nerve. **C:** motor nucleus in higher magnification showing localization of γ-synuclein in cell bodies (open arrowhead) and processes (filled arrowhead). Line through sagittal diagram shows level of coronal section.

assemblies of densely pact neurons (Fig. 5.2.15 to 5.2.17). Similarly, the primordia of the *substantia nigra and the ventral tegmental area* displayed neurons whose cell bodies were clearly labelled by the antibody (Fig. 5.2.18). However, the situation here is different as the definite structures are not yet formed and the primordia show bands of migrating neurons (Specht et al., 1981).

Thus the situation at E15 differed significantly from the one encountered in adult mouse brains. Whereas the pointillistic staining pattern that was so characteristic for anti-γ-synuclein stains of adult mouse brains was virtually absent from any part of the E15 brains, γ-synuclein was clearly localized in cell bodies and axons. This was an intriguing finding because it suggested that a switch in the protein's localization seemed to take part at some stage between E15 and the adult mouse brain. To establish a time frame when such a switch would occur further stainings were conducted on prenatal (E18) and postnatal (P2) mouse brains.

At E18, some changes were observed as opposed to three days earlier. Firstly, the labelled cells in all motor nuclei seemed less densely packed than seen before. Still, a significant number of neuronal cell bodies were labelled in all of the nuclei (Fig. 5.2.19). The changes seen could have very well been due to anatomical rearrangements inside the nuclei, and even more likely due to developmental cell death of motoneurons. Also, the dotted staining pattern that is suggestive of protein localization in synaptic terminals had become more prominent. If the dots were to represent synaptic terminals then at E18

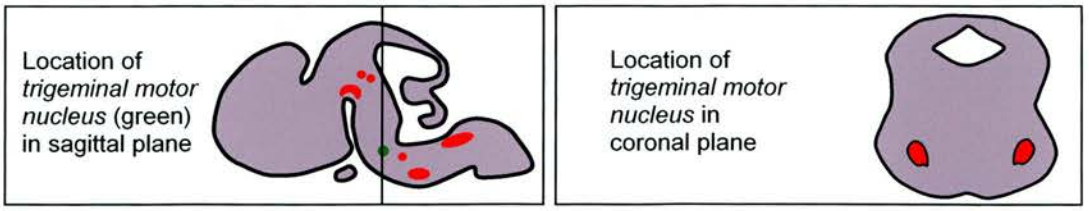
Location of *trigeminal motor nucleus* (green) in sagittal plane
Location of *trigeminal motor nucleus* in coronal plane

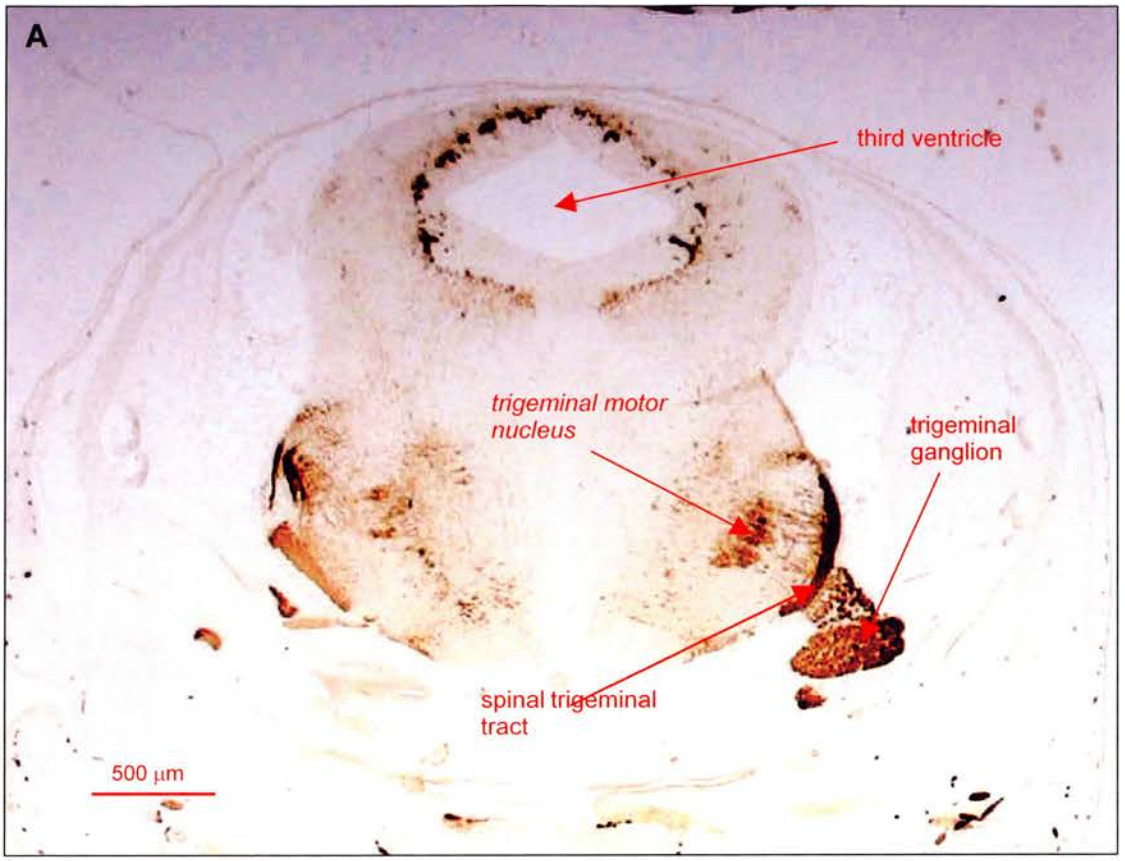
A
third ventricle
trigeminal motor nucleus
trigeminal ganglion
spinal trigeminal tract
500 μm

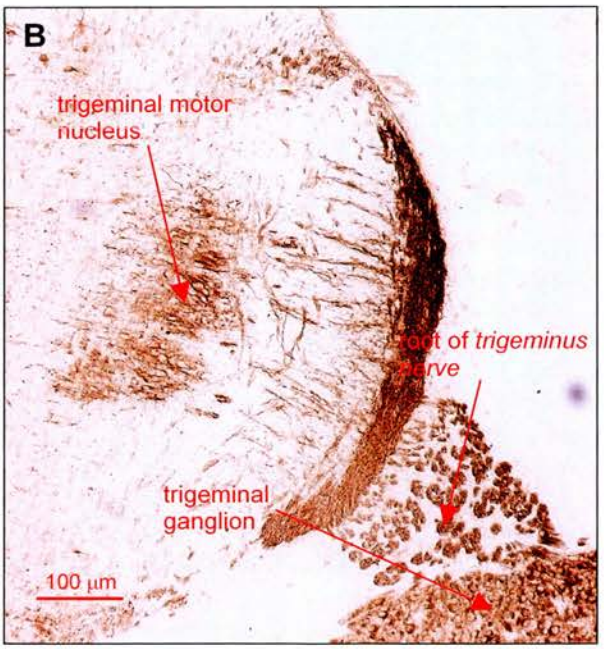
B
trigeminal motor nucleus
root of *trigeminus* nerve
trigeminal ganglion
100 μm

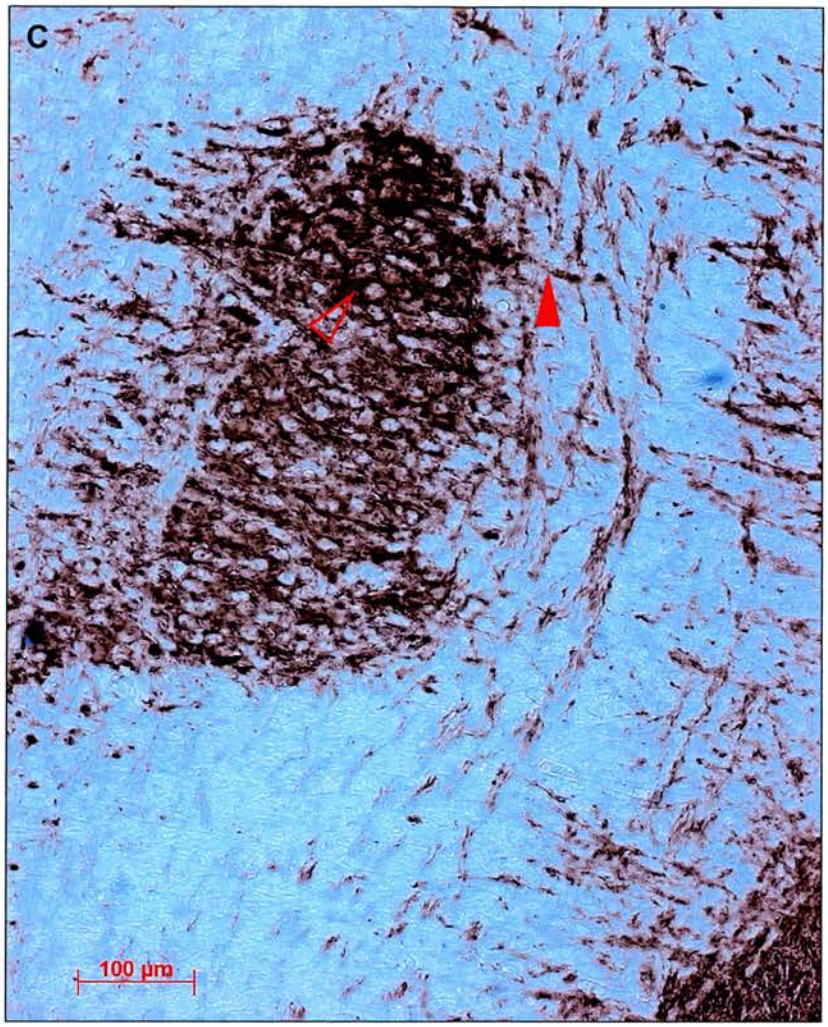

Fig. 5.2.15: Anti-γ-synuclein staining of the murine *motor nucleus of the trigeminal nerve* at E15. **A, B:** coronal overviews showing labelling of the motor nucleus as well as the spinal trigeminal tract, the trigeminal nerve root and the trigeminal ganglion. **C:** motor nucleus in higher magnification showing the detection of γ-synuclein inside the cell bodies (open arrowhead) and the emerging motor fibres (closed arrowhead). Line through sagittal diagram shows level of coronal section.

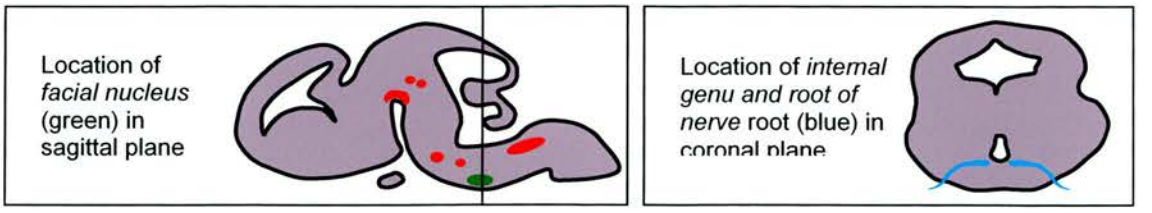
Location of *facial nucleus* (green) in sagittal plane
Location of *internal genu and root of nerve* root (blue) in coronal plane

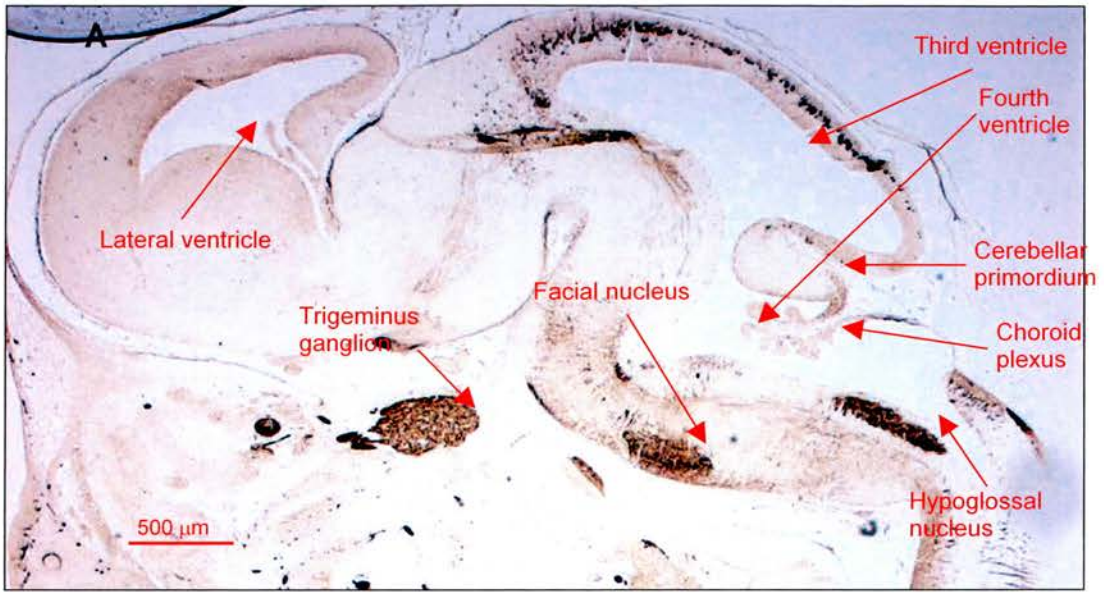
A
Third ventricle
Fourth ventricle
Lateral ventricle
Cerebellar primordium
Facial nucleus
Trigeminus ganglion
Choroid plexus
Hypoglossal nucleus
500 µm

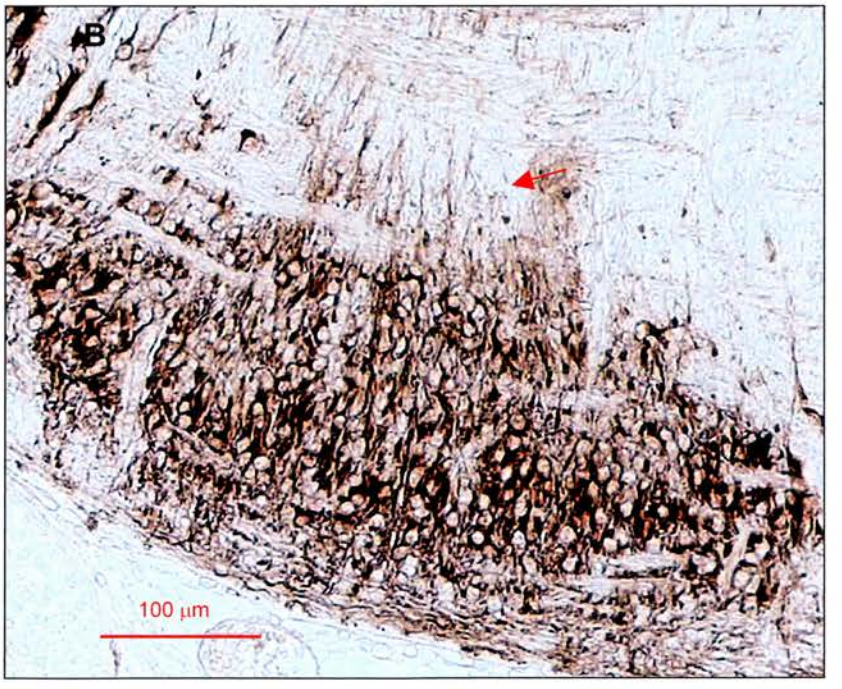
B
100 µm

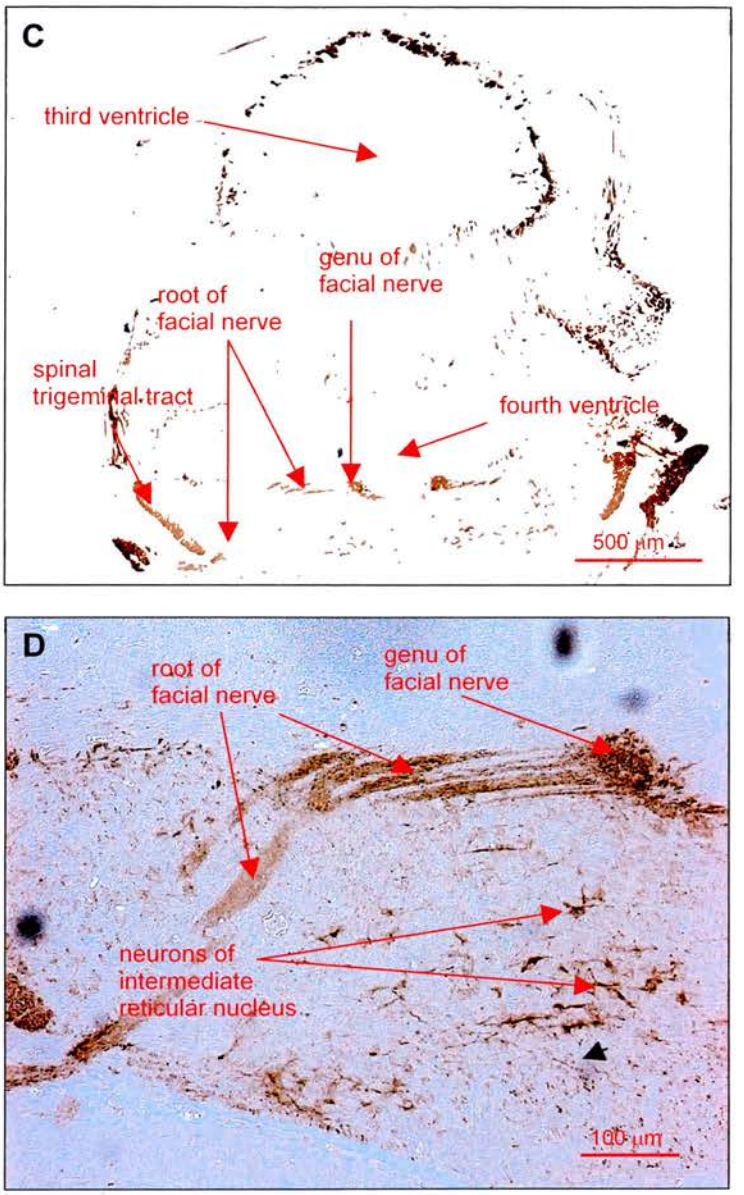

Fig. 5.2.16: Anti-γ-synuclein immunostaining of murine *facial nucleus and nerve root* at E15: **A:** sagittal overview showing distinct labelling of the facial nucleus (and the hypoglossal nucleus further caudally). **B:** higher magnification of facial nucleus shows labelling of cell somata and emerging nerve fibres (arrow). **C, E:** coronal sections showing γ-synuclein in the internal genu and the root of the facial nerve. Line through sagittal diagram shows level of coronal section

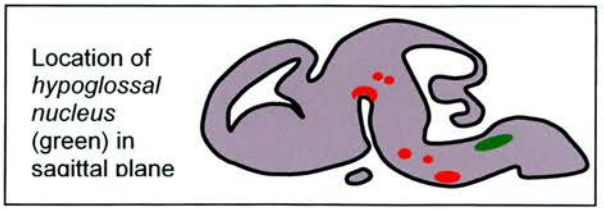
Location of
hypoglossal
nucleus
(green) in
sagittal plane

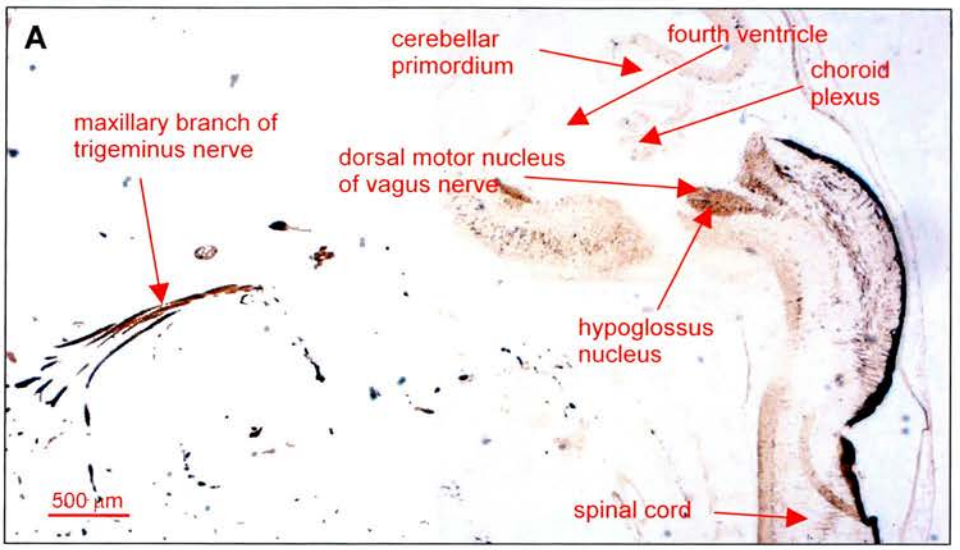
A
cerebellar
primordium
fourth ventricle
choroid
plexus
maxillary branch of
trigeminus nerve
dorsal motor nucleus
of vagus nerve
hypoglossus
nucleus
500 µm
spinal cord

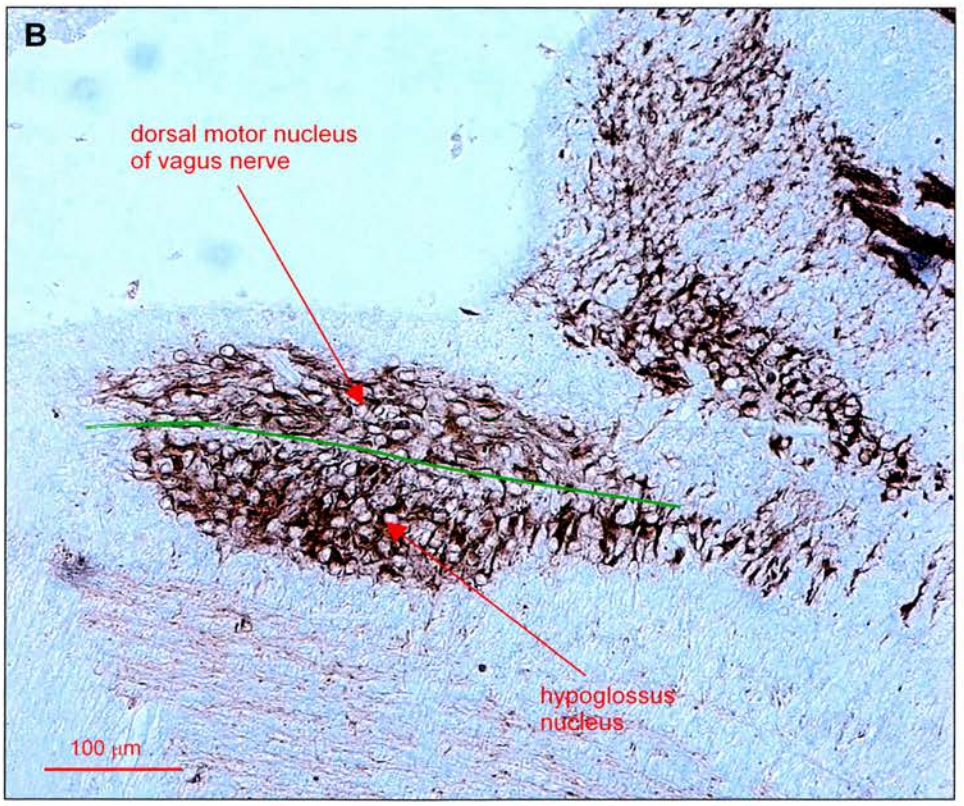
B
dorsal motor nucleus
of vagus nerve
hypoglossus
nucleus
100 µm

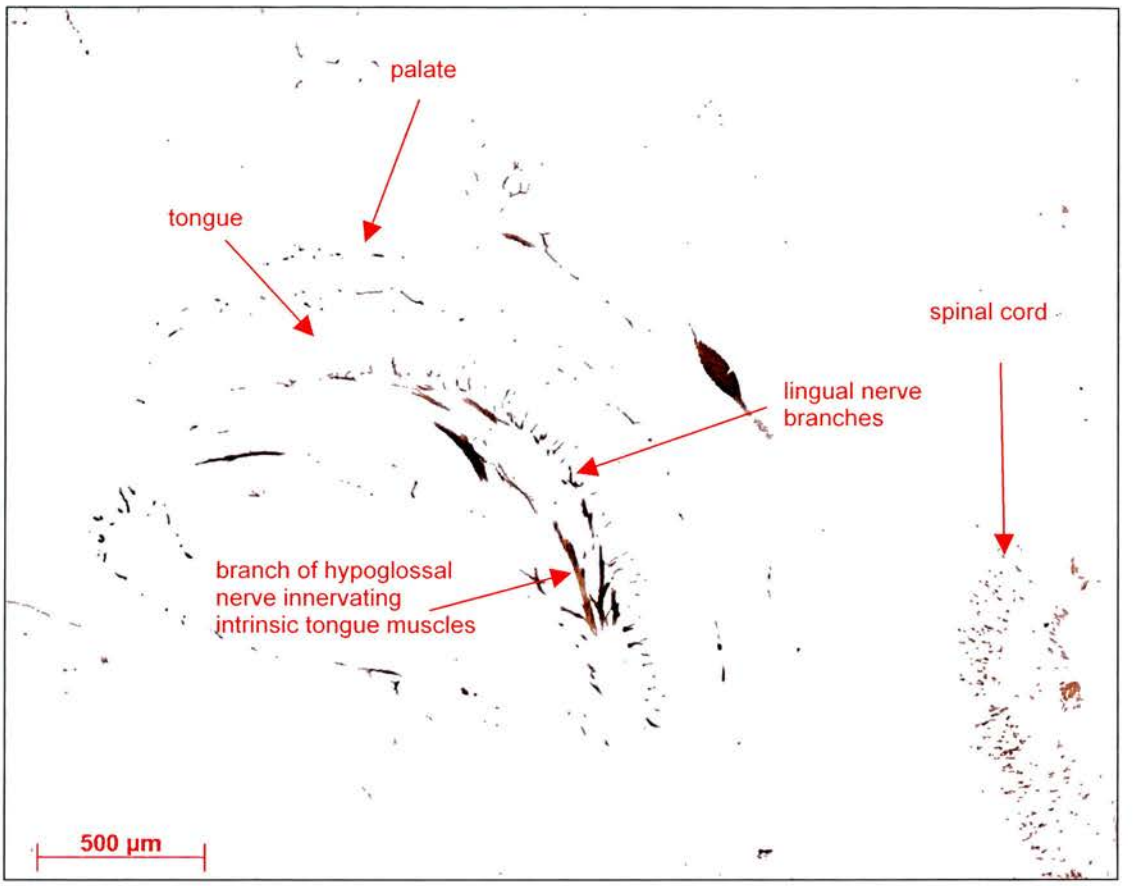

Fig. 5.2.17: Anti-γ-synuclein staining of *hypoglossal nucleus* at E15. **A:** overview in sagittal plane. **B:** Hypoglossal nucleus at higher magnification showing labelling of cell somata. The green line indicates the border between the hypoglossal nucleus and the (equally labelled) dorsal motor nucleus of the vagus nerve. **C:** sagittal section showing detection of γ-synuclein in the hypoglossal nerve. Note: the fibres of the sensory lingual nerve also stain positive for γ-synuclein.

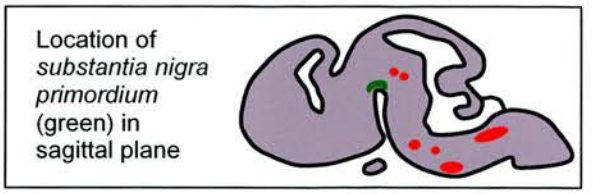

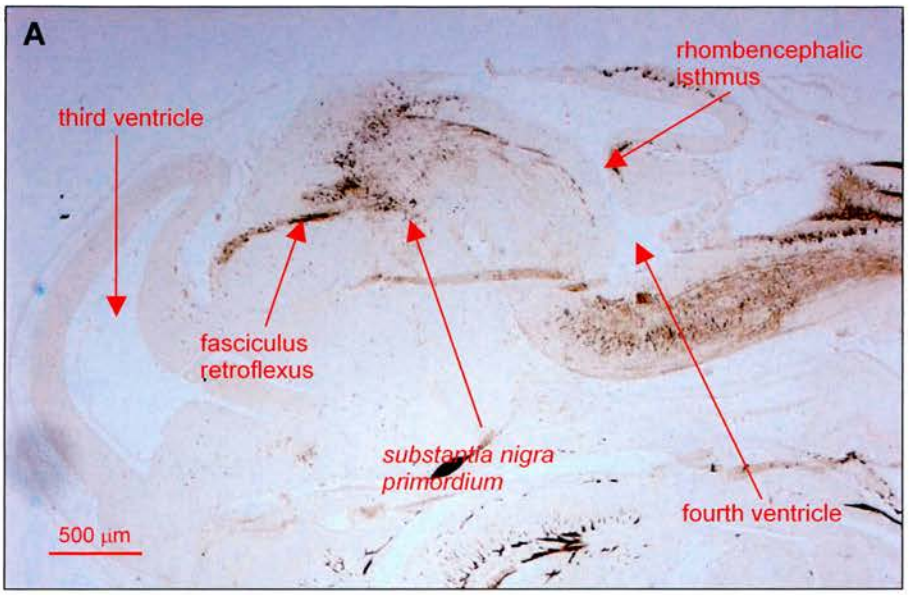

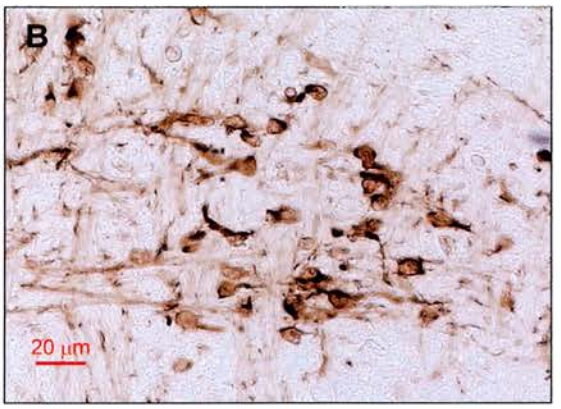

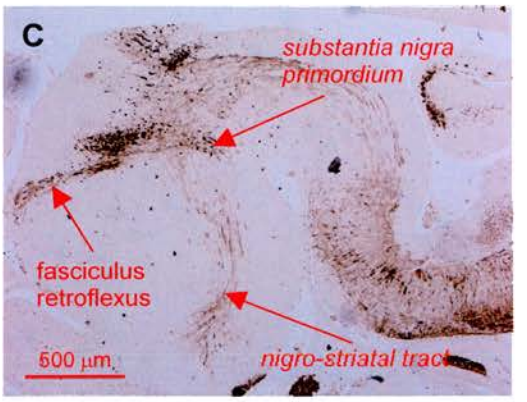

Fig. 5.2.18: Anti-γ-synuclein staining of the primordium of the murine *substantia nigra* at E15. **A:** sagittal overview. Note the strongly labelled fasciculus retroflexus, an important landmark in identifying the primordium of the substantia nigra. **B:** higher magnification of A showing the clearly labelled cell bodies of the primordium. **C:** sagittal section showing labelling of the nigro-striatal tract.

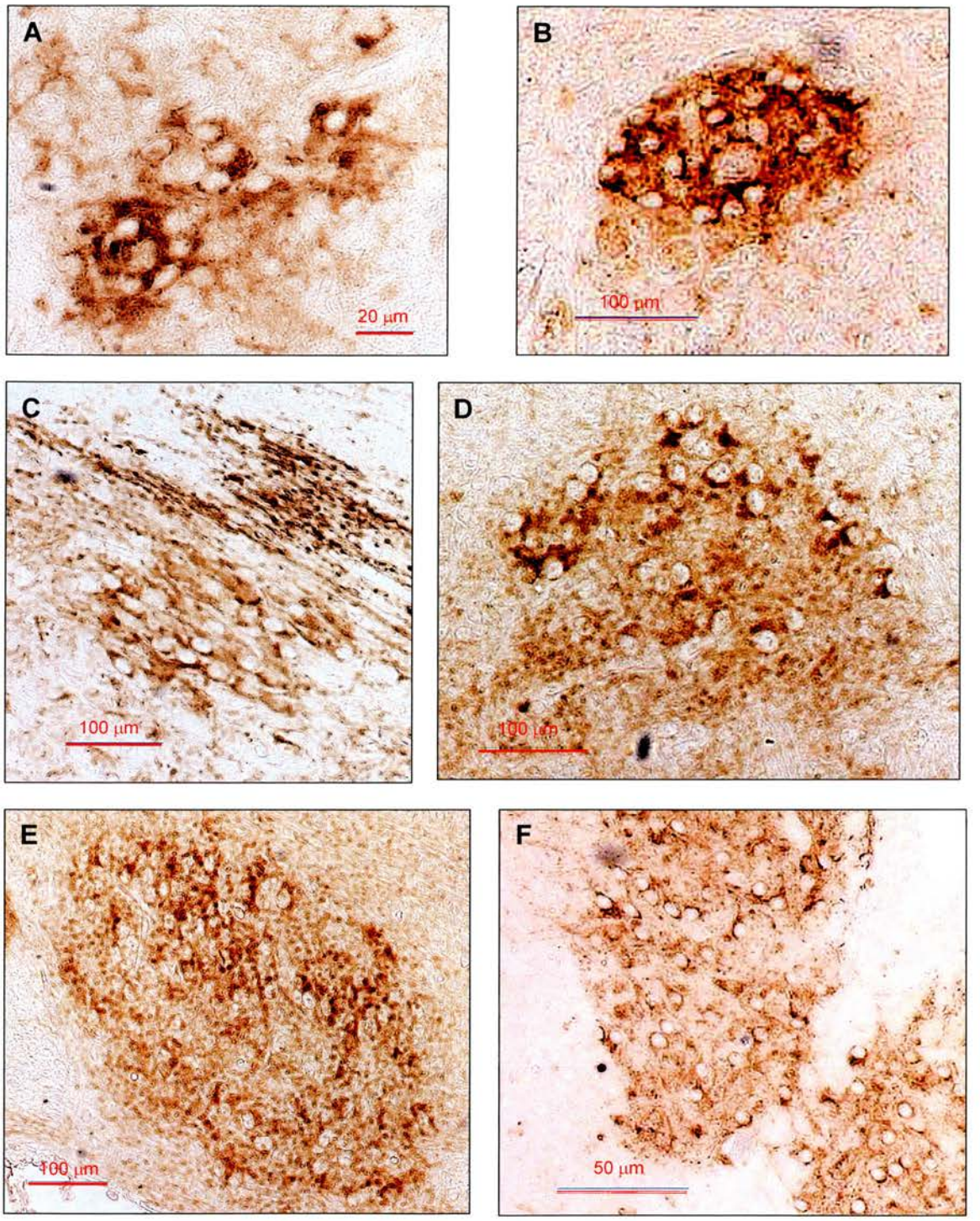

Fig. 5.2.19: Anti-γ-synuclein staining of the *somato- and branchiomotor* nuclei at E18. All nuclei still contain labelled neuronal cell bodies, but note the increasingly dotted neuropil stain.

A: oculomotor nucleus
B: trochlear nucleus
C: abducens nucleus
D: motor nucleus of trigeminus nerve
E: facial nucleus
F: hypoglossal nucleus

γ-synuclein was present all along the neuronal extent from cytoplasm to axon terminal. However, it is important to point that the presumed synaptic terminals stained inside the motor nuclei represent afferent inputs from other unaccounted parts of the nervous system, although every motor nucleus also receives projections from its contralateral counterpart. Anyway, the picture at E18 seemed to confirm that a localization shift was taking place indicating that in the end γ-synuclein might not be so much different from its two siblings with respect to its final destination (see Discussion). Interestingly, the primordia of the *substantia nigra and the ventral tegmental area* had already seized cytosolic expression of the protein (Fig. 5.2.20). On none of the sections depicting the primordia could any labelled cell bodies be found. Instead the area was marked by a densely dotted pattern.

Finally, at P2 the staining pattern resembled the one seen in the adult brain. The cytosolic stain had disappeared and given way to the pointillistic pattern in all motor nuclei as well as the SN and the VTA with the exception of the *facial nucleus* (Fig. 5.2.21). A significant number of facial motoneurons still retained γ-synuclein in their cytoplasm surrounded by a field of dots.

These findings strongly suggest that the localization of γ-synuclein at the cellular level undergoes a shift during development. Although not reported here, this shift has been seen in a number of structures inside the central nervous system. Shortly after neurons are born (i.e. have differentiated) and have become postmitotic, γ-synuclein is upregulated and

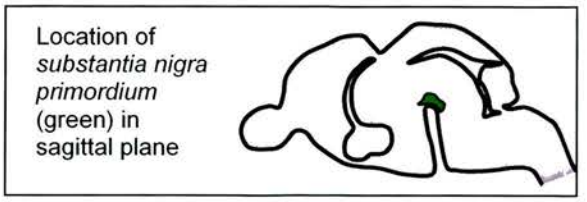

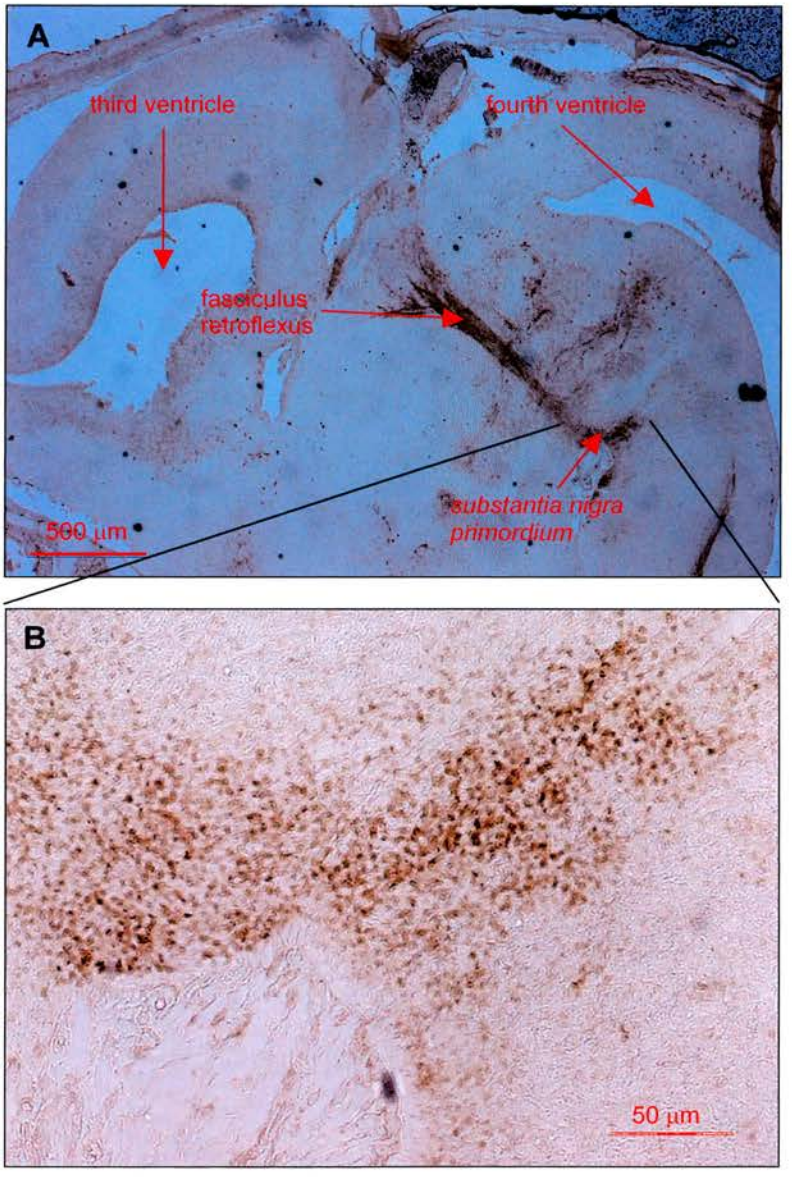

Fig. 5.2.20: Anti-γ-synuclein staining of the murine substantia nigra primordium at E18. **A:** sagittal overview. Note the strongly labelled fasciculus retroflexus, and important landmark in identifying the primordium of the substantia nigra. **B:** higher magnification of A. the primordial region is outlined by a dotted neuropil stain. No cell bodies are labelled.

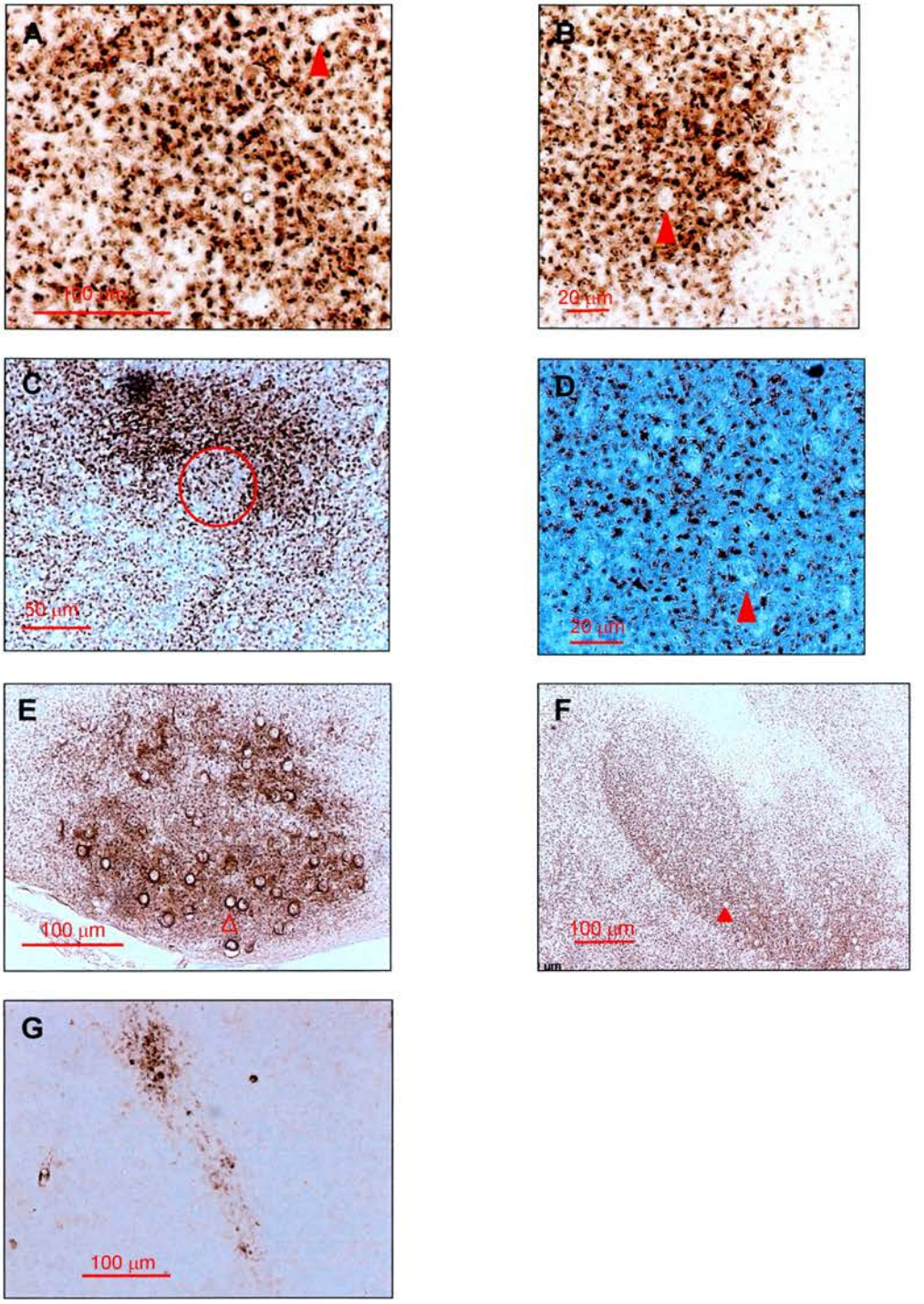

Fig. 5.2.21: Anti-γ-synuclein staining of the murine *somato- and branchiomotor nuc*lei and the *substantia nigra* at P2. All structures are characterized by a dense dotted neuropil stain. Cell bodies only remain clearly labelled in the facial nucleus (open arrowhead in E) whereas elsewhere they either appear as holes in the dotted neuropil stain (filled arrowheads in B, D, F) or can't be detected at all (A, C, G). All photos taken from sagittal sections of the same brain.

A: oculomotor nucleus
B: trochlear nucleus
C: abducens nucleus (red circle)
D: motor nucleus of the trigeminus nerve
E: facial nucleus
F: hypoglossal nucleus
G: substantia nigra

appears in the neurons' cell bodies and their outgrowing axons. In the cranial motor nuclei the protein seems to be moved away from the cytoplasm and assumes a more peripheral localization (with the curious exception of facial motoneurons) around the time of birth. In the SN and the VTA this shift seems to occur earlier although the definite structures – unlike the motor nuclei – have not yet been fully established.

5.3 Discussion

γ-synuclein is upregulated throughout the mouse brain at the beginning of the second half of the embryonic period. This has been previously been demonstrated on the mRNA level (Buchman et al., 1998b) and was confirmed here on the protein level. It was seen to be predominantly expressed in structures of the upper and lower brainstem. This seemed to set it apart from its two relatives, α- and β-synuclein which had been reported mainly in mid- and forebrain structures (Uéda et al., 1993, Iwai et al., 1995). However, a very recent publication described the immunocytochemical detection of the α- and β-synuclein proteins throughout the entire central nervous system of the rat (Li et al., 2002). This would allow for a far greater overlap of expression of all three synucleins than previously assumed. It would also provide stronger support for the balance hypothesis discussed in the previous chapter. If indeed an imbalance between α- and γ-synuclein was responsible for the demise of specific neuronal populations as speculated, then one would expect the neurons to co-express both proteins under normal circumstances. However, the article by Li and colleagues has several weaknesses. As α- and β-synuclein are both predominantly localized in nerve terminals, their immunocytochemistry of brain sections produced the dotted staining pattern that has been described here for γ-synuclein in the adult moue brain. This makes an exact description of the structures that actual express synucleins very difficult if not almost impossible. If one describes a

dotted synuclein staining inside the substantia nigra and assumes that these dots represent axon terminals (as has been done in Li's paper as well as here) then all one says is that neurons projecting onto the substantia nigra contain the protein. This means that any number or all of the following structures could express the synuclein: the striatum, the globus pallidus, the subthalamic nucleus, the amygdala, the nucleus accumbens, the pre-motor cortex, and the reticular formation. Which of these structures would indeed be responsible for the dotted stain in the substantia nigra is impossible to say.

Here, the focus had been on the cranial branchio- and somatomotor nuclei as well as the substantia nigra. In the adult mouse brain, all of them revealed a pointillistic staining pattern. Cytosolic staining which would have clearly indicated that γ-synuclein was indeed expressed by the structures themselves was only seen in a few neurons of the facial nucleus and the substantia nigra. However, the protein was detected in all motor nerve roots and the nigro-striatal tract. It is therefore possible to state that the cranial motoneurons and dopaminergic neurons of the substantia nigra express γ-synuclein.

The most intriguing finding was the clear cytosolic localization of γ-synuclein in embryonic neurons. Unlike in the adult brains, the protein appeared in the cytoplasm of motor neurons all along the midbrain, hindbrain and spinal cord axis as well as in the their nerve roots shortly after their birth. If γ-synuclein was indeed influencing neurofilament network integrity

as suggested by Buchman and colleagues (Buchman et al., 1998a), then the timing of its appearance in the motor neurons would make perfect sense. Shortly after differentiation, these neurons grow axons towards their targets (see Introduction). This requires the presence of a functional network of neurofilaments (Cleveland et al., 1991; Lee and Cleveland, 1996). Nevertheless, the exact function of γ-synuclein in regulating neurofilament network integrity is unknown. Buchman and colleagues have shown that overexpression of the gene in cultured sensory neurons leads to protease-dependent degradation of the heavy-chain neurofilament (NF-H) but has no effect on light and intermediate neurofilaments (NF-L, NF-M; Buchman et al., 1998a). This shines little light on the physiological function of γ-synuclein. But its upregulation at a time of increased neurofilament production further supports the notion that it might be involved in neurofilament network assembly and/or maintenance.

These studies have also shown that the localization of γ-synuclein is shifting during the perinatal phase of development and that the protein is finally compartmentalized in the axons and possibly nerve terminals. Again, if one assumes involvement of the molecule in axonal neurofilament network integrity, this shift makes sense. As the newly established motoneurons begin to grow out axons, γ-synuclein would be produced in significant amounts. Even if its domain of action were not to lie in the soma but in the outgrowing axon, detection of the protein in the cytoplasm could be due to a high rate of synthesis. Once the neurons have established synaptic contacts, synthesis of

γ-synuclein might be decreased to a baseline level. A swift shift of the protein towards its domain of action might then leave insufficient concentrations inside the cell body to be detectable by means of immunocytochemistry. This would explain why only a few cell somata still stained weakly for γ-synuclein in postnatal and adult brains. Depending on the individual needs of a single neuron, protein synthesis might be increased producing just enough γ-synuclein to be detected by immunohistochemistry before its transported into the periphery. Interestingly, Li and colleagues have detected the γ-synuclein in the somata of adult motoneurons in the rat brain. However, the antibody used by them was raised against recombinant human γ-synuclein and lacked the specificity of the SK23 antibody used in this study. Given also that their study was done on a different – albeit closely related - species one has to be cautious when making comparisons.

Another explanation for the shift phenomenon could concern the protein itself. Although no isoforms of γ-synuclein have been found (Buchman V., personal communication), it is conceivable that the protein undergoes differential posttranslational changes which lead to different quaternary structures. The proposal here is that in postnatal life cytosolic γ-synuclein would assume a quaternary structure that might mask the C-terminal binding site for the SK23 antibody and therefore avoid detection by immunohistochemistry. This hypothesis could be tested by producing an antibody directed against a different domain of the protein, e.g. the N-terminal and repeating the immunostainings with the new antibody. If this

would label neuronal somas then the assumption could be made that at least two quaternary forms of γ-synuclein existed and that these were differentially compartmentalized. However, this approach is not without problems since the N-terminals of the three synucleins exhibit a very high degree of similarity which would give rise to doubts about such an antibody's specificity.

It is important to point out that differences between different stainings might well be antibody-related. Antibody activity might differ between batches or an aliquot might render useless when kept at inadequate temperatures. Inconsistency in using the histological staining protocols can also seriously effect the outcome. However, there are good reasons to believe that these technical problems are unlikely to have produced the results presented above. All antibody aliquots that had been used originated from one batch only. Optimisation trials using different batches had been performed prior to the main experiments. All aliquots had been kept at –80 degrees and were used immediately after defrosting. At no time were defrosted antibodies kept in the fridge and used at a later stage. Staining protocols were strictly adhered to in order to minimize varying staining quality. Moreover, stainings were performed on a number of brains for every age group, and the results were persistent inside each group. Also, stainings of adult brains which revealed only weak and rare cytosomal labelling of individual neurons showed prominent labelling of other structures like the optic tract or the superior colliculus. This is not consistent with a somewhat inferior staining technique.

In summary, it is my belief that the differences in the compartmentalization of γ-synuclein between the embryo and the adult mouse are genuine. The predominantly peripheral localization of γ-synuclein in adult cranial motor nuclei and the substantia nigra resembled the expression pattern previously described for α- and β-synuclein (Uéda et al., 1993; Jakes et al., 1994; George et al., 1995; Iwai et al., 1995; Li et al., 2002). Given the results presented here, one has to entertain the possibility that the expression pattern of γ-synuclein is not as different from its relatives as previously suggested (Buchman et al., 1998b). In this context it would be interesting to study the expression pattern of α- and β-synuclein during development as has been done here for γ-synuclein. It could be possible that a similar shift of protein compartmentalization also affected those two synucleins. If this was the case then studies on embryos could also give a clearer picture of what neurons actually express which synuclein. As discussed above, the mere detection of protein or mRNA diffusely localized in a neural structure does not necessarily mean that this structure is the source of expression. Therefore a study as undertaken by Li and colleagues is only of limited value and especially so when using antibodies of different degrees of specificity as has been done by them. The detection of α- and/or β-synuclein inside specific neurons in the embryo might give us a clearer picture of their overall expression pattern then we have to date. A different but somewhat Herculean approach when applied to the whole of the central nervous system would be to conduct co-localization studies with the

synuclein in question and a variety of different markers (e.g. antibodies against various neurotransmitters).

Furthermore, the assumption has been made here that the characteristic dotted stain represents the presence of protein in axon terminals. Although, given the size and distribution of these dots, it is likely that they are indeed labelled terminals rather than transversely hit neuronal processes this is by no means a certainty. Co-localization studies with synaptic markers like synaptophysin and the utilization of electron microscopy might be helpful to support this claim.

In summary, the findings presented here have clearly shown that γ-synuclein is expressed by cranial motoneurons as well as the dopaminergic neurons of the substantia nigra. The protein is upregulated at a stage when these neurons have become postmitotic and started axonal outgrowth. This seems to support the hypothesis that γ-synuclein is somehow involved in neurofilament network assembly or maintenance as neurofilaments play an important role in axonal growth. Evidence has been presented that during development the protein undergoes a shift in intraneuronal localization and is finally compartmentalized in axons and axon terminals. This makes its expression pattern resemble that of its two relatives, α-and γ-synuclein and contrasts with previous conceptions stating that γ-synuclein is predominantly localized in cell somata and processes.

General Discussion

This thesis aimed at investigating the effects of Macrophage Stimulating Protein (MSP) and γ-synuclein on brainstem motor systems. MSP, a long known member of the kringle protein family, exerts a whole range of biological functions (Leonard and Skeel, 1978; Skeel et al., 1991; Skeel and Leonard, 1994; Banu et al., 1996; Broxmeyer et al., 1996; Wang et al., 1996). The present study showed for the first time that MSP can also act as a neurotrophic factor for developing hypoglossal motoneurons in E5.5 chick embryos. This is not only the developmental period when chick motoneurons underg physiological cell death (Lance-Jones, 1982), but also when axons of the hypoglossal nerve have reached their target, the tongue musculature (Kuratani et al., 1988, 1991). Furthermore, this study has shown that MSP mRNA is expressed in the chick tongue at E5.5. The receptor for MSP, RON is expressed in the hypoglossal nucleus of developing mice (Gaudino et al., 1994, 1995; Quantin et al., 1995; Thery et al., 1995). and has been shown to mediate growth signals on induction by MSP (Iwama et al., 1996). These findings provide strong evidence that MSP is a target-derived neurotrophic factor for hypoglossal motoneurons.

This adds MSP to the seemingly ever-growing list of neurotrophic substances. As discussed in Chapter 1, the conditions for neuronal survival are complex, and have to be coordinated in time and space. Firstly, motoneuron survival does not only depend on target-derived substances. Survival-enhancing factors can stem from the central nervous system, sources along the route of axon trajectories like the extracellular matrix (Edgar et al., 1984) or Schwann cells (Arce et al., 1990). Afferent influences

can also have effects on neuronal survival (Levi-Montalcini, 1947; Wakade et al., 1983; Sendtner et al., 2000). Secondly, trophic requirements of motoneurons might change during development (Henderson et al., 1993). Thirdly, trophic substances can act synergistically to potentiate each others efficacy (Arakawa et al., 1990, Unsicker and Kriegelstein, 2000). And fourthly, different subpopulations of motoneurons can depend on different trophic factors (Stoker et al., 1987; Nakamura et al., 1989, Novak et al., 2000).

The latter seems to be especially true for MSP as its receptor RON is expressed in the hypoglossal nucleus but in none of the other cranial motor nuclei (Gaudino et al., 1995). However, the study undertaken by Gaudino and colleagues had focused on the mouse hindbrain, and no information is available as to whether the same is true for the chick embryo. At the time the present study was undertaken, no specific antibody targeting murine motoneurons was available. Thus, it wasn't possible to immuno-purify hypoglossal motoneurons from mouse embryo hindbrains. An alternative would be to study RON expression in the chick hindbrain by means of in situ hybridisation. Furthermore, if RON expression in the chick embryo would be similar to the mouse embryo, one would expect MSP to have no effect on other cranial hindbrain motoneurons. In vitro studies of purified motoneurons from these nuclei could assist in answering that question. But at the time this proves a difficult undertaking, as there is a significant anatomical overlap between the cranial motor nuclei at E5.5 and many motoneurons have already downregulated SC1, the marker for chick

motoneurons used for immuno-purification (see Chapters 1 and 3). A way around this problem would be to create MSP null-mutant mice and to compare motoneuron numbers in all cranial motor nuclei with those in wildtype mice by histological means.

An interesting finding was that MSP also acted on neurite outgrowth of hypoglossal neurons. There is a plethora of molecules and structures involved in axonal outgrowth and guidance of cranial motoneurons. A number of them have been discussed in the introduction of this thesis. Remarkably little has been published yet on the role that neurotrophic factors can play in axon outgrowth and guidance. Caton and colleagues have shown that HGF which is produced by the branchial arches has outgrowth-promoting effects on cranial motoneurons (Caton et al., 2000). A very recent paper has described BDNF, CNTF, and CT-1 as promoting outgrowth of embryonic cranial motoneurons, while GDNF and NT-3 failed to have any effect (Naeem et al., 2002).

Further research in this area will have to focus on establishing a detailed picture as to when and under what conditions specific neurotrophic factors act on what neuronal (sub)populations. This is also of clinical importance. For instance, Amyotrophic Lateral Sclerosis (Motor Neuron Disease) is a neurodegenerative disorder that leads to a progressive loss of motoneurons. Interestingly, this loss is asymmetrical. Certain motoneuron subpopulations are more preferentially involved in the demise than others. In the brainstem, the disease affects predominantly the trigeminal ,the facial,

and the hypoglossal motor nuclei. In the spinal cord, the dorsolateral motoneuron pool is often more affected than the ventromedial pool (Chou, 1994). There is some evidence that apoptosis, the mechanism underlying physiological cell death in the developing nervous system (see Chapter 1), might play a role in the demise of these neurons (Rabizadeh et al., 1995; Bredesen et al., 1996; Vukosavic et al., 1999).

Another finding highlighted by the present findings is that a factor that enhances neuronal growth, can also have effects on neurite outgrowth. This aspect has so far been widely neglected in the literature about neuronal growth factors apart from of a few exceptions (e.g. Maina et al., 1998, Caton et al., 2000). Axonal outgrowth and guidance of cranial motoneurons is as complex as survival, and involves a range of factors. Axons can be guided by attractive and dispelling factors (reviewed by Tessier-Lavigne and Goodman, 1996).

These findings stress the importance of developmental studies that elucidate the mechanisms underlying neuronal survival, axonal and dendritic outgrowth and myelination, and the establishment of functional synapses between neurons and their targets. Thus, basic research has the potential to bring about specific therapeutic strategies not only to halt pathological processes but also to regenerate lost neurons. However, one has to restrain one's enthusiasm towards the therapeutic potential of neurotrophic factors themselves. Firstly, clinical trials employing a single neurotrophic substance are flawed from the outset as they don't take into account the complexities of

neuronal survival and growth. Secondly, neurotrophic factors are often multifunctional molecules with different biological activities that act on different targets. MSP is a good example: apart from its neurotrophic potential, which has been demonstrated here for the first time, it is also involved in immune response and osteoclastic activity (see above). Thirdly, it has become clear in recent years that the apparent inability of damaged central neurons to regenerate is not so much of their own making but due to unfavourable conditions in their diseased environment, which prevent a *restitutio ad integrum*.

The second part of this thesis focused on the effects that knocking out the γ-synuclein gene had on the dopaminergic neurons of the murine substantia nigra, pars compacta (SNpc) and the ventral tegmental area (VTA), and on cranial motoneurons. A significant reduction in neuron numbers of the SNpc and the VTA in the knockout mice was observed. This could be contributed to an increased loss of neurons during the period of physiological cell death in these structures shortly after birth. However, it remains unclear what mechanisms might be responsible for the increased cell demise. So far, little is known about the physiological functions of synucleins and in particular, γ-synuclein. On the one hand, γ-synuclein might be implicated in the assembly and/ or maintenance of the cytoskeletal network (Buchman et al., 1998b). On the other hand, there is evidence that an imbalance between α- and γ-synuclein might lead to α-synuclein-induced cytotoxicity, possibly involving caspase-dependent, apoptotic pathways (van

der Putten et al., 2000; Saha et al., 2000, Uversky et al., 2002, G. Middleton, personal communication). Which of these seemingly unrelated observations might be responsible for the observed loss of dopaminergic neurons in γ-synuclein is speculation. There is reason to favour the second possibility: Disturbances in the assembly of a functioning neurofilament network are likely to affect neurons particularly at a time when axonal outgrowth towards a target takes place. Given that cell numbers between knockout and wildtype mice did not differ at E18, a stage at which these neurons have already established contact with their target, the striatum, makes it unlikely that the cell loss can be contributed to an impaired neurofilament network. Furthermore, the timing of the cell loss seems conspicuous. It seems more plausible that at a time when pro-apoptotic mechanisms are most active inside these neurons (the time of physiological cell death), α-synuclein – not balanced by the presence of its relative - might exert a cytotoxic influence and lead to the demise of a certain number of neurons.

Also, it is not clear what percentage of dopaminergic neurons in the SNpc and the VTA actually express γ-synuclein. As has been shown here, there is a significant shift in the localization of γ-synuclein on the neuronal level during development towards the periphery. The cytosomal expression of the protein in adult animals as revealed by conventional immunostaining does not answer the important question whether γ-synuclein is expressed by all or only a subset of dopaminergic neurons in the SNpc and VTA. It is therefore impossible to relate the observed 20% loss of neurons to a similar

expression pattern. The situation gets even more confusing when comparing the cell count results in cranial motoneurons with the γ-synuclein expression pattern in cranial nuclei. Although, γ-synuclein has been shown to be expressed in all six of the studied motor nuclei, knocking out the gene led to a reduction of motoneurons in only two of these nuclei. If an imbalance between the synucleins was to be blamed for the demise of certain neuronal subpopulations, then it would be necessary to investigate what motor nuclei express α-synuclein. Until recently, the prevailing impression was that α-synuclein is predominantly expressed in rostrally located neuronal structures. Li and colleagues have found that α-synuclein is also present in the brainstem (Li et al., 2002). However, as discussed in Chapter 5, this study is not without flaws, since for many structures it only showed a dotted expression pattern which was contributed to the localization of α-synuclein in synaptic terminals. Even if one was to accept that the dotted staining represents pre-synaptic localization of the protein, it gives no clues about the source of its expression. It would therefore be interesting to perform a similar study for α-synuclein as has been presented here for γ-synuclein. Murphy and colleagues have shown a shift in α-synuclein localization from the cell soma to processes and synaptic terminal in cultured murine hippocampal neurons (Murphy et al., 2000). It is therefore feasible to assume that anti-α-synuclein stainings of mouse embryos at different developmental stages might reveal the true extent of the protein's expression pattern.

An interesting finding was that γ-synuclein was upregulated in cranial motoneurons at a time when these cells begin to grow axons towards their respective targets. As neurofilaments play an important role in the outgrowth of neuronal processes, this observation seemed to confirm the hypothesis of Buchman and colleagues that γ-synuclein was involved in the assembly and/ or maintenance of the neurofilament network. This is of particular interest in a slightly unrelated context. It has been shown that γ-synuclein is upregulated in the malignant cells of breast cancer. Furthermore, its concentration seems to increase in parallel with the clinical staging of this tumour (Ji et al., 1997; Ninkina et al.,. 1998). It is tantalizing to speculate that the protein's putative involvement in cytoskeletal network integrity might play a role in the invasiveness of malignant cells.

The knowledge about the possible functions of γ-synuclein remains patchy. Neither has its involvement in neurodegenerative or malignant diseases been elucidated yet nor is it clear what role the protein plays during the development of the nervous system. A lot of research remains to be done. But the same principle applied earlier to MSP and neurotrophic factors also holds true for γ-synuclein. The study of the developing nervous system does not merely quench the thirst for scientific knowledge in its own right but also has the potential to make us understand the nature of neurological diseases and to lead to therapeutic strategies that are desperately needed.

BIBLIOGRAPHY

Abeliovich A, Schmitz Y, Farinas I, Choi-Lundberg D, Ho W-H, Castillo PE, Shinsky N, Verdugo JMG, Armanini M, Ryan A, Hynes M, Phillips H, Sulzer D, Rosenthal A. (2000) Mice lacking alpha-synuclein display functional deficits the nigrostriatal dopamine system. *Neuron* **25**, 239-252

Abercrombie M (1946) Estimation of nuclear population from microtome sections. *Anat. Rec.* **94**, 239-247

Adams JM, Cory S. (1998) The Bcl-2 protein family: arbiters of cell survival. *Science* **281**, 1322-1326

Airaksinen MS, Titievsky A, Saarma M. (1999) GDNF family neurotrophic signalling: four masters, one servant? *Mol. Cell. Neurosci.***13**, 313-325

Akam M. (1987) The molecular basis for metameric pattern in the *Drosophila* embryo. *Development* **101**, 1-22

Akopian AN, Wood JN. (1995) Peripheral nervous system-specific genes identified by subtractive cDNA cloning. *J. Biol. Chem.* **270**, 21264-21270

Allsopp TE, Wyatt S, Paterson HF, Davies AM. (1993a) The proto-oncogene bcl-2 can selectively rescue neurotrophic factor-dependent neurons from apoptosis. *Cell* **73**, 295-307

Allsopp TE, Robinson M, Wyatt S, Davies AM. (1993b) Ectopic trkA expression mediates a NGF survival response in NGF-independent sensory neurons but not in parasympathetic neurons. *J. Cell. Biol.* **123**, 1555-1566

Altman J, Bayer SA. (1981) Development of the Brain Stem in the Rat. V. Thymidine-Radiographic Study of the Time of Origin of Neurons in the Midbrain Tegmentum *J. Comp.Neurol.* **198**, 677-716

Altman J, Bayer SA (1995) Atlas of prenatal rat brain development. *Boca Raton, London, CRC Press*

Alvarado-Mallart RM. (1993) Fate and potentialities of the avian mesencephalic/metencephalic neuroepithelium. *J. Neurobiol.* **24**, 1341-1355

Anderson JK, 2000. What causes the build-up of ubiquitin-containing inclusions in Parkinson's disease? *Mech. Age. Dev.* **118**, 15-22

Ang SL, Conlon RA, Jin O, Rossant J. (1994) Positive and negative signals from mesoderm regulate the expression od mouse Otx2 in ectoderm explants, *Development* **120**, 2979-2989

Arakawa Y, Sendtner M, Thoenen H. (1990) Survival effect of ciliary neurotrophic factor (CNTF) on chick embryonic motoneurons in culture: comparison with other neurotrophic factors and cytokines. *J. Neurosci.* **10**, 3507-3515

Arber S, Caroni P. (1996) Specificity of single LIM motifs in targeting and LIM/LIM interactions *in situ*. *Genes Dev.* **10**, 289-300

Arce V, Pollock RA, Philippe JM, Pennica D, Hender. (1998) Synergistic effects of Schwann- and muscle-derived factors on motoneuron survival involve GDNF and Cardiotrophin-1 (CT-1). *J. Neurosci.* **18**, 1440-1448

Auclair F, Valdes N, Marchand R (1996) Rhombomere-specific origin o branchial and visceral motoneurons of the facial nerve in the rat embryo. *J. Comp. Neurol.* **369**, 451-461

Baker JC, Harland RM. (1997) From receptor to nucleus: the SMAD pathway. *Curr Opin Genet Dev* **7**, 467-473

Bally-Cuif L, Cholley B, Wassef M. (1995) Involvement of Wnt-1 in the formation of the mes/metencephalic boundary. *Mech. Development.* **53**, 23-34

Bancroft JD, Stevens A (1996) Theory and practice of histological techniques. *Churchill Livingstone, New York, Edinburgh*

Banu N, Price DJ, London R, Deng B, Mark M, Godowski PJ, Avraham H. (1996) Modulation of megakaryocytopoesis by human macrophage-stimulating protein, the ligand for the RON receptor. *J. Immunol.* **156**, 2933-2940

Barde Y-A, 1990, The nerve growth factor family. *Prog. Growth Factor Res.* **2**, 237-248

Bardelli A, Ponzetto C, Comoglio PM. (1994) Identification of the functional domains in the hepatocyte growth factor and its receptor by molecular engineering. *J. Biotechnol.* **37**, 109-122

Barrow JR, Capecchi MR. (1996) Targeted disruption of the Hoxb-2 locus in mice interferes with expression of Hoxb-1 and Hoxb-4. *Development* **122**, 3817-3828

Baxter RM, Cohen P, Obermeier A, Ullrich A, Downes. (1995) Phosphotyrosine residues in the nerve-growth-factor receptor (Trk-A). Their role in the activation of inositol-phospholipid metabolism and protein kinase cascades in phaeochromocytoma (PC12) cells. *Eur. J. Biochem.* **234**, 84-91

Benedetti M, Levi A, Chao MV. (1993) Differential expression of nerve growth factor receptors leads to altered binding affinity and neurotrophin responsiveness. *Proc. Natl. Acad. Sci. USA* **90**, 7859-7863

Bentley CA, Lee K-F. (2000) p75 is important for axon growth and Schwann cell migration during development. *J. Neurosci.* **20**, 7706-7715

Berod A, Hartman BK, Keller A, Joh TH, Pujol JF (1982) A new double labelling technique using tyrosine hydroxylase and dopamine-beta-hydroxylase immunohistochemistry: evidence for dopaminergic cells lying in the pons of the beef brain. *Brain Res.* **240**, 235-243

Biere AL, Wood SJ, Wypych J, Steavenson S, Jiang Y, Anafi D, Jacobsen FW, Jarosinski MA, Wu GM, Louis JC, Martin F, Narhi LO, Citron M. (2000) Parkinson's disease associated alpha-synuclein is more fibrillogenic than

beta- and gamma-synuclein and cannot cross-seed its homologs. *J. Biol. Chem.* **275**, 34574-34579

Birgbauer E, SechristJ, Bronner-Fraser M, Fraser S. (1995) Rhombomere origin and rostrocaudal reassortment of neural crest cells revealed by intravital microscopy. *Development* **121**, 935-945

Bladt F, Riethmacher D, Isenmann S, Aguzzi A, Birchmeier C. (1995) Essential role for the c-met receptor in the migration of myogenic precursor cells into the limb bud. *Nature* **376**, 768-771

Bloch-Gallego E, Huchet M, El M'Hamdi H, Xie F-K, Tanaka H, Henderson CE. (1991) Survival *in vitro* of motoneurons identified or purified by novel antibody-based methods is selectively enhanced by muscle-derived factors. *Development*, **111**, 221-232

Blum M. (1998) A null mutation in TGF-a leads to a reduction in midbrain dopaminergic neurons in the substantia nigra. *Nat. Neurosci.* **1**, 374-377

Boldin MP, Goncharov TM, Goltsev YV, Wallach D. (1996) Involvement of MACH, a novel MORT1/FADD-interacting protease, in Fas/APO-1- and TNF receptor-induced cell death. *Cell* **85**, 803-815

Boldin MP, Varfolomeev EE, Pancer Z, Mett IL, Camonis JH, Wallach D. (1995) A novel protein that interacts with the death domain of Fas/APO1 contains a sequence motif related to the death domain. *J. Biol. Chem.* **270**, 7795-7798

Boncinelli E, Acampora D, Pannese M, D'Esposito M, Somma R, Gaudino G, Stornaiuolo A, Cafiero M, Faiella A, Simeone A. (1989) Organization of human class I homeobox genes. *Genome* **31**, 745-756

Boncinelli E, Gulisano M, Broccoli V. (1993) Emx and Otx homeobox genes in the developing mouse brain. *J. Neurobiol.* **24**, 1356-1366

Boncinelli E, Somma R, Acampora D, Pannese M, D'Esposito M, Faiella A, Simeone A. (1988) Organization of human homeobox genes. *Hum. Reprod.* **3**, 880-886

Bothwell M. (1995) Functional interactions of neurotrophins and neurotrophin receptors. *Ann. Rev. Neurosci.* **18**, 223-253

Bottaro DP, Rubin JS, Faletto DL, Chan AM, Kmiecik. (1991) Identification of the hepatocyte growth factor as the c-met proto-oncogene product. *Science* **251**, 802-804

Bredesen DE, Wiedau-Pazos M, Goto JJ, Rabizadeh S, Roe JA, Gralla EB, Ellerby LM, Valentine JS. (1996) Cell death mechanisms in ALS. *Neurology* **47 Suppl**, S36-S39

Brennan C, Rivas-Plata K, Landis SC. (1999) The p75 neurotrophin receptor influences NT-3 responsiveness of sympathetic neurons *in vivo*. *Nat. Neurosci.* **2**, 699-705

Broxmeyer HE, Cooper S, Li ZH, Lu L, Sarris A, Wang MH, Chang MS, Donner DB, Leonard EJ. (1996) Macrophage-stimulating protein, a ligand for the RON receptor protein tyrosine kinase, suppresses myeloid progenitor cell proliferation and synergizes with vascular endothelial cell growth factor and members of the chemokine family. *Ann. Hematol.* **73**, 1-9

Bruening HE, Giasson BI, Klein-Szanto AJ, Lee VM, Trojanowski JQ, Godwin AK (2000) Synucleins are expressed in the majority of breast and ovarian carcinomas and in preneoplastic lesions of the ovary. *Cancer* **88**, 2154-2163

Buchman VL, Adu J, Pinon LG, Ninkina NN, Davies AM. (1998a) Persyn, a member of the synuclein family, influences neurofilament network integrity. *Nat. Neurosci.* **1**, 101-103

Buchman VL, Hunter HJA, Pinon LGP, Thompson J, Privalova EM, Ninkina NN, Davies AM. (1998b) Persyn, a member of the synuclein family, has a distinct pattern of expression in the developing nervous system. *J. Neurosci.* **18**, 9335-9341

Bueker ED. (1948) Implantation of tumors in the hind limb field of the embryonic chick and the developmental response of the lumbosacral nervous system. *Anat. Rec.* **102**, 369-389

Burke WJ, Joh TH (1988) Effect of dopamine on tyrosine hydroxylase in cultured rat adrenal medulla. *Biochem. Pharmacol.* **37**, 1391-1397

Cantino D, Sisto-Daneo L. (1972) Cell death in the developing optic tectum *Brain Res.* **38**, 13-25

Caton A, Hacker A, Naeem A, Livet J, Maina F, Bladt F, Klein R, Birchmeier C, Guthrie S. (2000) The branchial arches and HGF are growth-promoting and chemoattractant for cranial motor axons. *Development* **127**, 1751-1766

Carpenter RL. (1933) Spinal ganglion responses to the transplantation of limbs after metamorphosis in Amblystoma punctatum. *J. Exp. Zool.* **64**, 287-301

Carpenter RL. (1932) Spinal ganglion responses to the transplantation of differentiated limbs in Amblystoma larvae. *J. Exp. Zool.* **61**, 149-173

Carter BD, Zirrgiebel U, Barde YA. (1995) Differential regulation of p21ras activation in neurons by nerve growth factor and brain-derived neurotrophic factor. *J. Biol. Chem.* **270**, 21751-21757

Caton A, Hacker A, Naeem A, Livet J, Maina F, Bladt F, Klein R, Birchmeier C, Guthrie S. (2000) The branchial arches and HGF are growth-promoting and chemoattractant for cranial motor axons. *Development* **127**, 1751-1766

Cattaneo E, Pelicci PG. (1998) Emerging roles for SH2/PTB-containing Shc adaptor proteins in the developing mammalian brain. *TINS* **21**, 476-481

Chalepakis G, Stoykova A, Wijnholds J, Tremblay P, Gruss P. (1993) Pax: gene regulators in the developing nervous system. *J. Neurobiol.* **24**, 1367-1384

Chang S, Fan J, Nayak J. (1992) Pathfinding by cranial nerve VII, (facial) motoneurons in chick hindbrain. *Development* **114**, 815-823

Chao MV. (1994) The p75 neurotrophin receptor. *J. Neurobiol.* **25**, 1373-1385

Chao M, Casaccia-Bonnefil P, Carter B, Chittka A, Kong H, Yoon SO. (1998) Neurotrophin receptors: mediators of life and death. *Brain Res. Brain Res. Rev.* **26**, 295-301

Chavrier P, Lemaire P, Revelant O, Bravo R, Charna. (1988) Characterization of a mouse multigene family encoding zinc finger structure. *Mol. Cell. Biol.* **8**, 1319-1326

Chavrier P, Zerial M, Lemaire P, Almendral J, Bravo R, Charnay P. (1988) A gene encoding a protein with zinc fingers is activated during G0/G1 transition in cultured cells. *EMBO* **7**, 29-35

Chen YP, Hyang L, Russo AF, Solursh M. (1992) Retinoic acid is enriched in Henson's node and is developmentally regulated in the early chicken embryo. *Proc. Natl. Acad. Sci. USA* **89**, 10056-10059

Chiang C, Litingtung Y, Lee E, Young KE, Corden JL, Westphal H, Beachy PA. (1996) Cyclopia and defective axial patterning in mice lacking sonic hedgehog gene function. *Nature* **383**, 407-413

Chinnaiyan AM, O'Rourke K, Tewari M, Dixit VM. (1995) FADD, a novel death domain-containing protein, interacts with the death domain of Fas and initiates apoptosis. *Cell* **81**, 505-512

Chomzcynski P, Sacchi N. (1987) Single step method of RNA isolation by acid guanidinium thiocyanate-phenol-chloroform extraction. *Anal. Biochem.* **162**, 156-159

Chu-Wang I-W, Oppenheim RW. (1978a) Cell death of motoneurons in the chick embryo spinal cord. I. A light and electron microscopic study of naturally-occurring and induced cell loss during development. *J. Comp.Neurol.* **177**, 33-58

Chu-Wang I-W, Oppenheim RW. (1978b) Cell death of motoneurons in the chick embryo spinal cord. II. A quantitative and qualitative analysis of degeneration in the ventral root, including evidence for axon outgrowth and limb innervation prior to cell death. *J. Comp.Neurol.* **177**, 59-86

Ciechanover A, Schwartz AL (1994) The ubiquitin-mediated proteolytic pathway: mechanisms of recognition of the proteolytic substrate and involvement in the degradation of native cellular proteins. *FASEB J.* **8**, 182-191

Clarke PGH, Cowan WM. (1976) The time of origin and the pattern of survival of neurons in the isthmo-optic nucleus of the chick. *J. Comp.Neurol.* **167**, 125-142

Clarke JDW, Lumsden A. (1993) Segmental repetition of neuronal phenotype sets in the chick embryo hindbrain. *Development* **118**, 151-162

Clary DO, Reichardt LF. (1994) An alternative spliced form of the nerve growth factor receptor TrkA confers an enhanced response to neurotrophin 3. *Proc. Natl. Acad. Sci. USA* **91**, 11133-11137

Clayton DF, George JM. (1999) Synucleins in synaptic plasticity and neurodegenerative disorders. *J. Neurosci. Res.* **58**, 120-129

Cleveland DW, Hoffman PN (1991) Slow axonal transport models come full circle: evidence that microtubule sliding mediates axon elongation and tubulin transport. *Cell* **67**, 453-456

Cohen S, Levi-Montalcini R. (1956) A nerve growth-stimulating factor isolated from snake venom. *Proc. Natl. Acad. Sci. USA* **42**, 571-574

Cohen S, Levi-Montalcini R, Hamburger V. (1954) A nerve growth-stimulating factor isolated from sarcomas 37 and 180. *Proc. Natl. Acad. Sci. USA* **40**, 1014-1018

Cohlan SQ. (1953) Excessive intake of vitamin A as a cause of congenital anomalies in the rat. *Science* **117**, 535-537

Colamarino SA, Tessier-Lavigne M. (1995) The axonal chemoattractant netrin-1 is also chemorepellent for trochlear motor axons. *Cell* **81**, 621-629

Collin R. (1906) Recherches cytologiques sur le developpement de la cellule nerveuse. *Névraxe* **8**, 181-308

Conlan RA. (1995) Retinoic acid and pattern formation in vertebrates. *TIGS* **11**, 314-319

Conti L, De Fraja C, Gulisano M, Migliaccio E, Govoni S, Cattaneo E. (1997) Expression and activation of SH2/PTB-containing ShcA adaptor protein reflects the pattern of neurogenesis in the mammalian brain. *Proc. Natl. Acad. Sci. USA* **94**, 8185-8190

Conway KA, Harper JD, Lansbury PT. (1998) Accelerated *in vivo* fibril formation by a mutant alpha-synuclein linked to early onset Parkinson's disease. *TINS* **21**, 249-254

Conway KA, Lee SJ, Rochet JC, Ding TT, Williamson RE, Lansbury PT Jr. (2000) Acceleration of oligomerization, not fibrillization, is a shared property of both alpha-synuclein mutations linked to early-onset Parkinson's disease: implications for pathogenesis and therapy. *Proc. Natl. Acad. Sci. USA* **97**, 571-576

Cooper ERA. (1946) The development of the substantia nigra. *Brain* **69**, 22-33

Couly GF, Coltey PM, Le Douarin NM.(1993) The triple origin of skull in hihger vertebrates: a study in quail-chick chimeras. *Development* **117**, 409-429

Cowan WM, Fawcett JW, O'Leary DDM, Stanfield BB. (1984) Regressive events in neurogenesis. *Science* **225**, 1258-1265

Cowan WM, Wenger E. (1967) Cell loss in the trochlear nucleus of the chick during normal development and after radical extirpation of the optic vesicle *J. Exp. Zool.* **164**, 265-280

Cowan WM, Wenger E. (1968) Degeneration in the nucleus of origin of the preganglionic fibers to the chick ciliary ganglion following early removal of the optic vesicle. *J. Exp. Zool.* **168**, 105-124

Coyle JT. (1977) Biochemical aspects of neurotransmission in the developing brain. *Int. Rev. Neurobiol.* **20**, 65-103

Creech Kraft J, Schuh T, Juchan MR, Kimelman D. (1994) Temporal distribution, localization and metabolism of all-trans retinol, didehydroretinol and all-trans-retinal during Xenopus development. *Biochem. J.* **301**, 111-119

Crossley PH, Martinez S, Martin GR. (1996) Midbrain development induced by FGF8 in the chick embryo. *Nature* **380**, 66-68

Curtis R, Adryan KM, Stark JL, Park JS, Compton DL. (1995) Differential role of the low affinity neurotrophin receptor (p75) in retrograde axonal transport of the neurotrophins. *Neuron* **14**, 1201-1211

Datta SR, Dudek H, Tao X, Masters S, Fu H, Gotoh Y. (1997) Akt phosphorylation of BAD couples survival signals to the cell-intrinsic death machinery. *Cell* **91**, 231-241

Davey F, Hilton M, Davies AM. (2000) Co-operation between HGF and CNTF in promoting the survival and growth of sensory and parasympathetic neurons. *Mol. Cell. Neurosci.* **15**, 79-87

Davies AM. (1994) Chemoattractants for navigating axons. *Curr. Biol.* **4**, 1142-1145

Davies AM, Lee KF, Jaenisch R. (1993) p75-deficient trigeminal sensory neurons have an altered response to NGF but not to other neurotrophins. *Neuron* **11**, 565-574

Davies AM, Minichiello L, Klein R. (1995) Developmental changes in NT-3 signalling via TrkA and TrkB in embryonic neurons. *EMBO J.* **14**, 4482-4489

Davies JA, Cook GMW, Stern CD, Keynes RJ. (1990) Isolation from chick somites of a glycoprotein fraction that causes collapse of dorsal route ganglion growth cones. *Neuron* **4**, 11-20

Davis CA, Joyner AL. (1988) Expression patterns of the homeobox containing genes En-1 and En-2 and the proto-oncogene int-1 diverge during mouse development. *Genes Dev.* **2**, 1736-1744

DeBernardo AP, Chang S. (1996) Heterophilic interactions of DM-GRASP: grasp-NgCam interactions involved in neurite extension. *J. Cell Biol.* **133**, 657-666

Detwiler SR. (1936) Neuroembryology. An Experimental Study, Macmillan New York

Dray A. (1979) The striatum and substantia nigra: a commentary on their relationships. *Neurosci.* **4**, 1407-1439

Duboule D, Dolle P. (1989) The structural and functional organization of the murine HOX gene family resembles that of *Drosophila* homeotic genes. *EMBO* **8**, 1497-1505

Durston AJ, Timmermans JP, Hage WJ, Hendriks HF, de Vries NJ, Heideveld M, Nieuwkoop PD. (1989) Retinoic acid causes an anteroposterior transformation in the developing central nervous system. *Nature* **340**, 140-144

Ebens A, Brose K, Leonardo ED, Hanson MG, Bladt F, Birchmeier C, Barres BA, Tessier-Lavigne M. (1996) Hepatocyte growth factor/ scatter factor is an axonal chemoattractant and a neurotrophic factor for spinal motoneurons *Neuron* **17**, 1157-1172

Ecchelard Y, Epstein DJ, St-Jaques B, Shen L, Mohler J, McMahon JA, McMahon AP. (1993) Sonic hedgehog, a member of a family of putative signalling molecules, is implicated in the regulation of CNS polarity. *Cell* **75**, 1417-1430

Edgar D, Timpl R, Thoenen H (1984) The heparin-binding domain of laminin is responsible for its effects on neurite outgrowth and neuronal survival. *EMBO J.* **3**, 1463-1468

Eisen JS. (1994) Development of motoneuronal phenotype. *Ann. Rev. Neurosci.* **17**, 1-30

Ericson J, Briscoe J, Rashbass P, van Heyningen V, Jessell TM. (1997) Graded sonic hedgehog signaling and the specification of cell fate in the ventral neural tube. *Cold Spring Harb. Symp. Quant. Biol.* **62**, 451-466

Ericson J, Morton S, Kawakami A, Roelink H, Jessell TM. (1996) Two critical periods of sonic hedgehog signaling required for the specification of motoneuron identity. *Cell* **87**, 661-673

Ericson J, Thor S, Edlund T, Jessell TM, Yamada T. (1992) Early stages of motoneuron differentiation revealed by expression of homeobox gene Islet-1. *Science* **256**, 1555-1560

Ernst M. (1926) Über Untergang von Zellen während der normalen Entwicklung bei Wirbeltieren *Z. Anat. Entwicklungsgesch.* **79**, 228-262

Ferguson BA. (1993) Development of motor innervation of the chick following dorsal-ventral limb bud rotations. *J. Neurosci.* **3**, 1760-1772

Fossom LH, Sterling CR, Tank AW (1992) Regulation of tyrosine hydroxylase gene transcription rate and tyrosine hydroxylase mRNA stability by cyclic AMP and glucocorticoid. *Mol. Pharmacol.* **42**, 898-908

Foster GA (1998) Chemical neuroanatomy of the prenatal rat brain. *Oxford University Press, Oxford, New York, Tokyo*

Fournier-Thibault C, Pourquié O, Rouaud T, LeDouarin NM. (1999) BEN/SC1/DM-GRASP expression during neuromuscular development: a cell adhesion molecule regulated by innervation. *J. Neurosci.* **19**, 1382-1392

Frade JM, Barde YA. (1999) Genetic evidence for cell death mediated by nerve-growth factor and the neurotrophin receptor p75 in the developing mouse retina and spinal cord. *Development* **126**, 683-690

Frade JM, Barde YA. (1998) Nerve growth factor: two receptors, multiple functions, *Bioessays* **20**, 137-145

Fraser S, Keynes R, Lumsden A. (1990) Segmentation in the chick embryo hindbrain is defined by cell lineage restrictions. *Nature* **344**, 431-435

Freyd G, Kim SK, Horvitz HR. (1990) Novel cysteine-rich motif and homeodomain in the product of Caenorhabditis elegans cell lineage gene lin-11. *Nature* **344**, 876-879

Friedman WJ, Greene LA. (1999) Early events in neurotrophin signalling via Trk and p75 receptors. *Curr. Opin. Neurobiol.* **5**, 579-587

Frohman MA, Boyle M, Martin GR. (1990) Isolation of the mouse Hox-2.9 gene; analysis of embryonic expression suggests that positional information along the anterior-posterior axis is specified by mesoderm. *Development* **110**, 589-607

Galvin JE, Uryu K, Lee VM, Trojanowski JQ. (1999) Axon pathology in Parkinson's disease and Lewy body dementia hippocampus contains alpha-, beta, and gamma-synuclein neuropathology. *Proc. Natl. Acad. Sci. USA* **96**, 13450-13455

Galvin JE, Giasson B, Hurtig HI, Lee VM, Trojanowski JQ (2000) Neurodegeneration with brain iron accumulation , type 1 is characterized by alpha-, beta-, and gamma-synuclein neuropathology. *Am. J. Pathol.* **157**, 361-368

Galvin JE, Schuck TM, Lee VM, Trojanowski JQ. (2001) Differential expression and distribution of alpha-, beta-, and gamma-synuclein in the developing human substantia nigra. *Exp. Neurol.* **168**, 347-355

Garces A, Haase G, Airaksinen MS, Livet J, Filippi P, deLapeyriere O. (2000) GFRa1 is required for development of distinct subpopulations of motoneuron. *J. Neurosci.* **20**, 4992-5000

Garel S, Garcia Domiquez M, Charney P (2000) Control of the migratory pathway of facial branchiomotor neurons. *Development* **127**, 5297-5307

Gaudino G, Follenzi A, Naldini L, Collesi C, Santoro M, Gallo KA, Godowski PJ, Comoglio PM. (1994) RON is a heterodimeric tyrosine kinase receptor activated by the HGF homologue MSP. *EMBO* **13**, 3524-3532

Gaunt SJ. (1991) Expression patterns of mouse Hox genes: clues to an understanding of developmental and evolutionary strategies. *Bioessays* **13**, 505-513

Gaunt SJ. (1988) Mouse homeobox gene transcripts occupy different but overlapping domains in embryonic germ layers and organs: a comparison of Hox-3.1 and Hox-1.5. *Development* **103**, 135-144

Gavalas A, Davenne M, Lumsden A, Chambon P, Rijli FM. (1997) Role of Hox-2 in axon pathfinding and rostral hindbrain patterning. *Development* **124**, 3693-3702

Gehring WJ. (1986) On the homeobox and its significance *Bioessays* **5**, 3-4

Gendron-Maguire M, Mallo M, Zhang M, Gridley T. (1993) Hoxa-2 mutant mice exhibit homeotic transformation of skeletal elements derived from cranial neural crest. *Cell* **75**, 1317-1331

George JM, Jin H, Woods WS, Clayton DF. (1995) Characterization of a novel protein regulated during the critical period for song learning in the zebra finch. *Neuron* **15**, 361-372

Gilardi P, Schneider-Manoury S, Charnay P. (1991) Krox-20: a candidate gene for the regulation of pattern formation in the hindbrain. *Biochimie* **73**, 85-91

Gilbert SF. (1997) An introduction to developmental biology, 5th edition; Sinauer Associates, Inc. Publishers, Sunderland Massachusetts

Gilland E, Baker R. (1993) Conservation of neuroepithelial and mesodermal segments in the embryonic vertebrate head. *Acta Anat. Basel* **148**, 110-123

Gilland E, Baker R. (1993) Conservation of neuroepithelial and mesodermal segments in the embryonic vertebrate head. *Acta Anat.* **148**, 110-123

Giroud A, Martinet M. (1959) Teratogenes pur hypervitaminose A chez le rat, la souris, le cobaye, et la lapin. *Arch. Fr. Pediatr.* **16**, 971-980

Goddard JM, Rossel M, Manley NR, Capecchi MR. (1996) Mice with targeted disruption of Hoxb-1 fali to form the motor nucleus of the VIIth nerve. *Development* **122**, 3217-3228

Gomez-Lechon MJ. (1999) Oncostatin M: signal transduction and biological activity. *Life Sciences* **65**, 2019-2030

Gordon-Weeks PR, Giffin N, Weekes CS, Barben C. (1989) Transient expression of laminin immunoreactivity in the developing rat hippocampus. *N Neurocytol.* **18**, 451-463

Gotz R, Koster R, Winkler C, Raulf F, Lottspeich F. (1994) Neurotrophin-6 is a new member of the nerve growth factor family. *Nature* **372**, 266-269

Graham A, Francis-West P, Brickell P, Lumsden A. (1994) The signalling molecule Bmp-4 mediates apoptosis in the rhombencephalic neural crest. *Nature* **372**, 684-686

Graham A, Heyman I, Lumsden A. (1993) Even-numbered rhombomeres control the apoptotic elimination of neural crest cells from odd-numbered rhombomeres in the chick hindbrain. *Development* **119**, 233-245

Graham A, Lumsden A. (1996) Interactions between rhombomeres modulate Krox-20 and follistatin expression in the chick embryo hindbrain. *Development* **122**, 473-480

Graham A, Maden M, Krumlauf R. (1991) The murine Hox-2 genes display dynamic dorsoventral patterns of expression during central nervous system development. *Development* **112**, 255-264

Graham A, Papalopulu N, Krumlauf R. (1989) The murine and *Drosophila* homeobox clusters have common features of organisation and expression. *Cell* **57**, 367-378

Graham A, Paplopulu N, Lorimer J, McVey J, Tuddenham EG, Krumlauf R. (1988) Characterization of a murine homeo box gene, Hox 2.6, related to the *Drosophila* deformed gene. *Genes Dev.* **2**, 1424-1438

Grapin-Botton A, Bonnin MA, Le Douarin MN. (1997) Hox gene induction in the neural tube depends on three parameters: competence, signal supply and paralogue group. *Development* **124** 849-859

Grapin-Botton A, Bonnin MA, McNaughton LA, Krumlauf R. (1995) Plasticity of tranposed rhombomeres: Hox gene induction is correlated with phenotypic modifications. *Development* **121**, 2707-2721

Greene LA, Kaplan DR. (1995) Early events in neurotrophin signalling via Trk and p75 receptors. *Curr. Opin. Neurobiol.* **5**, 579-587

Grewal SS, Horgan AM, York AD, Withers GS, Banker GA, Stork PJ. (2000) Neuronal calcium activates a Rap1 and B-Raf signaling pathway via the cyclic adenosine monophosphate-dependent protein kinase. *J. Biol. Chem.* **275**, 3722-3728

Grunz H, Tacke L. (1989) Neural differentiation of Xenopus laevis ectoderm takes place after disaggregation and delayed reaggregation without inducer. *Cell Diff. Dev.* **28**, 211-217

Gundersen HJG. (1986) Stereology of arbitrary particles. A review of unbiased number and size estimators and the presentation of some new ones, in the memory of William R. Thompson. *J. Microsc.* **143**, 3-45

Guthrie S, Butcher M, Lumsden A. (1991) Patterns of cell division and interkinetic nuclear migration in the chick embryo hindbrain. *J. Neurobiol.* **22**, 742-754

Guthrie S, Lumsden A. (1992) Motoneuron pathfinding following rhombomere reversals in the chick embryo hindbrain. *Development*, **114**, 663-673

Guthrie S, Muchamore I, Kuroiwa A, Marshall H, Krumlauf R, Lumsden A. (1992) Neuroectodermal autonomy of Hox 2.9 expression revealed by rhombomere transpositions. *Nature* **356**, 157-159

Guthrie S, Pini A. (1985) Chemorepulsion of developing motor axons by the floor plate. *Neuron* **14**, 1117-1130

Guthrie S, Prince V, Lumsden A. (1993) Selective dispersal of avian rhombomere cells in orthotopic and heterotopic grafts. *Development* **118**, 527-538

Hamanoue M, Takemoto N, Matsumoto K, Nakamura T, N. (1996) Neurotrophic effect of hepatocyte growth factor on central nervous system neurons *in vitro*. *J. Neurosci. Res.* **43**, 554-564

Hamburger V. (1958) Regression versus peripheral control of differentiation in motor hypoplasia. *Am. J. Anat.* **102**, 365-410

Hamburger V. (1946) Isolation of the brachial segments of the spinal cord of the chick embryo by means of tantalum foil blocks. *J. Exp. Zool.* **103**, 113-142

Hamburger V. (1958) Regression versus peripheral control of differentiation in motor hypoplasia. *Am. J. Anat.* **102**, 365-410

Hamburger V. (1939b) The development and innervation of transplanted limb primordia of chick embryos. *J. Exp. Zool.* **80**, 347-389

Hamburger V, Keefe EL. (1944) The effects of peripheral factors on the proliferation and differentiation in the spinal cord of chick embryos. *J. Exp. Zool.* **96**, 223-242

Hamburger V, Levi-Montalcini R. (1949) Proliferation, differentation and degeneration in the spinal ganglia of the chick embryo under normal and experimental conditions. *J. Exp. Zool.* **111**, 457-502

Hamburger, V (1939a) Motor and sensory hyperplasia following limb-bud transplantation in chick embryos. *Physiol. Zool.* **12**, 268-284

Hanaway J, McConnell JA, Netsky MG. (1971) Histogenesis of the Substantia Nigra, Ventral Tegmental Area of Tsai and Interpeduncular Nucleus: An Autoradiographic Study of the Mesencephalon in the Rat. *J. Comp.Neurol.* **142**, 59-74

Harris AE. (1969) Differentiation and degeneration in the motor horn of foetal mouse. *J. Morphol.* **129**, 281-305

Harrison SMW, Jones ME, Uecker S, Albers KM, Kudrycki KE, Davis BM. (2000) Levels of nerve growth factor and neurotrophin-3 are affected differentially by the presence of p75 in sympathetic neurons *in vivo*. *J. Comp.Neurol.* **424**, 99-110

Hattori T, McGeer PL. (1973) Synaptogenesis in the corpus striatum of infant rat. *Exp. Neurol.* **38**, 70-79

Haug H, Kuhl S, Mecke E, Sass NL, Washer K (1984) The significance of morphometric procedures in the investigation of age changes in cytoarchitectonic structures of human brain. *J. Hirnforsch.* **25**, 353-374

Heaton MB (1977) Retrograde axonal transport in lateral motoneurons of the chick embryo prior to limb bud innervation *Dev. Biol.* **58**, 421-427

Heaton MB, Moody SA.(1980) Early development and migration of the trigeminal motor nucleus in the chick embryo. *J. Comp.Neurol.* **189**, 61-99

Helmbacher F, Schneider-Manoury S, Topilko P, Tiret L, Charnay P. Targeting of the EphA4 tyrosine kinase receptor affects dorsal/ventral pathfinding of limb motor axons. *Development* **127**, 3313-3324

Henderson CE. (1996) Role of neurotrophic factors in neuronal development *Curr. Opin. Neurobiol.* **6**, 64-70

Henderson CE, Bloch-Gallego E, Camu E. (1995) Purified embryonic motoneurons. In Cohen J, Wilkin G (eds.) *Nerve Cell Culture: a practical approach.* Oxford university Press, London, 69-81

Henderson CE, Camu W, Mettling C, Gouin A, Poulsen. (1993) Neurotrophins promote motoneuron survival and are present in embryonic limb bud. *Nature* **363**, 266-270

Henderson CE, Phillips HS, Pollock RA, Davies AM Lemeulle C, Armanini M, Moffet B, Vandlen RA, Simmons L. (1994) GDNF: a potent survival factor for motoneurons present in peripheral nerve and muscle. *Science* **266**, 1062-1064

Henderson CE, Yamamoto Y, Livet J, Arce V, Garces A. (1998) Role of neurotrophic factors in motoneuron development. *J. Physiology (Paris)* **92**, 279-281

Heym C, Forssmann WG. (1981) Techniques in Neuroanatomical Research, Springer, Berlin-Heidelberg

Heyman I, Kent A, Lumsden. (1993) Cellular morphology and extracellular space at rhombomere boundaries in the chick embryo hindbrain. *Dev. Dyn.* **198**, 241-253

Hinds JW. (1968) Autoradiographic study of histogenesis in the mouse olfactory bulb. I. Time of origin of neurons and neuroglia *J. Comp.Neurol.* **134**, 287-304

Hogan BLM, Thaller C, Eichele G. (1992) Evidence that Henson's node is a site of retinoic acid synthesis. *Nature* **359**, 237-241

Holland P, Hogan B. (1988) Expression of homeobox genes during mouse development: a review. *Genes Dev.* **2**, 773-782

Hollyday M, Jacobson RD. (1990) Location of motor pools innervating chick wing. *J. Comp.Neurol.* **302**, 575-588

Honda S, Kagoshima M, Wanaka A, Tohyama M, Matsumoto K, Nakamura T. (1995) Localization and functional coupling of HGF and c-Met/HGF receptor in rat brain: implication as neurotrophic factor. *Mol. Brain Res.* **32**, 197-210

Howard CV, Reed MG (1998) Unbiased Stereology. Three-dimensional measurement in microscopy. *βios Scientific Publishers*

Huang EJ, Reichardt LF. (2001) Neurotrophins: Roles in neuronal development and function. *Ann. Rev. Neurosci.* **24**, 677-736

Huff JL, Jelinek MA, Borgman CA, Lansing TJ, Parsons JT. (1993) The protooncogene c-sea encodes a transmembrane protein-tyrosine kinase related to the MET/hepatocyte growth factor/scatter factor receptor. *Proc. Natl. Acad. Sci. USA* **90**, 6140-6144

Hughes A. (1961) Cell degeneration in the larval ventral horn of Xenopus laevis. *J Embryol. Exp. Morph.* **9**, 269-284

Hughes RA, Sendtner M, Thoenen H. (1993) Members of several gene families influence survival of rat motoneurons *in vitro* and *in vivo*. *J. Neurosci. Res.* **36**, 663-671

Hughes WF, McLoon SC. (1979) Ganglion cell death during normal retinal development in the chick: Comparisons with cell death induced by early target field destruction. *Exp. Neurol.* **66**, 587-601

Hunt P, Gulisano M, Cook M, Sham M, Faiella A, Wilkinson D, Boncinelli E, Krumlauf R. (1991a) A distinct Hox code for the branchial region of the head. *Nature* **353**, 861-864

Hunt P, Wilkinson D, Krumlauf R. (1991b) Patterning the vertebrate head: murine Hox 2 genes mark distinct subpopulations of premigratory and migrating neural crest. *Development* **112**, 43-51

Hynes M, Porter JA, Chiang C, Chang D, Tessier-Lavigne M, Beachy PA, Rosenthal A. (1995b) Induction of midbrain dopaminergic neurons by sonic hedgehog. *Neuron* **15**, 35-44

Hynes M, Poulsen K, Tessier-Lavigne M, Rosenthal A. (1995a) A control of neuronal diversity by the floor plate: contact-mediated induction of midbrain dopaminergic neurons. *Cell* **80**, 95-101

Hyppa M. (1969) A histochemical study of the primate catecholamines in the hypothalamic neurons of the rat in relation to ontogenetic and sexual differentiation. *Z. Zellforschung* **98**, 550-560

Irmler M, Thome M, Hahne M, Schnieder P, Hofmann K. (1997) Inhibition of death receptor signals by cellular FLIP. *Nature* **388**, 190-195

Iseki E, Odawara T, Li F, Kosaka K, Nishimura T, Akiyama H, Ikeda K. (1996) Age-related ubiquitin-positive granular structures in non-demented subjects and neurodegenerative disorders. *J Neurol Sci* **142**, 25-29

Itasaki N, Sharpe J, Morrison A, Krumlauf R. (1996) Reprogramming Hox expression in the vertebrate hindbrain: influence of paraxial mesoderm and rhombomere transposition. *Neuron.* **16**, 487-500

Iwai A, Masliah E, Yoshimoto M, Ge N, Flanagan L, de Siva HA, Kittel A, Saitoh T. (1995) The precursor protein of non-A beta component of Alzheimer's disease amyloid is a presynaptic protein of the central nervous system. *Neuron* **14**, 467-475

Iwama A, Yamaguchi N, Suda T. (1996) STK/ RON receptor tyrosine kinase mediates both apoptotic and growth signals via the multifunctional docking site conserved among the HGF receptor family. *EMBO* **15**, 5866-5875

Jackson-Lewis V, Vila M, Djaldetti R, Guegan C, Liberatore G, Liu J, O'Malley KL, Burke RE, Przedborski S. (2000) Developmental Cell Death in Dopaminergic Neurons of the Substantia Nigra of Mice. *J. Comp.Neurol.* **424**, 476-488

Jacob J, Guthrie S. (2000) Facial visceral motoneurons display specific rhombomere origin and axon pathfinding behavior in the chick. *J. Neurosci.* 20, 7664-7671

Jacob J, Tiveron M-C, Brunet J-F, Guthrie S. (2000) Role of the target in the pathfinding of facial visceral motor axons. *Mol. Cell. Neurosci.* **16**, 14-26

Jakes R, Spillantini MG, Goedert M. (1994) Identification of two distinct synucleins from human brain. *FEBS Lett.* **345**, 27-32

Janec E, Burke RE. (1993) Naturally-occurring cell death during postnatal development of the substantia nigra of the rat. *Mol. Cell. Neurosci.* **4**, 30-35

Ji H, Liu YE, Jia T, Wang M, Liu JW, Xiao G, Joseph BK, Rosen C, Shi YE. (1997) Identification of a breast cancer-specific gene, BCSG1, by direct differential cDNA sequencing. *Cancer Res.* **57**, 759-764

Jia T, Liu J, Shi YE. (1999) Stimulation of breast cancer invasion and metastasis by synuclein gamma. *Cancer Res.* **59**, 742-747

Jones RL. (1937) Split nuclei as a source of error in nerve cell counts. *Stain. Tech.* **13**, 91-95

Joseph LJ, Le Beau MM, Jamieson GA, Acharya S, Shows TB, Rowley JD, Sukhatme VP. (1988) Molecular cloning, sequencing, and mapping of EGR2, a human early growth response gene encoding a protein with zinc-binding finger structure. *Proc. Natl. Acad. Sci. USA* **85**, 7164-7168

Joyner A. (1996) Engrailed, Wnt and Pax genes regulate midbrain-hindbrain development. *TIGS* **12**, 15-20

Jungbluth S, Koentges G, Lumsden A. (1997) Coordination od early neural tube development by BDNF/trkB *Development* **124,** 1877-1885

Jurgensmeier JM, Xie Z, Deveraux Q, Ellerby L, Bredesen D, Reed JC. (1998) Bax directly induces release of cytochrome c from isolated mitochondria. *Proc. Natl. Acad. Sci. USA* **95**, 4997-5002

Källén B. (1962) Mitotic patterning in the central nervous system of chick embryos; studied by a colchicine method. *Z. Anat. Entwicklungsgeschichte* **123**, 309-319

Kania A, Johnson RL, Jessell TM. (2000) Coordinate roles for Lim homeobox genes in directing the dorsoventral trajectory of motor axons in the vertebrate limb. *Cell* **102**, 161-173

Karlsson O, Thor S, Norbert T, Ohlsson H, Edlund T. (1990) Insulin gene enhancer binding protein Isl-1 is a member ofa novel class of proteins containing both a homeo and a Cys-His domain. *Nature* **344**, 879-882

Kaufman MH (1992) The atlas of mouse development. *Academic Press*

Kennedy TE, Serafini T, de la Torre JR, Tessier-Lavigne M. (1994) Netrins are diffusible chemotropic factors for commissural axons in the embryonic spinal cord. *Cell* **78**, 425-435

Kerr JF, Searle J, Harmon BV, Bishop CJ. (1987) Apoptosis. Perspectives on Mammalian Cell Death. 93-128

Kerr JFR, Wyllie AH, Currie AR. (1972) Apoptosis: a basic biological phenomenon with wide-ranging implications in tissue kinetics. *Br. J. Cancer* **26**, 239-257

Kerr JFR, Harmon B, Searle J. (1974) An electron-microscope study of cell deletion in the anuran tadpole tail during sponataneous metamorphosis with special reference to apoptosis of striated muscle fibers. *J. Cell. Biol.* **14**, 571-585

Kessel M, Gruss P. (1991) Homeotic transformations of murine vertebrae and concomitant alteration of Hox codes induced by retinoic acid. *Cell* **67**, 89-104

Kim CN, Wang X, Huang Y, Ibrado AM, Liu L. (1997) Overexpression of Bcl-X(L) inhibits Ara-C induced mitochondrial loss of cytochrome c and other perturbations that activate the molecular cascade of apoptosis. *Cancer Res.* **57**, 3115-3120

Klein RD, Sherman D, Ho WH, Stone D, Bennett GL, M. (1997) A GPI-linked protein that interacts with Ret to form a candidate neurturin receptor. *Nature* **387**, 467-470

Kluck RM, Bossy-Wetzel E, Green DR, Newmeyer DD. (1997) The release of cytochrome c from mitochondria: a primary site for Bcl-2 regulation of apoptosis. *Science* **275**, 1132-1136

Kochhar DM, Penner JD, Tellone CI. (1984) Comparative teratogenic activities of two retinoids: Effects on palate and limb development. *Teratogen. Carcinogen. Mutagen.* **4**, 377-387

Köntges G, Lumsden A. (1996) Rhombencephalic neural crest segmentation is preserved throughout craniofacial ontogeny. *Development* **122**, 3229-3242

Krumlauf R, Marshall H, Studer M, Nonchev S, Sham. (1993) Hox homeobox genes and regionalisation of the nervous system. *J. Neurobiol.* **24**, 1328-1340

Kuhar MJ, Atweh SF. (1978) Distribution of some suspected neurotransmitters in the central nervous system. *Revues of Neuroscience* **3**, 35-76

Kuratani SC, Tanaka S, Ishikawa Y, Zukeran C (1988) Early development of the hypoglossal nerve in the chick embryo as observed by the whole-mount nerve staining method. *Am. J. Anat.* **182,** 155-168

Kuratani SC, Miyagawa-Tomita S, Kirby ML (1991) Development of cranial nerves in the chick embryo with spatial reference to the alterations of cardiac branches after ablation of the cardiac neural crest. *Anat. Embryol.* **183**, 501-514

Kuratani SC, Eichele G. (1993) Rhombomere transplantation repatterns the segmental organization of cranial nerves and reveals cell-autonomous expression of a homeodomain protein. *Development* **117**, 105-117

Kurihara N, Tatsumi J, Arai F, Iwama A, Suda T. (1998) Macrophage-stimulating protein (MSP) and its receptor, RON, stimulate human osteoclast activity but not proliferation: effect of MSP distinct from that of hepatocyte growth factor. *Exp. Hematol.* **26**, 1080-1085

Kuwana T, Smith JJ, Muzio M, Dixit V, Newmeyer DD, Kornbluth S. (1998) Apoptosis induction by caspase-8 is amplified through the mitochondrial release of cytochrome c. *J. Biol. Chem.* **273**, 16589-16594

Lamb TM, Harland RM. (1995) Fibroblast growth factor is a direct neural inducer, which combined with noggin generates anterior-posterior neural pattern. *Development* **121**, 713-718

Lamb TM, Knecht AK, Smith WC, Stachel SE, Economides AN, Stahl N, Yancopolous GD, Harland RM. (1993) Neural induction by the secreted polypeptide noggin. *Science* **262**, 713-718

Lammer EJ, Chen DT, Hoar RM, Agnish ND, Benke PJ, Braun JT, Curry CJ, Fernhoff PM, Grix AW, Lott IT. (1985) Retinoic acid embryopathy. *N. Engl. J. Med.* **313**, 837-841

Lance-Jones C. (1982) Motoneuron cell death in the developing lumbar spinal cord of the mouse, *Brain Res.*, **256**, 473-479

Lance-Jones C, Landmesser L (1980b) Motoneurone projection patterns in the chick limb following early partial reversals of the spinal cord. *J. Physiol.* **302**, 581-602

Lance-Jones C, Landmesser L. (1981b) Pathway selection by embryonic chick motoneurons in an experimentally altered environment. *Proc. R. Soc. Lond.* **214**, 19-52

Lance-Jones C, Landmesser L. (1980a) Motoneurone projection patterns in the embryonic chick limbs follow partial deletions of the spinal cord. *J. Physiol.* **302**, 559-580

Lance-Jones C, Landmesser L. (1981a) Pathway selection by chick lumbosacral motoneurons during normal development. *Proc. R. Soc. Lond.* **214**, 1-18

Landmesser L. (1992) Growth cone guidance in the avian limb: a search for cellular and molecular mechanisms. *The Nerve Growth Cone*, ed. Letourneau PC, Kater JB, Macagno ER, Raven Press New York, 373-85

Landmesser L, Pilar G. (1976) Fate of ganglionic synapses and ganglion cell axons during normal and induced cell death. *J. Cell. Biol.* **68**, 357-374

Langman J. (1969) Medical Embryology, Williams & Williams, Baltimore

Langston AW, Gudas LJ. (1992) Identification of a retinoic acid responsive enhancer 3' of the murine homeobox gene Hox-1.6. *Mech. Development* **38**, 217-227

Larmet Y, Dolphin AC, Davies AM. (1992) Intracellular calcium regulates the survival of early sensory neurons before they become dependent on neurotrophic factors. *Neuron* **9**, 563-574

Larramendi LM. (1969) Analysis of synaptogenesis in the cerebellum of the mouse, Neurobiology of Cerebellar Evolution and Development, 803-843

Lauder J, Bloom F. (1974) Ontogeny of monoamine neurons in the locus coeruleus, raphe nuclei, and substantia nigra of the rat. I. Cell differentiation. *J. Comp.Neurol.* **155**, 469-482

Lauder JM, Bloom FE. (1974) Ontogeny of Monoamine Neurons in the Locus Ceruleus, Raphe Nuclei and Substantia Nigra of the Rat. *J. Comp.Neurol.* **155**, 469-482

Le Douarin NM. (1993) Embryonic neural chimaeras in the study of brain development. *TINS* **16**, 64-72

Lee J, Platt KA, Censullo P, Ruiz I Altaba A. (1997) Gli1 is a target of sonic hedgehog that induces ventral neural tube development. *Development* **124**, 2537-2552

Lee KF, Bachman K, Lamdis S, Jaenisch R. (1994a) Dependence on p75 for innervation of some sympathetic targets. *Science* **263**, 1447-1449

Lee KF, Davies AM, Jaenisch R. (1994b) p75-deficient embryonic dorsal root sensory and neonatal sympathetic neurons display a decreased sensitivity to NGF. *Development* **120**, 1027-1033

Lee MK, Cleveland DW (1996) Neuronal intermediate filaments. *Annu. Rev. Neurosci.* **19**, 187-217

Leid M, Kastner P, Chambon P. (1992) Multiplicity generates diversity in the retinoic signalling pathways. *Trends Biochem. Sci.* **17**, 427-433

Leonard EJ, Skeel A. (1976) A serum protein that stimulates macrophage movement, chemotaxis and spreading. *Exp. Cell Res.* **102**, 434-438

Levi-Montalcini R. (1952) Effects of mouse tumor transplantation on the nervous system. *Ann. NY Acad. Sci.* **55**, 330-343

Levi-Montalcini R. (1949) The development of the acoustico-vestibular centers in the chick embryo in the absence of the afferent root fibers and of descending tracts. *J. Comp.Neurol.* **91**, 209-242

Levi-Montalcini R. (1975) NGF: An unchartered route. In *Neurosciences: Paths of Discovery,* Worden FG, Swazey JP, Adelman G (eds.), Chapman and Hall, London, 245-65

Levi-Montalcini R. (1947) Regressione secondaria del ganglio ciliare dopo aspotazione della resicola mesencefalica in embrione di pollo. *R. Acad. Naz. Linncie* **3**, 144-146

Levi-Montalcini R. (1945) Correlations dans le développement des différentes parties du systéme nervaux. II. Correlations entre le développement de l'encephale et celui de la moelle épinière dans l'embryon de poulet. *Arch. Biol.* **56**, 71-93

Levi-Montalcini R. (1950) The origin and development of the visceral system in the spinal cord of the chick embryo. *J Morphol.* **86**, 253-284

Levi-Montalcini R, Hamburger V. (1951) Selective growth stimulating effects of mouse sarcoma on the sensory and sympathetic nervous system of the chick embryo. *J. Exp. Zool.* **116**, 321-361

Levine MS, Harding KW. (1989) *Drosophila*: the zygotic contribution. *Genes and Embryos,* ed. Glover M, Hames BD, IRL New York, 39-94

Lewin GR, Barde YA. (1996) Physiology of the neurotrophins. *Ann. Rev. Neurosci.* **19**, 289-317

Lewis E. (1978) A gene complex controlling segmentation in *Drosophila*. *Nature*, **276**, 565-570

Li H, Zhu H, Xu CJ, Yuan J. (1998) Cleavage of BID by caspase 8 mediates the mitochondrial damage in the Fas pathway of apoptosis. *Cell* **94**, 491-501

Li JY, Henning Jensen P, Dahlstrom A (2002) Differential localization of alpha-, beta- and gamma-synucleins in the rat CNS. *Neuroscience* **113**, 463-478

Li P, Nijhawan D, Budihardjo I, Srinivasula SM, Ahmad M, Alnemri ES, Wang X. (1997) Cytochrome c and dATP-dependent formation of Apaf-1/caspase-9 complex initiates an apoptotic protease cascade. *Cell* **91**, 479-489

Lieb K, Anderson C, Lazarov N, Zienecker R, Urban I, Reisert I, Pilgrim C. (1996) Pre-and postnatal development of dopaminergic neuron numbers in the male and female mouse midbrain. *Brain Res. Dev. Brain Res.* **94**, 37-43

Liem Jr. KF, Tremml G, Roelink H, Jessell TM. (1995) Dorsal differentiation of neural plate cells induced by BMP-mediated signals from epidermal ectoderm. *Cell* **82**, 969-979

Liu X, Li P, Widlak P, Zou H, Luo X, Garrard WT, Wang X. (1998) The 40-kDa subunit of DNA fragmentation factor induces DNA fragmentation and chromatin condensation during apoptosis. *Proc. Natl. Acad. Sci. USA* **95**, 8461-8466

Liu X, Zou H, Slaughter C, Wang X. (1997) DFF, a heterodimeric protein that functions downstream of caspase-3 to trigger DNA fragmentation during apoptosis. *Cell* **89**, 175-184

Liu X, Zou H, Widlak P, Garrad W, Wang X. (1999) Activation of the apoptotic endonuclease DFF40 (CAD/CPAN): oligomerization and direct interaction with histone H1. *J. Biol. Chem.* **274**, 13836-13840

Löfberg J, Nynas-McCoy A, Olsson C, Jönsson L, Perris R. (1985) Stimulation of initial neural crest cell migration in the axolotl embryo by tissue grafts and extracellular matrix transplanted on microcarriers. *Dev. Biol.* **107**, 442-459

Loizou LA. (1971) The postnatal development of monoamine-containing structures in the hypothalamo-hypophyseal system of the albino rat. *Z. Zellforschung* **114**, 234-252

Lumsden A. (1995) A 'LIM code' for motoneurons? *Curr. Biol.* **5**, 491-495

Lumsden A. (1990) The cellular basis of segmentation in the developing hindbrain. *TINS* **13**, 329-335

Lumsden A, Krumlauf R. (1996) Patterning the vertebrate neuraxis. *Science* **274**, 1109-1292

Lumsden A, Keynes R. (1989) Segmental patterns of neuronal development in the chick hindbrain. *Nature* **337**, 424-428

Lumsden A, Sprawson N, Graham A. (1991) Segmental origin and migration of neural creast cells in the hindbrain region of the chick embryo. *Development* **113**, 1281-1291

Mahadeo D, Kaplan L, Chao MV, Hempstead BL. (1994) High affinity nerve growth factor binding displays a faster rate of association than p140Trk binding. Implications for multi-subunit polypeptide receptors. *J. Biol. Chem.* **269**, 6884-6891

Maina F, Casagranda F, Audero E, Simeone A, Comoglio PM, Klein R, Ponzetto C. (1996) Uncoupling of Grb2 from the Met receptor *in vivo* reveals complex roles in muscle development *Cell* **87**, 531-542

Maina F, Hilton MC, Andres R, Wyatt S, Klein R, Davies AM. (1998) Multiple roles for hepatocyte growth factor in sympathetic neuron development. *Neuron* **20**, 835-846

Maina F, Hilton MC, Ponzetto C, Davies AM, Klein R. (1997) Met receptor signalling is required for sensory nerve development. *Genes Dev.* **11**, 3341-3350

Malicki J, Schugart K, McGinnis W. (1990) Mouse Hox-2.2 specifies thoracic segmental identity in Drospophila embryos and larvae. *Cell* **63**, 961-967

Marchand R, Poirier LJ. (1983) Isthmic Origin of Neurons of the Rat Substantia Nigra. *Neurosci.* **9**, 373-381

Marigo V, Davey RA, Zuo Y, Cunningham JM, Tabin CJ. (1996) Biochemical evidence that patched is the hedgehog receptor. *Nature* **384,** 176-179

Marin F, Puelles L. (1994) Patterning of the embryonic avian midbrain after experimental inversions: a polarizing activity from the isthmus. *Dev. Biol.* **163**, 19-37

Marín F, Puelles L. (1995) Morphological fate of rhombomeres in quail/chick chimeras: a segmental analysis oh hindbrain nuclei. *Eur. J. Neurosci.* **7**, 1714-1738

Maroteaux L, Campanelli JT, Scheller RH. (1988) Synuclein: a neuron-specific protein localized to the nucleus and presynaptic nerve terminal. *J. Neurosci.* **8**, 2804-2814

Marshall H, Nonchev S, Sham MH, Muchamore I, Lumsden A, Krumlauf R. (1992) Retinoic acid alters Hox code and induces transformation of rhombomeres 2/3 into a 4/5 identity. *Nature* **360**, 737-741

Marshall H, Studer M, Pöpperl H, Aparicio S, Kuroiwa A, Brenner S, Krumlauf R. (1994) A conserved retinoic acid response element required for early expression of the homeobox gene Hoxb-1. *Nature* **18**, 567-571

Martinez S, Marin F, Nieto MA, Puelles L. (1995) Induction of ectopic engrailed expression and fate change in avian rhombomeres: intersegmental boundaries as barriers. *Mech. Development* **51**, 289-303

May RM. (1933) Reactions neurogenique de la moelle à la greffe en surnombre, ou à l'ablation d'une ébauche de patte posterieure chez l'embryon de l'anoure, Disglossus pictus. *Bull. Biol.* **67**, 327-349

Mayr R. (1985) Makroskopische Anatomie des unteren Hirnstammes. Benninghoff Anatomie 3, Urban & Schwarzenberg, München-Wien-Baltimore, 130

Mayeux R, Chen J, Mirabello E, Marder K, Bell K, Dooneief G, Cote L, Stern Y. (1990) An estimate of the incidence of dementia in idiopathic Parkinson's disease. *Neurology* **40**, 1513-1517

McGinnis W, Krumlauf R. (1992) Homeobox genes and axial patterning. *Cell* **68**, 283-302

McMahon AP, Joyner AL, Bradley A, McMahon JA. (1992) The midbrain-hindbrain phenotype of Wnt-1⁻/Wnt-1⁻ mice results from stepwise deletion of engrailed-expressing cells by 9.5 days postcoitum. *Cell* **69**, 581-595

Meredith GE. Comparative view of the central organization of the afferent and efferent circuitry for the inner ear. *Acta Biol. Hung.* **39**, 229-249

Meyer-Franke A, Kaplan MR, Pfrieger FW, Barres BA. (1995) Characterization of the signaling interactions that promote the survival and growth of developing retinal ganglion cells in culture. *Neuron* **15**, 805-819

Meyer-Franke A, Wilkinson GA, Kruttgen A, Hu M, Munro E, Hanson MG, Reichardt LF, Barres BA. (1998) Depolarization and cAMP elevation rapidly recruit TrkB to the plasma membrane of CNS neurons. *Neuron* **21**, 681-693

Millen KJ, Wurst W, Herrup K, Joyner A. (1994) Abnormal embryonic cerebellar development and patterning of postnatal foliation in two mouse Engrailed-2 mutants. *Development* **120**, 695-706

Møller A, Strange P, Gunderson HJG (1990) Efficient estimation of cell voume and number using the nucleator and dissector. *J. Microsc.* **159**, 61-71

Moody SA, Heaton MB. (1983a) Developmental relationships between trigeminal ganglia and trigeminal motoneurons in chick embryos. I. Ganglion development is necessary for motoneuron migration. *J. Comp.Neurol.* **213**, 327-343

Moody SA, Heaton MB. (1983b) Developmental relationships between trigeminal ganglia and trigeminal motoneurons in chick embryos. II. Ganglion axon ingrowth guides motoneuron migration. *J. Comp.Neurol.* **213**, 344-349

Moody SA, Heaton MB. (1983) Developmental relationships between trigeminal motoneurons in chick embryos. III. Ganglion perikarya direct motor axon outgrowth in the periphery. *J. Comp.Neurol.* **213**, 350-364

Mori C, Nakamura N, Kimura S, Irie H, Takigawa T. (1995) Programmed cell death in the interdigital tissue of the fetal mouse limb is apoptosis with DNA fragmentation. *Anat. Rec.* **242**, 103-110

Morin X, Cremer H, Hirsch MR, Kapur RP, Goridis C, Brunet JF. (1997) Defects in sensory and autonomic ganglia and absnce of locus coeruleus in mice deficient for the homeobox gene Phoxa. *Neuron* **18**, 411-423

Murone M, Rosenthal A, de Sauvage FJ. (1999) Sonic hedgehog signalling by the patched-smoothened receptor complex. *Curr. Biol.* **9**, 76-84

Murphy P, Davidson D, Hill R. (1989) Segment-specific expression of a homeobox-containing gene in the mouse hindbrain *Nature* **341**, 156-159

Murphy P, Hill RE. (1991) Expression of the mouse labial-like homeobox-containing genes, Hox 2.9 and Hox 1.6, during segmentation of the hindbrain. *Development* **111**, 61-74

Muzio M, Chinnaiyan AM, Kischkel FC, O'Rourke K, Shevchenko A, Ni J, Scaffidi C, Bretz JD, Zhang M, Gentz R, Mann M, Krammer PH, Peter ME, Dixit VM.. (1996) FLICE, a novel FADD-homologous ICE/CED-3-like protease, is recruited to the CD95 (Fas/APO-1) death-inducing signaling complex. *Cell* **85**, 817-827

Naeem A, Abbas L, Guthrie S (2002) Comparison of the effects of HGF, BDNF, CT-1, CNTF, and the branchial arches on the growth of embryonic cranial motor neurons. *J. Neurobiol.* **51**, 101-114

Nagata S. (1997) Apoptosis by death factor. *Cell* **88**, 355-365

Nakajo S, Tsukada K, Omata K, Nakamura Y, Nakaya K. (1993) A new brain-specific 14-kDa protein is a phosphoprotein. Its complete amino acid sequence and evidence for phosphorylation. *Eur. J. Biochem.* **217**, 1057-1063

Nakajo SJ, Omata T, Aiuchi T, Shibayama I, Okahashi H, Ochiai Y, Nakai K, Nakaya K, Nakamura Y. (1990) Purification and characterization of a novel brain-specific 14-kDa protein. *J. Neurochem.* **55**, 2031-2038

Nakamura T, Nishizawa T, Hagiya M, Seki T, Shimoni. (1989) Molecular cloning and expression of human hepatocyte growth factor. *Nature* **342**, 440-443

Nakamura T, Sanokawa R, Sasaki Y, Ayusawa D, Oishi. (1996) N-Shc: a neural-specific adapter molecule that mediates signaling from neurotrophin/Trk to Ras/Mapk pathway. *Oncogene* **13**, 1111-1121

Naldini L, Weidner KM, Vigna E, Gaudino G, Bardell. (1991) Scatter factor and hepatocyte growth factor are indistinguishable ligands for the met receptor. *EMBO* **10**, 10, 2867-2878

Narhi L, Wood SJ, Steavonson S, Jiang Y, Wu GM, Anafi D, Kaufman SA, Martin F, Sitney K, Denis P, Loious JC, Wypech J, Biere AL, Citron M. (1999) Both familial Parkinson's mutations accelerate alpha-synuclein aggregation. *J. Biol. Chem.* **274**, 9843-9846

Neff NT, Prevette D, Houenou LJ, Lewis ME, Glicksman MA, Yin QW, Oppenheim RW. (1993) Insulin-like growth factors: putative muscle-derived trophic agents that promote motoneuron survival. *J. Neurobiol.* **24**, 1578-1588

Nicholson DW, Thornberry NA. (1997) Caspases: killer proteases. *Trends Biochem. Sci.* **22**, 299-306

Nieuwkoop PD, Boterenbrood EC, Kremer A, Blousma FFSN, Hoessels ELMJ, Meyer G, ver Heyen FJ. (1952) Activartion and organisation of the central nervous system in amphibians *J. Exp. Zoology* **120**, 83-108

Nilsson AS, Fainzilber M, Falck P, Ibanez CF. (1998) Neurotrophin-7: a novel member of the neurotrophin family from the zebrafish. *FEBS Lett.* **424**, 285-290

Ninkina NN, Alimova-Kost MV, Paterson JW, Delaney L, Cohen BB, Imreh S, Gnuchev NV, Davies AM, Buchman VL. (1998) Organization, expression and polymorphism of the human persyn. *Hum. Mol. Genet.* **7**, 1417-1424

Noden DM. (1983) Morphogenetic movements of avian cephalic and cervical muscles and associated connective tissues. *Am. J. Anat.* **168**, 257-276

Nonchev S, Vesque C, Maconochie M, Seitanidou T, Ariza McNaughton L, Frain M, Marshall H, Sham MH, Krumlauf R, Charnay P. (1996) Segmental expression of Hoxa-2 in the hindbrain is directly regulated by Krox-20. *Development* **122**, 543-554

Novak KD, Prevette D, Wang S, Gould TW, Oppnheim R. (2000) Hepatocyte growth factor/ scatter factor is a neurotrophic survival factor for lumbar but not for other somatic motoneuons in the chick embryo. *J. Neurosci.* **20**, 326-337

O'Connor TM, Wyttenbach CR. (1974) Cell death of the embryonic chick spinal cord. *J. Cell. Biol.* **60**, 448-459

Ogura T, Evans RM. (1995) A retinoic acid-triggered cascade of Hoxb-1 gene activation. *Proc. Natl. Acad. Sci. USA* **92**, 387-391

Ogura T, Evans RM. (1995) Evidence for two distinct retinoic acid response pathways for Hoxb-1 gene regulation. *Proc. Natl. Acad. Sci. USA* **92**, 392-396

Okamura H, Kitahama K, Nagatsu I, Geffard M (1988) Comparative topopgraphy of dopamine- and tyrosine hydroxylase-immunoreactibve neurons in the rat arcuate nucleus. *Neurosci. Lett.* **95**, 347-353

Okura Y, Arimoto H, Tanuma N, Matsumoto K, Nakamur. (1999) Analysis of neurotrophic effects of hepatocyte growth factor in the adult hypoglossal nerve axotomy model. *Eur. J. Neurosci.* **11**, 4139-4144

Olson L, Seiger A. (1972) Early prenatal ontogeny of central monoamine neurons in the rat: Fluorescence histochemical observations. *Z. Anat. Entwicklungsgesch.* **137**, 301-316

Oppenheim RW. (1991) Cell death during development of the nervous system. *Annu. Rev. Neurosci.* **14**, 453-501

Oppenheim RW. (1996) Neurotrophic survival molecules for motoneurons: an embarrassment of riches. *Neuron* **17**, 195-197

Oppenheim RW, Cole T, Prevette D. (1989) Early regional variations in motoneuron numbers arise by differential proliferation in the chick embryo spinal cord. *Dev. Biol.* **133**, 468-474

Oppenheim RW, Houenou LJ, Johnson JE, Lin LF, Li L. (1995) Developing motoneurons rescued from programmed and axotomy-induced cell death by GDNF. *Nature* **373**, 344-346

Oppenheim RW, Houenou LJ, Parsadanian AS, Prevette D, Snider WD, Shen L. (2000) Glial Cell Line-derived neurotrophic factor and developing mammalian motoneurons: regulation of programmed cell death among motoneuron subtypes. *J. Neurosci.* **20**, 5001-5011

Parks TN. (1979) Afferent influences on the development of the brain stem auditory nuclei of the chicken: Otocyst ablation. *J. Comp.Neurol.* **183**, 665-678

Pattyn A, Morin X, Cremer H, Goridis C, Brunet JF. (1997) Expression and interactions of the two closely related homeobox genes Phox2a and Phox2b during neurogenesis. *Development* **124**, 4064-4075

Pawson T, Nash P. (2000) Protein-protein interactions define specificity in signal transduction. *Genes Dev.* **14**, 1027-1047

Paxinos G, Franklin KBJ (2001) The mouse brain in stereotaxic coordinates. *Academic Press*

Pfaff SL, Mendelsohn M, Stewart CL, Edlund T, Jessell TM. (1996) Requirement for LIM homeobox gene Isl-1 in motoneuron generation reveals a motoneuron-dependent step in interneuron differentiation. *Cell* **84**, 309-320

Piccolo S, Sasai Y, Lu B, De Robertis EM. (1996) Dorsoventral patterning in Xenopus: inhibition of ventral signals by direct binding of chordin to BMP-4. *Cell* **86**, 589-598

Plazcek M, Tessier-Lavigne M, Jessell TM, Dodd J. (1990) Orientation of commissural axons *in vitro* in response to a floor plate-derived chemoattractant. *Development* **110**, 19-30

Porter JA, Young KE, Beachy PA. (1996) Cholesterol modification of hedgehog signaling proteins in animal development. *Science* **274**, 255-259

Pöpperl H, Featherstone RM. (1993) Identification of a retinoic acid response element upstream of the murine Hox-4.2 gene. *Mol. Cell. Biol.*, **13**, 257-265

Pourquié O, Coltey M, Thomas J-L, Le Douarin NM. (1990) A widely distributed antigen developmentally regulated in the nervous system. *Development* **10,** 743-752

Pourquié O, Hallonet MER, Le Douarin NM. (1992) Association of BEN glykoprotein expression with climbing fiber axogenesis in the avian cerebellum. *J. Neurosci.* **12**, 1548-1557

Prestige MC. (1967) The control of cell number in the lumbar ventral horn during the development of Xenopus laevis tadpoles. *J Embryol. Exp. Morph.* **18**, 359-387

Prestige MC, Wilson MA. (1972) Loss of axons from ventral roots during development. *Brain Res.* **41**, 467-470

Prince V, Lumsden A. (1994) Hoxa-2 expression in normal ad transposed rhombomeres: independent regulation in the neural tube and neural crest. *Development* **120**, 911-923

Putten H van der, Wiederhold KH, Probst A, Barbieri S, Mistl C, Danner S, Kauffmann S, Hofele K, Spooren WPJM, Ruegg MA, Lin S, Caroni P, Sommer B, Tolnay M, Bilbe G. (2000) Neuropathology in mice expressing human alpha-synuclein. *J. Neurosci.* **20**, 6021-6029

Quantin B, Schuhbaur B, Gesnel MC, Doll'e P, Breathnach R. (1995) Restricted expression of the ron gene encoding the macrophage stimulating protein receptor during mouse develoment. *Dev. Dyn.* **204**, 383-390

Rabizadeh S, Gralla EB, Borchelt DR, Gwinn R, Valentine JS, Sisodia S, Wong P, Lee M, Hahn H, Bredesen DE. (1995) Mutations associated with amyotrophic lateral sclerosis convert superoxide dismutase from an antiapoptotic gene to a proapoptotic gene: studies in yeast and neural cells. *Proc. Natl. Acad. Sci. USA* **92**, 3024-3028

Raoul C, Henderson CE, Pettmann B. (1999) Programmed cell death of embryonic motoneurons triggered through the Fas death receptor. *J. Cell. Biol.* **147**, 1049-1062

Raoul C, Pettmann B, Henderson CE. (2000) Active killing of neurons during development and following stress: a role for p75NTR and Fas? *Curr. Opin. Neurobiol.* **10**, 111-117

Reichardt LF, Farinas I. (1997) Neurotrophic factors and their receptor. Roles in neuronal development and function. In: *Molecular and Cellular Approaches To Neural Development*, Cowan WM, Jessell TM, Zipurski SL (eds.), Oxford University Press, New York, 220-263

Reifers F, Böhli H, Walsh EC, Crossley PH, Stainier DYR, Brand M. (1998) FGF8 is mutated in zebrafish acerebellar mutants and is required for maintenance of

midbrain-hindbrain boundary development and somitogenesis. *Development* **125**, 2381-2395

Rickmann M, Fawcett J, Keynes RJ. The migration of neural crest cells and the growth of motor axons through the rostral half of the chick somite. *J. Embryol. Exp. Morph.* **90**, 437-455

Riddle R, Johnson RL, Laufer E, Tabin C. (1993) Sonic hedgehog mediates the polarity activity of the ZPA. *Cell* **75**, 1401-1416

Riethmacher D, Sonnenberg-Riethmacher E, Brinkmann V, Yamaai T, Lewin GR, Birchmeier C. (1997) Severe neuropathies in mice with targeted mutations in the ErbB3 receptor. *Nature* **389**, 725-730

Rijli FM, Gavalas A, Chambon P. (1998) Segmentation and specification in the branchial region of the head: the role of the Hox selector genes. *Int. J. Dev. Biol.* **42**, 393-401

Rijli FM, Mark M, Lakkaraju S, Diedrich A, Dolle P. (1993) A homeotic transformation is generated in the rostral branchial region of the head by disruption of Hoxa-2, which acts as a selector gene. *Cell* **75**, 1333-1349

Riley DE, Lang AE. (1996) Movement disorders, *Neurology in Clinical Practice*, Bradley WG, Daroff RB, Fenichel GM, Marsden CD (eds.), Butterworth-Heinemann, 1733-1772

Rodella L, Rezzani R, Corsetti G, Stachiotti A, Ventura RG (1994) The rat abducens nucleus: a histo- and immunohistochemical study. *Boll. Soc. Ital. Biol. Sper.* **70**, 69-74

Rodriguez-Tebar A, Dechant G, Barde YA. (1991) Neurotrophins: structural relatedness and receptor interactions. *Philos. Trans. R. Soc. London Ser. B.* **331**, 255-258

Roelink H, Augsberger A, Heemskerk J, Korzh V, Norlin S, Ruiz I Altaba A, Tanabe Y, Placzek M, Edlund T, Jessell TM, Dodd J. (1994) Floor plate and

motoneuron induction by vhh-1, a vertebrate homolog of hedgehog expressed by the notochord. *Cell* **76**, 761-775

Roelink H, Porter JA, Chiang C, Tanabe Y, Chang DT, Beachy PA, Jessell TM. (1995) Floor plate and motoneuron induction by different concentrations of the amino-terminal cleavage product of sonic hedgehg autoproteolysis. *Cell* **81**, 445-455

Rogers LA, Cowan WM. (1973) The development of the mesencephalic nucleus of the trigeminal nerve in the chick. *J. Comp. Neurol.* **147**, 291-320

Romer SA, Parsons TS. (1991) Hilfsapparate des Auges, *Vergleichende Anatomie der Wirbeltiere*, Verlag Paul Parey, Hamburg Berlin, 456

Ronsin C, Muscatelli F, Mattei M-G, Breathnach R. (1993) A novel putative receptor protein tyrosine kinase of the met family. *Oncogene* **8**, 1195-1202

Rosenthal A. (1999) The GDNF protein family: Gene ablation studies reveal what they really do and how. *Neuron* **22**, 201-207

Rothman SM. (1992) Excitotoxins: possible mechanisms of action, *NY Acad Sci*, **648**, 132-138

Rothstein JD, Bristol LA, Hosler B, Brown RH, Kuncl RW. (1994) Chronic inhibition of superoxide dismutase produces apoptotic death in spinal neurons. *Proc. Natl. Acad. Sci. USA* **91**, 1455-4159

Rowitch DH, McMahon AP. (1995) Pax-2 expression in the murine neural plate precedes and encompasses the expression domains of Wnt-1 and En-1. *Mech. Development* **52**, 3-8

Ruiz I Altaba A. (1998) Combinatorial Gli gene function in floor plate and neuronal inductions by sonic hedgehog. *Development* **125**, 2203-2212

Sachs LM, Abdallah B, Hassan A, Levi G, De Luze A. (1997a) Apoptosis in Xenopus tadpole tail muscles involves Bax-dependent pathways. *FASEB J.* **11**, 801-808

Sachs LM, Lebrun JJ, De Luze A, Kelly PA, Demeneix BA. (1997) Tail regression, apoptosis and thyroid hormone regulation of myosin heavy chain isoforms in Xenopus tadpoles. *Mol. Cell. Endocrinology* **131**, 211-219

Sadler TW. Langman's Medical Embryology. Seventh edition (1995) Williams & Wilkins, Baltimore

Saha AR. (2001) The role of α-synuclein in the molecular pathogenesis of Parkinson's disease and dementia with Lewy bodies. Ph.D. thesis, University of London

Saha AR, Ninkina NN, Hanger DP, Anderton BH, Davies AM, Buchman VL. (2000) Induction of neuronal death by alpha-synuclein. *Eur. J. Neurosci.* **12**, 3073-3077

Sasai Y, Lu B, Steinbeisser, De Robertis EM. (1995) Regulation of neural induction by the Chd and BMP-4 antagonistic patterning signals in Xenopus. *Nature* **376**, 333-336

Sato SM, Sargent TD. (1989) Development of neural inducing capacity in dissociated Xenopus embryos. *Dev. Biol.* **134**, 263-266

Sauer FC. (1936) The interkinetic migration of embryonic epithelial nuclei. *J Morphol.* **60,** 1-11

Saunders JW Jr., Fallon JF. (1966) Cell death in morphogenesis. *Major Problems of Developmental Biology*, Locke M (ed.), Academic Press, New York, 289-314

Saunders JW Jr., Gasseling MT, Saunders LC. (1962) Cellular death in morphogenesis of the avian wing. *Dev. Biol.* **5**, 147-178

Schmidt C, Bladt F, Goedecke S, Brinkmann V, Zschiesche W, Sharpe M, Gherardi E, Birchmeier C. (1995) Scatter factor/ hepatocyte growth factor is essential for liver development. *Nature* **373**, 699-702

Schmidt JE, Suzuki A, Ueno N, Kimelman D. (1995) Localized BMP-4 mediates dorsal/ventral patterning in the early Xenopus embryo. *Dev. Biol.* **169**, 37-50

Schmidt O, Doxakis E, Davies AM. (2002) Macrophage stimulating protein is a neurotrophic factor for embryonic chicken hypoglossal motoneurons. *Eur. J. Neurosci.* **15**, 101-108

Schneider-Manoury S, Seitanidou T, Charnay P, Lumsden A. (1997) Segmental and neuronal architecture of the hindbrain of Krox-20 mouse mutants. *Development* **124**, 1215-1226

Schneider-Manoury S, Topilko P, Seitanidou T, Levi G, Cohen Tannoudji M, Pournis S, Babinet C, Charnay P. (1993) Disruption of Krox-20 results in alteration of rhombomeres 3 and 5 in the developing hindbrain. *Cell* **75**, 1199-1214

Schubert FR, Fainsod A, Gruenbaum Y, Gruss P. (1995) Expression of the novel murine homeobox gene Sax-1 in the developing nervous system. *Mech. Development* **51**, 99-114

Schuldiner S, Shirvan A, Linial M. (1995) Vesicular neurotransmitter transporters: from bacteria to humans. *Physiol. Rev.* **75**, 369-392

Schweichel IU, Merker HJ. (1973) The morphology of various types of cell death in prenatal tissues. *Teratology* **7**, 253-266

Scott MP. (1992) Vertebrate homeobox gene nomenclature *Cell* **71**, 551-553

Sedel F, Bechade C, Triller A. (1999) Nerve growth factor (NGF) induces motoneuron apoptosis in rat embryonic spinal cord *in vitro*. *Eur. J. Neurosci.* **11**, 3904-3912

Segal RA, Greenberg ME. (1996) Intracellular signalling pathways activated by neurotrophic factors. *Ann. Rev. Neurosci.* **19**, 463-489

Sendtner M, Arakawa Y, Stöckly KA, Kreutzberg GW, Thoenen H. (1991) Effect of ciliary neurotrophic factor (CNTF) on motoneuron survival., *J. Cell Sci. Suppl.* **15**, 103-109

Sendtner M, Holtmann B, Kolbeck R, Thoenen H, Barde Y. (1992) Brain-derived neurotrophic factor prevents the death of motoneurons in newborn rats after nerve section. *Nature* **360**, 757-758

Sendtner M, Pei G, Beck M, Schweizer U, Wiese S. (2000) Developmental motoneuron cell death and neurotrophic factors. *Cell Tissue Res.* **301**, 71-84

Serafini T, Kennedy TE, Galko MJ, Mirzayan C, Jessell TM, Tessier-Lavigne M. (1994) The netrins define a family of axon outgrowth-promoting proteins homologous to C. elegans UNC-6. *Cell* **78**, 409-424

Sham MH, Vesque C, Nonchev S, Marshall H, Frain M. (1993) The zinc finger gene Krox-20 regulates HoxB2 (Hox2.8) during hindbrain segmentation. *Cell* **72**, 183-196

Shaner RF. (1932) Development of nuclei and tracts of mid-brain. *J. Comp.Neurol.* **55**, 493-512

Shaner RF. (1936) Development of the finer structures and finer connections of the globus pallidus, corpus of Luys and substantia nigra in the pig. *J. Comp.Neurol.* **64**, 213-233

Shimamura K, Hartigan DJ, Martinez S, Puelles L, Rubenstein JLR. (1995) Longitudinal organization of the anterior neural plate and neural tube. *Development* **121**, 3923-3933

Shorey ML. (1909) The effect of the destruction of peripheral areas on the differentiation of the neuroblasts. *J. Exp. Zool.* **7**, 25-64

Simeone A, Acampora D, Gulisano M, Stornaiuolo A, Boncinelli E. (1992) Nested expression domains of four homeobox genes in developing rostral brain. *Nature* **358**, 687-690

Simon H, Guthrie S, Lumsden A. (1994) Regulation of SC1/ DM-GRASP during the migration of motoneurons in the chick embryo brain stem. *J. Neurobiol.* **25**, 1129-1143

Simon H, Hornbruch A, Lumsden A. (1995) Independent assignment of antero-posterior and dorso-ventral positional values in the developing chick hindbrain. *Curr. Biol.* **5**, 205-214

Skeel A, Yoshimura T, Showalter SD, Tanaka S, Appel. (1991) Macrophage stimulating protein: purification, partial amino acid sequence, and cellular activity. *J. Exp. Med.* **173**, 1227-1234

Skeel AH, Leonard EJ. (1994) Action and target cell specifity of human macrophage-stimulating protein (MSP). *J. Immunol.* **152**, 4618-4623

Sohal GS, Weidman T. (1978) Ultrastructural sequence of embryonic cell death in normal and peripherally deprived trochlear nucleus. *Exp. Neurol.* **66**, 619-628

Sohal GS, Weidman TA, Stoney SD. (1978) Development of the trochlear nerve: Effects of early removal of periphery. *Exp. Neurol.* **59**, 331-341

Sottrup-Jensen L, Zaijdel M, Claeys H, Petersen TE. (1975) Amino-acid sequence of activation cleavage site in plasminogen homology with "pro" part of prothrombin. *Proc. Natl. Acad. Sci. USA*, **72**, 577-581

Spatz H. (1923-1924) Zur Ontogenese des Striatum und des Pallidum, *D. Z. Nervenheilkunde* **81**, 185-188

Specht LA, Pickel VM, Joh TH, Reis DJ. (1981a) Light-Microscopic Immunocytochemical Localization of Tyrosine Hydroxylase in Prenatal Rat Brain. I. Early Ontogeny. *J. Comp.Neurol.* **199**, 233-253

Specht LA, Pickel VM, Joh TH, Reis DJ. (1981b) Light-Microscopic Immunocytochemical Localization of Tyrosine Hydroxylase in Prenatal Rat Brain. II. Late Ontogeny. *J. Comp.Neurol.* **199**, 255-276

Spemann H, Mangold H. (1924) Über Induktion von Embryoanlagen durch Implantation artfremder Organisatoren. *Wilhelm Roux Arch Entwicklung Org.* **100**, 599-638

Srinivasula SM, Ahmad M, Fernandes-Alnemri T, Litwack G, Alnemri ES. (1996) Molecular ordering of the Fas-apoptotic pathway: the Fas/APO-1 protease that activates multiple Ced-3/ICE-like cysteine proteases. *Proc. Natl. Acad. Sci. USA* **93**, 14486-14491

Stella MC, Vercelli A, Repici M, Follenzi A, Comoglio PM. (2001) Macrophage stimulating protein is a novel neurotrophic factor. *Mol. Biol. Cell*, **12**, 1341-1352

Stern CD, Sisodiya SM, Keynes RJ. (1986) Interactions between neurites and somite cells: inhibition and stimulation of nerve growth in the chick embryo. *J Embryol. Exp. Morph.* **91**, 209-226

Stoker M, Gherardi E, Perryman M, Gray J. (1987) Scatter factor is a fibroblast-derived modulator of epithelial cell mobility. *Nature* **327**, 239-242

Stone DM, Hynes M, Armanini M, Swanson TA, Gu Q, J. (1996) The tumour-suppressor gene patched encodes a candidate receptor for sonic hedgehog. *Nature* **384**, 129-134

Straznicki C, Tay C. (1983) The localization of motoneuron pools innervating wing muscles in the chick. *Anat. Embryol.* **166**, 209-218

Studer M, Lumsden A, Ariza McNaughton L, Bradley A, Krumlauf R (1996) Altered segmental identity and abnormal migration of motor neurons in mice lacking Hoxb-1. *Nature* **384**, 630-634

Surguchov A, Palazzo RE, Surguchova I. (2001) Gamma synuclein: subcellular localization in neuronal and non-neuronal cells and effect on signal transduction. *Cell Motil. Cytoskel.* **49**, 218-228

Swiatek PJ, Gridley T. (1993) Perinatal lethality and defects in hindbrain development in mice homozygous for a targeted mutation of the zinc finger gene Krox-20. *Genes Dev.* **7**, 2071-2084

Tan K, Le Douarin N. (1991) Development of the nuclei and cell migration in the medulla oblongata. Application of the quail-chick chimera system. *Anat. Embryol.* **183**, 321-343

Tanabe Y, Jessell TM. (1996) Diversity and patterning in the spinal cord. *Science* **274**, 1115-1123

Tanaka H, Matsui T, Agata A, Tomura M, Kubota I, M. (1991) Molecular cloning and expression of a novel adhesion molecule, SC1. *Neuron* **7**, 535-545

Tanaka H, Obata K. (1984) Developmental changes in unique cell surface antigens of chick embryo spinal motoneurons and ganglion cells. *Dev. Biol.* **106**, 26-37

Tank AW, Ham L, Curella P (1986a) Induction of mRNA for tyrosine hydroxylase by cyclic AMP and glucocorticoids in a rat pheochromocytoma cell line: effect of the inducing agents alone or in combination on the enzyme levels and rate of sunthesis of tyrosine hydroxylase. *Mol. Pharmacol.* **30**, 486-496

Tank AW, Curella P, Ham L (1986b) Induction of mRNA for tyrosine hydroxylase by cyclic AMP and glucocorticoids in a rat pheochromocytoma cell line: evidence for the regulation of tyrosine hydroxylase synthesis by multiple mechanisms in cells exposed to elevated levels of both inducing agents. *Mol. Pharmacol.* **30**, 497-503

Tennyson VM, Mytilineou C, Barrett RE. (1973) Fluorescence and electron microscopic studies of the early development of the substantia nigra and area ventralis tegmenti in the fetal rabbit. *J. Comp.Neurol.* **149**, 233-258

Tessier-Lavigne M, Plazcek M, Lumsden AGS, Dodd J. (1988) Chemotropic guidance of developing axons in the mammalian central nervous system *Nature* **336**, 775-778

Theiler K. (1989) The House Mouse. Atlas of embryonic development. *Springer-Verlag, New York, Berlin, Heidelberg, London, Paris, Tokyo*

Thery C, Sharpe MJ, Batley SJ, Stern CD, Gherardi E. (1995) Expression of HGF/ SF, HGF1/ MSP, and c-met suggests new functions during early chick development. *Dev. Genet.* **17**, 90-101

Thornberry NA, Lazebnik Y. (1998) Caspases: enemies within. *Science* **281**, 1312-1316

Tiunova AA, Anokhin KV, Saha AR, Schmidt O, Hanger DP, Anderton BH, Davies AM, Ninkina NN, Buchman VL. (2000) Chicken synucleins: cloning and expression in the developing embryo. *Mech. Development* **99**, 195-198

Tosney KW. (1991) Cells and cell-interactions that guide motor axons in the developing chick embryo. *Bioessays* **13**, 17-23

Tosney KW. (1988) Proximal tissues and patterned neurite outgrowth at the lumbosacral level of the chick embryo: partial and complete deletion of the somite. *Dev. Biol.* **127**, 266-286

Tosney KW. (1987) Proximal tissues and patterned neurite outgrowth at the lumbosacral level of the chick embryo: deletion of the dermomyotome. *Dev. Biol.* **122**, 540-558

Tosney KW, Landmesser L. (1984) Pattern and specificity of axonal outgrowth following varying degrees of chick limb bud ablation. *J. Neurosci.* **4**, 2518-2527

Tsuchida T, Ensini M, Morton SB, Baldassare M, Edlund T, Jessell TM, Pfaff SL. (1994) Topographic organization of embryonic motoneurons defined by expression of LIM homeobox genes. *Cell* **79**, 957-970

Ueda K, Fukushima H, Masliah E, Xia Y, Iwai A, Yoshimoto M, Otero DA, Kondo J, Ihara Y, Saitoh T. (1993) Molecular cloning of cDNA encoding an unrecognized component of amyloid in Alzheimer's disease. *Proc. Natl. Acad. Sci. USA* **90**, 11282-11286

Uehara Y, Minowa O, Mori C, Shiota K, Kuno J, Noda T, Kitamura N. (1995) Placental defect and embryonic lethality in mice lacking hepatocyte growth factor/ scatter factor. *Nature* **373**, 702-705

Unsicker K, Krieglstein K. (2000) Co-activation of TGF-b and cytokine signalling pathways are required for neurotrophic functions. *Cytokine Growth Factor Rev.* **11**, 97-102

Urbanek P, Wang ZQ, Fetka I, Wagner EF, Busslinger M. (1994) Complete block of early B cell differentiation and altered patterning of the posterior midbrain in mice lacking Pax5/BSAP. *Cell* **79**, 901-912

Uversky VN, Li J, Souillac P, Millett IS, Doniach S, Jakes R, Goederts M, Fink AL. (2002) Biophysical properties of the synucleins and their propensities to fibrillate. *J.Biol. Chem.* **277**, 11970-11978

Valarche I, Tissier-Seta JP, Hirsch MR, Martinez S, Goridis C, Brunet JF (1993) The mouse homeodomain gene Phox2a regulates Ncam promotor activitiy in concert with Cux/CDP an is a putative determinant of neurotransmitter phenotype. *Development* **119**, 881-896

Van Straaten HWM, Hekking JWM, Wiertz-Hoessels EL, Thors F, DrukkerJ. (1985) Effect of a notochordal implant on the early morphogenesis of the neural tube and neuroblasts: histometrical and histological results. *Dev. Biol.* **110**, 247-254

Varela-Echavarría, Pfaff SL, Guthrie S. (1996) Differential expression of LIM homeobox genes aming motoneuron subpopulations in the developing chick brain stem. *Mol. Cell. Neurosc.* **8**, 242-257

Verdi JM, Birren SJ, Ibanez CF, Persson H, Kaplan DR, Benedetti M, Chao MV, Anderson DJ. (1994) p75LNGFR regulates Trk signal transduction and NGF-induced neuronal differentiation in MAH cells. *Neuron* **12**, 733-745

Villavicencio EH, Walterhouse DO, Iannaccoune PM. (2000) The sonic hedgehog-patched-gli pathway in human development. *Am. J. Hum. Genet.* **67**, 1047-1054

Voorn P, Kalsbeek A, Jorritsma-Byham B, Groenewegen HJ. (1988) The Pre- and Postnatal Development of the Dopaminergic Cell Groups in the Ventral Mesencephalon and the Dopaminergic Innervation of the Striatum of the Rat. *Neurosci.* **25**, 857-887

Wagner M, Han B, Jessell TM. (1992) Regional differences in retinoid release from embryonic neural tissue detected by an *in vitro* reporter assay. *Development* **116**, 55-66

Wagner M, Thaller C, Jessell TM, Eichele G. (1990) Polarizing activity and retinoid synthesis in the floor plate of the neural tube. *Nature* **345**, 819-822

Wahl CM, Noden DM, Baker R. (1994) Developmental relations between sixth nerve motoneurons and their targets in the chick embryo. *Dev. Dyn.* **201**, 191-202

Wakabayashi K, Yoshimoto M, Fukushima T, Koide R, Horikawa Y, Morita T, Takahashi H. (1999) Widespread occurrence of alpha-synuclein/NACP-immunoreactive neuronal inclusions in juvenile and adult-onset Hallervorden-Spatz disease with Lewy bodies. *Neuropathol. Appl. Neurobiol.* **25**, 363-368

Wakade AR, Edgar D, Thoenen H. (1983) Both nerve growth factor and high K concentration support the survival of chick embryo sympathetic neurons. *Exp. Cell Res.* **144**, 377-384

Walsh GS, Krol KM, Crutcher KA, Kawaja MD. (1999a) Enhanced neurotrophin-induced axon growth in myelinated portions of the CNS in mice lacking the p75 neurotrophin receptor. *J. Neurosci.* **19**, 4155-4168

Walsh GS, Krol KM, Kawaja MD. (1999b) Absence of the p75 neurotrophin receptor alters the pattern of sympathosensory sprouting in the trigeminal ganglia of mice overexpressing nerve growth factor. *J. Neurosci.* **19**, 258-273

Wang MH, Dlugosz AA, Sun Y, Suda T, Skeel A, Leonard EJ. (1996) Macrophage-stimulating protein induces proliferation and migration of murine keratinocytes. *Exp. Cell Res.* **226**, 39-46

Wang MH, Ronsin C, Gesnel MC, Coupey L, Skeel A, L. (1994) Identification of the ron gene product as the receptor for the human macrophage stimulating protein. *Science* **266**, 117-119

Wang MZ, Jin P, Burncrot DA, Marigo V, McMahon AP, Wang EA, Woolf T, Pang K. (1995) Induction of dopaminergic neuron phenotype in the midbrain by sonic hedgehog. *Nat. Medicine.* **1**, 1184-1188

Warrilow J, Guthrie S. (1999) Rhombomere origin plays a role in the specificity of cranial motor axon projections in the chick. *Eur. J. Neurosci.* **11**, 1403-1413

Way JC, Chalfie M. (1988) mec-3, a homeobox-containing gene that specifies differentiation of the touch receptor neurons in C. elegans. *Cell*, **54**, 5-16

Whitman M. (1998) Smads and early developmental signalling by the TGF beta superfamily. *Genes Dev.* **12**, 2445-2462

Wiese S, Metzger F, Holtmann B, Sendtner M. (1999) The role of p75NTR in modulating neurotrophin survival effects in developing motoneurons. *Eur. J. Neurosci.* **11**, 1668-1676

Wild JM, Zeigler HP. (1980) Central representation and somatotopic organization of the jaw muscles within the facial and trigeminal nuclei of the pigeon (Columba livia). *J. Comp.Neurol.* **92**, 175-201

Wilkinson D, Bhatt S, Cook M, Boncinelli E, Krumlauf R. (1989b) Segmental expression of hox 2 homeobox-containing genes in the developing mouse hindbrain. *Nature* **341**, 405-409

Wilkinson DG, Bhatt S, Chavrier P, Bravo R, Charnay P. (1989b) Segment-specific expression of a zinc-finger gene in the developing nervous system of the mouse. *Nature* **337**, 461-464

Wilkinson DG, Krumlauf R. (1990) Molecular approaches to the segmentation of the hindbrain, TINS, 13, 335-339

Windle WF. (1933) Neurofibrillar development in the central nervous system of cat embryos between 8 and 12 mm long. *J. Comp.Neurol.* **50**, 643-723

Windle WF, Fitzgerald JE. (1942) Development of the human mesencephalic trigeminal root and related neurons. *J. Comp.Neurol.* **77**, 597-608

Wingate R, Lumsden A. (1996) Persistence of rhombomeric organisation in the postsegmental avian hindbrain. *Development* **122**, 2143-2152

Wong V, Glass DJ, Arriaga R, Yancapoulos GD, Lindsay RM, Conn G. (1997) Hepatocyte growth factor promotes motoneuron survival and synergizes with ciliary neurotrophic factor. *J. Biol. Chem.* **272**, 5187-5191

Wurst W, Auerbach AB, Joyner A. (1994) Multiple developmental defects in Engrailed-1 mutant mice: an early mid-hindbrain deletion and patterning defects in forelimbs and sternum. *Development* **120**, 2065-2075

Wyllie AH. (1981) Cell death: A new classification separating apoptosis from necrosis. *Cell Death in Biology and Pathology*, 9-34

Wyllie AH, Kerr JFR, Currie AR. (1980) Cell death: The significance of apoptosis. *Int. Rev. Cytol.* **68**, 251-306

Xue L, Fletcher GC, Tolkovski AM. (1999) Autophagy is activated by apoptotic signalling in sympathetic neurons: an alternative mechanism of death execution. *Mol. Cell. Neurosci.* **14**, 180-198

Yaginuma H, Tomito M, Takashita N, McKay SE, Cardwell C, Yin QW, Oppenheim RW. (1996) A novel type of programmed neuronal death in the cervical spinal cord of the chick embryo. *J. Neurosci.* **16**, 3685-3703

Yamada T, Pfaff SL, Edlund T, Jessell TM. (1993) Control of cell pattern in the neural tube: motoneuron induction by diffusible factors from notochord and floor plate. *Cell* **73**, 673-686

Yamada Y, Placczek M, Tanaka H, Dodd J, Jessell TM. (1991) Control of cell pattern in the developinmg nervous system: polarizing activity of the floor plate and notochord. *Cell* **64**, 635-647

Yamamoto Y, Livet J, Pollock RA, Garces A, Arce V, Henderson CE. (1997) Hepatocyte growth factor (HGF/SF) is a muscle-derived survival factor for a subpopulation of embryonic motoneurons. *Development* **124**, 2903-2913

Yan Q, Matheson C, Lopez OT. (1995) *In vivo* neurotrophic effects of GDNF on neonatal and adult facial motoneurons. *Nature* **373**, 341-344

Yang J, Liu X, Bhalla K, Kim CN, Ibrado AM, Cai J, Peng TI, Jones DP, Wang X. (1997) Prevention of apoptosis by Bcl-2: release of cytochrome c from mitochondria blocked. *Science* **275**, 1129-1132

Yang XM, Toma JG, Bamji SX, Belliveau DJ, Kohn J., (1998) Autocrine hepatocyte growth factor provides a local mechanism for promoting axonal growth. *J. Neurosci.* **18**, 8369-8381

Ye W, Shimamura K, Rubenstein JLR, Hynes MA, Rosenthal A. (1998) FGF8 and SHH signals create inductive centers for dopaminergic and serotonergic neurons in the anterior neural plate. *Cell* **93**, 755-766

Yeh WC, Pompa JL, McCurrach ME, Shu HB, Elia AJ, Shahinian A, Ng M, Wakeham A, Khoo W, Mitchell K, El Deiry WS, Lowe SW, Goeddel DV, Mak TW. (1998) FADD: essential for embryo development and signaling from some, but not all, inducers of apoptosis. *Science* **279**, 1954-1958

Yoshimura T, Yuhki N, Wang MH, Skeel A, Leonard EJ. (1993) Cloning, sequencing, and expression of human macrophage stimulating protein (MSP, MST1) confirms MSP as a member of the family of kringle proteins and locates the MSP gene on chromosome 3. *J. Biol. Chem.* **268**, 15461-15480

Zha J, Harada H, Yang E, Jockel J, Korsmeyer SJ. (1996) Serine phosphorylation of death agonist BAD in response to survival factor results in binding to 14-3-3 not BCL-X(L). *Cell* **87**, 619-628

Zhadanov AB, Bertuzzi S, Taira M, Dawid IB, Westphal H. (1995) Expression pattern of murine LIM class homeobox gene Lhx3 in subsets of neural and neuroendocrine tissues. *Dev. Dyn.* **202**, 354-364

Zhang M, Kim HJ, Marshall H, Gendron Maguire M, Lucas DA, Baron A, Gudas LJ, Gridley T, Krumlauf R, Grippo JF. (1994) Ectopic Hoxa-1 induces rhombomere transformation in mouse hindbrain. *Development* **120**, 2431-2442

Zilles K, Wingert F. (1973) Quantative studies of the development of the fresh volumes and the number of neurones of the N. oculomotorii of white mice during ontogenesis. *Brain Res.* **56**, 63-75

Zou H, Henzel WJ, Liu X, Lutschg A, Wang X, Xu M. (1998) Apaf-1, a human protein homologous to C. elegans CED, participates in cytochrome c-dependent activation of caspase-3. *Cell* **90**, 405-413

Zou H, Li Y, Liu X, Wang X. (1999) An APAF-1 cytochrome c multimeric complex is a functional apoptosome that activates pro-caspase-9. *J. Biol. Chem.* **274**, 11549-11556